UNIVERSIDADE DE SÃO PAULO

FACULDADE DE CIÊNCIAS FARMACÊUTICAS DE RIBEIRÃO PRETO

Synthesis of GPI anchor analogues to support the discovery of new molecular targets of *Trypanosoma cruzi*

Síntese de análogos de âncora de GPI: uma contribuição para a descoberta de novos alvos moleculares de *Trypanosoma cruzi*

Ana Luísa Malaco Morotti

Ribeirão Preto
2018

ANA LUÍSA MALACO MOROTTI

Synthesis of GPI anchor analogues to support the discovery of new molecular targets of *Trypanosoma cruzi*

Síntese de análogos de âncora de GPI: uma contribuição para a descoberta de novos alvos moleculares de *Trypanosoma cruzi*

Corrected version of the doctoral thesis presented to the Graduate Program in Pharmaceutical Sciences on 11/12/2018. The original version is available at the School of Pharmaceutical Sciences of Ribeirão Preto/USP.

Doctoral thesis presented to the Graduate Program of School of Pharmaceutical Sciences of Ribeirão Preto/USP for the degree of Doctor in Sciences.

Concentration Area: Natural and Synthetic Products

Supervisor: Prof Dr Ivone Carvalho

Co-supervisor: Prof Dr Robert A. Field

Ribeirão Preto
2018

I AUTHORIZE THE REPRODUCTION AND TOTAL OR PARTIAL DISCLOSURE OF THIS
WORK, BY ANY CONVENTIONAL OR ELECTRONIC MEANS

APPROVAL PAGE

Name: Ana Luísa Malaco Morotti

Title: Synthesis of GPI anchor analogues to support the discovery of new molecular targets of *Trypanosoma cruzi*

Doctoral thesis presented to the Graduate Program of School of Pharmaceutical Sciences of Ribeirão Preto/USP for the degree of Doctor in Sciences.

Concentration Area: Natural and Synthetic Products

Supervisor: Ivone Carvalho

Approved on:

Examiners

Prof. Dr. _____

Institution: _____ Signature:_____

Prof. Dr. _____

Institution: _____ Signature:_____

Prof. Dr. _____

Institution: _____ Signature:_____

Prof. Dr. _____

Institution: _____ Signature:_____

Prof. Dr. _____

Institution: _____ Signature:_____

Prof. Dr. _____

Institution: _____ Signature:_____

This thesis is dedicated to my treasured parents José Mario and Telma.

ACKNOWLEDGEMENTS

"Whatever you decide to do, make sure it makes you happy"
(Unknown author)

ABSTRACT

MOROTTI, A. L. M. Synthesis of GPI anchor analogues to support the discovery of new molecular targets of *Trypanosoma cruzi.* 2018. 178p. Thesis (Doctoral). School of Pharmaceutical Sciences of Ribeirão Preto-University of São Paulo-Ribeirão Preto, 2018.

Glycosylphosphatidylinositol (GPI) anchors are essential molecules to attach glycoconjugates and proteins in protozoan's cell surface. *Trypanosoma cruzi* produces a range of unique GPI structures that anchor mucins and *trans*-sialidases which participate in important processes involved in the interaction between parasite and host. As an effort to study *T. cruzi* GPI anchor biosynthesis and possibly use it as a potential target for an antichagasic drug, this work aims to synthesize GPI anchor analogs (labelled or not) and analyze the potential of these molecules as substrates in the GPI biosynthetic pathway. In this context, a pseudo-disaccharide **31** was synthesized by *O*-glycosylation reaction between azide glycosyl donors (**32 or 33a-d**) and *myo*-inositol acceptor (**34**), prepared from glucosamine (**35**) hydrochloride and methyl α-D-glucopyranoside (**36**), respectively, using orthogonal protection/ deprotection. Five different glycosyl donors (**32** and **33a-d**) were prepared to investigate the influence of their protective groups on the stereoselectivity of the *O*-glycosylation reaction in the presence of different solvents to afford the required GPI α-linkage. In addition, the synthesis of the *myo*-inositol acceptor **34** was achieved using several protection/deprotection steps, besides the Ferrier rearrangement, to form a functionalized cyclitol derivative that enables the regioselective introduction of the azide glycoside unit and phospholipid moiety on its C-1 and C-6 positions, respectively. Then, *O*-glycosylation of acceptor **34** with donor **33c** was accomplished in diethyl ether, using TMSOTf as promoter to give exclusively α-anomer **31c** in high yield. After deallylation of **31c**, the phosphodiester moiety bearing an octyl chain (**87**), prepared by the H-phosphonate approach, was appended to the pseudo-disaccharide to yield, after deprotection, target compounds **30a**. The same synthetic strategy was applied to the preparation of **30c**, even though in the protective form, compound **91** bearing an alkyl-naphthyl side chain (**90**). Currently, compound **30a** is being tested as substrates of GPI anchor biosynthesis in *Euglena gracilis* cell membranes, a non-pathogenic unicellular algae, which may potentially be used as a model for phylogenetically related human parasites. After incubation of the potential

GPI substrate **30a** with *E. gracilis* microsomal membranes for generation of metabolites, the analysis by LC-MS and, eventually, isolation of the products will be performed for further characterization. Products that show any substrate or inhibitory activities will be also assayed in *T. cruzi* microsomal membrane.

RESUMO

MOROTTI, A. L. M. Síntese de análogos de âncora de GPI: uma contribuição para a descoberta de novos alvos moleculares de *Trypanosoma cruzi*. 2018. 178p. Tese (Doutorado). Faculdade de Ciências Farmacêuticas de Ribeirãi Preto-Universidade de São Paulo, Ribeirão Preto, 2018.


Âncoras de glicosilfosfatidilinositol (GPI) são estruturas essenciais para a ancoragem de glicoconjugados e proteínas na superfície celular de protozoários. *Trypanosoma cruzi* produz uma gama de estruturas únicas de GPI, as quais ancoram mucinas e *trans*-sialidases, que participam de processos envolvidos na interação entre parasita e hospedeiro. Afim de estudar a biossíntese de âncora de GPI de *T. cruzi* e possivelmente utilizá-la como um potencial alvo anti-*T.cruzi*, este trabalho visa sintetizar análogos de âncoras de GPI e analisar o potencial destas moléculas como substratos da via biossintética de GPIs. Neste contexto, um pseudo-dissacarídeo **31** foi sintetizado através de *O*-glicosilação entre os doadores derivados de azido-glicopiranosídeo (**32** ou **33a-d**) e o acceptor de *mio*-inositol (**34**), preparados a partir de cloridrato de glucosamina (**35**) e metil-α-D-glucopiranósido (**36**), respectivamente, usando proteção/desproteção ortogonais. Cinco diferentes dadores de glicosídicos (**32** e **33a-d**) foram preparados para investigar a influcia dos seus grupos protetores na estereoselectividade da reações de *O*-glicosilação na presença de diferentes solventes para estudar o favorecimento da configuração α, presente em GPIs. Ademais, a síntese do aceptor de *mio*-inositol **34** foi realizada em 12 etapas pela estratégia do rearranjo Ferrier para formar um derivado de ciclitol, além de diversas proteções/desproteções, funcionalizado que permite a introdução regiosselectiva da unidade de azido glicose (**32-33a-d**) e uma porção de fosfolípido no seu C-1 e posições C-6, respectivamente. Assim, *O*-glicosilação entre doador **33c** e o acceptor **34**, foi realizada utilizando TMSOTf como promotor para originar o composto **31c** com boa estereoseletividade para α, com elevado rendimento (~70%). Após a dealilação de **31c**, a porção fosfodiéster contendo uma cadeia C-8 (**87**), preparada pela abordagem do H-fosfonato, foi anexada ao pseudo-dissacarídeo para gerar, após desprotecção global, o composto alvo **30a**. A mesma estratégia sintética foi aplicada ao preparo do composto **91** contendo uma cadeia lateral alquil-naftil (**90**) que está em últimas etapas de desproteção para gerar o composto final **30c**.

Atualmente, o composto **30a** está sendo testado como substrato da biossíntese de âncoras de GPI em membranas microssomais de *Euglena gracilis*, uma alga unicelular não patogênica, que pode potencialmente ser utilizada como modelo para parasitas humanos filogeneticamente relacionados. Após a incubação do potencial substrato de GPI **30a** com membranas microssomais de *E. gracilis* para geração de metabólitos, será realizada análise do extrato por LC-MS e, eventualmente, isolamento dos produtos formados para posterior caracterização. Os produtos que apresentarem atividade como substrato ou como inibidores da biossíntese de GPI em *E. gracilis* serão também ensaiados na membrana microsomal do *T. cruzi.*

Palavras-chave: âncoras de GPI, proteção/desproteção ortogonal, glicosamina, *mio*-inositol, fosfodiéster.

LIST OF COMPOUNDS

33a

33b

33c

33d

31a

31b

31c

31d

77

89

91

34

92

84

85
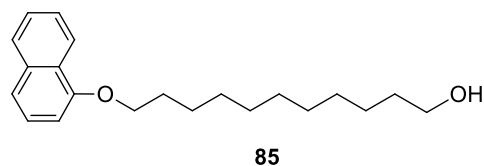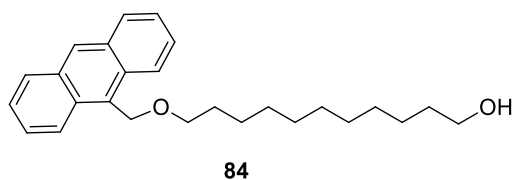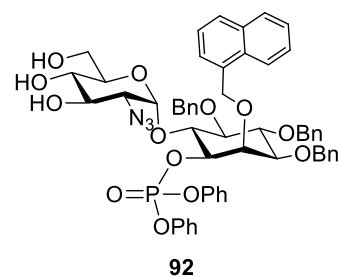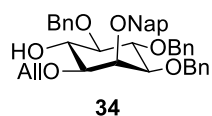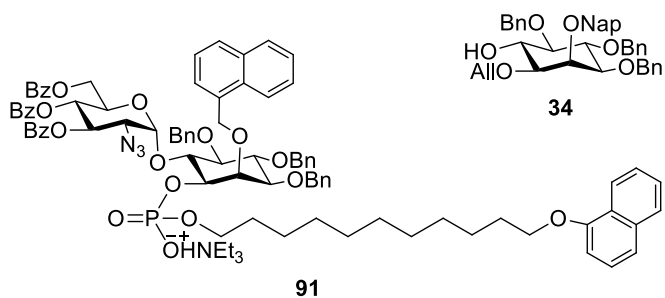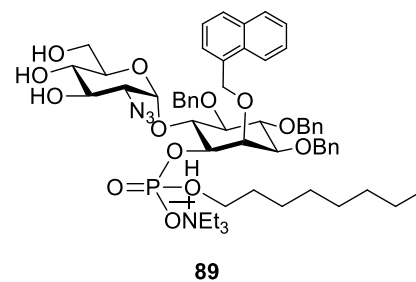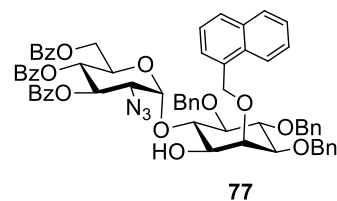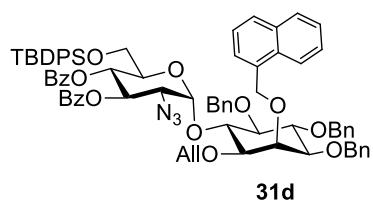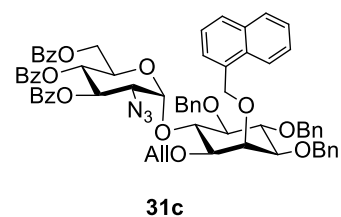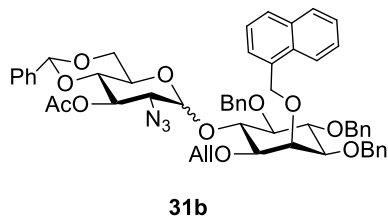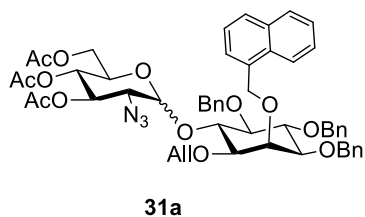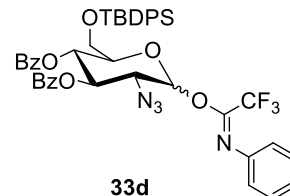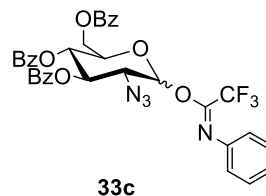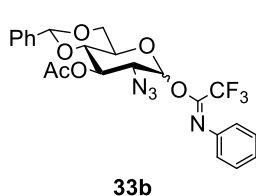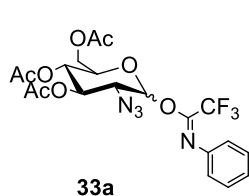
LIST OF ABBREVIATONS

Ac: acetyl

AcOH: Acetic acid

AcOEt: ethyl acetate

AEP: Aminoethylphosphonate

AgOTf: Silver trifluoromethanesulfonate

All: Allyl

Bn: Benzyl

Bz: Benzoyl

DCE: 1,2-ichloroethane

DCM: Dichloromethane

DMP: Dess-Martin Periodinane

EG: *Euglena gracilis*

ER: Endoplasmatic Reticulum

ESI- TOF: Electrospray ionisation time-of-flight mass espectrometry

Et$_2$O: Diethyl ether

EtN-P: Ethanolamine phosphate

EtN-P-T: Ethanolamine phosphate transferase

EVE: Ethyl vinyl ether

FDG: 2-Fluoro-2-deoxyglucose

GDP-Man: Guanosine diphosphate mannose

GIPLs: Glycoinositol phospholipids

Glc: Glucose

GlcNAc: *N*-acetyl-glucosamine

GlcNAcT: *N*-acetyl-glucosamine transferase

GlcN: Glucosamine

GPI: Glycosylphosphatidylinositol

HPLC: High performance liquid chromatography

HR-MS: High resolution mass spectrometry

Ino: Inositol

IPC: Inositolphosphorylceramide

LC-MS: Liquid chromatography coupled to mass spectrometry

Man: Mannose

ManN: Mannosamine

ManT: Mannosyltransferase

Me: Methyl

MeCN: Acetonitrile

MP: Melting point

MS: Molecular sieves

MS/MS: Tandem mass spectrometry

MW: Molecular weight

Nap: Naphtylmethyl

NMR: Nuclear magnetic resonance

PARP: Procyclic Acidic Repetitive Protein

PE: Phosphatidylethanolamine

PI: Phosphatidylinositol

Pi: Precursor ion

ppm: Parts *per* million

PPTS: Pyridinium *p*-toluenesulfonate

p-TSOH: *p*-toluenesulfonic acid

r.t.: Room temperature

TBDPSCl: *terc*-butyldiphenylsilyl chloride

TBDPS: *terc*-butyldiphenylsilyl

TBDMSCl: *terc*-butyldimethylsilyl chloride

TBS or **TBDMS**: *terc*-butyldimethylsilyl

TFA: Trifloroacetic acid

TfN$_3$: Triflic azide

TLC: Thin layer chromatography

TMSOTf: Trimethylsilyl trifluoromethanesulfonate

Tol.: Toluene

VSG: Variant Surface Glycoprotein

LIST OF TABLES

LIST OF FIGURES

LIST OF SCHEMES

SUMMARY

1. INTRODUCTION

_____

1.1. Chagas Disease and *Trypanosoma cruzi*

Chagas disease affects around 7 millions of people worldwide, being a substantial cause of morbidity and mortality, particularly in developing countries, being the source of about 7500 deaths annually. Low financial returns and reduced income of affected individuals do not arouse interest in research and development of new treatments by the pharmaceutical industry (WHO, 2018). Chagas disease was a concern limited to Latin American territory. However, due to an increase in immigration in the last decades, the disease has started to spread around other continents (DNDi, 2018).

The causative agent of Chagas disease is the hemiflagellate protozoan *Trypanosoma cruzi*, which belongs to the family of *Trypanosamatidae* and order *Kinetoplastida*. The parasite was discovered by Carlos Chagas in 1909, who first identified *T. cruzi* in the blood of a domestic cat and later in a two years old girl. The main transmitter of *T. cruzi* is a vector bug, *Triatoma infestans*, which infects humans (and other mammals) through their contaminated feces while feeding with the individual blood. Other forms of infection also occur through the ocular or oral mucosa, blood transfusion, congenital and laboratory accidents (WHO, 2018). The protozoan has a heteroxenic life cycle, which consists in one phase in the invertebrate vector and another phase in vertebrates (mammals) (NOIREAU; DIOSQUE; JANSEN, 2009; NEVES, 2000). *T. cruzi* undergoes intracellular multiplication phases in the vertebrate host being found as trypomastigotes (blood) and amastigotes (tissues). In the insect, the protozoan is present as epimastigotes. Chagas' disease presents three clinical phases: the acute one, generally asymptomatic or with unspecific symptoms, which the parasite is in abundance in the individual's bloodstream; the intermediate phase, in which the host is asymptomatic until manifestation of the third phase, the chronic one, characterized by irreversible lesions in different organ tissues. Among individuals in the chronic phase, 30% of them develop cardiopathies while 10% suffer from damage to the esophagus, colon, nervous system or more than one organ, remaining with the disease until the end of their lives (WHO, 2018). In Brazil, cardiac complications related to Chagas disease are significant cause of implantation of pacemakers and heart transplantations, as

well as an important cause of death in adults between 30 and 60 years old (BRAZIL, 2013).

1.2. Therapy against Chagas Disease

Currently, there is no vaccine against Chagas Disease, being prevention and elimination of the vector bug the most effective means of protection against the illness. The scarce therapeutic arsenal for the treatment of affected individuals consists of two drugs: benznidazole and nifurtimox (Figure 1) (SALES-JUNIOR et al., 2017). Both compounds act as pro-drugs that require nitro-reduction for further formation of free radicals and metabolites which bind to the parasite's nuclear and mitochondrial DNAs, causing damage to these structures (SALES-JUNIOR et al., 2017; RAJAO et al., 2014). On the other hand, these nitroaromatic compounds are also responsible for significant side effects, lack of selectivity, and are only effective in the early stage of the infection. Patients in the acute phase of the disease, which are those who could successfully respond to treatment with benznidazole or nifurtimox represent less than 1% of infected ones. Moreover, nifurtimox was discontinued in Brazil, because some *T. cruzi* strains have shown to be resistant to this drug. In summary, all these facts call attention to the urgent search for more selective and specific treatments against Chagas disease (SUETH-SANTIAGO et al., 2017; ANDRADE et al., 1999).

Benznidazole   **Nifurtimox**
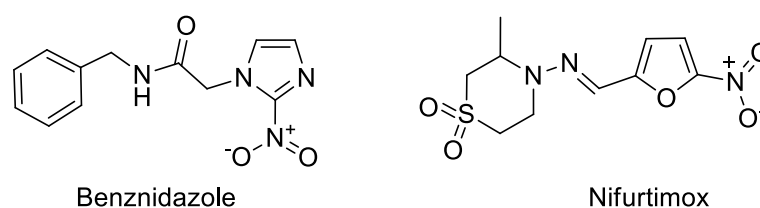
Figure 1: Currently approved drugs for the treatment of Chagas Disease

1.2.1. Drug discovery and the search for specific targets in T. cruzi

Studies towards drug discovery for Chagas Disease continues to be a challenge, even after more than 100 years of the discovery of *T. cruzi* (WHO, 2009). The search for novel molecules that are selectively injurious to the parasite is the primary quest in the exploration for new drugs. Antiparasitic chemotherapy is usually

based on two classes of targets: the ones that are specific to *T. cruzi*, and those which are common to parasite and host. In the last case, there must be some selectivity by the bioactive compound for the protozoan's receptors or enzymes, aiming a more significant effect on the parasite and fewer impacts on the host (SUETH-SANTIAGO et al., 2017). In a study performed by Sueth-Santiago and collaborators (2017), *T. cruzi's* specific targets such as *trans*-sialidases, trypanothione reductase, and cruzipain have been gaining significant interest in the search for molecules against the parasite in the last two decades. In this context, our research group has shown interesting results by putting efforts on synthesizing new structures and by exploring higher selectivity on analogues of existing drugs against *T. cruzi* (MARCHIORI et al., 2017; ANDRADE et al., 2015; MARTINS-TEIXEIRA et al., 2013). Examples of compounds synthesised by our group against *T. cruzi* are shown in Figure 2. Andrade and co-workers (2015) synthesised a series of 27 analogues of benznidazole which some presented very good *in vitro* activities against trypomastigote and amastigote forms of two different strains of *T. cruzi.* Among them, compound **1** (Figure 2) showed IC$_{50}$= 7,0 µM and low toxicity in spleen cells isolated from C57BL/6 mice, leading to high selectivity for the parasite's cell.
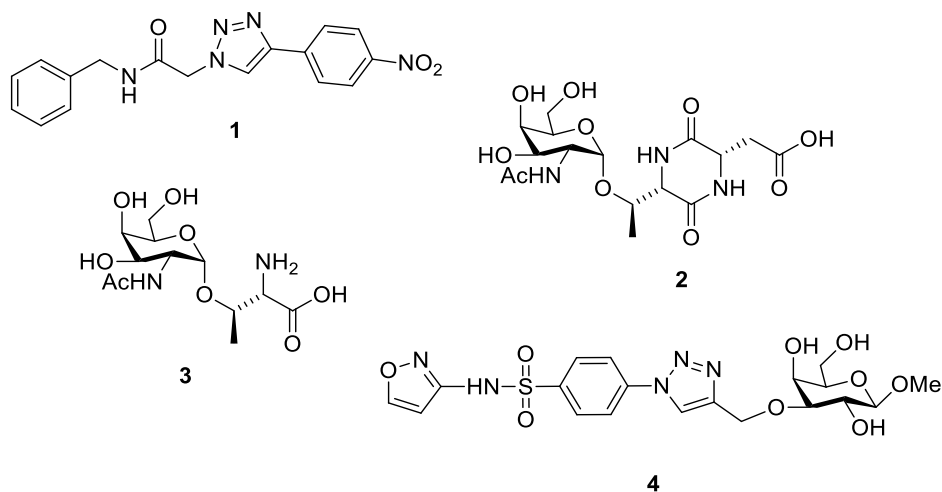
Figure 2*:* Compounds synthesised by our research group aiming for trypanocidal activity.

Diketopiperazine analogue **2** and precursor **3** (Figure 2) were proposed as a *trans*-sialidase inhibitor. Compound **3** showed the best activity towards the TcTS (79% of inhibition at 1.0 mM and IC$_{50}$ value of 0.32 mM), whereas compound **2** appeared to have higher anti-trypanosomal activity against *T. cruzi* Tulahuen strain, presenting an IC$_{50}$ value of 124 µM (benznidazole was used as control with value of 0.03 mM for IC$_{50}$). Moreover, compound **2** did not show cytotoxicity against mouse spleen cells.

Finally, compound **4** (Figure 2) was evaluated in its ability to avoid *T. cruzi's* tripomastigostes invasion in the host's cells. Compound **4** blocked the parasite invasion by a galectin-3 binding-related mechanism, revealing that galectin-3 may be an essential host target for the design of anti-trypanosomal agents.

1.3. Glycosylphosphatidylinositol Anchors

Glycosylphosphatidylinositol (GPI) anchors are glycophospholipid-based structures which are found in the membrane leaflet of many eukaryotic cells. These molecules can be found attached to complex phosphosaccharides, glycoproteins and as surface glycolipids in protozoans, being predominantly abundant in these organisms (McCONVILLE; FERGUSON, 1993; FERGUSON, HART, KINOSHITA, 2017). More specifically in *T. cruzi*, GPI anchors are responsible for anchoring essential mucins and enzymes, such as *trans*-sialidase on the parasite's cell surface. Several studies revealed that GPI anchors are important for invasion and survival of parasites in host cells. The high density of GPI structures at all life-cycle stages of protozoan parasites suggests that the GPI biosynthetic pathway might be an interesting object of study towards the development of anti-parasitic drugs/vaccines. (MENDONCA-PREVIATO, et al. 2008; McCONVILLE; FERGUSON, 1993).

GPIs comprise a glycan core with a phosphoethanolamine linker and a phospholipid chain (Figure 3, part A). Most GPI anchors so far elucidated have a conserved scaffold: **$H_2N(CH_2)_2OPO_3H6Man\alpha1\rightarrow2Man\alpha1\rightarrow6Man\alpha1\rightarrow4GlcN\alpha1\rightarrow6$*myo*-Ino1-OPO$_3$H-Lipid,** except for *Entamoeba histolytica* (FERGUSON, 1997; MCCONVILLE; FERGUSON, 1993).

Given that all eukaryotes produce GPI anchors, it is essential to understand the differences regarding structural features (Figure 3, Parts A and B). The different GPI structures according to each organism are highlighted in Table 1. For instance, in mammalians, a fourth mannose residue is linked to Man III as well as a second phosphorylation in Man II (Figure 3, Part A). Lipid is usually alkylacylglycerol, or diacylglycerol derivatives and C-2 of inositol moiety present a palmitate lipid moiety (Table 1, Line 6). (TSAI et al., 2012).
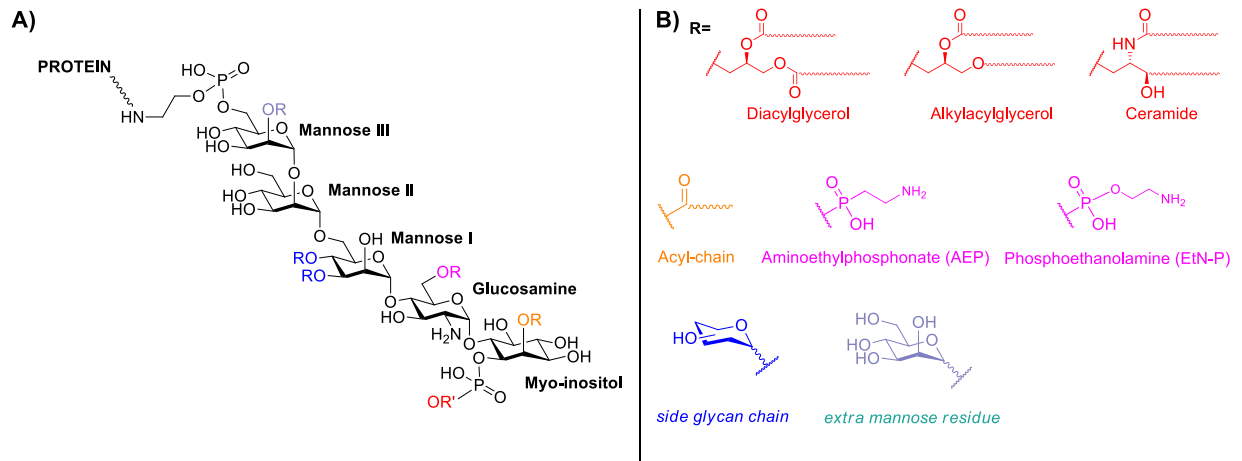
Figure 3: A: Common structure of GPI anchors. B: Main components linked to the glycan core in specific colours, which correlates to the positions of same colours in the glycan core in part A.

Regarding *T. brucei*, the variant surface glycoprotein (VSG) GPI anchor contains a saccharide chain branch at the C-3 of Man I. Dimyristoylglycerol, and *lysO*-1-*O*-stearoylglycerol are the main lipids composing *T. brucei*'s VSG and Procyclic Acidic Repetitive Protein (PARP) anchors. In addition, procyclic forms of the parasite present acylated inositol moiety in their GPIs and a residue of ethanolaminophosphate is only found in Man III (Table 1, Line 1). (MCCONVILLE; FERGUSON, 1993; FANKHAUSER et al., 1993; CONZELMANN et al., 1992).

T. cruzi GPI´s glycan core comprises four mannose residues besides a 2-aminoethylphosphonate (AEP) group linked at the C-6 position of the GlcN. (Table 1, Line 2). The lipid linked to the PI moiety varies along the parasite's developmental state: Epimastigotes GPIs contain mainly 1-*O*-($C_{16:0}$)-alkyl-2-*O*-($C_{16:0}$)-acylglycerol-3-PI; metacyclic trypomastigotes present GPI anchors predominantly composed by different types of phosphoceramide-inositol, containing dihydrosphingosine ($C_{18:0}$), lignoceric ($C_{24:0}$) or palmitic acid ($C_{16:0}$) (Figure 1) (CARDOSO et al., 2013; SERRANO et al., 1995; MCCONVILLE; FERGUSON, 1993).
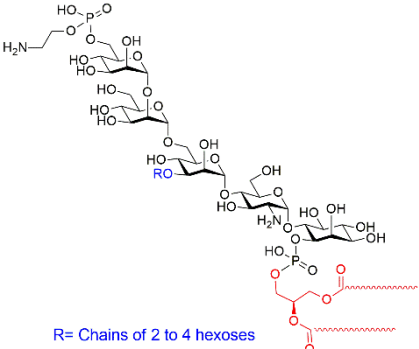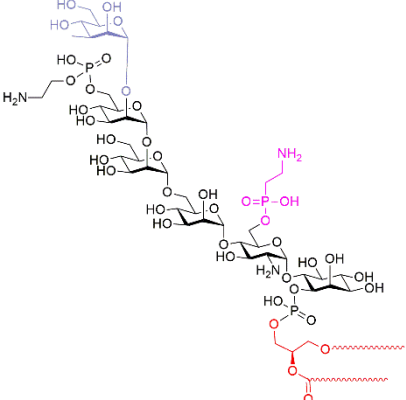
Leishmania spp. lipophosphoglycans (LPGs) are made of 1-*O*-alkyl-2-*lyso* phosphatidylinositol with one saturated C_{24} or C_{26} alkyl chain, which supports a negatively charged repeating polysaccharide, richly expressed by promastigote forms (up to 5×10^6 per cell). Glycoinositol phospholipids (GIPLs), related to 1-*O*-alkyl-2-*O*-acyl- or *lysO*-1-*O*-acylglycerol, and varied external glycans, are found in large quantities (approximately 10^7 molecules per cell) in all developmental stages (Table 1, Line 3, for *L. major*). (MCCONVILLE; FERGUSON, 1993).
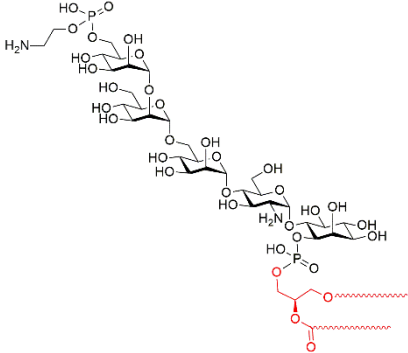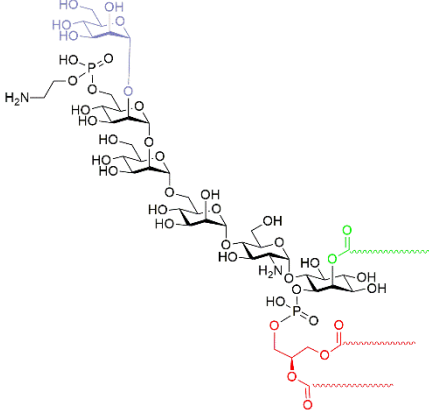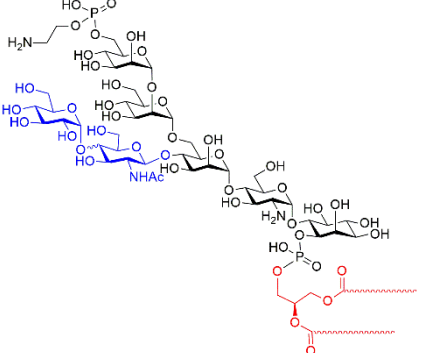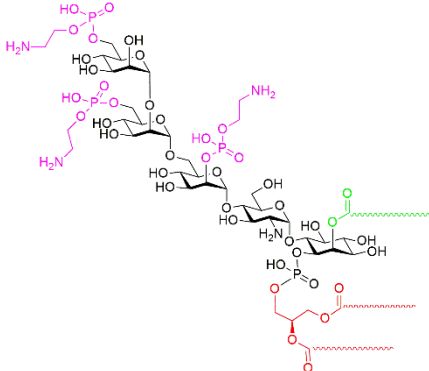
Plasmodium spp. parasites present four mannose moieties at their GPI glycan core. The PI part of intraerythrocytic *P. falciparum* GPIs is varied on fatty acyl substituents, with palmitate or myristic acid frequently linked to C-2 of inositol. *Plasmodium spp*. GPIs do not contain any additional phosphoethanolamine substitution in their glycan core structures (Table 1, Line 4, for *P. falciparum*) (SUKHAREVA-BUELL, 2003; NAIK; DAVIDSON; GOWDA, 2000).

Finally, *Toxoplasma gondii* GPI anchors are found as free structures or anchoring proteins, and these structures mainly differ among themselves in carbohydrate composition connected to the glycan core. Type A GPIs contain a residue of GalNAc-linkedβ1→4 to Man I, whereas type B presents Glcα1→4GalNAc linked to the same mannose residue in the main core. Fatty acids are typically $(C_{18:1})$-diacylglycerol, but the length varies depending on the life stage and virulence of *T. gondii* strain (Table 1, Line 5). (ECKERT; GEROLD; SCHWARZ, 2002; MCCONVILLE; FERGUSON, 1993).

Table 1. Structures of some protozoan parasites and mammalian GPIs. Table adapted from Morotti, Martins-Teixeira and Carvalho (2017).

Species	GPI structure
1. Trypanosoma brucei	
2. Trypanosoma cruzi	

Species	GPI structure
3. Leishmania major	
4.Plasmodium falciparum	
5. Toxoplasma gondii	
6. Mammalian	

1.3.1. Biosynthesis of GPI anchors

The first GPI structure elucidated was *T. brucei*'s Variant Surface Glycoprotein (VSG), and this parasite has been extensively used as an experimental model for

studies involving GPI anchor pathways. Since *T. brucei* GPI structures and pathways have been characterised, much of what is known about this class of molecules is related to this parasite, and the order of the events in a GPI biosynthesis is also based on these existing studies (MCCONVILLE; FERGUSON, 1993). What is identified about *T. cruzi* GPI anchors have been recently reported by Cardoso et al. (2013) although the order of each step may follow *T. brucei*'s GPI biosynthesis, as standard. On the other hand, structural variances between GPI anchors lead to the fact that biosynthesis of these molecules in different organisms is also diverse. Herein, what is acknowledged about the biosynthesis of *T. cruzi* is described with the assistance of Figure 4, and some examples of divergent biosynthesis from other eukaryotes will be discussed.
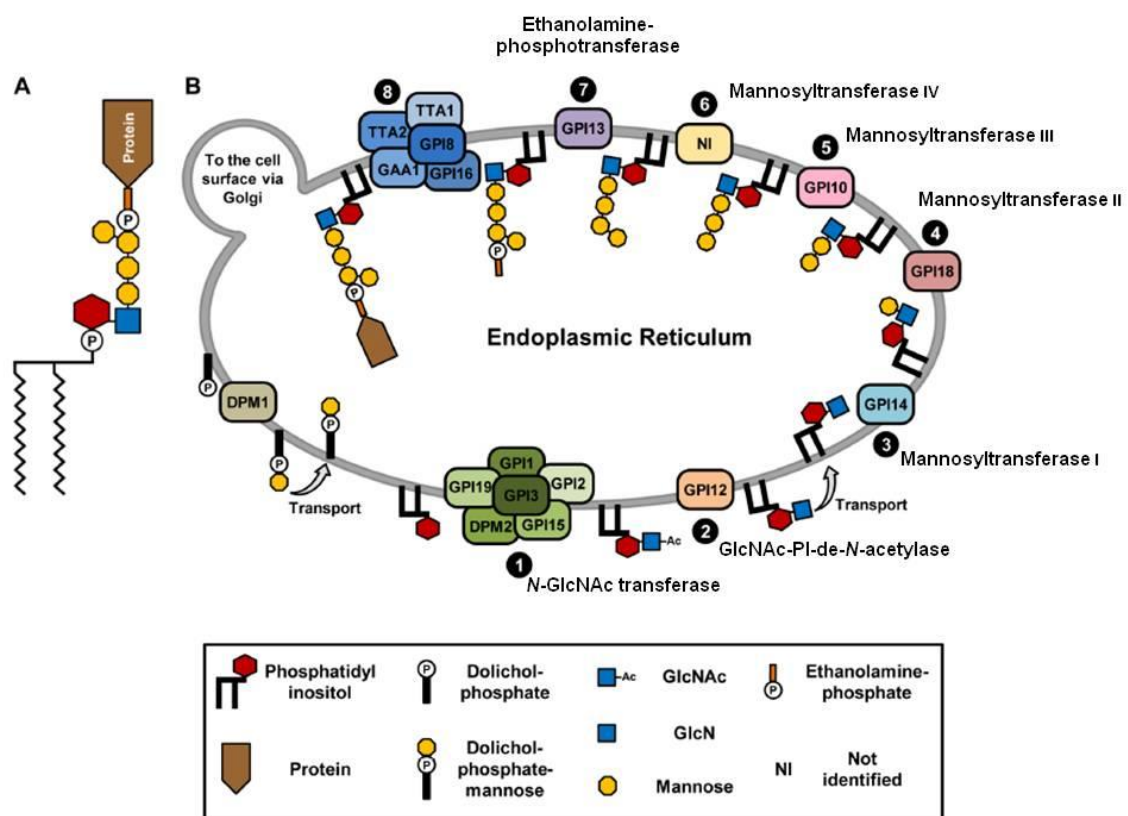
Figure 4: Biosynthesis of *T. cruzi* GPI anchors according to Cardoso and co-workers (2013). Coloured squares bring the names of genes Identified so far for the enzymes involved in the pathway. Abbreviations: **Glc*N*Ac**: *N*-acetylgucosamine; **Glc*N***: guclosamine; **Glc*N*Ac-PI-de-*N*- acetylase**: *N*-acetylglucosamine-phosphatidylinositol-de-*N*-acetylase.

The first step is the attachment of *N*-acetyl glucosamine by a *N*-GlcNAc transferase to the phosphatidylinositol (PI) moiety (Step 1, Figure 4). De-*N*-acetylase of glucosamine moiety allows the entrance of the molecule in the endoplasmic

reticulum (Step 2, Figure 4). Four different mannosyltransferases link, respectively, mannoses I, II, III, and IV to the GlcN-PI block; UDP-Mannose is the donor of all mannose residues in the GPI pathway (Steps 3 to 6, Figure 4). An ethanolamine phosphate moiety is linked to Man III of the central core by an ethanolamine-phosphotransferase for further linkage of a protein (Step 7 and 8, Figure 4). The ready GPI anchor leaves the endoplasmic reticulum in a vesicle towards the Golgi apparatus for later attachment to the cell membrane.

Some differences in the biosynthetic pathway of other organisms are emphasised: In *T. gondii*, conversion of Glc*N*Ac to Glc*N* also occurs outside the ER- when compared to *T. cruzi* biosynthesis, which contrast with common biosynthetic routes, that require GlcNAc to occur inside ER (SMITH et al., 2007). PI-acylation occurs in mammalian GPI biosynthesis and *T. gondii* at a particular step, which is after de-*N*-acetylation of PI-GlcNAc and before the addition of any mannose residue. In mammalian GPIs, the addition of the first mannose residue is followed by linkage of an extra ethanolamine phosphate in C-6 of this moiety (NIEHUS et al., 2014; PEKARI et al., 2001). Deacylation occurs after addition of all mannose residues, and failure in this process leads to inhibition of later steps (SMITH et al., 2007). In contrast, biosynthesis of *T. brucei*'s bloodstream form GPI counts on several acylations/deacylations along the pathway. Conversely, in *L. mexicana*, an additional ethanolaminephosphate is unusually linked to the core GlcN of some hybrid type GIPL anchor (MCCONVILLE; FERGUSON, 1993). *T. cruzi* and *P. falciparum* biosynthetic pathways appear to be similar to *T. brucei*'s, although there's no evidence of fatty acid remodelling before attachment of a protein to the ethanolaminephosphate residue (NAIK; KRISHNEGOWDA; GOWDA, 2003). Finally, *T. cruzi* GPIs undergo a change of PI lipids from alkylacylglycerol derivative to ceramide by an inositolphosphorylceramide (IPC) synthase during epimastigote to metacyclic trypomastigote stages. However, this stage is not considered part of the parasite's GPI biosynthesis (RALTON; MCCONVILLE, 1998).

1.3.2.GPI Anchors as a target against protozoan parasites

Biosynthetic and structural differences between organisms are some of the reasons why GPI anchor can be useful as drug targets against parasites. Moreover, normal levels of GPI synthesis are not essential, in some instances, for mammalian

cell survival (SMITH et al., 2001; FERGUSON, 1999). Although eukaryotes have similar GPI pathways, differences in the timing of specific biosynthetic steps and substrate specificities of the enzymes have been reported. In the last two decades, various research groups have been investigating the possibility of validating proteins involved in GPI biosynthesis as drug targets against parasites such as protozoans and fungus (MOROTTI; MARTINS-TEIXEIRA; CARVALHO, 2017, SMITH et al., 2004). In this context, it is important to cite some examples of studies towards inhibition of GPI pathway.

GPI intermediates from *T. brucei* and *Leishmania* spp. undergo myristic acid remodelling, at some point of the biosynthesis. Myristate analogues containing oxygen substituting one methylene group were used as inhibitors of myristic acid remodelling process. The *O*-11 (Compound **5**; Figure 5) analogue killed almost all the parasites in culture within few hours at a concentration of 10 μM. The compound was able to cause alterations in the parasites' morphology, with impaired motility, loss of integrity shape and vacuole inclusions. Moreover, the analogue **5** showed no toxicity for human T lymphoid cells (DOERING et al., 1991).

Some molecules showed GPI inhibition although it was not possible to identify the specific biosynthetic step or particular target molecule involved. Synthetic cell-permeable analogues of a GPI intermediate, (Compounds **6** and **7;** Figure 5) were recognised, incorporated and metabolised by the *T. brucei* GPI pathway, but not by the HeLa cells representing the human pathway. This finding served as a chemical validation of the GPI biosynthetic pathway as a drug target against African sleeping sickness (SMITH et al., 2004).

The specificity of mannosyltransferases was studied in *T. brucei* with a series of synthetic analogues. In summary, a simple C_{18} alkyl chain could substitute the natural diacylglycerol lipid moiety, and the substrate recognition by MTIII required hydroxyl groups at positions C-2 and C-3 of the terminal mannose. On the other hand, the amine in glucosamine residue was not essential for the recognition. This examination led to the identification of **8** (Figure 5) as an inhibitor of Mannosyltransferase III with an IC_{50} of 1.7 μM, leading to the accumulation of $Man_2GlcN-PI$, (URBANIAK, et al., 2008). Most straightforward structures such as **9** (Figure 5) also inhibited the GPI pathway, possibly by competing with endogenous GPI intermediates for mannosyltransferase(s) (BROWN et al., 1997).
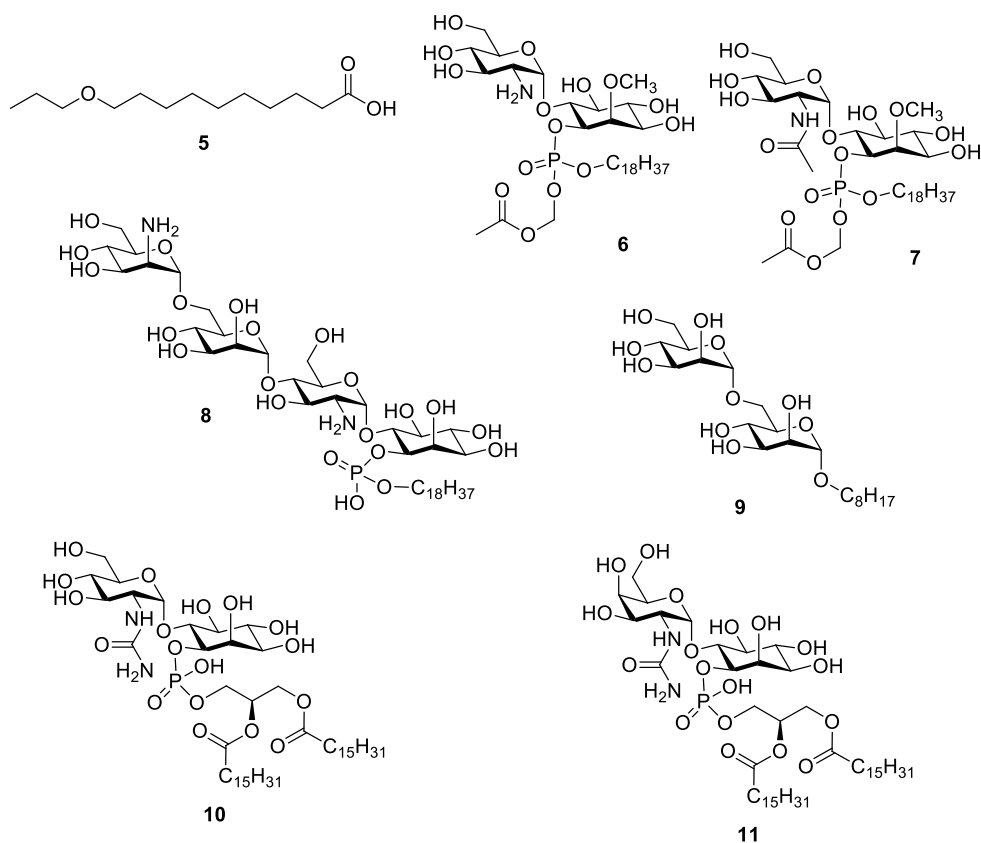
Figure 5: Compounds designed for Inhibition of GPI anchors of various organisms.

Smith and co-workers (2002) evaluated the substrate specificities of enzymes from *Plasmodium* GPI biosynthesis using analogues of D-GlcNR1→6-D-*myo*-inositol-1-HPO$_4$-*sn*-1,2-dipalmitoylglycerol. Similarities were found comparing *Plasmodium* and mammalian (HeLa cells) enzymes, such as: (i) the 2-acetamido/amino and 3-OH groups in GlcN moiety are essential for the de-*N*-acetylase, inositol acyltransferase, and further mannosyltransferase I recognition; (ii) the 6-OH group in GlcN is not critical for substrate recognition by de-*N*-acetylase, inositol acyltransferase, the four mannosyltransferases, and the ethanolamine phosphate transferase; (iii) the 4-OH group of GlcN is required for recognition of the inositol acyltransferase and mannosyltransferase I. Conversely, differences between both pathways were also revealed: (i) Inhibition of *Plasmodium* inositol acyltransferase was observed with GlcN-[L]-PI, while GlcN-(2-*O*-alkyl) PI weakly and competitively inhibited the mannosyltransferase I; (ii) the *Plasmodium* de-*N*-acetylase is able to recognise analogues containing *N*-benzoyl, *α*-D-GlcNAc or *α*-D-GalNAc, whereas the human enzyme cannot. Two analogues, (Compounds **10** and **11**; Figure 5) were designed and found to be potent *Plasmodium*-specific de-*N*-acetylase suicide inhibitors (IC$_{50}$

~0.2 µM), being potential lead compounds for the development of antimalarial drugs (SMITH et al., 2002; SMITH et al., 2001).

1.3.3. Synthetic approaches for GPI anchors

According to examples cited above, several compounds, most of them being carbohydrate/lipid based, have shown to be successful in inhibiting enzymes involved in GPI anchor biosynthesis of various parasites when assayed *in vitro*. However, using these molecules *in vivo* is still a challenge regarding pharmacokinetic and pharmacodynamic aspects, considering that many parasites are intracellular (MITRAGOTRI; BURKE; LANGER, 2014). On the other hand, various strategies can be used to enable the entrance of carbohydrate-like molecules inside cells. Most procedures consist in proper functionalization of the carbohydrate moiety or formulation of carriers to circumvent problems such as lack of pharmacokinetic properties, poor bioavailability, fast serum clearance, and rapid degradation (MITRAGOTRI; BURKE; LANGER, 2014; AICH et al., 2010). Moreover, convincing evidences have shown that this class of molecules is a versatile platform for drug discovery (IVANOVA et al., 2017; HATAKEYAMA et al., 2011; AICH et al., 2010; MONTOYA-PELEAZ et al., 2005; BROWN et al., 2001).

Natural GPIs are structurally diverse. Furthermore, GPI-anchored proteins are amphiphilic and associated with the cell membrane, making their isolation from nature difficult (LU; GAO; GUO, 2015). Studies of isolated GPIs from *P. falciparum* showed that parasitic GPIs can trigger an immune response of mammalian hosts. However, other groups could not find the same reported results. The discrepancies between these results might be due to the impurities associated with the isolation process of the parasitic GPI. To circumvent this problem, a series of synthetic fragments structurally related to P. falciparum GPI were synthesized and evaluated. This strategy allowed to observe that there were higher levels of IgG in sera which were exposed to the synthesized structures, compared to those not exposed to these synthesized molecules (BOUTLIS et al., 2002, BOUTLIS et al., 2003; HUDSON et al., 2003; SUGUITAN (2006). The progress in the chemical synthesis enabled the preparation of several GPIs and analogues of *P. falciparum* and *T. brucei* that allowed the study of these molecules against the immune response of the host. These findings, together with the fact that all protozoan parasites express large

amounts of GPIs, in comparison with mammals, suggest that these molecules offer a good alternative for the development of vaccines (TSAI et al., 2012).

Numerous GPI anchor structures of various organisms have been synthesised. Synthesis of the *O*-glycan core usually starts with a suitably protected D-glucosamine to an optically pure, also protected *myo*-inositol derivative. From this block, there are basically two ways to synthesize the oligosaccharide chain present in GPIs: the linear and the convergent forms. The linear form is derived from monosaccharide donors which are individually added one by one to form an oligosaccharide (NIKOLAEV; MAHARIK, 2011). The first GPI anchor structure was synthesized by Murakata et al. (1991-1992), who proposed a linear synthesis. Glycosyl donors containing fluorine and chlorine were used in this attempt (Compounds **16-19**, Scheme 1), as well as a protected *myo*-inositol moiety as acceptor (Compound **20**, Scheme 1). The benzyl groups were used as permanent protective groups along the entire synthesis. The H-phosphonate chemistry allowed the insertion of two different phosphodiester units (Compounds **14-15**, Scheme 1). Overall deprotection was carried out by hydrogenolysis, in the presence of Pd(OH)$_2$/C (Compound **12**, Scheme 1). This first synthetic strategy gave the VSG GPI of *T. brucei* (11) with 23% yield (Scheme 1) (MURAKATA; OGAWA, 1991; MURAKATA; OGAWA, 1992).

The convergent approach occurs with ready and more complex blocks, which are prepared in parallel for later union to form one single molecule resulting in less management of the protecting groups of the oligosaccharide chain. The portions related to ethanolamine phosphate and phospholipids are added before the overall deprotection of the GPI structure.

Several authors have reported GPI anchor synthesis using different strategies in a convergent way (CAMPBELL; FRASER-REID, 1994; CAMPBELL; FRASER-REID, 1995; BAESCHLIN et al., 1998; MAYER, SCHMIDT, 1999; KWON et al., 2005; LIU; STOCKER; SEEBERGER, 2006). As an example of convergent synthesis, Ley and collaborators (1998) performed the VSG GPI of *T. brucei*, which was adaptable for the synthesis of other GPIs (Scheme 2). Briefly, the strategy was based on three building blocks prepared in parallel, using butane-2,3-diacetal and chloroacetate as protecting groups (Compounds **23** and **24**, Scheme 2). (BAESCHLIN et al., 1998).
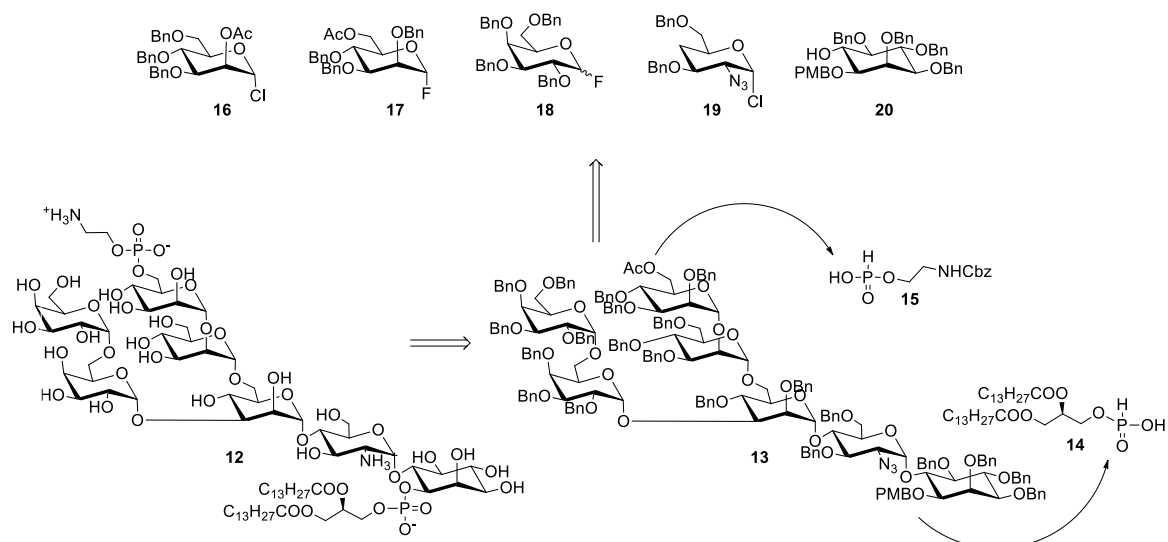
Scheme 1: Retrosynthesis of *T. brucei* GPI anchor performed by Ogawa and co-workers (1991/1992). Adapted from Nikolaev and Maharik, 2011*.*
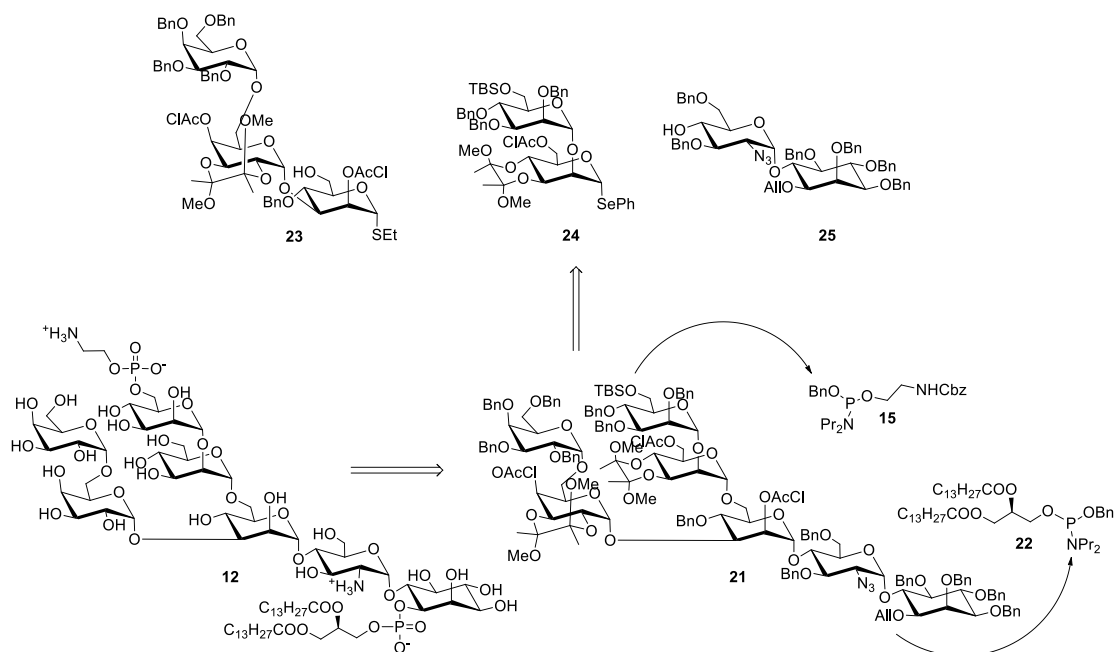
Scheme 2: Retrosynthesis of *T. brucei* GPI anchor performed by Ley and co-workers (1998). Adapted from Nikolaev and Maharik, 2011.

Another example of convergent GPI synthesis was performed by Konradsson and Hederos groups (2005) for the preparation of *P. falciparum* phosphorylated *myo*-nositol heptassacaride (Scheme 3). The proposed synthetic route came from three building blocks (Compounds **27**, **28** and **29**). Donors derived

from galactofuranose, containing *O*-acetyl group, were coupled to mannose residues to obtain block **27** (Scheme 3), by *O*-glycosylation promoted by AgOTf. Stereochemistry (β) was assisted by the *O*-acetyl groups. Block **28** was obtained by *O*-glycosylation of two mannose residues, followed by 2'-*O*-debenzylation. Block **29** was obtained in six steps.
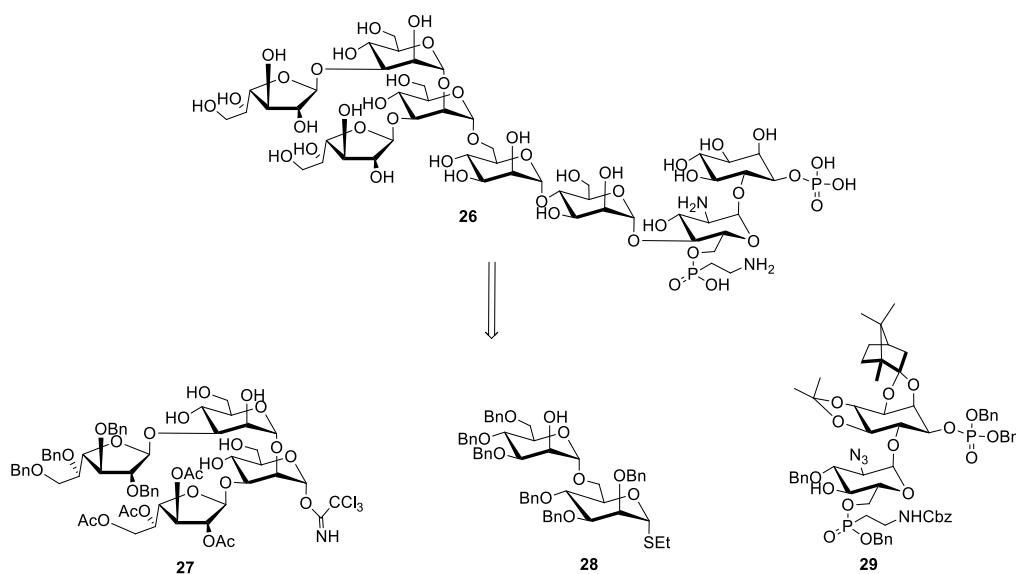
Scheme 3: Retrosynthesis of the heptasaccharide derivative of *P. falciparum* GPI anchor performed by Konradson and co-workers (2005). Adapted from Nikolaev and Maharik, 2011.

After the addition of all the blocks, the overall deprotection of the heptassacaride was first performed with deacetylation, under Zemplen conditions followed by *O*-debenzylation using sodium in ammonium solution. Finally, the acetal groups were removed by acid hydrolysis, generating the final product **26** (Scheme 3).

1.3.4. Labelled GPI Anchors as a strategy to study GPI pathways

Labelled GPI anchors have been used as part of efforts to elucidate molecular details of GPI biosynthesis and structural features. Many studies on the structure and components of the GPI anchor have relied on the incorporation of labelled lipids and sugars into GPIs anchor (FERGUSON; HALDAR; CROSS, 1985). Structural characterization of intermediates led to the initial elucidation of GPI anchors biosynthetic pathways (SHARMA et al., 1999; VARMA; HENDRICKSON, 2010). Currently, different chemical approaches have been applied to understand GPI-anchoring and its significance.

Lili Lu and co-workers (2015) developed a strategy for metabolic engineering of cell surface GPIs and GPI-anchored proteins using inositol derivatives carrying an azido group. The inositol containing azido group was exposed to cancer cell lines, MCF-7, Hela, K562, and SKM28, and could be incorporated to the GPI pathway. The cells were then tagged with biotin via click chemistry forming a fluorescent coat of GPIs with the modified inositol. This approach was suggested to be used to label GPI-anchored proteins with various tags for biological studies (LU; GAO; GUO, 2015). Another application of labelled GPI anchor was developed by the same research group which synthesised the first biotin-labeled GPI core glycans. These GPI conjugates were useful tool by their use to the scrutiny of pore-forming bacterial toxin-GPI interaction, revealing that the phosphate group at the C-1 position of GPI inositol had a significant impact on GPI-toxin binding (GAO et al., 2017).

GPI glycan moieties labelled with 2-aminobenzamide were also useful to compare the structure of phylamentous fungi *Aspergillus fumigatus* and yeasts *Saccharomyces cerevisiae* GPI anchors. The study showed that the nature of the inositol-linked phospholipids of *A. fumigatus* is phosphoceramide containing mainly phytosphingosine and monohydroxylated $C_{24:0}$ fatty acid. In contrast, *S. cerevisiae* presented diacylglycerol phospholipid moieties instead of a ceramide derivative (FONTAINE et al. 2003).

Imhof and co-workers (2004) have reported that the ethanolamine phosphate side chain added to the first mannose residue is a prerequisite for the addition of the third mannose to its GPI precursor in *Saccharomyces cerevisiae (yeast)*. These findings were performed after incorporation of labelled *myo*-[2-^{3}H] inositol precursor to the growing cells of the yeast.

1.4. *Euglenis gracilis*

Euglena gracilis is a free-living microalga, unicellular and flagellated, which inhabits fresh water. However, due to its high adaptability, it can survive to conditions such as very low pH (around 0.9), high salinity and high energetic ionising radiation (BUETOW, 1962; 2011). *Euglena* presents both plant and animal characteristics: it can live in the light, producing food by photosynthesis, or it can exist in the dark and using environmental sources, storing them as a *paramylon* (starch-like β-1,3-glycan).

Euglena is composed of all organelles of the eukaryotic cell and it does not have a cell wall like plant. Instead, it is composed of repetitive membrane domains

know as ridges and groves (Figure 6) (AHMADINEJAD; DAGAN; MARTIN, 2007; SOMMER, 1965). *Euglena* belongs to the phylum *Euglenozoa*, (NAKANO et al., 1987); which also includes Trypanosomatid parasites, such as *T. cruzi, T. brucei* and *Plasmodium.*
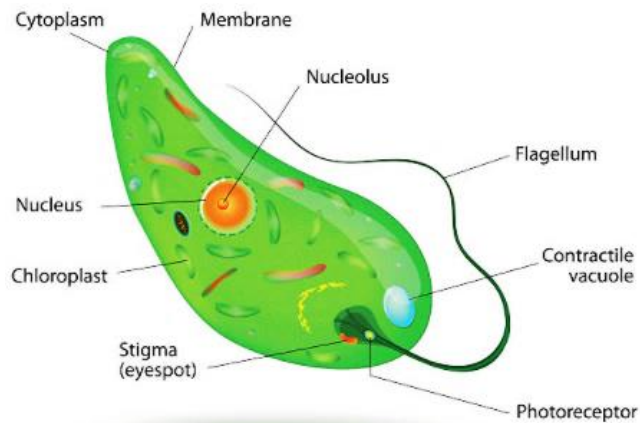
Figure 6: *Euglena gracilis* and cellular components

1.4.1. E. gracilis as a safe protozoan model

There is very limited data regarding research to elucidate the structural composition of glycoproteins in *E. gracilis* (IVANOVA, 2015). In a study conduced by Delacanal and Parodi (1985), *E. gracilis* entire cells were incubated with UDP-[^{14}C]Glc and radiolabelled lipid-linked *N*-glycans. Thus, *N*-linked glycoproteins were extracted at different time of incubation. The lipid-linked *N*-glycans were hydrolysed in mild acidic conditions to release monosaccharides, whereas *N*-linked glycoproteins were treated with endo-β-*N*-acetylglucosaminidase to cleave the bond between two *N*-acetylglucosamine moities to release *N*-linked oligosaccharides. The free monosaccharides and *N*-linked oligosaccharides were then compared to standards using paper chromatography. The results disclosed that dolichol-P-P-bound oligosaccharide migrated together with $Glc_3Man_9GlcNAc_2$ standard and appeared to contain glucose, mannose and *N*-acetylglucosamine residues. Based on these results, the authors suggested that the mechanism of protein *N*-glycosylation in *E. gracilis* is similar to higher eukaryotic cells phenomena.

A study performed by Ivanova and co-workers (2017) showed that fluorescent labelling could be successfully applied in glycosyl derivatives to track membrane-bound glycosyltransferases involved in the biosynthesis of various glycoconjugates in

Euglena gracilis. This methodology can be powerfully useful to probe the biosynthesis of other glycoconjugates, such as GPIs in *E. gracilis* and related organisms as *T cruzi.*

The investigation towards GPI anchor enzymes on microsomal membranes can also be extended to *T. cruzi.* Previato and co-workers (1998) conducted a characterization of the activity of a GlcNAc-transferase from Trypanosoma cruzi's microsomes. The authors were able to analyse the optimal environment for the enzyme's activity by incorporating N-[^{3}H] acetylglucosamine to a synthetic peptide acceptor (KPPTTTTTTTKPP) and proved that the best conditions are related to pH 7.5-8.5 and the requirement of Mn^{2+}. The enzyme also proved to be unaffected by the natural products tunicamycin and amphomycin and is powerfully inhibited by UDP (PREVIATO et al., 1998).

The importance of GPI anchors on the cell surface of parasites and position of *Euglena* in the same phylum (*Euglenozoa*) of several protozoan parasites, as well as the lack of knowledge in this area of research, both in *E. gracilis* or in trypanosomatids, prompted the professor Rob Field's research group to investigate biosynthesis of these glycoconjugates in *E. gracilis*, with the possibility that *Euglena* could be used as an alternative model system for parasites. Given these findings, this work proposes that carbohydrate moieties to mimic GPI anchor precursors and serve as probe for GPI pathways in *E. gracilis* as an alternative and safe method to support drug discovery for Chagas disease.

The approach of using *E. gracilis* to uncover glycan pathways is recentlyand exclusively being standardized by the Rob Field's laboratory at John Innes Centre, in which *this* fresh-water algae have been used as source of several enzymatic and biochemical studies. Some advantages of this approach can be pointed out, such as the fact that no biosafety structure or training are necessary to manipulate *E. gracilis,* since it not a pathogen, making this algae a safe organism to standardize methodologies that can be applied to other organisms. *It also gives the opportunity* to obtain new compounds by enzymatic approach and to uncover the own *E. gracilis*' GPI pathways, as well as *T. cruzi*'s pathway. On the other hand, disadvantages can be related to the lack of validate methodologies in *E. gracilis* since GPI anchor precursors that may serve as controls are unknown, leading to the uncertainty that perhaps the GPI *E. gracilis* biosynthesis can be very different from *T. cruzi*'s.

The complexity and broad spectrum of mechanisms in which anchor GPIs may be involved in the parasite survival and infectivity arouse interest from a chemical and biological point of view. The synthesis of parts of GPI anchor becomes an interesting tool for the deepening of studies concerning the biological functions and interactions performed by this class of molecules for the search of new molecular targets, allowing the planning and development of new effective drugs. In addition, it may assist in the identification and development of potential structures to be used as antigen or adjuvant vaccines, capable of mimicking GPI anchor carbohydrates (BOONYARATTANAKALIN et al., 2008; SWARTS; GUO, 2010; TSAI et al., 2012).

2. OBJECTIVES

_____

2.1. General objective

This work aimed to synthesize part of GPI anchor derivatives (Figure 7), containing simplified lipid moiety or UV visible lipid derivative to be tested in *Euglena gracilis* microsomal membranes (a simple protozoan model) as a strategy to improve and complement studies about GPI anchor biosynthetic pathway. This approach may assist the discovery of either GPI anchor inhibitors or GPI anchor substrates. The strategy might be extended to *T. cruzi* GPI biosynthesis, giving clues for the development of possible inhibitors for GPI biosynthesis in the parasite.

30

30a R$_1$= (CH$_2$)$_7$CH$_3$

30b R$_2$=
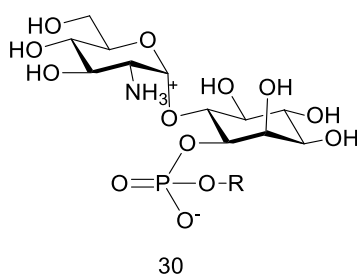
30c R$_3$=
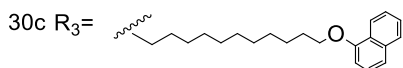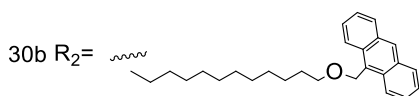
Figure 7: Proposed molecules to be used as substrates of GPI anchor pathway.

2.2. Specific Objectives

- To perform a study of glycosamine derivatives as glycosyl donors. This study will be conducted by modifying the protecting groups at position 3, 4 and 6 of an 2-azido-2-deoxy-D-glucopyranoside as an attempt to obtain better α configuration selectivity during the *O*-glycosyl linkage in order to mimic the GPI anchor.

- To perform a study of synthesis of *myo*-inositol derivatives to work as acceptor in *O*-glycosylation reactions. The acceptor may contain a proper enatiomeric resolution and undergo orthogonal protections and deprotections in order to achieve the desired block for a GPI anchor mimic.

- To study *O*-glycosylation reaction between the synthesized blocks of glucosamine derivatives (donors) and protected myo-inositol (acceptor) to standadyze the better conditions to obtain pseudo-disaccharides **30a-c** in the desired α configuration in good yields and selectivity.

- To synthesize phospholipid derivatives with simplified 8-carbon chain or containing UV visible moieties which may serve as "trackers" for the biological assays.

- To isolate microsomal membranes of *Euglena gracilis* and implement conditions to investigate the GPI pathway with *Euglena* cell microsomes by using compounds **30a-c,** in presence of GDP-mannose, as substrate or inhibitor of GPI biosynthesis.

3. MATERIAL AND METHODS

3.1. Material

3.1.1. Laboratorial Equipment

• Discovery microwave reactor - CEM® Discovery, with cooling and pressure system.

• Rotary evaporators BÜCHI Model R-215 and R-210 with cold-tip condenser.

• Analytical balances Mettler PE 400/Sartorius BP 121S

• Magnetic stirrers IKA-RCT BASIC and Corning PC-320.

• Ultraviolet light: Spectroline CM-10

• Mufla Thermolyne 47900

• Precision Model D 150 High Vacuum Pump

• Biotage Horizon and Isolera TM Chromatograph

• High Performance Liquid Chromatography Shimadzu SCL-10AVP with Class-VP 5.0 software, or Thermo Fisher Dionex system equipped with Corona charged aerosol detector (CAD) and UV detector.

• Polarimeter Perkin-Elmer 341

•Infrared spectrometer Perkin-Elmer Spectrum BX equipped with MIRacle single reflection horizontal accessory.

3.1.2. Other material

Chemicals were acquired as reagent grade and used with no extra purification. When necessary, solvents and some reagents were treated and purified according to methods described in the literature (PERRIN; AMAREGO; PERRIN, 1996). All moisture-sensitive reactions were performed under Argon or Nitrogen or argon atmosphere and oven-dried glassware was used for this type of reaction. Anhydrous solvents were purchased from Merck® or Acrós®. Buffers were freshly prepared prior to use.

Reactions were monitored by thin-layer chromatography (TLC) on silica gel coated aluminium plates (Silica Gel 60 F254, Merck®) with indicated eluents and *Advion* Plate Express®. Compounds were visualised under UV light (λ 254 nm), by dipping in ethanol-sulphuric acid (95:5, v/v), in orcinol solution (20 mg/mL orcinol monohydrate in $EtOH/H_2SO/H_2O$ 4:75:10:5, v/v) followed by heating. Other

chromogenic agents for detection were also used when necessary: Phosphoric Vanillin (2.5 g of vanillin in 50 ml of ethanol and 12.5 ml of 85% orthophosphoric acid); Sulfuric Anisaldehyde (0.5mL anisaldehyde and 5mL sulfuric acid in 10mL glacial acetic acid and 85mL methanol). Fluorescent products were purified on semi-preparative TLC on pre-coated silica gel glass plates (Silica Gel 1000 UV$_{254}$, Analtech).

Flash chromatography was performed on a Biotage Isolera MPLC system using pre-packed silica gel cartridges. Manual column chromatography was performed in glass columns using silica gel with particle sizes: 40-63 μm and 63-200 μm (Merck®). HPLC was carried out using a Dionex HPLC system with reverse phase (C18 stationary phase) column, equipped with Corona charged aerosol detector (CAD) or UV detector (at 274 nm).

Nuclear magnetic resonance spectra were obtained in Bruker Avance III 400 NMR (John Innes Centre), Bruker Avance DPX-300 MHz, DRX-400 MHz e DRX-500 MHz (Faculty of Phylosophy Sciences and Letters of Ribeirão Preto), and Bruker UltraShield 300 FT-NMR (School of Pharmaceutical Sciences of Ribeirão Preto).

High Resolution Mass sprectra were obtained in positive or negative inonization mode in Bruker Daltonics micrOTOF-Q II - ESI-TOF (School of Pharmaceutical Sciences of Ribeirão Preto) or Waters Synapt G2 mass spectrometer (John Innes Centre).

3.2. Methods

3.2.1. Methods for glycosyl of donors

2-azido-2-deoxy-D-glucopyranose (37) (NYFFELER et al., 2002; ANSELME; FISCHER, 1969).
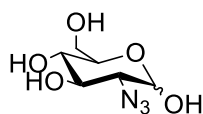
Triflic azide solution was prepared by addition of 6.0 g sodium azide (NaN$_3$) in 15.0 mL of water, followed by 25.0 mL of DCM. Triflic anhydride (3.1 mL) was then added

dropwise for 10 minutes. The solution was left to stir for 2 hours, then aqueous and organic solution were separated. Aqueous phase was extracted with DCM (2x 10.0 mL) and all organic solutions were combined and neutralised with $NaHCO_3$.

In parallel, 2-amino-2-deoxy-D-glucose hydrochloride **35** (2.0 g; 9.3 mmol) was added in flask containing 30.0 mL of water. Potassium carbonate (K_2CO_3) (2.3 g; 1.66 mmol) and copper sulphate ($CuSO_4$) (14.0 mg; 0.09 mmol) were added followed by 60.0 mL of MeOH and the entire solution of triflic azide. The mixture was left to stir overnight and then solvents were evaporated. The compound **37** was purified by silica flash chromatography (EtOAc/MeOH 4:1) and obtained as a white solid with 96% yield (1.8 g; 8.9 mmol). MW: 205.17 g/mol; IV= 2150 cm^{-1}. MP: >152 ºC (with decomposition). R_f= 0.25 (EtOAc/MeOH 4:1); δH (ppm) (MeOD; 300 MHz) 5.24 (1H, d, J= 3.6 Hz, H-1α); 4.60 (1H, d, J= 8.2 Hz, H-1β); 3.80-3.60 (4H, m); 3.40-3.33 (4H, m); 3.16 (1H, dd, J= 9.5 Hz, 8.2 Hz, H-2). Ratio α/β: 1: 2.

2-azido-1,3,4,6-tetra-O-acetyl-D-glucopyranose (41)
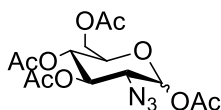
To a solution of **37** (1.0 g; 4.8 mmol) in pyridine (5.0 mL), acetic anhydride (3.0 mL) was added. The reaction mixture was left to stir overnight. After this period, the mixture was diluted with DCM, washed with solution 1N HCl (2x 10 mL) and saturated solution of $NaHCO_3$. The organic layer was dried with $MgSO_4$ and solvent was evaporated. Compound **41** was isolated by silica flash chromatography (Hexane/EtOAc 7:3 to 1:1) and obtained in quantitative yield (1.78 g; 4.7 mmol) as a clean yellow syrup. MW: 373.11 g/mol; R_f= 0.3 (Hexane/ EtOAc 7:3); δH (ppm) (CDCl$_3$; 400 MHz) 6.24 (1H, d, J= 3.6 Hz, H-1α); 5.49 (1H, d, J= 8.8 Hz, H-1β); 5.03 (1H, t, J= 9.3 Hz, H-3); 4.98 (1H, t, J= 9.2 Hz, H-4); 4.22 (1H, dd, J= 12.5 Hz, 4.7 Hz, H-6a); 4.01 (1H, dd, J= 12.5 Hz, 2.1 Hz, H-6b); 3.85 (1H, m, H-5); 3.59 (1H, dd, J= 9.7 Hz, 8.8 Hz, H-2); 2.13 - 1.95 (12H, 4s, 4-COCH$_3$) Ratio α/β: 3: 7.

2-azido-3,4,6-tri-O-acetyl-D-glucopyranose (42) (FIANDOR et al., 1985)
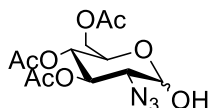
Compound **41** (1.0 g; 2.6 mmol) together with THF/NH$_3$.MeOH 7 N (7:3), under N$_2$ stirred under room temperature for 2 hours. The reagents were neutralized by bubbling N$_2$ into the reaction mixture. Solvents were evaporated, and the product **42** was obtained after purification by silica flash chromatography (Hexane/EtOAc 7:3 to 1:1) as a yellow syrup with 78% yield (0.67 g; 2.0 mmol). MW: 331.10 g/mol; R$_f$= 0.42 (Hexane/EtOAc 1:1); δH (ppm)(CDCl$_3$; 400 MHz) 5.46 (1H, dd, J= 10.6 Hz; 9.3 HZ, H-3); 5.33 (1H, d, J= 3.3 Hz, H-1α); 4.97 (1H, t overlapped, J= 9.5 Hz H-4); 4.67 (1H, d, J= 8.0 Hz, H-1β); 4.16 (1H, dd overlapped, J= 12.5 Hz; 3.1 Hz; H-6a); 4.08 (1H, dd overlapped, J= 12.1 Hz; 2.3 Hz, H-6b); 3.66 (1H, m, H-5); 3.36 (1H, dd, J= 10.5 Hz; 3.4 Hz, H-2); 2.04- 1.95 (9 H, 3s, 3 COCH$_3$) Ratio α/β: 1.25:1.

2-azido-3,4,6-tri-O-acetyl-2-deoxy-1-trifluoroacetimidoyl-D-glucopyranose (33a)
(YANG et al., 2012; YU & TAO; 2002).
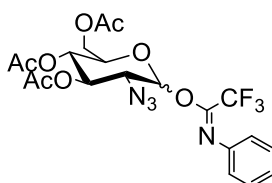
To a solution of compound **42** (0.3 g; 0.9 mmol) in DCM, K$_2$CO$_3$ (0.25 g; 1.8 mmol) was added and the solution stirred under N$_2$ for 15 minutes. *N*-phenyl-2,2,2 trufluoroacetimidoyl chloride (0.3 mL; 1.8 mmol) was added to the mixture and reaction stirred for 2 hours under N$_2$ and room temperature. The mixture was then filtered, and solvent was evaporated. The product **33a** was obtained as a white solid with 89% yield (0.4 g; 0.80 mmol), after purification in silica flash chromatography (Hexane/EtOAc 9:1 to 7:3). MP: >152 ºC MW: 502.4 g/mol; R$_f$= 0.63 (Hexane/EtOAc 7:3); δH (ppm)(CDCl$_3$; 400 MHz 7.2 (2H, m, Ar); 7.14 (1H, m, Ar); 6.85 (2H, d, J= 7.6 Hz, Ar); 5.62 (1H, br, H-1); 5.05 (2H, m, H-3, H-4); 4.26 (1H, dd J= 12.4 Hz; 4.6 Hz, H-6a); 4.10 (1H, dd, J= 12.4 Hz; 1.7 Hz, H-6b); 3.80 (2H, m, H-5, H-2); 2.14-1.98 (9 H, 3s, 3-OCOCH$_3$).

2-azido-4,6-O-benzylidene-2-deoxi-D-glucopyranose (38) (DASGUPTA et al., 2011)
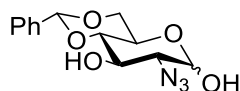
To a solution of compound **37** (1.0 g; 3.4 mmol) in dry MeCN (10.0 mL), benzaldehyde dimethyl acetal (2.5 mL; 17.0 mmol) and p-toluenesulphonic acid monohydrate (32.4 mg; 0.17 mmol) were added. The reaction stirred overnight at room temperature, and Et$_3$N (0.1 mL) was added to the mixture. After stirring for more 10 minutes, the solvents were evaporated and compound **38** was obtained as a white solid after purification by silica flash chromatography (Hexane/EtOAc 7:3) with 68% yield (0.68g; 2.3 mmol). MW: 293.28 g/mol; R$_f$= 0.55 (Hexane/EtOAc 1:1); δH (ppm) (CDCl$_3$; 300 MHz): 7.51-7.48 (2H, m, Ar); 7.42-7.39 (3H, m, Ar); 5.56 (0.5H, s, H-7); 5.55 (0.5, s, H-7); 5.31 (0.5 H, d, J= 3.5 Hz;, H-1α); 4.68 (0.5H, d, J=7.9 Hz, H-1β); 4.34 (0.5H, dd, J= 4.8 Hz; 10.4 Hz, H-6aβ); 4.29-4.22 (1H, m, H-6aα; H-5α); 4.10 (0,5H, m, H-5β); 3.82-3.67 (2H, m, H-6bα; H-6bβ; H-4α; H-4β); 3.60-3.51 (1H, m); 3.47-3.39 (1,5H, m) 3.35 (0.5H each, 2s broad,2-OH); Ratio α/β= 1:1

2-azido-1,3-di-O-acetil-4,6-O-benzylidene-2-deoxi-D-glucopyranose (39)

The same procedure to obtain compound **41** was used to prepare compound **39**. The product **39** was obtained as a brown solid with 71% yield. MW: 377.35 g/mol; R$_f$= 0.28 (Hexane/EtOAc 7:3); δH (ppm) (CDCl$_3$; 400 MHz): 7.46-7.34 (12H, m, Ar); 6.28 (1H, d, J= 3.7 Hz, H-1α); 5.65 (1H, d, J= 8.4 Hz H-1β); 5.60 (1H, t, J= 9.9 Hz, H-3); 5.50 (1H, s, H-7); 4.31 (1H, dd, J=4.7 Hz; 10.3 Hz, H-6a); 3.75-3.60 (4H, m, H-2; H-3; H-6b; H-5) 2.20 (3H, s, 1-OCOCH$_3$); 2.15 (3H, s, OCOCH$_3$). Ratio α/β= 1:1.5.

2-azido-3-O-acetil-4,6-O-benzylidene-2-deoxi-D-glucopyranose (40) (FIANDOR et al., 1985).
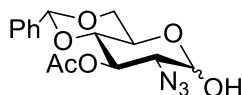
The same procedure to prepare compound **42** was used to obtain compound **40**. The product was obtained after purification by silica flash chromatography (Hexane/EtOAc 7:3 to 1:1), as a brown syrup with 78% yield. MW: 335.31 g/mol; R_f= 0.55; δH (ppm) (CDCl$_3$; 300 MHz): 7.46-7.40 (2H, m, Ar); 7.37-7.34 (3H, m, Ar); 5.65 (0.5H, t apparent, J= 9.9 Hz, H-3α); 5.50 (0.5H, s, H-7); 5,49 (0.5, s, H-7); 5.39 (0.5 H, d, J= 3.4 Hz;, H-1α); 5.18 (0.5H, t apparent, J= 9.7 Hz, H-3β); 4.81 (0.5H, d, J=7.9 Hz, H-1β); 4.34 (0.5H, dd, J= 4.3Hz; 9.9 Hz, H-6aβ); 4.29 (0.5H, dd, J= 4.9 Hz; 9.9 Hz, H-6aα); 4.19 (0.5H, ddd, J= 4.9 Hz; 9.9 Hz, H-5α); 3.82-3.60 (2.5H, m, H-6bα; H-6bβ; H-4α; H-4β; H-5β); 3.34 (0.5H, dd, J= 7.9 Hz; 10.0 Hz, H-2β); 2.17 (3H, s, OCOCH$_3$); 2.14 (2.5H, s, OCOCH$_3$). Ratio α/β= 1.5:1.

2-azido-3-O-acetyl-4,6-O-benzylidene-2-deoxy-1-α-trichloroacetimidoyl-D-glucopyranose (32) (SCHMIDT; KINZY, 1992; SCHMIDT; MICHEL, 1942).
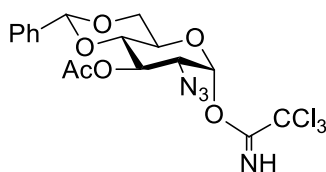
In a two-necked flask containing solution of **40** (30 mg, 0.089 mmol) in dry dichloromethane under argon atmosphere, trichloroacetonitrile (35.0 μL, 0.35 mmol) and DBU (4 μL, 0.025 mmol) at 0° C. The mixture was stirred for 1 hour in an ice bath. After this period, the reaction was transferred to a one-neck flask and the solvent was evaporated under reduced pressure. Product **32** was obtained as a yellowish solid, in 45% yield (17 mg, 0.04 mmol) after purification on a column chromatography (stationary phase: silica, mobile phase: Hexane/EtOAc 1:1). MW: 479.69 g/mol. R_f = 0.6 (Hexane/EtOAc 1:1); δ H (ppm) (CDCl$_3$, 400 MHz): 8.82 (1H, s, N-H); 7.46-7.43 (2H, m, Ar); 7.7.38-7.34 (3H, m, Ar); 6.47 (1H, d, J= 3.7 Hz, H-1);

5.68 (1H, apparent t, *J*= 9.9 Hz, H-3); 5.53 (1H, s, H-7); 4.33 (1H, dd, *J*= 4.9Hz, 9.4Hz H-6a); 4.13 (1H, m, H-5); 3.76 (2H, m, H-4; H-6b); 3.70 (1H, dd, *J*= 3.7 Hz, 10.3 Hz, H-2); 2.17 (3H, s, -OCOCH$_3$).

2-azido-3-O-acetil-4,6-O-benzylidene-2-deoxi-1-trifluoroacetimidoyl- D-glucopyranose (33b) (YANG et al., 2012; YU & TAO; 2002).
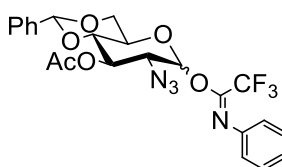
The same procedure to prepare compound **33a** was used to obtain compound **33b.** The product was obtained after purification by silica flash chromatography (Hexane/EtOAc 7:3), as a white powder with 84% yield. MW: 506.43 g/mol**.** R$_f$= 0.66 (Hexane/EtOAc 7:3). δH (ppm)(CDCl$_3$; 400 MHz) 7.44-7.30 (7H, m, Ar); 7.15 (1H, m, Ar); 6.86 (2H, d, *J*= 7.55 Hz, Ar); 5.70 (1H, br, H-1); 5.20 (1H, m, H-3); 4.32 (1H, m, H-4); 3.82- 3.22 (4H, m, H-6a, H-6b, H-5, H-2); 2.12 (1H, s, -OCOCH$_3$).

2-azido-1,3,4,6-tetra-O-benzoyl-2-deoxy-D-glucopyranose (43)
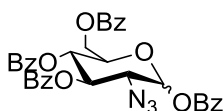
To a solution of **37** (1.0 g; 4.8 mmol) in pyridine (5.0 mL), benzoyl chloride (5.0 mL) was carefully added by the walls of the flask. The reaction mixture was left to stir for 1 hour. After this period, the mixture was cooled down to 0 ºC and water was slowly added. Reaction was diluted in EtOAc and then washed with solution 1N HCl (2x 10 mL) and saturated solution of NaHCO$_3$. The organic layer was dried in MgSO$_4$, solvent was evapored and compound was isolated by silica flash chromatography (Hexane/EtOAc 9:1 to 7:3) to give product **43** in quantitative yield (3.1 g; 4.85 mmol) as a white solid. MW: 621.59 g/mol; R$_f$= 0.41 (Hexane/EtOAc 7:3); δH (ppm) (CDCl$_3$; 400 MHz) 8.18-7.88 (8H, m, Ar); 7.64-7.32 (14H, m, Ar); 6.05 (1H, d, *J*= 8.4 Hz, H-1β); 6.69 (0.2 H, d, *J*= 3.6 Hz, H-1α); 5.69 (2H, m, H-3, H-4); 4.61 (1H, dd, *J*= 12.4

Hz; 2.9 Hz; H-6a); 4.47 (1H, dd, *J*= 12.4 Hz; 4.9 Hz, H-6b); 4,.9 (1H, m, H-5); 4.12 (1H, dd, *J*= 10.0 Hz; 8.5 Hz, H-2) Ratio α/β: 1:5.

2-azido-3,4,6-tri-O-benzoyl-2-deoxy-D-glucopyranose (44) (FIANDOR et al., 1985)
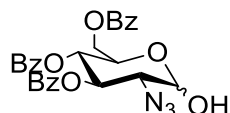
Compound **43** (3.1 g; 4.85 mmol) together with THF/NH₃.MeOH 7 N (6:4), under N₂ stirred at room temperature for 18 hours. The reagents were neutralized by bubbling N₂ into the reaction mixture. Solvents were evaporated, and the product **44** was obtained after purification by silica flash chromatography (Hexane/EtOAc 9:1 to 7:3), as a white solid with 41% yield (1.0 g; 1.98 mmol). MW: 517.49 g/mol; R$_f$= 0.21 (Hexane/EtOAc 7:3); δH (ppm) (CDCl₃; 400 MHz) 8.19-7.35 (15H, m, Ar); 5.49 (1H, d, *J*= 8.4 Hz, H-1β); 5.73 (1H, t, *J*= 9.8 Hz, H-3); 5,.49 (1H, t, *J*= 9.6 Hz, H-4); 3.87 (2H, m, H-6a, H-6b); 3.67 (1H, m, H-5); 2.61 (1H, dd, *J*= 9.7 Hz; 8.8 Hz, H-2) Ratio α/β: not detected.

2-azido-3,4,6-tri-O-benzoyl-2-deoxy-1-trifluoroacetimidoyl-D-glucopyranose (33c) (YANG et al., 2012; YU & TAO; 2002)
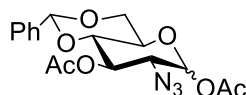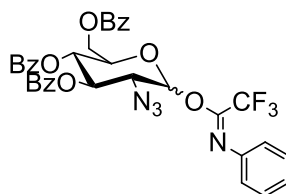

The same procedure to prepare compound **33c** was used to obtain compound **33a**. The product was obtained after purification by silica flash chromatography (Hexane/EtOAc 9:1 to 7:3), as a white powder with 91% yield. MW: 688.18 g/mol; R$_f$= 0.56 (Hexane/EtOAc 7:3); δH (ppm) [α]$_D^{25}$ +47.9 (*c* 1.0, CHCl₃); (CDCl₃; 500 MHz) 8.07-7.25 (34H, m, Ar); 7.15 (4H, m, Ar) 7.11 (4 H, m, Ar); 6.80 (4H,m, Ar); 6.51 (1H, br, H-1α); 6.01 (1H, t, *J*= 10.0 Hz, H-4α); 5.91 (1H, br, H-1β); 5.69 (1H, t, *J*= 9.8 Hz, H-4β); 5.61 (2H, m, H-3α; H-3β); 4.62-4.40 (5H, m, H-6,H-5α); 4.15-4.06 (2H, m, H-

5β; H-2β); 3.94 (1H, d apparent, H- 2β) Ratio α/β: 1:0.9. ^{13}C NMR (126 MHz, CDCl$_3$) δ 166.11 (C=O), 166.07 (C=O), 165.62 (C=O), 165.57 (C=O), 165.42 (C=O), 165.38 (C=O), 143.03 (C=N), 142.99 (C=N), 133.78 (C-Ar), 133.74 (C-Ar), 133.71 (C-Ar), 133.67 (C-Ar), 133.34 (C-Ar), 133.26 (C-Ar), 131.93 (C-Ar), 130.08 (C-Ar), 130.00 (C-Ar), 129.89 (C-Ar), 129.87 (C-Ar), 129.71 (C-Ar), 129.64 (C-Ar), 129.23 (C-Ar), 128.98 (C-Ar), 128.88 (C-Ar), 128.84 (C-Ar), 128.61 (C-Ar), 128.60 (C-Ar), 128.57 (C-Ar), 128.50 (C-Ar), 127.16 (C-Ar), 124.80 (C-Ar), 120.36 (C-Ar), 119.42 (C-Ar), 119.33 (C-Ar), 117.09 (C-Ar), 114.98 (C-Ar), 95.69 (C-1β), 93.60 (C-1α), 73.38 (C-4β), 72.75 (C-5β), 70.77 (C-4α), 70.73 (C-5α), 69.20 (C-3α), 69.09 (C-3β), 63.48 (C-2β), 62.90 (C-6β), 61.16 (C-2α), 60.48 (C-6α).

2-azido-3,4,6-tri-O-acetyl-1-tert-butyldimethylsilyl-D-glucopyranose (45) (LI; YU 2015)
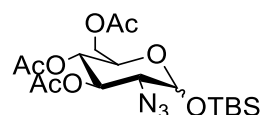
To a solution of **42** (1.0 g; 3,0 mmol) in DCM (5 mL) and imidazole (0.6 g; 9.0 mmol), under N$_2$ tert-butyldimethylsilyl chloride (TBDMSCl) (0.9 g; 6.0 mmol) was added at 0⁰ C. The reaction was left to warm up to room temperature and stirred for 3 hours. After this time, saturated solution of NaHCO$_3$ was added and the layers were separated. Organic phase was washed more 2 times with solution of NaHCO$_3$, dried with MgSO$_4$ and solvent was evapored under reduced pressure. Compound **45** was obtained as a yellow syrup after purification by silica flash chromatography (Hexane/EtOAc 8:2 to 7:3) with 79 % (1.05 g; 2.37 mmol) yield. MW: 445.54 g/mol. R$_f$= 0.44 (Hexane/EtOAc 7:3). δH (ppm) (CDCl$_3$; 400 MHz) 4.80 (2H, m, H-3, H-4); 4.46 (1H, d, *J*= 7.6 Hz, H-1β); 4.00 (1H, dd, *J*= 12.1 Hz; 6.0 Hz; H-6a); 3.95 (1H, dd, *J*= 12.1 Hz; 2.5 Hz, H-6b); 3.49 (1H, m, H-5); 3.25 (1H, dd, *J*= 10.3 Hz; 7.7 Hz, H-2); 1.92- 1.85 (9 H, 3s, 3 COCH$_3$); 0.77 (12 H, s, 3-CH$_3$); 0.75 (6 H, s, 2 -CH$_3$) Ratio α/β: 1:2.5.

2-azido-1-tert-butyldimethylsilyl-β-D-glucopyranose (46) (LI; YU 2015)
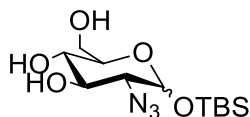
A solution of MeONa 1M was added dropwise to a solution of compound **45** (1.05 g; 2.37 mmol) in MeOH until pH 9-10. The mixture stirred overnight and then resin (Dowex 50WX8-200) was added to the reaction to reach Ph 7. The mixture was filtered, and solvent was evaporated. Compound **46** was obtained as a yellow syrup without further purification with 99% yield (0.75 g; 2.35 mmol). MW: 319.43 g/mol. R_f= 0.12 (Hexane/EtOAc 7:3). δH (ppm)(CDCl$_3$; 400 MHz) 4.39 (1H, d, J= 7.6 Hz, H-1β); 3.64 (1H, dd, J= 12.0 Hz; 2.3 Hz; H-6a); 3.50 (1H, dd, J= 11.9 Hz; 5.2 Hz, H-6b); 3.14 (1H, m, H-5); 2.90 (1H, dd, J= 9.8 Hz; 7.7 Hz, H-2); 1.92-1.85 (9 H, 3s, 3-COCH$_3$); 0.77 (12 H, s, 3 -CH$_3$); 0.76 (6 H, s, 2-CH$_3$) Ratio α/β: 1:2.5.

2-azido-3,4-di-benzoyl-2-deoxy-6-tert-butyldiphenylsilyl-1-tert-butyldimethylsilyl-β-D-glucopyranose (48) (LI; YU 2015)
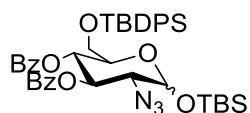
 To a solution of **46** (0.75 g; 2.35 mmol) in DMF (5 mL) and imidazole (0.48 g; 7.0 mmol), under N$_2$ tert-butyldiphenylsilyl chloride (TBDPSCl) (0.92 mL; 3.52 mmol) was added at 0º C. The reaction was left to warm up to room temperature and stirred for 7 hours. After this time, EtOAC and saturated solution of NaHCO$_3$ was added and the layers were separated. Organic phase was washed more 2 times with solution of NaHCO$_3$, dried with MgSO$_4$ and solvent was evaporated under reduced pressure. Compound **47** was subjected to same procedure for benzoylation to obtain compound **43** to obtain compound **48**. Product was obtained with 73% yield in two steps (1.3 g; 1.71 mmol), as a white solid. MW: 766.04 g/mol. R_f= 0.62 (Hexane/EtOAc 7:3). δH (ppm) (CDCl$_3$; 400 MHz) 4.9 (1H, d, J= 7.6 Hz, H-1β); 3.64 (1H, dd, J= 12.0 Hz; 2.3 Hz; H-6a); 3.50 (1H, dd, J= 11.9 Hz; 5.2 Hz, H-6b); 3.14 (1H, m, H-5); 2.90 (1H, dd, J= 9.8 Hz; 7.7 Hz, H-2); 0.77 (12 H, s, 3-CH$_3$); 0.76 (6 H, s, 2-CH$_3$) Ratio α/β: 1:2.5.

2-azido-3,4-O-benzoyl-6-tert-butyldiphenylsilyl-D-glucopyranose (49) (LI; YU 2015)
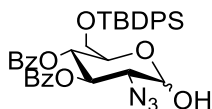
A solution of **48** (1.3 g; 1.68 mmol) in THF (7.0 mL), under N_2, was cooled down to -20⁰ C and TBAF (0.5 mL; 1.9 mmol) followed by AcOH (0.1 mL; 1.8 mmol) were added. The reaction stirred for 12 hours. Saturated solution of $NaHCO_3$ was added and mixture was allowed to warm up to room temperature. Organic layer was separated, and washed more 2 times with $NaHCO_3$ solution, dried with $MgSO_4$ and solvent was evaporated under reduced pressure. Product **49** was purified by silica flash chromatography (Hexane/EtOAc 7:3) with 70% yield (0.76 g; 1.17 mmol). MW: 651.78 g/mol. R_f= 0.52 (Hexane/EtOAc 7:3). δH (ppm) ($CDCl_3$; 400 MHz) 5.87 (1H, dd, J= 10.4 Hz, 9.6 Hz, H-3); 5.52 (1H, t, J= 9.8 Hz, H-4); 5.41 (1H, d, J= 3.4 Hz, H1α); 4.66 (1H, d, J= 7.9 Hz, H-1β); 4.25 (1H, ddd, J= 10.1 Hz, 4.0 Hz, 2.6 Hz, H-5); 3.76-3.71 (2H, m, H-6a; H-6b); 3.48 (1H, dd, J= 10.5 Hz, 3.4 Hz, H-2); 0.95 (12 H, s, 3-CH_3); Ratio α/β: 2:1.

2-azido-3,4-O-benzoyl-6-tert-butyldiphenylsilyl-D-glucopyranosyl trifluoroacetamidate 33d (YANG et al., 2012; YU & TAO; 2002)
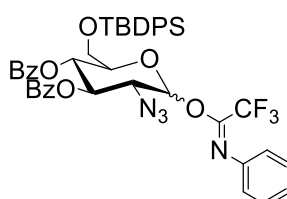
The same procedure to obtain compounds **33a-c** was used to achieve **33d**. Due to instability, product was used as donor in *O*-glycosylation reactions with no further purification after 4 hours in vacuum manifold. MW: 822.9 g/mol. R_f= 0.66 (Hexane/EtOAc 7:3).

3.2.2. Methods for myo-inositol acceptor block

2,3-4,5-di-O-cyclohexylidene-myo-inositol (51) (XUE, J.; SHAO, N.; GUO, 2003; GAREGG et al., 1984)
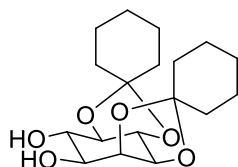
To a solution of *myo* inositol **50** (1.0 g, 5.5 mmol) commercially obtained in N, N, dimethylformamide (DMF) (10 mL) was added cyclohexanone dimethyl acetal (2.11 mL, 13.0 mmol) and p-toluenesulfonic acid (3.0 µg, 0.13 mmol). The reaction was kept under reflux for three hours. After this period, the reaction mixture was cooled to room temperature and Et₃N drops were added. DMF was evaporated under reduced pressure and compound **51** was obtained as a white crystal, in 16% yield (0.3 g, 0.88 mmol) after purification on a column chromatography (stationary phase: silica; mobile phase: dichloromethane/EtOAc 2:1). MW: 340.41 g/mol. Mp: 129-132 °C; R_f= 0.22; δ H (ppm) (CDCl₃, 400 MHz): 4.49 (1H, dd, *J*= 4.0 Hz, 6.2 Hz, H-2); 4.33 (1H, dd, *J*= 6.5 Hz, 8.2 Hz, H-5); 4.03 (1H, dd, *J*= 4.6 Hz, 9.0 Hz, H-1); 3.96 (1H, dd, *J*= 8.1 Hz, 10.6 Hz, H-4); 3.85 (1H, m, H-3); 3.40 (1H, dd, J= 9.0 Hz, 10.6 Hz); 1.73-1.41 (20H, m, 2-*O*-cyclohexylidenes).

1,6-di-O-allyl-2,3-4,5-di-O-cyclohexylidene-myo-inositol (52) (SWARTS, GUO, 2010).
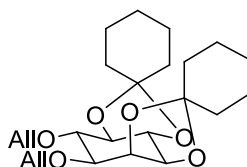
In a 2-neck flask under an argon atmosphere, a solution of **51** (0.1 g; 0.3 mmol) in DMF was kept under stirring on ice bath. To this solution, sodium hydride (NaH, 60% in mineral oil), previously washed with dry hexane, was added (0.053 g; 0.44 mmol). The ice bath was removed, and the reaction was stirred for one hour at room temperature. After this period, allyl bromide (4.0 µL; 0.44 mmol) was dropped

into the reaction mixture. The reaction was left stirring until starting material was no longer observed by TLC. The reaction was quenched with cold methanol and then ethyl acetate. The mixture was poured into separatory funnel and washed with saturated NaCl solution. The organic fractions were combined, dried over anhydrous MgSO₄, filtered and the solvent was evaporated under reduced pressure. Product **52** was purified by column chromatography (stationary phase: silica, mobile phase: 1: 1 hexane/EtOAc) and obtained as a clear oil with 78% (0.1 g; 0.23 mmol) in yield. MW: 420.53 g/mol. R_f = 0.56; δ H (ppm) (CDCl₃, 400 MHz): 5.96-5.85 (2H, m, Al); 5.35 - 5.27 (2H, m, Al); 5.21 - 5.16 (2H, m, Al); 4.37 (1H, dd, *J*= 3.3 Hz, 6.9 Hz, H-2); 4.31 (1H, dd, *J*= 4.5 Hz, 9.8 Hz, H-1) 4.27-4.22 (1H, m, Al); 4.21-4.19 (1H, dt, *J*= 1.46 Hz, 5.3 Hz, Al); 4.17-4.15 (2H, m, Al); 4.12-4.07 (1H, m, Al); 3.78 (1H, dd, *J*= 3.0 Hz, 7.6 Hz, H-3); 3.66 (1H, m, H-4); 3.40 (1H, dd, *J*= 7.7 Hz, 10.7 Hz, H-4); 1.73-1.41 (20H, m, 2-*O*-cyclohexylidenes).

1,6-di-O-allyl-myo-inositol (53) (SWARTS, GUO, 2010).
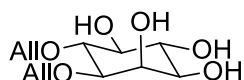
In a flask under an argon atmosphere containing compound **52** (15.0 mg, 0.003 mmol) was added 2:1 dry dichloromethane and methanol. Then acetyl chloride was added, and the reaction remained under stirring for one hour and 30 minutes. The mixture was quenched with Et₃N and the solvents were evaporated under reduced pressure. Product **53** was purified by column chromatography (stationary phase: silica, mobile phase: EtOAc/methanol 4:1) and obtained as a colorless oil in 28% yield. MW: 260.28 g/mol. R_f= 0.17 (EtOAc/methanol 4:1); δ H (ppm) (MeOD; 300 MHz): 5.95-5.85 (2H, m, Al); 5.25 (1H, dd, *J*= 2.1 Hz, 16.9 Hz, Al); 5.17 (1H, dd, *J*= 2.0 Hz, 16.9 Hz, Al); 5.10-5.05 (2H, m, Al), 4.40-4.36 (1H, m, H-1); 4.31 (1H, dd, *J*= 5.5Hz, 10.0Hz, H-6) 4.25-4.20 (1H, m, Al); 4.21-4.19 (1H, m, Al); 4.17-4.15 (2H, m, Al); 4.12-4.07 (1H, m, Al); 3.76 (1H, dd, *J*= 2.9 Hz, 9.0 Hz, H-3); 3.49 (1H, m, H-4); 3.24 (1H, dd, *J*= 5.2 Hz, 10.5 Hz, H-1).

4,6-O-benzylidene-1-O-methyl-α-D-glucopyranose (66)
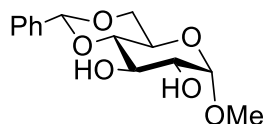
The same procedure to obtain compound **36** was used for compound **66** Product was obtained after purification in silica gel chromatography (EtOAc/methanol, 4:1) as a white solid with 89% yield. MP**:** 163-165ºC; R_f 0.23; δH (ppm) (CDCl3; 300 MHz): 7.51-7.44 (2H, m, Ar); 7.38-7.35 (3H, m, Ar); 5.52 (1H, s, H-7); 4.78 (1H, d, *J*= 3.8 Hz; H-1); 4.89 (1H, dd, *J*= 3.5 Hz; 8.9 Hz, H-6a); 3.92 (1H, t, *J*= 9.2 Hz, H-3); 3.84-3.72 (2H, m, H-6b; H-5) 3.43 (1H, dd, *J*= 4.0 Hz; 9.1 Hz, H-2), 3.36 (3H, s, OCH3); 3.32 (1H, dd, *J*= 4.5 Hz; 9.5 Hz, H-4).

2,3-di-O-benzyl-4,6-O-benzylidene-1-O-methyl-α-D-glucopyranose (67)
(BOONYARATTANAKALIN et al., 2008)
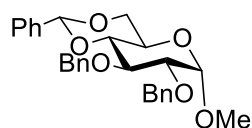
Method 1: To a flask containing compound **66** (1.5 g; 5.3 mmol), benzyl chloride (BnCl) (5 mL; 42.4 mmol) e and potassium hydroxide (KOH) (1.19 g; 21.2 mmol) were added and left to stir for 5 hours at 100 ºC. The mixture was allowed to cool down to room temperature and the remaining benzyl chloride was evaporated under reduced pressure. Compound **67** was obtained as a white powder with 53% yield (1.3 g; 2.8 mmol), after purification by silica flash chromatography (Hexane/EtOAc 9:1 to 7:3). **Method 2** (for low scale only): Compound **66** (1.0 g; 3.5 mmol), BnCl (2.0 mL) and KOH (0.23 g; 4.2 mmol) were added to a sealed microwave tube and subjected to irradiation for 5 minutes at 145º C and 200 W. Work up was performed according Method 1 and product **67** was obtained with 89% yield (1.4 g; 3.1 mmol). **Method 3:** To a flask under N_2 containing solution of compound **66** in DMF**,** NaH was added at 0º C. The mixture stirred for 30 minutes and then BnBr was added dropwise for 15 minutes. The reaction was allowed to warm up to room temperature and stirred overnight. Mixture was then diluted in ethyl acetate, washed with saturated NaCl solution (3x), organic layers were dried in $MgSO_4$ and solvent was evaporated in

reduced pressure. Purification in silica flash chromatography (Hexane/EtOAc 9:1 to 7:3) gave compound **67** as a white powder in 76% yield. MP: 94-98 °C; R_f= 0.68 δH (ppm) (CDCl$_3$; 300 MHz): 7.51-7,44 (2H, m, Ar); 7.38-7.31 (13H, m, Ar); 5.55 (1H, s, H-7); 4.91 (1H, d, *J*=11.2 Hz, CH$_2$-Ph); 4.86 (2H, 2d, *J*=11.2 Hz; 12.3 Hz, CH$_2$-Ph); 4.70 (1H, d, *J*= 12,1 Hz; CH$_2$-Ph); 4,59 (1H, d, *J*= 3,6 Hz, H-1); 4,27 (1H, dd, *J*= 4,7 Hz; 10,0 Hz, H-6a); 4.05 (1H, t, *J*= 9.3 Hz, H-3); 3.82 (1H, ddd, *J*= 4.7 Hz; 9.8 Hz, H-5) 3.71 (1H, t apparent, *J*= 10.2 Hz, H-6b), 3.60 (1H, t, *J*= 9.4 Hz, H-4), 3.56 (1H, dd, *J*= 3.7 Hz; 9.3 Hz, H-2); 3.24 (3H, s, OCH$_3$).

2,3,4-Tri-O-benzyl-1-O-methyl-α-D-glucopyranose (68)
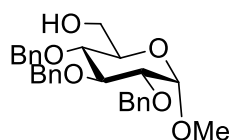
To a twin neck round bottom flask, compound **67** (1.1 g; 2.4 mmol) was dissolved in Et$_2$O/DCM (1:1) (40.0 mL). lithium and aluminium hydride (LiAlH$_4$) (0.28 g) was added and reaction was stirred at 40° C under reflux and anhydrous atmosphere. When solvents started to boil, freshly prepared solution of aluminium chloride (AlCl$_3$) (1.27 g) in Et2O (10 mL) was added dropwise for 30 minutes. The mixture stirred in reflux for 2 hours. Reaction was interrupted by addition of EtOAc and poured into separatory funnel. Water was carefully added to allow precipitation of Al(OH)$_3$. Aqueous phase was washed with Et$_2$O and organic layers were combined, dried with MgSO$_4$ and solvents were evaporated under reduced pressure. Compound **68** was purified in silica flash chromatography (Hexane/EtOAc 1:1) and obtained as a colourless syrup with 90% yield (1.0 g; 2.1 mmol). MW: 464.55 g/mol. R_f= 0.42 (Hexane/EtOAc 1:1). δH (ppm) (CDCl$_3$; 300 MHz): 7.35 (15H, m, Ar); 5.55 (1H, s, H-7); 4.98 (1H, d, *J*=10.8 Hz, CH$_2$-Ph); 4.88 (1H, d, *J*= 11.0 Hz, CH$_2$-Ph); 4.86 (1H, d, *J*= 10.0 Hz, CH$_2$-Ph); 4.83 (1H, d, *J*= 10.8 Hz, CH$_2$-Ph); 4.79 (1H, d, *J*= 12.0 Hz, CH$_2$-Ph); 4.70 (1H, d, *J*= 12.1 Hz; CH$_2$-Ph); 4.66 (2H, 2d, *J*= 11.0 Hz; 12.1 Hz, CH$_2$-Ph); 4.56 (1H, d, *J*= 3.5 Hz, H-1); 4,.7 (1H, dd, *J*= 4.7 Hz; 10.0 Hz, H-6a); 4.01 (1H, t, *J*= 9.3 Hz, H-3); 3,75 (1H, dd, *J*= 2.7 Hz; 11.6 Hz, H-6b) 3.70-3.61 (2H, m, H-6b; H-5), 3.52 (1H, t apparent, *J*= 9.4 Hz, H-4), 3.49 (1H, dd, *J*= 3.6 Hz; 9.6 Hz, H-2); 3.35 (3H, s, OCH$_3$).

6-O-acetyl-2,3,4-tri-O-benzyl-1-O-methyl-α- D-gluco-hex-5-enopyranose (70)

(BOONYARATTANAKALIN et al., 2008)
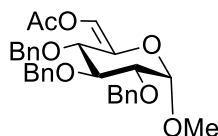
To a flask containing compound **68** (0.07 g; 0.15 mmol) in dry (2 mL), a solution of Dess-Martin periodinane (DMP) (0.095 g; 0.22 mmol) in 4,0 mL of DCM was added dropwise for 10 minutes. Reaction stirred at room temperature for 1 hour and then 10 mL of Et_2O followed by 6 mL saturated solution of $NaHCO_3$ containing $Na_2S_2O_3$ (1.5 g; 5.2 mmol) were added. Mixture stirred for 30 minutes and then aqueous and organic phases were separated. Organic layer was dried under reduced pressure and left overnight at vacuum manifold. After this period, crude product was dissolved in dry MeCN (20.0 mL) and acetic acid (0.04 mL; 0.43 mmol) followed by potassium carbonate (K_2CO_3) (0.1 g; 0.86 mmol) were added. Reaction was kept overnight under reflux and then, washed with saturated $NaHCO_3$ solution. Organic layer was dried in $MgSO_4$, and solvent was evaporated under reduced pressure. Product **70** was purified by silica flash chromatography (Hexane/EtOAc 7:3) and obtained as a colourless syrup with 87% yield (0.09 g; 0.18 mmol). MW: 504.57 g/mol. R_f = 0.62 (Hexane/EtOAc 7:3). δH (ppm) ($CDCl_3$; 300 MHz): 7.51- 4.43 (15H, m, Ar); 7.0 (1H, s, H-6); 5.05 (1H, d, J= 1.0 Hz, CH_2-Ph); 4.98 (1H, d, J= 11.2 Hz, CH_2-Ph); 4.90 (1H, d, J= 10.5 Hz, CH_2-Ph); 4.86 (1H, d, J= 10.8 Hz, CH_2-Ph); 4.75 (1H, d, J= 1.0 Hz, CH_2-Ph); 4.73 (1H, d, J= 12.1 Hz; CH_2-Ph); 4.70- 4.68 (2H, 2d, J= 11.2 Hz; 12.3 Hz, CH_2-Ph); 4.52 (1H, d, J= 3.5 Hz, H-1); 4.36 (1H, m, H-3); 3.99 (1H, t ap., J= 8.9 Hz, H-4), 3.58 (1H, m, H-2); 3.35 (3H, s, OCH_3), 2.15 (3H, s, $OCOCH_3$).

1-acetoxy-3,4,5-tri-O-benzyl-6-hydroxy-cyclohexanone (71)

(BOONYARATTANAKALIN et al., 2008)
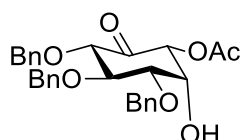
To a solution of compound **70** (0.97 g; 1.9 mmol;) in acetone/water (4:1), $Hg(CF_3COO)_2$ (0.9 g; 2.3 mmol) was added and mixture stirred for 1 hour at room temperature. The mixture was then cooled down to 0° C and 3M aqueous solution of sodium acetate (0.8 mL) was added, followed by 4.5 mL of saturated NaCl solution. Reaction stirred overnight at room temperature and then Et_2O was added. Mixture was washed with saturated $NaHCO_3$ solution and then saturated NaCl solution. Organic phases were combined, dried with $MgSO_4$, and solvents were evaporated under reduced pressure. The desired product **71** was purified by silica flash chromatography (Hexane/EtOAc 9:1 to 1:1) and obtained as a yellow syrup with 60% yield (0.8 g; 1.64 mmol). MW: 490.54 g/mol. R_f = 0.38 (Hexane/EtOAc 1:1). $[\alpha]_D^{25}$ -0.09 (c 0.1, $CHCl_3$). δH (ppm) ($CDCl_3$; 500 MHz): 7.51-4.43 (15H, m, Ar); 5.17 (1H, d ap, J= 1.9 Hz, H-1); 5.05 (1H, d, J=11.0 Hz, CH_2-Ph); 4.93 (1H, d, J=11.2 Hz, CH_2-Ph); 4.90 (1H, d, J=10.5 Hz, CH_2-Ph); 4.86 (1H, d, J=10.8 Hz, CH_2-Ph); 4.75 (1H, d, J=12.0 Hz, CH_2-Ph); 4.73 (1H, d, J= 12.1 Hz; CH_2-Ph); 4.70-4.53 (2H, 2d, J=11.2 Hz; 12.3 Hz, CH_2-Ph); 4.34 (1H, d ap, J= 2.5 Hz, H-6); 4.16 (1H, dd, J=0.6 Hz; 9,4 Hz, H-3), 4.8 (1H, t, J= 9.2 Hz, H-4); 3.86 (1H, dd, J= 2.4 Hz; 9.0 Hz, H-5), 2.24 (3H, s, OAc).

1-O-acetyl-3,4,5-tri-O-benzyl- D -myo-inositol 72 (TAKAHASHI; KITTAKA; IKEGAMI, 2001; BENDER; BUDHU, 1991).
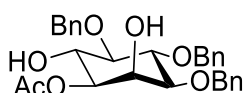
To a flask in ice bath and under N_2, containing solution of **71** (0.1 g; 0.2 mmol) in dry MeCN, $NaBH(OAc)_3$ and AcOH (0.2 mL) were added. Mixture was allowed to warm up to room temperature and stirred overnight. Ethyl ether was added and washed with saturated $NaHCO_3$ solution. Organic layers were combined, dried with $MgSO_4$ and solvents were evaporated under reduced pressure. Compound **72** was purified by silica flash chromatography (Hexane/EtOAc 7:3 to 1:1) and obtained a colourless syrup with 44% yield (0.45 g; 0.09 mmol). R_f= 0.14 (Hexane/EtOAc 1:1) $[\alpha]_D^{20}$ -10.09 (c 0.1, $CHCl_3$). δH (ppm) ($CDCl_3$; 300 MHz): 7.51- 7.43 (15H, m, Ar); 5.09-4.75 (8H, m); 4.31 (1H, t, J= 2.4 Hz, H-2); 4.14 (1H, t, J=9,6 H-6), 3.96 (1H, t, J= 9.4 Hz, H-4);

3.59 (1H, dd, J= 2.6 Hz; 9.4 Hz, H-3), 3.41 (1H, t, J= 9.4 Hz, H-5) 2.25 (3H, s, OCOCH$_3$).

1-O-allyl-3,4,5-tri-O-benzyl-D-myo-inositol (74)
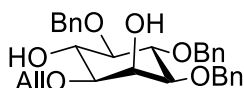
To a solution of compound **72** (0.1 g; 0.16 mmol) in DCM (2 mL), pyridinium *p*-toluenesulfonate (PPTS) (6.0 mg; 0.024 mmol) and ethyl vinyl ether (EVE) (0.3 mL; 0.32 mmol) were added. Solution stirred at room temperature and under N$_2$ overnight and then solvents were evaporated. The crude mixture was then dissolved in MeOH (2 mL) and solution of 1M MeONa was added until pH 10. The reaction was left stirring overnight at 50ºC and then solvent was evaporated at reduced pressure. The crude product **73** was filtered in silica pad (CHCl$_3$: MeOH 19:1; 20 mL) and left overnight at vacuum manifold. Compound **73** was dissolved in DMF under N$_2$ and cooled down to 0º C for addition of NaH. The reaction stirred under N$_2$ at room temperature for 30 minutes and then allyl bromide was added. After overnight period, reaction was diluted in DCM, washed with saturated NaCl solution, dried in MgSO$_4$ and solvent was evaporated. Compound **74** was purified by silica flash chromatography (Hexane/EtOAc 7:3 to 6:4) and obtained as a yellow solid with 67% overall yield (53.0 mg; 0.1 mmol). MW: 433.51 g/mol. R$_f$= 0.19 (Hexane/EtOAc 7:3). [α]$_D^{20}$ -10.07 (*c* 0.1, CHCl$_3$). δH (ppm) (CDCl$_3$; 400 MHz): 7.32- 7.20 (15H, m, Ar); 5.86 (1H, m, allyl); 5.22 (1H, ddd, J= 17.2 Hz; 2.6 Hz; 1.5 Hz, allyl); 5.14 (1H, ddd, J= 10.3 Hz; 2.6 Hz; 1,9 Hz, allyl); 4.87-4.62 (6H, m, CH$_2$-Ph); 4.15-4.00 (2H, m, allyl); 3.95 (1H, dt, J= 9.5 Hz; 1.3 Hz, H-1); 3.89 (1H, t, J= 9.3 Hz, H-5); 3.36 (1H, dd, J= 9.5 Hz; 2.7 Hz, H-3); 3.28 (1H, t, J=9.6 H-4), 3,09 (1H, dd, J= 9.6 Hz; 2.6 Hz, H-2), 2.38 (1H, d, J= 1.9 Hz, H-6); 2.35 (1H, s, OH).

1-O-allyl-3,4,5-tri-O-benzyl-2-O-naphtylmethyl-D-myo-inositol (34) (LIU et al., 2006).
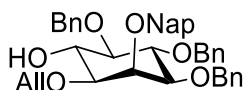
To a solution of **74** (0.59 g; 1.2 mmol) in DMF (5 mL) under N_2 tetrabutylammonium iodine (TBAI) (0.44 g; 1.2 mmol) was added. The mixture was cooled down to 0º C for addition of NaH (0.11 g; 4.8 mmol). After 10 minutes, reaction was cooled down to -20º C and a freshly prepared solution of 2-(Bromomethyl) naphthalene (0.3 g; 1.3 mmol) in DMF (3.0 mL) was added dropwise for 15 minutes. The reaction was allowed to warm up to room temperature and stirred overnight. Mixture was diluted in DCM, washed with $NaHCO_3$, dried in $MgSO_4$ and solvent was evaporated under reduced pressure. Product **34** was purified by silica flash chromatography (Hexane/EtOAc 8:2 to 6:4) and obtained as a yellow solid with 76% yield (0.57 g; 0.91mmol). MW: 630.33 g/mol. R_f= 0.49 (Hexane/EtOAc 7:3). $[\alpha]_D^{20}$ -11.02 (*c* 0.1, $CHCl_3$). δH (ppm) ($CDCl_3$; 400 MHz): 7.50-7.19 (22H, m, Ar); 5.82 (1H, m, allyl); 5.19 (1H, ddd, *J*= 17.2 Hz; 2.6 Hz; 1,5 Hz, allyl); 5.10 (ddd, *J*= 10.4 Hz; 2.6 Hz; 1.2 Hz, H-Allyl); 4.94-4.75 (6H, m, CH_2-Ph); 4.63 (1H, d, *J*= 11.7 Hz, CH_2-Ph); 4.56 (1H, d, *J*= 11.7 Hz, CH_2-Ph); 4.09 (1H, t, *J*= 9.5 Hz, H-3); 4.05-3.87 (4H, m, 2 allyl, H-1, H-5); 3.36-3.26 (2H, m, H-4, H-6); 3.05 (1H, dd, *J*= 9.8 Hz; 2.2 Hz, H-2); 2.42 (1H, br, OH).

3.2.3. O-glycosylation procedures

General procedure for *O*-glycosylation reactions: To an oven-dried flask containing 0.2 g of 4Å molecular sieves, donor (0.03 g; 1.0 Eq.) and acceptor (1.0 Eq.) dissolved in anhydrous Et_2O were added at -50º C under N_2. The mixture stirred for 10 minutes and then, a solution of TMSOTf in Et_2O was added (0.2 Eq.). The reaction was allowed to warm up between -30º C and -10º C and stirred until TLC showed absence of donor. The pseudo-disaccharide was purified by silica flash chromatography (Hexane/EtOAc 9:1 to 8:2 and 10% DCM) and obtained as a white foam in a range of 22% to 82% yield (results were solvent and donor-dependent).

1-O-allyl-6-O(2-azido-3,4,6-O-acetyl-2-deoxy-α-D-glucopyranosyl)-3,4,5-tetra-O-benzyl-2-O-naphtylmethyl-myo-inositol (31aα)
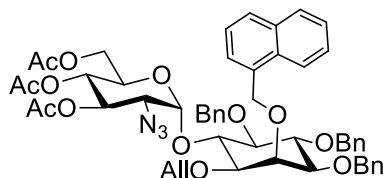
General procedure for *O*-glycosylation was applied, using as donor compound **33a** (30.0 mg; 59.0 μmol) and compound **34** (31.0 mg; 59.0 μmol) as acceptor. The product **31a** was obtained in 27% (15.7 mg; 17.7 μmol; proportion α/β 1.3:1) in DCE, 34% (18.9 mg; 21.3 μmol; proportion α/β 1.3:1) in Toluene/Et$_2$O and 40% in Et$_2$O (22.5 mg; 25.3 μmol; proportion α/β 2:1). MW: 886.96 g/mol. R$_f$= 0.59 (Hexane/EtOAc 7:3). [α]$_D^{20}$ +11.0 (*c* 0.1, CHCl$_3$). δH (ppm) (CDCl$_3$; 400 MHz): 7.85-7.24 (22H-Ar); 5.90 (1H, m, allyl); 5.81 (1H, d, *J*= 3.6 Hz, H1); 5.25 (1H, ddd, *J*= 17.2 Hz; 2.9 Hz; 1.4 Hz, allyl); 5.18 (1H, ddd, *J*= 10.4 Hz; 2.8 Hz; 1.4 Hz, allyl); 5.14 (1H, d, *J*= 11.6 Hz, CH$_2$-Ph); 5.0 (2H, s, CH$_2$-Ph); 4.94 (2H, m, H-3, CH$_2$-Ph); 4.83 (1H, d, *J*= 10.5 Hz, CH$_2$-Ph); 4.74 (1H, d, *J*= 11.5 Hz, CH$_2$-Ph); 4,69 (1H, d, *J*= 11,6 Hz, CH$_2$-Ph); 4.61 (1H, d, *J*= 11.6 Hz, CH$_2$-Ph), 4.28 (2H, m, H-4, H-6'); 4.16 (1H, t, *J*=9.5 Hz, H-4'); 4.06 (1H, t, *J*= 2.1 Hz, H-2'); 3.97 (2H, dddd, *J*= 5.5 Hz; 12.1 Hz; 27 8Hz, allyl); 3.64 (1H, dd, *J*=12.7 Hz; 1.9 Hz, H-6a); 3.56 (1H, dd, *J*= 12.7 Hz; 2.9 Hz, H-6b); 3.42 (3H, m, H-5, H-3', H-5'); 3.20 (1H, dd, *J*= 10.9 Hz; 3.6 Hz, H-2), 2.07-1.86 (9H, 3s, OCOCH$_3$). HRMS (ESI +) *m/z* calcd. for C$_{53}$H$_{57}$NaN$_3$O$_{13}$ 966.3784, found 966.3778 [M+Na$^+$].

1-O-allyl-6-O(2-azido-3,4,6-O-acetyl-2-deoxy-β-D-glucopyranosyl)-3,4,5-tetra-O-benzyl-2-O-naphtylmethyl-myo-inositol (31aβ)
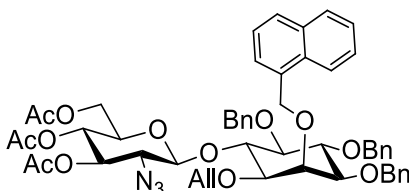
General procedure for *O*-glycosylation was applied, using as donor compound **33a** (30.0 mg; 59.0 μmol) and compound **34** (31.0 mg; 59.0 μmol) as acceptor. The product **31a** was obtained in 27% (15.7 mg; 17.7 μmol; proportion α/β 1.3:1) in DCE, 34% (18.9 mg; 21.3 μmol; proportion α/β 1.3:1) in Toluene/Et$_2$O and 40% in Et$_2$O

(22.5 mg; 25.3 µmol; proportion α/β 2:1). MW: 886.96 g/mol. R_f= 0.59 (Hexane/EtOAc 7:3). $[α]_D^{20}$ +11.0 (c 0.1, CHCl₃). δH (ppm) (CDCl₃; 400 MHz): 7.85-7.26 (22H-Ar); 5.90 (1H, m, allyl); 5.32 (1H, m, allyl); 5.15 (1H, ddd, J= 10.4 Hz; 3.1 Hz; 1.4 Hz, allyl); 5.14 (1H, d, J= 11.6 Hz, CH₂-Ph); 5.05-4.90 (6H, m, CH₂-Ph, H-1); 4.82 (1H, d, CH₂-Ph); 4.82 (1H, d, J= 10.7 Hz, CH₂-Ph); 4.78 (1H, d, J= 10.0 Hz, CH₂-Ph); 4.61 (2H, br, CH₂-Ph); 4.39 (1H, t, J= 9.4 Hz, H-3), 4.27 -4.20 (2H, m, H-4, H-6a); 4.13 (1H, t, J= 9.5 Hz, H-6'); 4.09- 4.0 (3H, m, allyl, H-2', H-6b); 3.58 (1H, t, J= 9.2 Hz, H-5'); 3.64 (1H, dd, J= 12.7 Hz; 1.9 Hz, H-6a); 3.58 (1H, t, J= 9.2 Hz, H-4'); 3.50 (2H, m, H-5, H-2); 3.42 (1H, dd, J= 9.7 Hz; 2.2 Hz, H-3'), 3.24 (1H, dd, J= 9.7 Hz; 2.2 Hz, H-1'), 2.10-1.92 (9H, 3s, 3 OCOCH₃). HRMS (ESI +) m/z calcd. for C₅₃H₅₇NaN₃O₁₃ 966.3784, found 966.3778 [M+Na⁺].

1-O-allyl-6-O(2-azido-3-O-acetyl-4,6-benzylidene-2-deoxy-α-D-glucopyranosyl)- 3,4,5-tetra-O-benzyl- 2-O-naphtylmethyl-myo-inositol (31bα)

General procedure for O-glycosylation was applied, using as donor compound **33b** (30.0 mg; 59.2 µmol) and compound **34** (31.0 mg; 59.2 µmol) as acceptor. The product **31b** was obtained in 22% (12.7 mg; 14.2 µmol; proportion α/β 1:1.25) in DCE, 73% (41.1 mg; 46.1 µmol; proportion α/β 1:1.5) in Toluene/Et₂O and 68% in Et₂O (38.5 mg; 43.2 µmol; proportion α/β 1:1.5). MW: 890.99 g/mol. R_f= 0.62 (Hexane/EtOAc 7:3). $[α]_D^{20}$ +17.3° (c 0.1, CHCl₃). δH (ppm) (CDCl₃; 400 MHz): 7.08-7.00 (27H, m, Ar); 5.98 (1H, m, allyl); 5.75 (1H, d, J= 3.7 Hz, H-1); 5.49 (1H, t, J= 10.0, H-3); 5.18 (1H, m, allyl); 5.11 (1H, m, H-allyl); 4.95-4.80 (4H, m, 4d, CH₂-Ph); 4.74 (1H, d, J= 10.7 Hz, CH₂-Ph); 4.62 (1H, d, J=11.7 Hz, CH₂-Ph); 4.54 (1H, d, J= 11.7 Hz, CH₂-Ph); 4.23 (1H, t, J= 9.6 Hz, H-4); 4.15 (1H, m, H-6a); .4.1 (1H, t, J= 9.5 Hz, H-6'); 4.0 (1H, m, H-2'); 3.99-3.92 (2H, m, H-allyl, H-6b); 3.85 (1H, m, H-allyl); 3.52- 3.40 (3H m, H-4', H-5', H-5); 3.35 (2H, br m, H-3', H-1'); 3.03 (1H, dd, J= 10.4 Hz, 3.8 Hz, H-2); 2.05 (3H, s, OCOCH₃). HRMS (ESI+) m/z calcd. for C₅₆H₅₇N₃NaO₁₁ 970.3885, found 970.3870 [M+Na⁺].

1-O-allyl-6-O(2-azido-3-O-acetyl-4,6-benzylidene-2-deoxy-β-D-glucopyranosyl)-3,4,5-tetra-O-benzyl-2-O-naphtylmethyl-myo-inositol (31bβ)
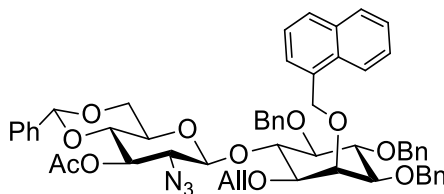
General procedure for *O*-glycosylation was applied, using as donor compound **33b** (30.0 mg; 59.2 µmol) and compound **34** (31.0 mg; 59.2 µmol) as acceptor. The product **31b** was obtained in 22% (12.7 mg; 14.2 µmol; proportion α/β 1:1.25) in DCE, 73% (41.1 mg; 46.1 µmol; proportion α/β 1:1.5) in Toluene/Et_2O and 68% in Et_2O (38.5 mg; 43.2 µmol; proportion α/β 1:1.5). MW: 890.99 g/mol. R_f= 0.62 (Hexane/EtOAc 7:3). $[\alpha]_D^{20}$ +17.3° (*c* 0.1, $CHCl_3$). δH (ppm) ($CDCl_3$; 400 MHz): 7.79-7.20 (27H, m, Ar); 5.85 (1H, m, allyl); 5.40 (1H, s, CH-Ph); 5.29 (1H, m, H-allyl); 5.11 (1H, m, allyl); 5.05-4.90 (6H, m, 4 CH_2-Ph, H -1, H-3); 4.72 (2H, m, 2- CH_2-Ph); 4.57 (1H, d, *J*= 11.7 Hz, CH_2-Ph); 4,53 (1H, d, *J*= 11.7 Hz, CH_2-Ph); 4.36 (1H, t, *J*= 9.6 Hz, H-4); 4.22 (1H, dd, *J*= 10.5 Hz; 5.0 Hz, H-6'); 4.15 (1H, m, H-allyl); 4.09- 4.02 (2H, m, H-4, H-allyl); 3.99 (1H, m, H-2'); 3.68 (1H, t, *J*= 10.2, H-3'); 3.51 (2H t, H-4', H-5'); 3.40- 3.32 (2H, m, H-6b; H-2) 3.25 (1H, m, H-5); 3.17 (1H, dd, *J*= 9.8 Hz; 2.2 Hz, H-1'); 2.05 (3H, s, $OCOCH_3$). HRMS (ESI +) *m/z* calcd. for $C_{56}H_{57}N_3NaO_{11}$ 970.3885, found 970.3870 [M+Na+].

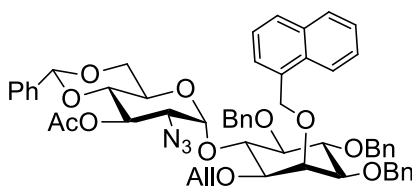***1-O-allyl-6-O(2-azido-3,4,6-O-benzoyl-2-deoxy-α-D-glucopyranosyl)-3,4,5-tetra-O-benzyl-2-O-naphtylmethyl-myo-inositol (31c)***
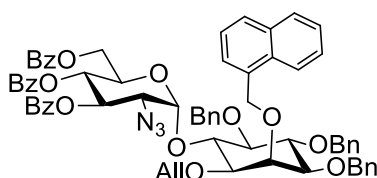
General procedure for *O*-glycosylation was applied, using as donor compound **33c** (30.0 mg; 43.5 µmol) and compound **34** (23.0 mg; 43.5 µmol) as acceptor. The product **31c** was obtained in 82% (37.8 mg; 35.2 µmol) in DCE, 74% (36.0 mg; 33.5

µmol) in Toluene/Et$_2$O and 77% in Et$_2$O (35.6 mg; 33.1 µmol). MW: 1073.16 g/mol. R$_f$= 0.64 (Hexane/EtOAc 7:3). [α]$_D^{20}$ +16.0° (c 0.1, CHCl$_3$). δH (ppm) (CDCl$_3$; 400 MHz): 8.09-7.09 (37H, m, Ar); 5.99 (3H, m, allyl, H-1, H-3); 5.50 (1H, t, J= 9.9 Hz, H-4); 5.20 (2H, m, 2 allyl); 5.05-4.55 (8H, m, 8 CH$_2$-Ph); 4.46 (1H, t, J= 9.4 Hz, H-6'); 4.23- 4.1 (3H, m, H-6a, H-2', H-4'); 4.0 (2H, m, 2 allyl); 3.76 (1H, dd, J= 12.4 Hz; 4.7 Hz, H-6b); 3.56 (1H, t, J= 9.3 Hz, H-3'); 3.46 (2H, m, H-5, H-1'); 3.39 (1H, dd, J= 10.7 Hz, 3.7 Hz, H-2). δ$_C$ (ppm) (CDCl$_3$; 100 MHz) 166.1 (C=O), 165.8 (C=O), 165.1 (C=O), 138.2 (C-Ar), 138.0 (C-Ar), 136.1(C-Ar), 134.0 (C-Ar), 133.3 (C-Ar-Bz), 133.1 (C-Ar-Bz), 133.0 (C-Ar-Bz), 132.8 (C-Ar-Bz), 129.8 (C-Ar-Bz), 129.7 (C-Ar-Bz), 129.0 (C-Ar-Bn), 128.8 (C-Ar-Bn), 128.6 (C-Ar-Bn), 128.5 (C-Ar-Bn), 128.4 (C-Ar-Bn), 128.3 (C-Ar-Bn), 128.2 (C-Ar-Bn), 128.1 (C-Ar-Bn), 128.0 (C-Ar-Bn), 127.9 (C-Ar-Bn), 127.6 (C-Ar-Bn), 126.9 (C-Ar-Bn), 126.6 (C-Ar-Bn), 126.6 (C-Ar-Bn), 126.3, 126.01 (C-Ar-Bn), 125.8 (C-Ar-Bn), 97.6 (C-1) 80.8 (C-1'), 80.8 (C-5'), 78.2 (C-4'), 75.0 (C-2'), 73.4 (C-5), 73.0 (C-CH$_2$Ph), 72.4 (C-6'), 69.1 (C-4), 62.4 (C-6), 61.7 (C-2) (Signs can be exchanged). HRMS (ESI+) m/z calcd. for C$_{68}$H$_{63}$NaN$_3$O$_{13}$ 1152.4253, found 1152.4415 [M+Na$^+$].

1-O-allyl-6-O(2-azido-3,4-O-benzoyl-6-terc-butyldiphenylsilyl-2-deoxy-α-D-glucopyranosyl)-3,4,5-tetra-O-benzyl-2-O-naphtylmethyl-myo-inositol (31d)
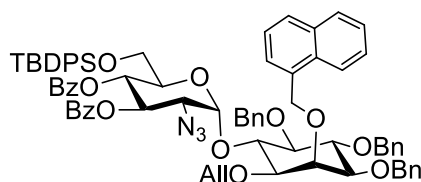
General procedure for O-glycosylation was applied, using as donor compound **33d** (approximately 30.0 mg; 36.4 µmol) and compound **34** (20.0 mg; 36.4 µmol) as acceptor. The product **31d** was obtained in 63% (31.4 mg; 26.0 µmol) in DCE, 68% (33.7 mg; 27.9 µmol) in Toluene/Et$_2$O and 68% in Et$_2$O (33.2 mg; 27.4 µmol). MW: 1207.46 g/mol. R$_f$= 0.67 (Hexane/EtOAc 7:3). [α]$_D^{20}$ +19.5° (c 0.1, CHCl$_3$). δH (ppm) (CDCl$_3$; 400 MHz): 7.79-7.20 (42H, m, Ar); 5.95 (1H, m, allyl); 5.87 (1H, d, J= 3.7 Hz, H-1); 5.78 (1H, dd, J= 10.5Hz; 9.6 Hz, H-3); 5.57 (1H, t, J= 9.9 Hz, H-4); 5.21 (1H, m, allyl); 5.15 (1H, m, allyl); 5.05-4.95 (3H, m, CH$_2$-Ph); 4.85 (1H, d, J= 11.9 Hz, CH$_2$-Ph); 4.82 (1H, d, J=10.5 Hz, CH$_2$-Ph); 4.67- 4.50 (3H, m, CH$_2$-Ph); 4.31 (1H, t, J= 9.6 Hz, H-6'); 4.15- 3.90 (5H; m, 2-allyl, H-2', H-6a); 3.62 (1H, m, H-6b, H-5'); 3.45- 3.35

(4H, m, , H-3', H-4', H-5); 3.29 (1H, dd, *J*= 10.9Hz; 3.6 Hz, H-1'); 3.06 (1H, dd, *J*= 11.8 Hz; 3.1 Hz, H-2); 0.9 (9H, s, but). HRMS (ESI+) *m/z* calcd. for $C_{77}H_{77}NaN_3O_{12}Si$ 1286.5169, found 1286.5621 [M+Na$^+$].

3.2.4. Deprotection of O-allyl group

6-O(2-azido-3,4,6-benzylidene-2-deoxy-α-D-glucopyranosyl)-3,4,5-tetra-O-benzyl-2-O-naphtylmethyl-myo-inositol (77) (LEE; SEEBERGER; VARON-SILVA, 2015).
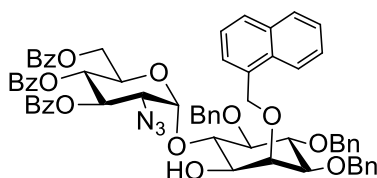
Pseudo-disaccharide **33c** was left to dry in high-vacuum overnight in a round flask (0.15 g; 0,13 mmol), then $PdCl_2$ and $NaCO_3$ was added followed by addition of AcOH and water. Reaction was left to stir for 24 hours under N_2 atmosphere. After this period, reaction was diluted in EtOAc and aqueous solution of saturated $NaHCO_3$ was carefully added. Layers were separated, and organic phase was washed with $NaHCO_3$, dried with $MgSO_4$ and solvent was evaporated under reduced pressure. Compound **77** was obtained with 83% (0.12 g; 0.10 mmol) yield after purification by silica flash chromatography (Hexane/EtOAc 9:1 to 8:2). MW: 1090.17 g/mol. R_f= 0.63 (Hexane/EtOAc 7:3). δH (ppm) (CDCl$_3$; 400 MHz): 8.05- 7.1 (37H, m, Ar); 5.93 (1H, dd, *J*= 10.5 Hz; 9.6 Hz, H-3); 5.84 (1H, d, *J*= 3.6 Hz, H-1); 5.0- 4.72 (8H, m, 8- CH$_2$-Ph); 4,6 (1H, m, H-6'); 4.20- 4.09 (4H, m, H-6a, H-5', H-4'); 4.04 (1H, t, *J*= 2.5 Hz, H-2'); 3.76 (2H, m, H-6b, H-5); 3.57 (1H, t, *J*= 9.3 Hz, H-3'); 3.52 (2H, m, H-1', H-2); 2.49 (1H, d, *J*= 9.0 Hz, OH). δ ^{13}C NMR (100 MHz, CDCl$_3$): 166.0 (C=O), 165.7 (C=O), 165.1 (C=O), 165.0 (C=O), 138.2 (C-Ar-OBz), 138.0 (C-Ar-OBz), 135.4 (C-Ar-OBz), 133.2 (C-Ar-OBz), 129.9 (C-Ar-OBz), 129.8 (C-Ar-OBz), 129.7 (C-Ar-OBz), 128.5 (C-Ar-Bn), 128.3 (C-Ar-Bn), 128.3 (C-Ar-Bn), 128.1 (C-Ar-Bn), 128.0 (C-Ar-Bn), 127.9 (C-Ar-Bn), 127.7 (C-Ar-Bn), 127.6 (C-Ar-Bn), 127.2 (C-Ar-Bn), 126.8 (C-Ar-Bn), 126.2 (C-Ar-Bn), 126.1 (C-Ar-Bn), 126.0 (C-Ar-Bn), 97.4 (C-1), 81.8 (C-1'), 80.8 (C-

5'), 78.2 (C-4'), 75.0 (C-2'), 73.4 (C-5), 73.0 (C-CH$_2$Ph), 72.4 (C-6'), 69.1 (C-4), 62.4 (C-6), 61.7 (C-2) (Signs can be exchanged).

3.2.5. Synthesis of phospholipid mimics

11-(anthracen-9-ylmethoxy)undecan-1-ol (84) (RILEY; XU; BROCKHAUSEN, 20010; MONTOYA-PELEAZ et al., 2005)
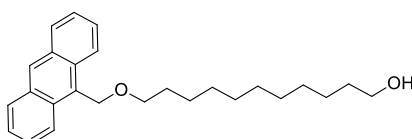
Commercially purchased 11-Bromo-1-undecanol (7.54 g, 30.0 mmol) and 3,4 dihydro-2H-pyran (12.62 g, 150.0 mmol) were dissolved in dry CH$_2$Cl$_2$ (140 mL) and the solution was cooled to 0º C. *p*-Toluenesulfonic acid monohydrate (0.057 g, 0.3 mmol) was then added and the solution was allowed to warm up to room temperature; it was then stirred overnight. The mixture was partitioned between Et$_2$O and a mixture of aqueous solution of saturated NaCl (70 mL), aqueous solution of saturated NaHCO$_3$ (70 mL), and water (140 mL). Organic layers were combined, dried with MgSO$_4$, and concentrated to yield a clear yellow oil. Product **82** was used without further purification in the following step. 9-Anthracenemethanol was dissolved in anhydrous DMF (5 mL) and NaH was added at 0º C. Mixture was stirred for 30 minutes, then compound (number) previously left under high-vacuum for 16 hours was added dropwise for 10 minutes and reaction was left overnight at room temperature. The mixture was diluted in CH$_2$Cl$_2$ (15 mL), washed wish NaHCO$_3$ (3x 15 mL), dried with MgSO$_4$ and solvent was evaporated under reduced pressure. Product was then resuspended in MeOH and *p*-toluenesulfonic acid (10.0 mg) was then added. Reaction was left to stir for 4 hours at room temperature and then interrupted with Et$_3$N. Solvents were evaporated, and compound **84** was obtained with 45% (0.51 g; 1.35 mmol) overall yield after purification by silica flash chromatography (Hexane/EtOAc 9:1). MW: 378. 55 g/mol. R$_f$= 0.73 (Hexane/EtOAc 7:3). δH (ppm) (CDCl$_3$; 400 MHz): 8.5-7.4 (9H, m, Ar); 5.41 (2H, s, CH$_2$-Ph); 3.62 (4H, m, 2 CH$_2$-O); 1,6 (4H, m, 2 CH$_2$); 1.37- 1.20 (8H, m, 4 CH$_2$).

11-(naphthalen-1-yloxy)undecan-1-ol(85) (RILEY; XU; BROCKHAUSEN, 20010; MONTOYA-PELEAZ et al., 2005).
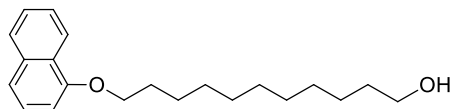
The same methodology to obtain compound **84** was used to obtain compound (number), however, naphthalen-1-ol was used in second step, instead of 9-Anthracenemethanol. Product **85** was isolated by silica flash chromatography (Hexane/EtOAc 9:1) and obtained with 30% yield (0.28 g; 0.9 mmol) MW: 314.46 g/mol. R_f= 0.71 (Hexane/EtOAc 7:3). δH (ppm) (CDCl$_3$; 400 MHz): 8.25- 6.75 (7H, m, Ar); 4.13 (2H, t, *J*= 6.4 *Hz*, CH$_2$-O); 3.62 (2H, t, *J*= 6.6 Hz, CH$_2$-O); 1.92 (2H, m, CH$_2$); 1.51 (4H, m, 2 CH$_2$); 1.45- 1.29 (8H, m, 4 CH$_2$).

Triethylammonium-1-octanoyl- H-phosphonate (87) (CROSSMANN, et al., 2002).
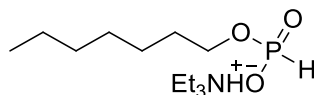
1-Octanol (0.2 g, 1.5 mmol) was dissolved in dry THF/pyridine (10:1; 11 mL). This solution was added dropwise over 10 min to a stirred solution of salicylchlorophosphite (0.36 g, 1.8 mmol) in dry THF (5 mL) under N$_2$ at room temperature *overnight*. The reaction mixture was quenched with 1 M triethylammonium hydrogen carbonate (TEAB) buffer solution (10 mL) and the resulting aqueous solution was stirred for 30 min. Chloroform (30 mL) was then added and the organic layer was separated and washed with 1 M TEAB buffer solution (3×10 mL), dried with MgSO$_4$, and concentrated under reduced pressure. The crude hydrogenphosphonate TEA salt **87** was used in the next experiment without further purification.

3.2.6. Methods for attachment of phospholipds

Triethylammonium-1-D-6-O-(2-azido-2-deoxy-α- D -glucopyranosyl)-3,4,5-tetra-O-benzyl-2-O-naphtylmethyl-myo-inositol-1-(octanoyl phosphate) (89)

(CROSSMANN, et al., 2002).
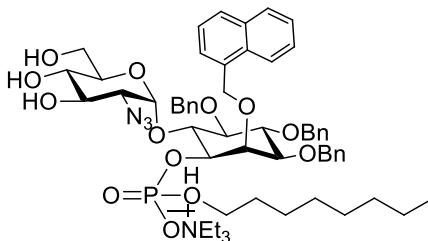
Each of the compounds **87** (0.1 g, 0.1 mmol) and **77** (0.2 g, 0.7 mmol) were previously dried overnight in a vacuum desiccator. They were then dissolved in dry pyridine (10 mL), pivaloyl chloride (0.23 mL, 2.1 mmol) was added and the resulting solution was stirred under N_2 at room temperature for 1 h. Freshly prepared solution of iodine (173 mg, 0.68 mmol) in pyridine/water (19:1; 10 mL) was then added and reaction mixture continued stirring for 2 hours. After the addition of $CHCl_3$ (30 mL), the organic solution was washed successively with 5% aqueous $NaHSO_3$ (25 mL), water (25 mL), and 1 M TEAB buffer solution (3×15 mL), dried with $MgSO_4$, and concentrated under reduced pressure. Compound **88** was then subjected to partial deprotection of benzoyl groups by adding NaOMe 1M to a solution of (number) in methanol (5 mL), until pH 9-10. Reaction mixture was filtered in Dowex resin with chloroform/methanol (19:1) and 0.1% Et_3N to give compound **89** which was separated by semi-prep. HPLC (isolation will be further described), with 8% yield (8.0 mg; 0.08 mmol). MW: 1071.24 g/mol. R_f= 0.5 (EtOAc/methanol 8:2). δH (ppm) (DMSO-D; 400 MHz): 7.9-7.15 (22H, m, Ar); 5.91 (1H, d, *J*= 3.1 Hz, H-1); 5.14- 4.55 (10H, m, 8- CH_2-Ph, H1', H-6´); 4.47 (1H, m, H-2'); 4.22 (1H, t, *J*= 9.3 Hz, H-5'); 4.15 (1H, m, H-4'); 3.89- 3.77 (6H, m); 3.57 (1H, m, H6a); 3.0 (4H, m, 2 CH_2); 2.9 (1H, dd, *J*= 10.2 Hz; 3.5 Hz, H-2); 1.53 (2H, q, CH_2); 1.33- 1.14 (8H, m, $4CH_2$), 0.84 (3H, t, *J*= 6.8 Hz, CH_3). ^{3}P NMR (202 MHz, $CDCl_3$): -0.84. ^{13}C NMR (125 128.49, 128.15, 127.97, 95.64, 81.69, 82.29, 81.51, 76.96, 76.73, 74.49, 74.46, 71.76, 72.11, 64.71, 63.34, 45.63, 40.17, 31.60, 31.10, 29.26, 25.82, 22.29, 22.43, 14.22, 9.19 (Signals based on HSQC and HMBC). HRMS (ESI-) *m/z* calcd. for $C_{52}H_{63}N_3O_{13}P^-$ 968.4182, found 968.4152 [M-H].

Triethylammonium-1-D-6-O-(2-azido-2-deoxy-α- D -glucopyranosyl)-3,4,5-tetra-O-benzyl-2-O-naphtylmethyl-myo-inositol-1-(1-undec-11-O-naphthyl-phosphate)(91)
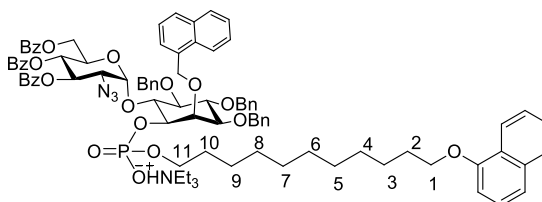
Each of the compounds **90** (0.03 g, 0.006 mmol) and **77** (0.02 g, 0.005 mmol) were previously dried overnight in a vacuum desiccator. They were then dissolved in dry pyridine (10 mL), pivaloyl chloride (47μL, 0.38 mmol) was added and the resulting solution was stirred under N_2 at room temperature for 1 h. Freshly prepared solution of iodine (173 mg, 0.68 mmol) in pyridine/water (19:1; 10 mL) was then added and reaction mixture continued stirring for 2 hours. After the addition of $CHCl_3$ (15 mL), the organic solution was washed successively with 5% aqueous $NaHSO_3$ (15 mL), water (15 mL), and 1 M TEAB buffer solution (3×10 mL), dried with $MgSO_4$, and concentrated under reduced pressure. Compound **91** was purified by flash chromatography (stationary phase: silica, mobile phase: DCM/Methanol 9:1) and obtained as a clear oil with 20% yield (6.0 mg; 4.0 μmol). R_f= 0.68 DCM/Methanol 9:1). MW: 1464.57 g/mol. δH (ppm) (CDCl₃; 500 MHz): 8.27-7.07 (43H, m, Ar); 6.80 (1H, d, J= 7.4 Hz, Ar-Nap), 5.99 (1H, J= 3.2Hz H-1); 5.91 (1H, t, J= 9.9 Hz, H-4); 5.46 (1H, t, J= 9.9 Hz, H-3); 5.15 (1H, d, J=11.8 Hz, CH₂-Ph); 5.11(1H, d, J=11.2 Hz, CH₂-Ph); 5.04 (1H, d, J=10.7 Hz, CH₂-Ph); 4.99 (1H, d, J=10.7 Hz, CH₂-Ph); 4.87 (1H, d, J=10.2 Hz, CH₂-Ph); 4.80 (1H, m); 4.73 (1H, d, J=11.2 Hz, CH₂-Ph); 4.68-4.52 (4H, m); 4.40 (1H, m); 4.22 (1H, d ap., J= 12.0 Hz, H-6a); 4.15 (1H, m); 4.10 (2H, t, J= 6.0 Hz, CH₂); 4.0- 3.85 (4H, m); 3.62-3.55 (2|H, m); (1H, dd, J= 12.4 Hz; 4.7 Hz, H-6b); 3.46 3.46 (1H, dd, J= 10.7 Hz, 3.7 Hz, H-2); 1.91 (2H, m, CH₂); 1.56 (4H, m, CH₂); 1.21 (13H, m, 5 CH₂, 1 CH₃). HRMS (ESI-) m/z calcd. For $C_{86}H_{87}N_3O_{17}P^-$ 1464.5778, found 1464.5713 [M – Et₃N]⁻.

1-D-6-O-(2-azido-2-deoxy-α-D-glucopyranosyl)-3,4,5-tetra-O-benzyl-2-O-naphtylmethyl-myo-inositol-1-(di-O-phenyl-phosphate) (92)
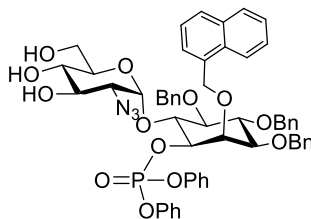
To a solution of compound **77** (0.05 g; 4.0 μmol) in dry DCM, Et₃N (0.01 mL; 0.04 mmol) and catalytic amount of DMAP were added, under inert atmosphere. Next, diphenyl chlorophosphite (0.01 mL; 0.04 mmol) was then carefully added to the stirring mixture. The reaction was left stirring for 72 hours. Solvents were evaporated and the product **92** was purified by column chromatography (toluene/EtOAc 9.5: 0.5) and obtained as a white solid in 82% yield (0.04 g; 3.3 μmol). MW: 1321.43 g/mol. R_f= 0.53 (Hexane/EtOAc 7:3) δH (ppm) (CDCl₃; 500 MHz): 8.27-7.07 (41H*, m, Ar); 5.91 (1H, t, J= 10.0 Hz, H-4); 5.58 (1H, J= 3.2Hz H-1); 5.48 (1H, t, J= 9.9 Hz, H-3); 5.22 (1H, d, J=11.6 Hz, CH₂-Ph); 5.08 (1H, d, J=11.4 Hz, CH₂-Ph); 5.01 (1H, d, J=11.7 Hz, CH₂-Ph); 4.93 (1H, d, J=10.4 Hz, CH₂-Ph); 4.82 (1H, d, J=11.4 Hz, CH₂-Ph); 4.79-4.71 (5H, m); 4.66 (1H, t, J= 2.2 Hz, H-3'); 4.62 (1H, d, J= 9.7 Hz); 4.28-4.19 (2H, m); 3.84 (1H, dd, J= 12.3 Hz; 5.0 Hz, H-6b); 3.67-3.61 (2H, m); 3.22 (1H, dd, J= 10.7 Hz, 3.7 Hz, H-2). HRMS (ESI+) *m/z* calcd. for C₇₇H₆₉N₃O₁₆P 1321.4337, found 1322.4409 [M+1]⁺ and *m/z* calcd. for C₇₇H₆₉N₃O₁₆ 1321.4337, found 1344.4245 [M+Na]⁺. *Aromatic signals could not be properly integrated due to the chloroform signal.

*3.2.7. HPLC Separation of compound **89** Using Reverse Phase C18 Chromatography*
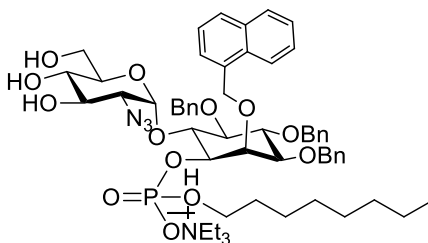
Separation was performed in DIONEX Ultimate 3000 instrument equipped with UV/vis detector and using column Phenomenex Luna 5 C18 (2) (10 x 250 mm, CV ~ 19.6 mL). Compound **89** was pre-purified in silica gel chromatography using 3 g of

silica and linear gradient CHCl₃/MeOH (starting with 100% CHCl₃ to 90% CHCl₃ and 10% MeOH). The product was then dissolved in MeOH to give concentration of about 4 mg/ml. Sample was filtered through 0.45 µm filter disc (The disc was washed it with MQ to remove preservatives). The sample in methanol was eluted with 50 mM Et₃NHOAc, pH 6.8 with 1.5% MeCN (Bottle A) and MeCN (Bottle B) at a flow rate of 5 ml/min and detection with on-line UV detector to monitor A₂₇₄. (Chromatograms in Appendix). The separation was done with 1 CV of isocratic elution with buffer in line A and 20% MeCN (line B). Then, linear gradient was applied from 20% to 100% MeCN for 5 CVs. More 4 CVs were eluted with 100% MeCN and then back to initial conditions (80% Buffer and 20% MeCN). Fractions containing the desired compound were pooled and freeze-dried. Time for full injection separation: 40 minutes.

3.2.8. Overall deprotection

1-D-6-O-(2-amino-2-deoxy-α-D-glucopyranosyl)-myo-inositol-1-(octanoyl-phosphate) (30a) (CROSSMANN, et al., 2002)
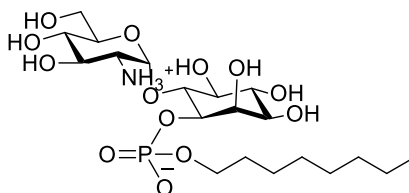
A solution of **89** (8 mg; 0.08 mmol) in methanol (1 mL) containing Pd on carbon (5.0 mg) was stirred under 10 atm of hydrogen for 1 hour. Then the mixture was before it was filtered on a bed of Celite and washed several times with Et₂O. The eluent was concentrated under reduced pressure and then product was purified in C₁₈ cartridge (0.5g) MeCN/Et₃NHOAc, pH 6.8 to give compound **30a** in 70% yield (0.3 mg, 5.6 µmol). MW: 533.50 g/mol. (8 mg; 0.08 mmol). HRMS (ESI-) *m/z* calcd. For $C_{20}H_{40}NO_{13}P$- 533.2237, found 532.2170 [M – H]⁻ and 533.2195.

3.2.10. Injection of standard **30a** for LC-MS profile

Injection of compound **30a** was performed on Zevo TQ-S Acquity UP-LC made by WATERS with loop of 10.0 μL. Injections of 2-7.5 μl were done with the diluted compound (10 μM in MeOH/water; calculation based on estimate of sample quantity to be about 0.1 mg or less) in column *Hypercarb* 1 x 100 mm, particle 5 μm, CV ~ 78.5 μL, and flow rate of 80 μl/min. Detection of the product by ESI(-). The following mobile phases were applied: Mobile phase **A**: Formic acid 0.3% (79.5 mM) brought to pH 9.0 with ammonia; mobile phase **B**: Acetonitrile; mobile phase **C**: Acetonitrile 80%, water 20 %, TFA 0.1%. A peak at retention time= 22 minutes.

3.2.11. Preparation of Euglena gracilis microsomal membranes

Euglena gracilis were grown in EG-JM (*Euglena gracilis*-Jaworski's medium for freshwater algae), for 13 days in dark conditions. Protocol for the media was obtained in the website: www.ccap.ac.uk. Procedures for isolation of microsomal membranes were performed between 0 and 4 °C. *E. gracilis* cells were de-flagelated by freezing to 0 ºC for 18 hours. re-suspended in *Euglena* lysis buffer [20 mM, pH 7.0 HEPES/KOH, 50 mM NaCl, plant protease inhibitor (1 tablet per 100 mL) and ribonuclease A (1 mg)] and disrupted by bursts of ultrasonic waves for 1 minute (1 second ON, and 3 seconds OFF) over three consecutive cycles. Residual un-lysed cells, large fragments and paramylon were removed by centrifugation (300 g for 3 min) and supernatant was centrifuged at 4200 g for 30 min to remove mitochondria. The supernatant was layered onto a 1.5 M sucrose cushion in 20 mM HEPES buffer (pH 7.0) and centrifuged at 15000 g for 45 min. The supernatant was removed and layered over a step gradient consisted of 1.3 M, 1.0 M, 0.8 M and 0.5 M sucrose in 20 mM HEPES buffer (pH 7.0). The separation of microsomal fraction was achieved by centrifugation at 150000 g for 3 h. Microsomal-enriched fractions were collected, re-suspended in 20 mM HEPES buffer (pH 7.0) and centrifuged at 150000 g for 2 h. The pellets were re-homogenised in 20 mM HEPES buffer (pH 7.0) and aliquots of the membranes were put into Eppendorfs to be further stored at -80 °C freezer. Bradford test was used to check protein concentration.

4. RESULTS AND DISCUSSION

_____

4.1. Experimental Planning

Euglena gracilis is being used by the group of professor Rob Field (John Innes Centre-Norwich/UK) as a tool to investigate important glycan pathways in eukaryotic cells. Based on the fact that this free-living algae belongs to the same phylum as tripanosomatids, such as *T cruzi*, this work proposed the synthesis of three GPI anchor analogues (compounds **30a-c**, Figure 8) to investigate the scope that *E. gracilis* could serve as a safe protozoan model to study GPI anchor pathways. On a search for better targets in *T. cruzi*, compounds **30a-c** could be useful tools for either to uncover GPI anchor biosynthesis, acting as substrates, or to inhibit this pathway. Validating the studies of synthetic GPI anchor derivatives in *E. gracilis* GPI pathway would give clues on the application of the same methodology on *T. cruzi*, with the benefit of working on validation of a methodology in a non-pathogenic organism.
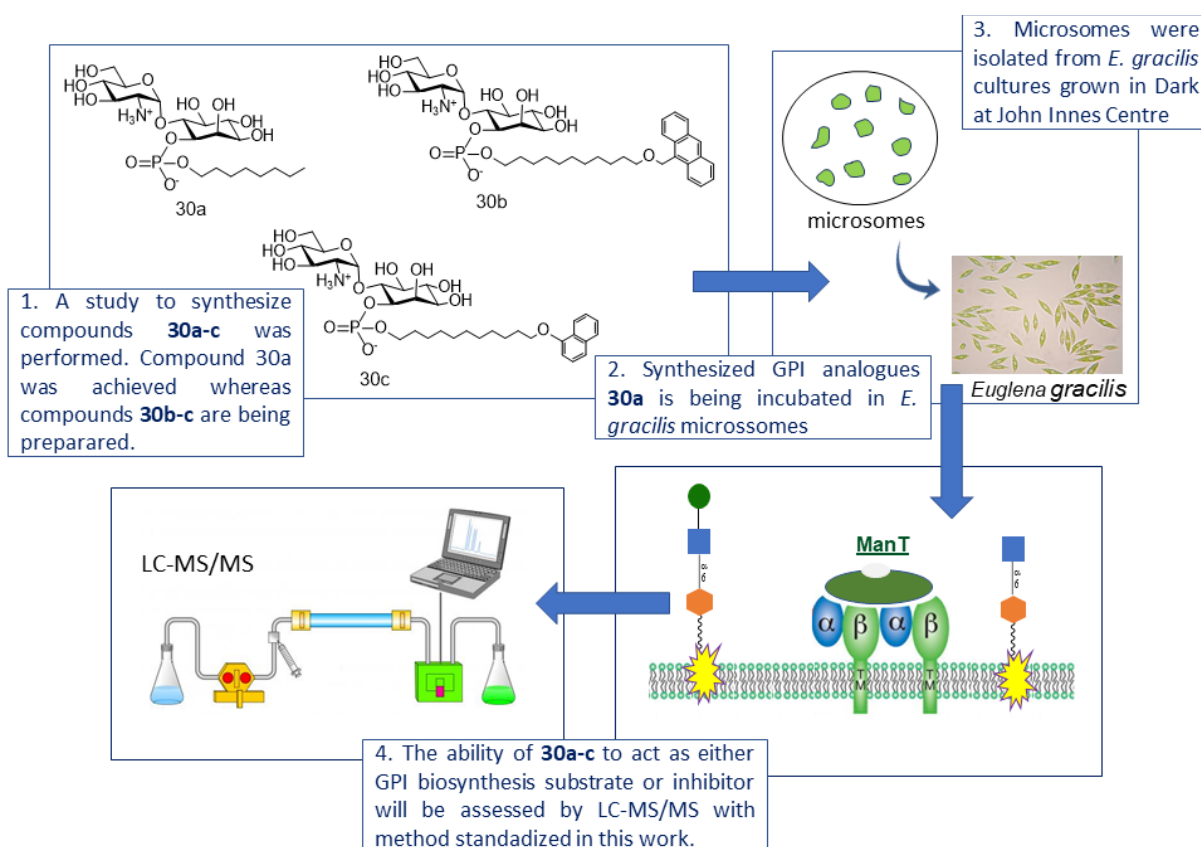
Figure 8: Experimental planning with overall view of the proposed work.

It is important to highlight that the GPI anchors were selected as a possible target due to the high variety of molecules involved in protozoan parasite's virulence.

These virulence structures are usually a point of mutation for the parasite's protection against the host's immune system and drugs (CARDOSO et al., 2013; McCONVILLE; FERGUSON, 1993).In spite of that, most protozoan's GPIs keep a conserved core which can be explored for the inhibition of several protozoan anchored proteins .

Thus, we proposed the use of microsomal membranes (microsomes) of *E. gracilis* as a source of enzymes that participate in GPI anchor biosynthesis. Those membranes are Golgi and Endoplasmic reticulum residues that, when properly isolated and stored, keep their active enzymes for up to one year. *Euglena gracilis* was then grown in dark for later isolation of the microsomes with well stablished methodology and the assays with the synthesized compound **30a** is under validation (GILLOTT; TRIEMER; VASCONCELOS, 1980). Compounds **30b-c** are yet being prepared.

4.2. Synthesis of Proposed Molecules 30a-c

To achieve the desired products, three different blocks were synthesised separately for the further union of each ready block at one time, in a linear synthesis. Moreover, a study towards orthogonal protection and deprotection was necessary with each of the moieties to afford the right linkage and right configuration of the blocks and final compounds.

Retrosynthesis of targeted molecules is presented in Scheme 4. The pseudo disaccharide **30** (Scheme 1) is composed by a *myo*-inositol unit and a glucosamine moiety, connected through the anomeric position (C-1) of donors **32** or **33a-d** with position C-6 of acceptor **34**, in an α configuration, as observed in the *T. cruzi* GPI anchor. A hydrocarbon chain would be linked to the *myo*-inositol block as a phosphodiester to simulate the GPI lipid part, and at the extremity of this chain, a fluorophore, such as naphthol or anthracenyl derivatives could be attached to track any metabolic change during the analysis of the assays in microsomal membranes of *Euglena gracilis* by liquid chromatography coupled to mass spectrometer (LC-MS).

Compound **31** was obtained via *O*-glycosylation reaction. According to classical theory, glycosylation reactions occur between a glycosyl donor and an acceptor in the presence of a promoter. Thus, for this work, a block of glucosamine derivative (Compounds **32** and **33a-d**, Scheme 4) was prepared as five different glycosyl

donors for a *myo*-inositol block as an acceptor to give **31** that mimic the natural GPI component.
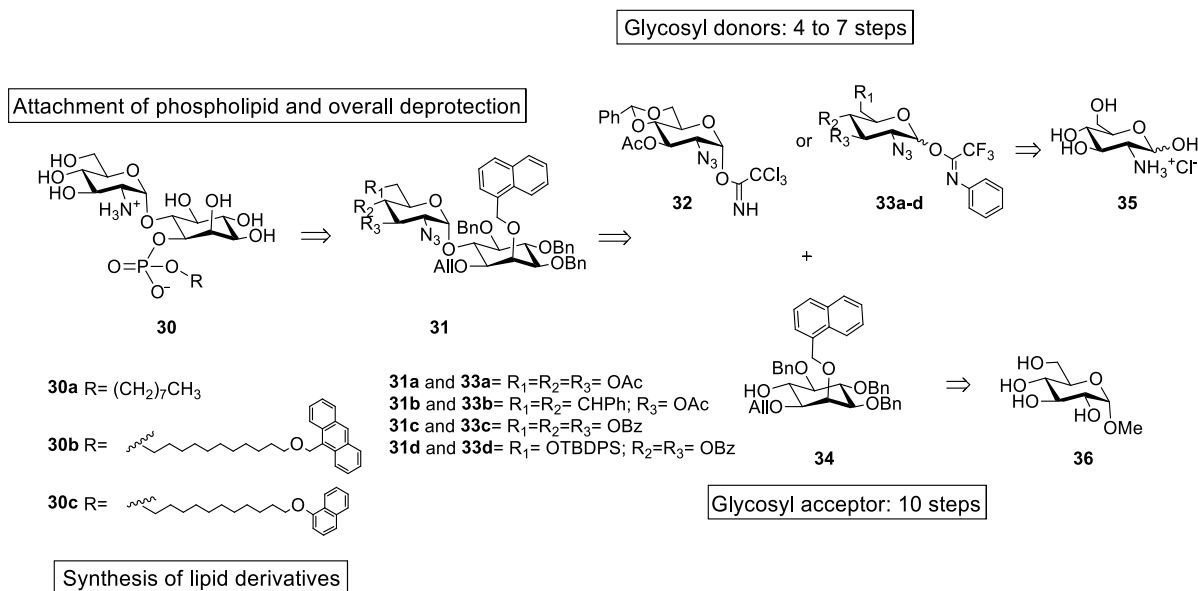
Scheme 4: Retrosynthesis of proposed compounds **30a-c**.

Compounds **32 and 33a-d** were synthesised from D-glucosamine hydrochloride (**35**) in four different ways to explore the influence of several protecting groups over the anomeric configuration on *O*-glycosylation reactions since the α-linkage between **32**, **33a-d** and **34** was required to maintain structural similarities to GPI. The activator groups of choice for the donors were trichloroacetimidate and *N*-phenyl-trifluoroacetimidate due to good accessibility, stability and effectiveness of *O*-glycosylation of complex molecules when compared to other classical glycosyl donors (YU, TAO, 2001). *Ferrier* rearrangements strategy was pursued for *myo*-inositol acceptor formation using methyl α-D-glucopyranoside (**36**) as starting material in order to obtain the regioselective free hydroxyl group at C-6 of the cyclitol in the corrected configuration (SWARTS, GUO, 2010; BOONYARATTANAKALIN et al., 2008; LIU; STOCKER; SEEBERGER, 2006). Furthermore, a different protecting group at C-1 of *myo*-inostol moiety was *O*-allyl group, which enabled the selective deprotection for further introduction of lipid derivatives. These phospholipid moieties were attached as phosphodiester to compounds **30a-c** (Scheme 4) via H-phosphonate strategy according to Crossmann and co-workers (2002). Small hydrocarbon chains were used as choice for the lipidic part (8 to 11 carbons) to avoid

solubility issues. All building blocks will be better discussed in their respective section.

4.2.1. Synthesis of donors

4.2.1.1. First strategy: Synthesis of trichloroacetimidate donor

Initially, the proposed donor **32**, containing trichloroacetimidate leaving group, was synthesized in 5 steps, according to Scheme 5 (NYFFELER et al., 2002; LINDBERG et al., 2002; YAN; KAHNE, 1996; SCHIMIDT; MICHEL, 1980, ANSELME; FISCHER, 1969). The benzylidene group would allow the deprotection of C-4 or C-6 selectively, and this attempt would permit the insertion of a residue of α-mannose (position C-4) or aminoethyl phosphonate (position C-6), according to *T. cruzi* GPI core structure, for example. A proper group at C-2 would favour the desired configuration on *O*-glycosylation reaction. Additionally, the methodologies to obtain **32** were already stablished and standardized in our research group (CAMPO et al., 2015; MOROTTI et al., 2015; ANDRADE, 2008).
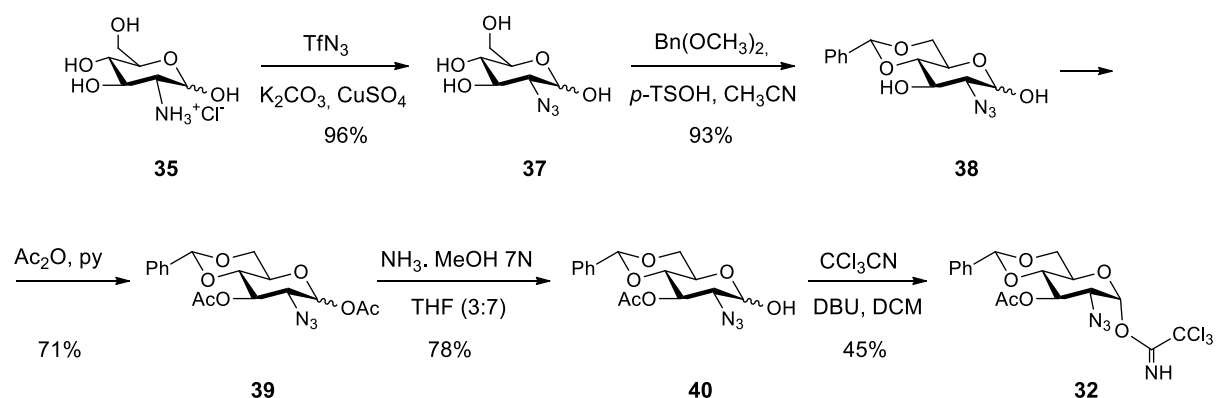
Scheme 5: Proposed synthetic route for donor **32**

Since the desired final product **30** might be linked at C-1 to an inositol moiety in α-configuration, choosing a proper protecting group for the amine at C-2 is essential to favour the formation of the right anomer. Acyl groups (acetyl and benzoyl groups, for example) at C-2 of the pyranose ring promote the neighbouring group participation, also called anchimeric assistance (SMITH, MARCH 2013; WINSTEIN; BUCKLES, 1942), which consists on the involvement of the protecting group at C-2 in the stabilization of an *acyloxonium* ion, during *O*-glycosylation reactions (Scheme

6). This phenomenon favours the attack by the nucleophile by the upper face of the pyranose ring, leading to the formation of β-*O*-glycosylated compounds.
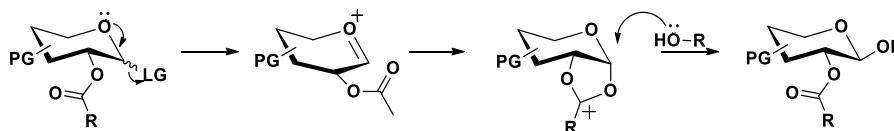
Scheme 6: Neighbouring participation on *O*-glycosylation mechanism of pyranoses.

Thus, the protecting group of choice for C-2 in this work was the non-participating azido group, which could be easily obtained by diazo transfer reaction (NYFFELER et al., 2002; ANSELME; FISCHER, 1969).
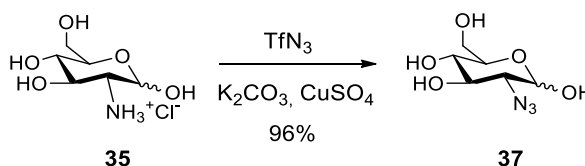
Scheme 7: Conversion of the amino group in **35** to azido group with diazo transfer reaction

Initially, the reagent azide triflate was generated *in situ* by slow addition of triflic anhydride to a solution of sodium azide in dichloromethane (DCM) (Scheme 8).
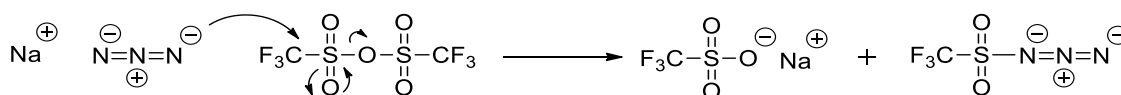
Scheme 8: *In situ* generation of triflic azide from sodium azide and trifluoromethanosulfoic anhydride.

After stirring for 2 hours, the solution was neutralized and immediately poured to a solution of glucosamine hydrochloride (compound **35**, mixture of α and β anomers) in water/methanol containing potassium carbonate and copper sulphate. The reaction occurred at room temperature for 24 hours. Product **37** was obtained in 96% yield, after neutralization of the reagents and purification by flash chromatography. Azido group was confirmed by infra-red (IR) spectroscopy, in which a typical strong band of *N=N=N* stretch could be observed at 2150 cm^{-1} (See Appendix).

The proposed mechanism[1] of reaction involves the attack of the nitrogen of the monosaccharide unit to one of the nitrogens of the triflate reagent forming a complex. Deprotonation leads to the formation of a copper-neutralized dianion tetrazene intermediate. In sequence, this intermediate is converted, via reverse bipolar cycloaddition, to the imino-copper-triflyl complex and, then, to the product containing azido at C-2 (NYFFELER et al., 2002) (Scheme 9).
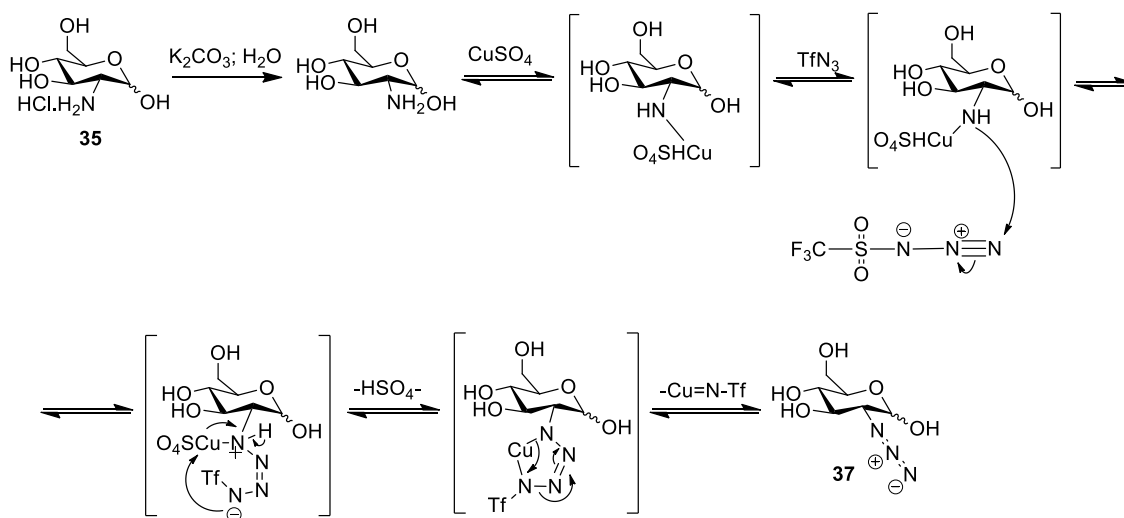
Scheme 9: Proposed mechanism for the diazo-tranfer reaction.

The next step was the protection positions C-4 and C-6 of the pyranose **37** via *trans*-acetalization. Thus, compound **37** was subjected to reaction with benzaldehyde dimethyl ketal and *p*-toluenesulfonic acid to form product **38** with 89% yield (Scheme 10).
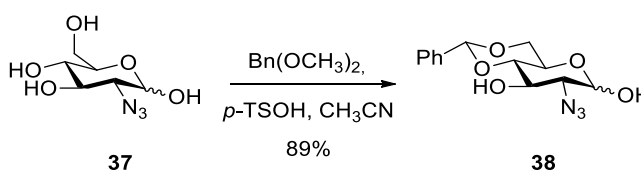
Scheme 10: Reaction to obtain benzylidene derivative **38**.

The ^{1}H NMR spectra of **38** presented signals at 7.51-7.39 ppm, with relative integration for five hydrogens, referring to the aromatic ring and singlet at 5.55 ppm relating to the methinic hydrogen. Also, the compound's α/β ratio was 1:1, based on the integration of the H-1 signals (Appendix).

---

[1] All the mehanisms of reaction presented in this work are simplified mechanisms.

The mechanism of reaction is proposed in Scheme 11. The first step consists of the acid-catalysed addition of the alcohol to the acetal carbon to give a hemiacetal, followed by a substitution that occurs by the S$_N$1 mechanism. The mechanisms of *trans*-acetalization is reversible, in which the acid promotes the hydrolysis of the product if in excess (BRUCKNER, 2010).
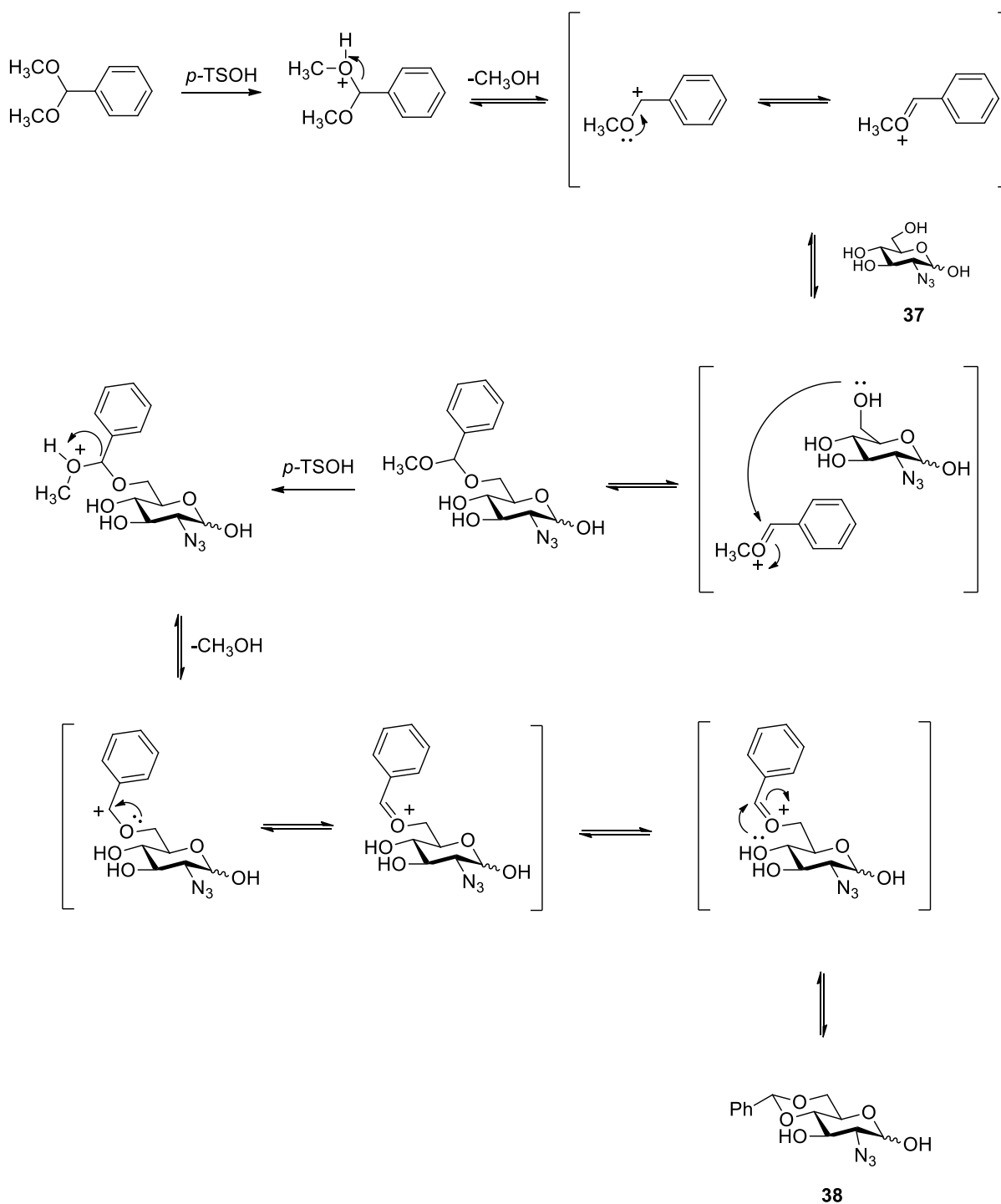
Scheme 11: Proposed mechanism of *trans*-acetalization of **37** to form compound **38**.

Subsequently, compound **38** was subjected to classical acetylation reaction at C-1 and C-3 with acetic anhydride and pyridine. (Scheme 12). Product **39** was obtained, after purification on column chromatography, with 71% yield.
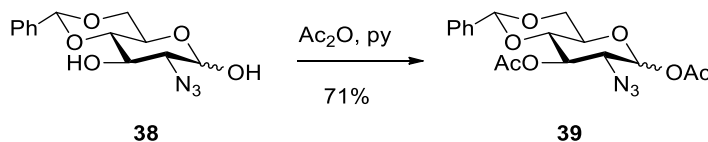
Scheme 12: Acetylation of positions C-3 and C-1 of compound **38**.

In the ^{1}H NMR spectra (Appendix) the signals at 6.28 ppm and 5.60 ppm related to H-1 and H-3, were more deshielded when compared to the starting material's (**38**) spectra. The α/β-anomers ratio was 1:1.5, based on the relative integration of H-1 signals. Moreover, two singlets in the region of 2.20 and 2.15 ppm with relative integral for three hydrogens (for the β isomers) were characterized as the methyl hydrogens from the acetyl groups.

The mechanism of reaction comprises the nucleophilic attack of the pyridine to the acetic anhydride, leading to the formation of a reactive intermediate susceptible to the attack of the free hydroxyl groups of the pyranose ring and consequent formation of the *O*-acetyl groups. In addition, pyridine also assists in the uptake of the protons generated in the reaction medium (Scheme 13).
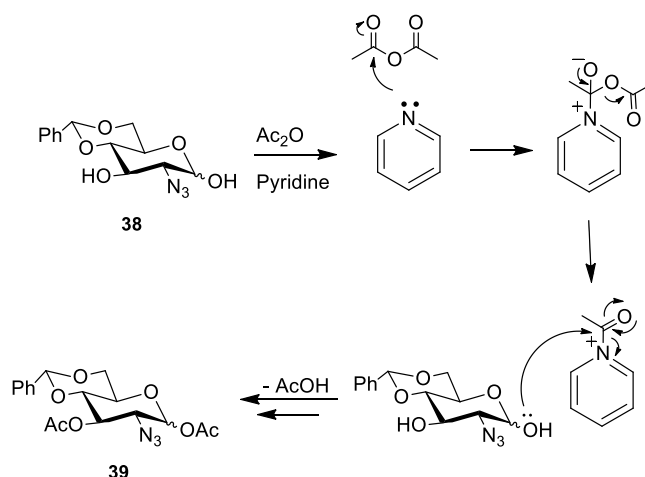
Scheme 13: Mechanism of reaction of acetylation in the presence of acetic anhydride and pyridine

After that, compound **39** was subjected to the selective deprotection of the C-1 acetyl group (Scheme 14). The reaction was carried out by treating **39** in THF with ammonia solution in methanol. The reaction occurred at room temperature for 30

minutes to 2 hours, when the TLC chromatography of the reactions showed the total consumption of the starting material. After bubbling nitrogen gas to help evaporate the remaining ammonia from the reaction mixture, evaporation of the solvents and purification on a column chromatography gave compound **40** with 78% yield.
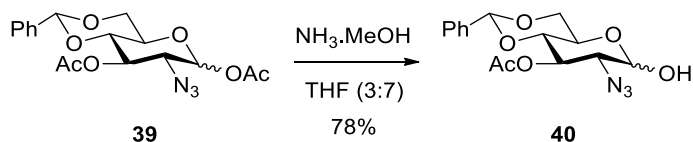
Scheme 14: Reaction of selective deprotection of anomeric position of **39**.

The ^{1}H NMR spectra (Appendix) showed a singlet with relative integration for 3 hydrogens referring to the only acetyl group at C-3 at 2.18 ppm. The doublets related do H-1 (5.50 ppm for α and 4.81 ppm for β, respectively) were observed as more shielded signals when compared to the starting material (6.28 ppm for α and 5.65 ppm for β anomer for precursor **39**, Scheme 14).

In this reaction mechanism, ammonia acts as a nucleophile by attacking the carbonyl carbon of the acetyl group from the anomeric position, following the formation of the hemiacetal, as shown in Scheme 15 (FIANDOR et al., 1985). The anomeric position is the first one to be attached by the nucleophile due to the anomeric effect providing higher reactivity of position 1, when compared to position 3. A longer length of reaction or higher equivalents of ammonia in the reaction may also lead to deacetylation at C-3 (FENG; BAGIA; MPOURMPAKIS, 2013).
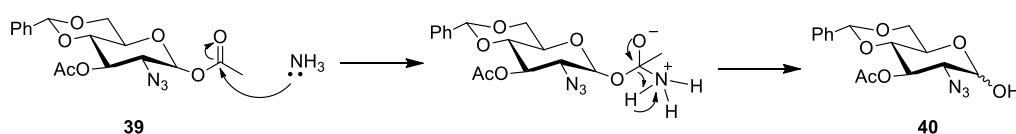
Scheme 15: Proposed mechanism of reaction for selective deprotection of anomeric position with ammonia.

In the latter step, functionalization of the anomeric position of compound **40** with a leaving group was necessary. The trichloroacetimidate group was initially described by Schmidt and Michael in 1980 and became widely used from the 1990s, since donors containing this leaving group have better stability when compared to donors bearing bromine or chlorine, and also provide good yields in *O*-glycosylation reactions (SCHMIDT; KINZY, 1992; SCHMIDT; MICHAEL, 1942). Thus, compound

40 was subjected to reaction with trichloroacetonitrile and DBU base, in an ice bath and under inert atmosphere, for one hour (Scheme 16). After this period, it was possible to observe the formation of a non-polar product in relation to the starting material **40**, by TLC analysis of the reaction mixture. Product **32** was purified by column chromatography and obtained in moderate yield (45%), compared to literature (above 90%) (SCHMIDT; KINZY, 1992). Finally, the overall yield to obtain compound **32** was 31%
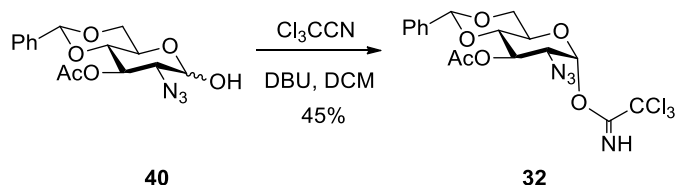
Scheme 16: Synthesis of trichloroacetimidate donor **32**.

The ¹H NMR mechanism is explained according to Scheme 17. DBU removes a proton from the hydroxyl group of the sugar, favoring the nucleophilic attack to the reagent trichloroacetonitrile. Once the alkoxide attacks the nitrile carbon, protonated DBU donates its proton to the nitrogen of the nitrile, forming the imidate derivative (MILJKOVIC, 2009).
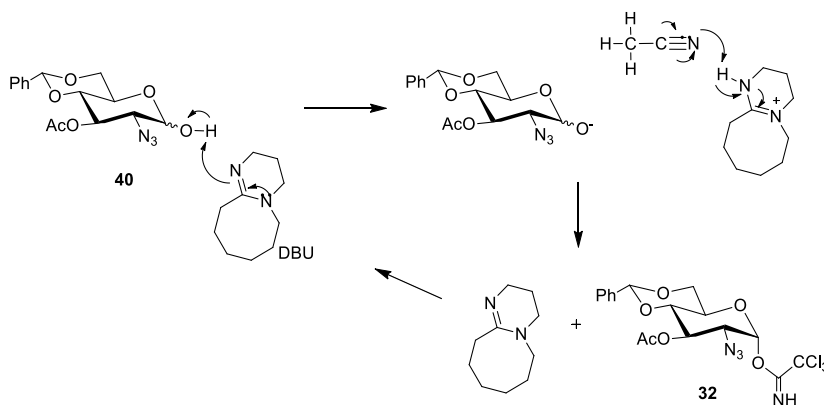
Scheme 17: Proposed mechanism of trichloroacetimidate attachment with DBU as base.

The ¹H NMR spectra (Appendix), showed a singlet at 8.82 ppm, which is characteristic for nitrogen-coupled hydrogen, present in the imidate group. Moreover, the doublet which corresponds to the hydrogen of the anomeric position was identified at 6.50 ppm being more deshielded when compared to the starting material (5.50 ppm for α and 4.81 ppm for β in compound **40**). The value of the coupling constant $J_{1,2} = 3.7$ Hz indicates the formation of only α isomer, a fact that can be explained by the base used in the reaction. Strong bases, such as DBU, lead to the

formation of α, thermodynamic product, whereas weak bases induce the formation of the β product, obtained by kinetic control (MILJKOVIC, 2009).

4.2.1.2. Second strategy: Synthesis of trifluoroacetimidate donors

A second series of donors were proposed during sandwich proposal at John Innes Centre/England under supervision of Professor Robert A. Field and Dr. Irina Ivanova. Based on the well-established influence of the protective groups of the glycosyl donors on the anomeric configuration (GUO; YE, 2010), four distinct protecting groups were selected, namely acetyl (**33a**), benzylidene (**33b**), benzoyl (**33c**) and *terc*-butyldiphenylsilyl (TBDPS) (**33d**) (Figure 9) to verify their impact over the preference on α configuration and on the yield of *O*-glycosylation reactions. The leaving group of choice was the *N*-phenyl-trifluoroacetimidate, which was being used by Field's group, and also reported in the literature as a good alternative over trichloroacetimidate donors for *O*-glycosylation with complex acceptors (YANG et al., 2012; YU & TAO; 2002). Moreover, *N*-phenyl trifluoroacetimidate donors have demonstrated to minimize the number of by-products that is often encountered in a trichloroacetimidate glycosylation, considering the leaving group liberated from the donor can give rise to *N*-glycosides (YU; SUN, 2010; TANAKA et al., 2005). The donors of this series were obtained in overall yields varying from 34% to 64%
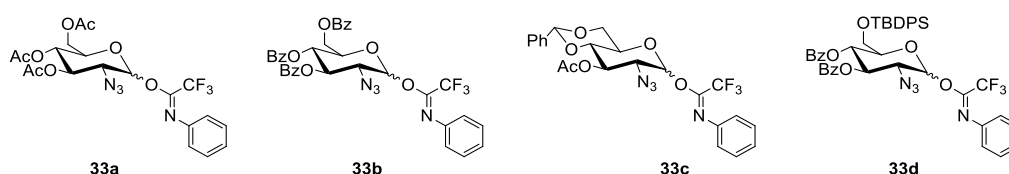
Figure 9: Proposed donors for the study of *O*-glycosylation reactions.

Typically, a protecting group is introduced into a carbohydrate moiety to temporarily block a functional group from the required reagents or chemical environment in a specific step. Protecting groups in carbohydrates not only distinguish the same sort of functional groups to expose the one needed to be reacted, but also confer effects to the molecules in *O*-glycosylation reactions. They can increase or decrease the reactivity, participating in the reactions and affecting the stereochemical results of *O*-glycosylation (GUO, YE, 2010).

4.2.1.2.1. Synthesis of acetylated donor **33a**

Acetyl groups are widely used as protective groups in organic chemistry due to easy assessment, frequently leading to good yields in protection and deprotection steps. Furthermore, these groups have been used to improve carbohydrate-based molecules as temporally protective groups or to improve absorption of very polar molecules in physiological environment (LU; GAO; GUO, 2015; GREENE, WUTS, 2007; PÉTURSSON, 1997). In this context, a 3,4,6-*O*-acetyl- 2-azido 2-deoxy-glucopyranosyl trifluoroacetamidate donor was proposed for *O*-glycosylation reaction.

The donor **33a** was obtained according to synthetic route depicted in Scheme 18. Initially, the free hydroxyl groups of compound **37**, previously described, were acetylated with acetic anhydride and pyridine (99% yield, compound **41**), followed by selective deprotection of the anomeric position (compound **42**, 78% yield) with ammonium solution in methanol 7N with same methodologies discussed in earlier Section (*4.2.1.1*).
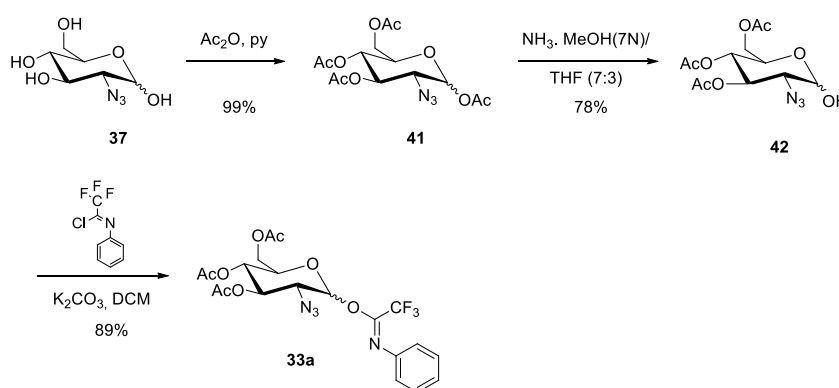
Scheme 18: Synthesis of 2-deoxy-2-azido-3,4,6-tri-*O*-acetyl-*N*-phenyl trifluoroacetimidate donor **33a**

The last step consisted on the attachment of leaving group *N*-phenyl-trifluoroacetimidate, according to Yu & Tao (2002), which gave donor **33a** with 89% yield.

The mechanism of reaction involves the formation of alkoxide for the further attack to the olefinic carbon (Scheme 19). All products were characterized by ^{1}H NMR (Appendix) and spectra are in accordance to literature (WALVOORT et al., 2011).
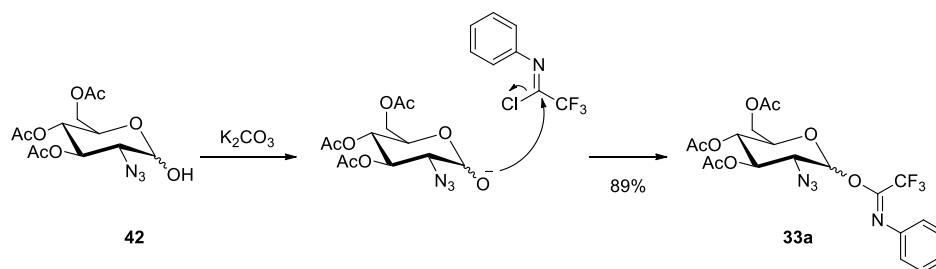
Scheme 19: Proposed mechanism for attachment of *N*-phenyl-trufluoroacetimidoyl group.

4.2.1.2.2. Synthesis of donor containing benzylidene ring *33b*

In order to compare results in *O*-glycosylation with the first proposed donor containing trichloroacetimidate as leaving group (compound **32**), a version of the same donor containing *N*-phenyl-trifluoroacetamidate was proposed. Donor **33b** was obtained from intermediate **40** accordingly to methodologies already discussed in Section *4.2.1.1* in similar yields. The attachment of the *N*-phenyl-trufluoroacetimidoyl group gave donor **33b** with 84% yield (Scheme 20). NMR assignments were based on described 4,6-*O*-benzylidene trifluoroacetamidate donors (SATO et al., 2017; BEDINI; CIRILLO; PARRILLO, 2012) (Appendix).
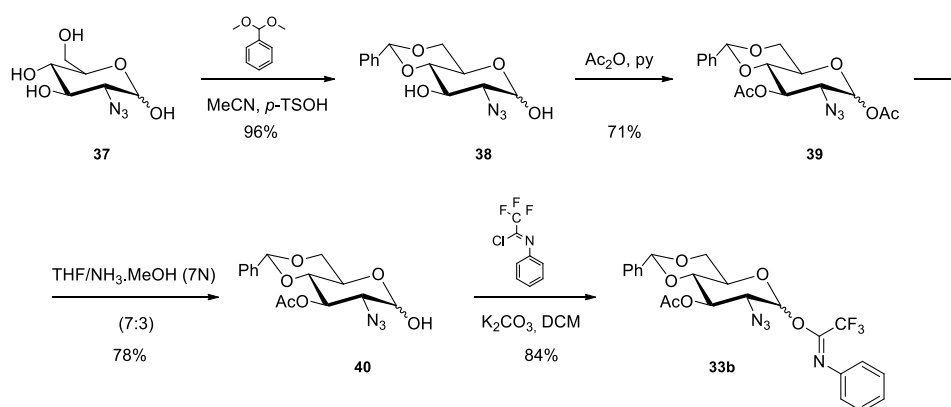
Scheme 20: Synthetic route for the preparation of donor **33b.**

4.2.1.2.3. Synthesis of benzoyl donor *33c*

Benzoyl protective groups are easily accessed using benzoyl chloride under basic conditions, which is a cheap strategy to protect carbohydrates, as described for acetyl groups. Furthermore, some advantages can be highlighted, such as better stability when compared to *O*-acetyl groups and lower ability to migrate (*trans-*

esterification) (GREENE; WUTS, 1999). Thus, compound **33c** was planned and synthesised according to Scheme 21.
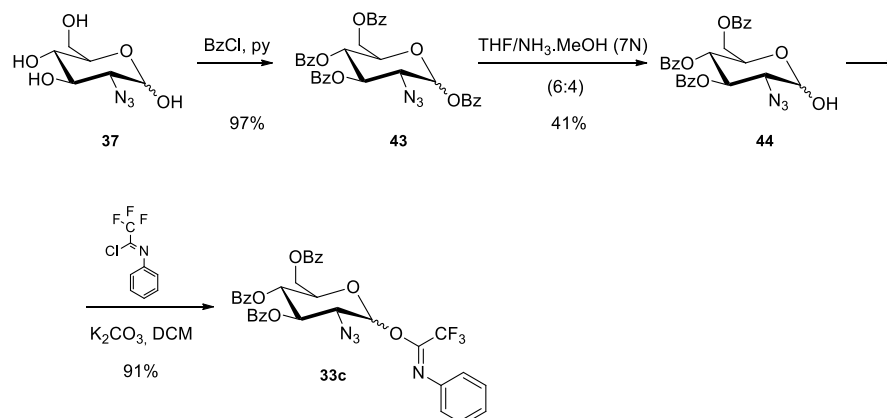
Scheme 21: Synthesis of donor **33c**

The common intermediate **37** was subjected to reaction with benzoyl chloride in pyridine to give the 2-azido-2-deoxy-1,3,4,6-*O*-benzoylated derivative **43**. For selective deprotection of anomeric position, an adjustment in the initial proportion of THF and NH$_3$.MeOH 7N (7:3) to 6:4 and longer hours of reaction was necessary to afford product **44** with 41% yield. Donor **33c** was synthesised according to procedures previously discussed for compounds 3**3a** and 3**3b** and was obtained in good yield (91%).

The ^{1}H NMR spectra (Appendix) showed two broad signals at 6.65 and 5.92 ppm related to the anomeric β and α hydrogens, respectively. These signals are in more deshielded region if compared to the precursor (5.49 ppm for the α Relative integration of signals located at the more deshielded area of the spectra (8.1-6.75 ppm) gave value close to 40 hydrogens, which are related to the aromatic hydrogens of both anomers (benzoyl and *N*-phenyl groups). Signals associated to *N*-phenyl groups were assigned at 7.15 ppm with integration to 2 hydrogens (one of each anomer) and 6.80 ppm with relative integration for 4 hydrogens.

4.2.1.2.4. Synthesis of donor containing 6-OTBDPS, *33d*

The steric influence of a bulky *terc*-butyldiphenylsilyl (TBDPS) group at C-6 position of the glucopyranose donor on the α/β ratio in *O*-glycosylation reactions led to the preparation of **33d** (Scheme 22). Previous results published by Biao Yu's group (2015) showed that the presence of bulky protecting groups at C-6 position

favours the formation of α-linked glycosides, since it provoques a sterical hindrance at the β-face of the carbohydrate, leaving only the α-face available for the nucleophilic attack. However, there is no report on the literature of glucopyranose containing both *N*-phenyl trifluoroacetamidate and 6-*O*-TBDPS groups. The synthetic route proposed for synthesis of donor comprising bulky group on C-6 position of the 2-azido glucose derivative (**3d**) is presented in Scheme 22.
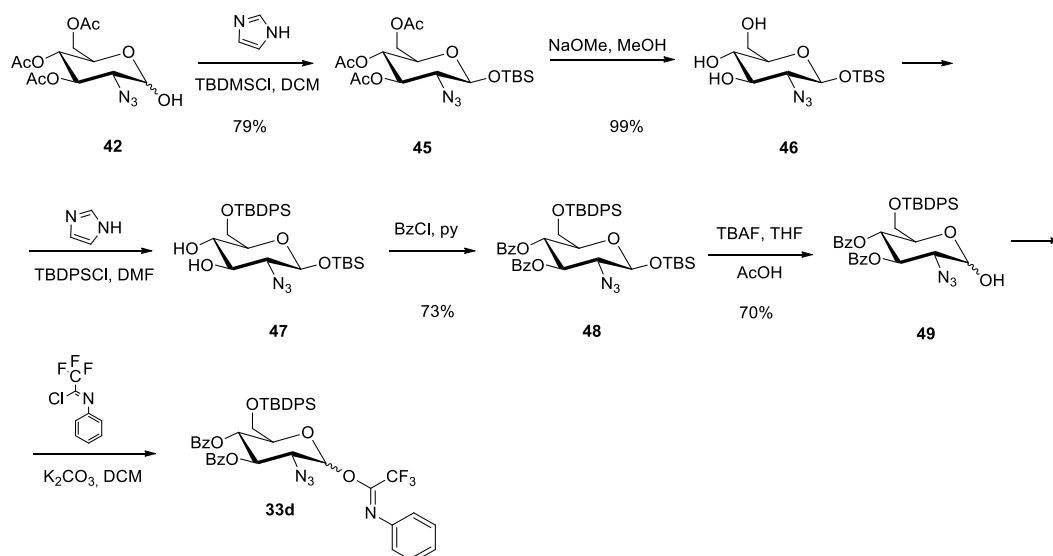
Scheme 22: Synthesis for donor **33d.**

Preparation of intermediate **49** was performed according to Jiakun Li & Biao Yu (2015) with similar yields. Common intermediate **42** had the anomeric position functionalised with *terc*-butyldimethylsilyl (TBS) group giving **45** with 79% yield. The mechanism of reaction to form the silyl ether involves the activation of the silicon species by the imidazole, for further attack of the free hydroxyl group (Scheme 23).
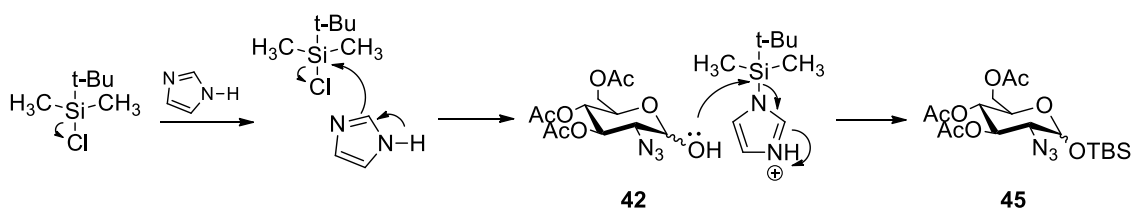
Scheme 23: Proposed mechanism for establishment of silyl ether.

Zemplén deacetylation of **45** gave compound **46** in quantitative yield for further attachment of the *terc*-butyldiphenylsilyl on C-6 of the glucopyranose derivative, giving compound **47**. Protection of remaining positions C-3 and C-4 was performed with benzoyl chloride. Selective elimination of *O*-TBS group from anomeric position

was possible due to the treatment of intermediate **48** with tetrabutylammonium fluoride (TBAF) in THF solution and low temperature (-20 °C), without cleavage of TBDPS at C-6, which is 10^4 times more stable than OTBS (GREENE; WUTS, 1999). Attachment of *N*-phenyl trifluoroacetimidate was performed as previously described for donors **33a-c.** However, donor **3d** showed to be very labile. One of the reasons may be due to a remaining source of fluorine (contaminant) from the reagent 2,2,2-trifluoro-*N*-phenylacetimidoyl chloride, which may have catalysed the cleavage of the *O*-Si bond of TBDPS group (Scheme 24).
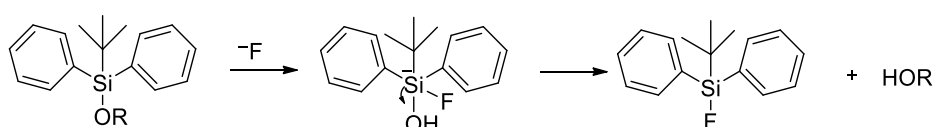
Scheme 24: Cleavage of OTBDPS group promoted by Fluorine.

To avoid degradation, donor **3d** was prepared again and the reaction was carefully monitored by TLC. When molecular weight of product was identified by the mass spectrometer *Advion* Plate Express® (found m/z= 845.5 calculated for $C_{44}H_{41}F_3N_4O_7SiNa$, Figure 10) the reaction was interrupted, solvent was evaporated and mixture containing donor **33d** was dried in high vacuum manifold for 3 hours and directly used in the following *O*-glycosylation reactions with no previous purification.
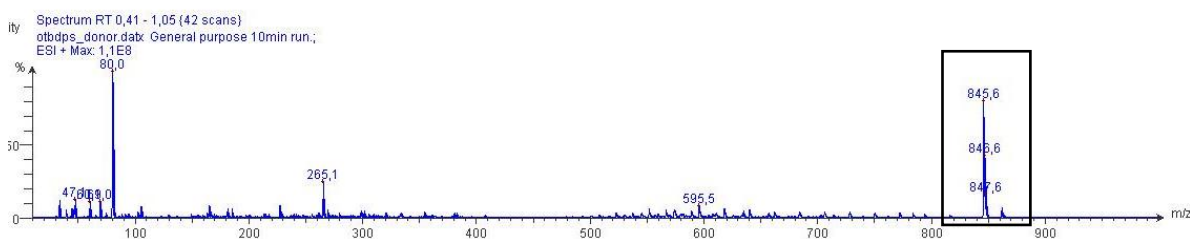
Figure 10: Mass spectra of mixture containing donor **33d**.

4.2.2. Synthesis of myo-inositol block (acceptor)

The *myo*-inositol is a six-membered ring *meso* compound containing 6 secondary hydroxyl groups and an axis of symmetry through 2nd and 5th carbon (Figure 11). Thus, any modification on positions 1,3,4, and 6 leads molecular chirality and formation of racemic mixtures that may be resolved at some point.
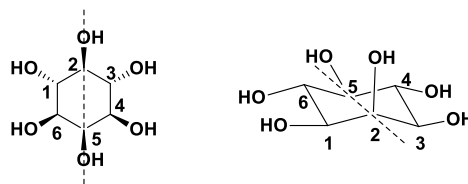
Figure 11: Axis of symmetry between 2nd and 5th carbons in *myo*-inositol

Many studies were focused on the establishment of methods to obtain enantiomerically pure *myo*-inositol derivatives. Thus, these methods can be divided into three categories: The first category is based on the conversion of naturally occurring chiral inositol derivatives into desired structures. The second one comprises the chemical modification of meso *myo*-inositol and further resolution of synthetic enantiomers by chemical or enzymatic approaches. Finally, the third category is the *de novo* synthesis, that is, the preparation of enantiomerically pure *myo*-inositol derivatives from *chirons* (GUO; BISHOP, 2004; SURESHAN et al., 2003).

Originally, the synthetic strategy was planned to obtain intermediate **58** by using *myo*-inositol as the starting material (Scheme 25), according to the second approach mentioned above (SWARTS; GUO, 2010).
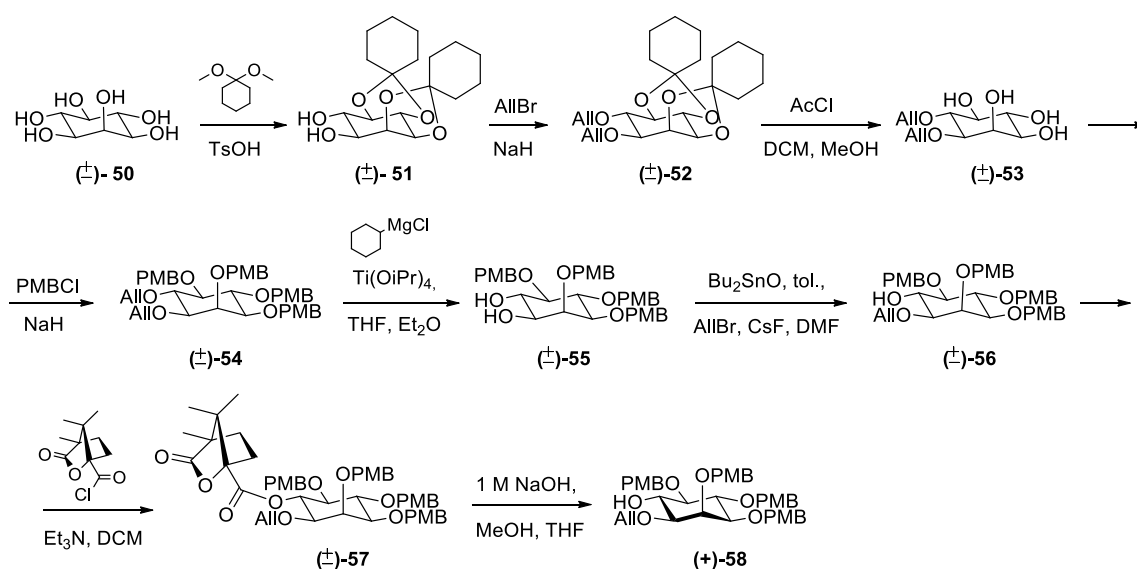
Scheme 25: Initial proposed route to obtain *myo*-inositol block **58.**

The first reaction consisted in selectively protect positions 2, 3, 4 and 5 of the cyclitol ring **50**, using *O*-cyclohexylidenes as protective group. Thus, the commercially available starting material *myo*-inositol was treated with cyclohexanone

dimethyl ketal *and p*-toluenesulfonic acid as catalyst in DMF at 100 °C for three hours to give compound **51** (Scheme 26).
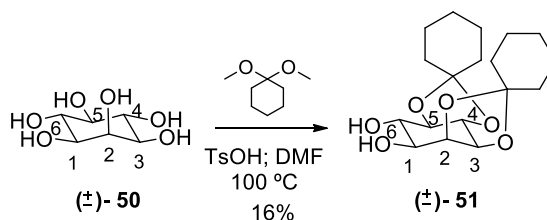
Scheme 26: Synthesis of di-*O*-cyclohexilidenes (compound **51**).

Three main products were observed by TLC due to the *meso* characteristics of *myo*-inositol (Figure 11). The products were identified by ^{1}H NMR as position isomers, in which different hydroxyls were protected, as in Figure 12. No protected derivatives were observed with one or three cyclohexylidene groups.
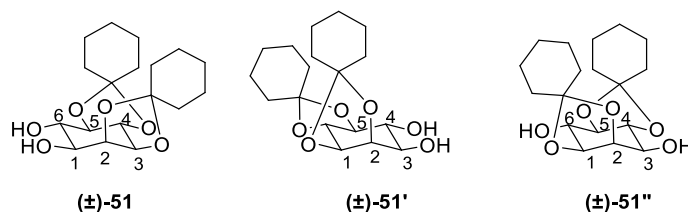
Figure 12: Products obtained in the attempt to protect compound **51** with di-*O*-cyclohexilidene.

The formation of other regioisomers in the same proportion of the target product reduced the yield of compound (±)-51 to 16%. However, this result was already expected, according to the literature (19%) (GAREGG, et al., 1984).

In the ^{1}H NMR spectra (Appendix) signals were observed at 1.73-1.41 ppm, with relative integration to 20 hydrogens, corresponding to the hydrogens of two cyclohexylidene groups, and a double doublet at 4.48 ppm, corresponding to H-2, linked to the unique axial substituent of *myo*-inositol, which presented coupling constants (axial/equatorial) with its axial neighbouring hydrogens H-3 (4.33 ppm, $J_{2,3}$ = 4.6 Hz) and H-1 (3.85 ppm, $J_{1,2}$ = 4.16 Hz). Signals were appropriately assigned according to the literature (XUE; SHAO; GUO, 2003).

The reaction mechanism for the formation of acetals occurs through the *trans*-acetalization of the cyclohexanone dimethyl ketal, after protonation by *p*-toluenesulfonic acid, as previously described for compound **38**, in Section 4.*2.1.1.*

Then, compound **51** was subjected to reaction with allyl bromide and sodium hydride as the catalyst in DMF to protect hydroxyl groups at positions C-1 and C-6

(Scheme 27). The allyl group was selected so that selective deprotection of positions 2, 3, 4 and 5 was possible in subsequent steps under mild acidic conditions. Product **52** was obtained as a colourless oil in 78% yield.
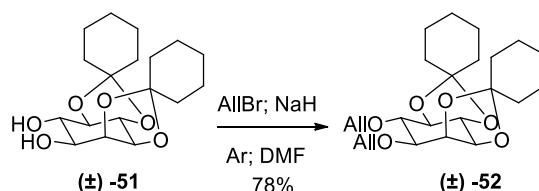
Scheme 27: Protection of C-1 and C-6 with *O*-allyl groups of derivative **51** to form **52**.

The ^{1}H NMR spectra (Appendix) showed three multiplets at 6.00-5.82 ppm; 5.35-5.27 ppm and 5.21-5.16 ppm with relative integration for two hydrogens each, referring to the olefinic hydrogens of the two allyl protecting groups. The mechanism of allylation (Williamson Reaction) consists in an S$_N$2 type reaction. Sodium hydride promotes deprotonation of the hydroxyl groups, forming alkoxides which consequently attack the allyl bromide (Scheme 28):
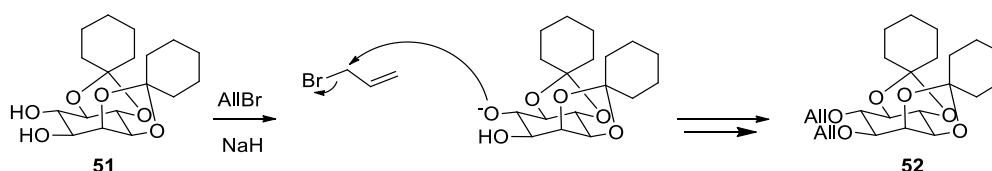
Scheme 28: Proposed mechanism for Williamson Reaction to form compound **52**.

Subsequently, compound **52** was subjected to deprotection with acetyl chloride in a mixture of dichloromethane and methanol (2:1) (Scheme 29). The TLC analysis of the reaction showed that the starting material was totally consumed, although chromogenic agents used could not detect the product. The literature reports the purification of compound **53** by classical column chromatography yielding the desired product in 90% (SWARTS; GUO, 2010). However, after purification according to literature, compound **53** was obtained as a clear oil in low yield (28%). A possible explanation for the obtained result could be the strong interaction of the hydroxyl groups with the stationary phase (silica).
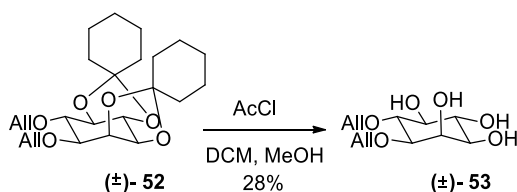
Scheme 29: Acidic cleavage of acetals of compound **52** forming **53**.

The ^{1}H NMR spectra (Appendix) showed the absence of the signals referred to the cyclohexylidene hydrogens at 1.70-1.40 ppm. All other NMR signals of **53** were assigned according to the literature (SWARTS; GUO, 2010).

The mechanism of reaction involves the attack of the methanol to the acetyl chloride generating hydrochloric acid (Scheme 30). In sequence, protonation of the acetal generates de hemiacetal and forming the *oxonium* ion. The attachment of the methanol to this ion followed by deprotonation leads to the recovery of cyclohexanone dimethyl ketal reagent (SMITH; MARCH, 2013) (Scheme 31).
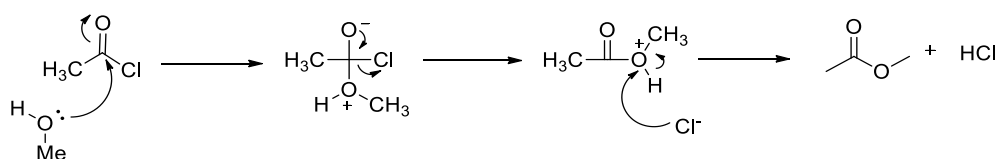
Scheme 30: Generation of the acidic environment for the cleavage of the acetals.
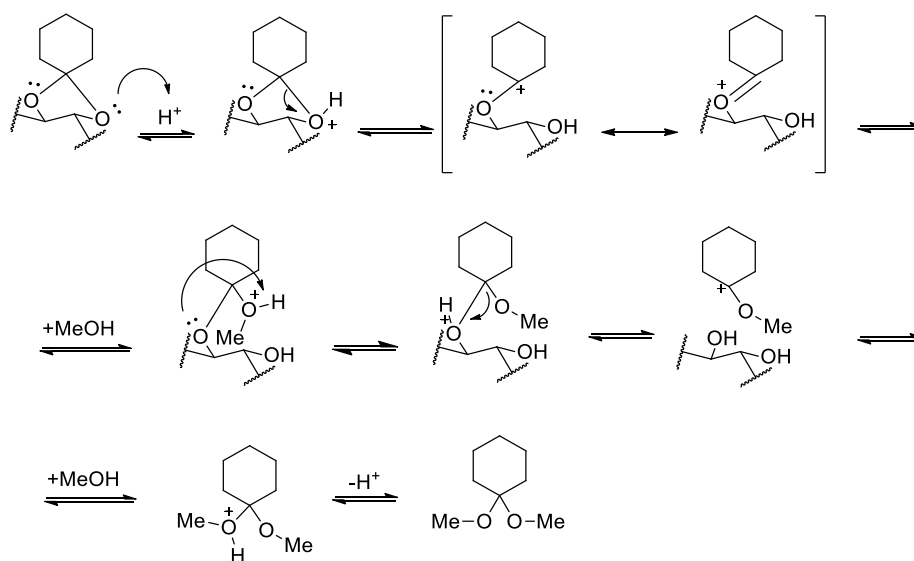
Scheme 31: Proposed mechanism of cleavage of acetal with recovery of cyclohexanone dimethyl ketal.

The low yield in this step (28%), as well as in the stage of formation of the di-cyclohexylidene derivative (16%) led to the concern that a very large scale would be necessary to reach the later steps of the route in Scheme 25. Thus, some alternative synthetic procedures were tested parallelly in a search for the best strategy to obtain the desired inositol moiety in the right configuration that would work as a glycosyl acceptor.

An alternative route with less steps (5 steps), compared to the one initially proposed (10 steps), would lead to the *myo*-inositol block **63** containing the phosphodiester already linked to C-1, in accordance to GPI anchor structure (Scheme 32).
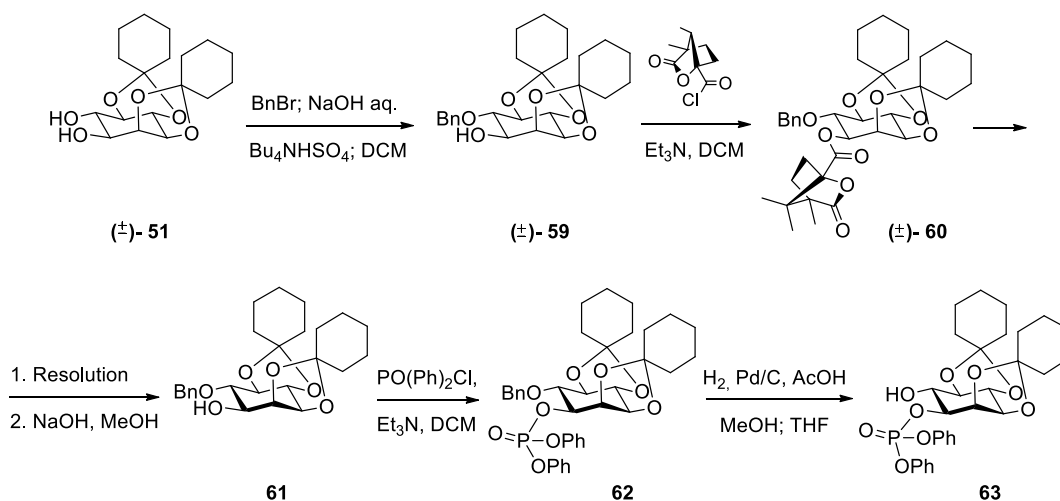
Scheme 32: New proposed route with reduced number of steps to achieve block **63**.

Considering the possibility of selective protection of one of the hydroxyl groups of **51**, the selective benzylation reaction of hydroxyl at C-6 was performed to form compound **59** (Scheme 32), in which literature reported the yield of 57% for this step (MADSEN et al., 1995). The reaction was performed in aqueous solution of NaOH (5%), DCM, and benzyl bromide (Scheme 33). Follow-up of the CCD reaction indicated the presence of a complex mixture of products of difficult separation. The starting material was also not totally consumed, even after attempts, such as increasing equivalence of reagents, heating, and longer duration of reaction. Separation of the mixture of products by classical column chromatography led to the isolation of products with very low mass. The ^{1}H NMR analysis showed that they were still impure, and no conclusive result regarding the success of the reaction was reached. Although the literature describes the obtention of regioselectively protected

myo-inositol in good yields for the regioisomer **59**, these results could not be reproduced in our laboratory (MADSEN et al., 1995).
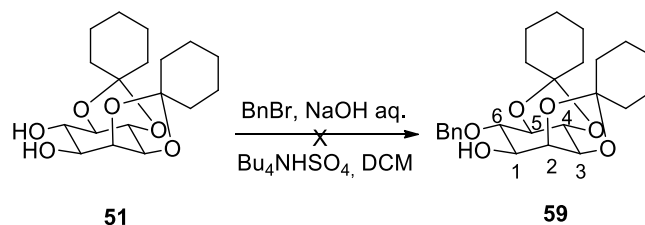
Scheme 33: Proposed reaction for regioselective benzylation of **51**.

In another attempt, the racemic resolution of the *myo*-inositol moiety at the beginning of the proposed synthesis was desired. In this context, some efforts for the resolution of compound **51** (Scheme 34) with lipases, available in the laboratory (*Mucor mehiei* lipase and porcine pancreas lipase, both from *Sigma Aldrich*®), were tested. The works of Ling and collaborators (LING; OZAKI, 1994; LING et al. 1993) were used to set up a reaction protocol (Scheme 34), although it is important to emphasize that the enzymes used in the mentioned articles were not the same as the ones experienced in this work. However, the strategy also led to inconclusive results and very low yields.
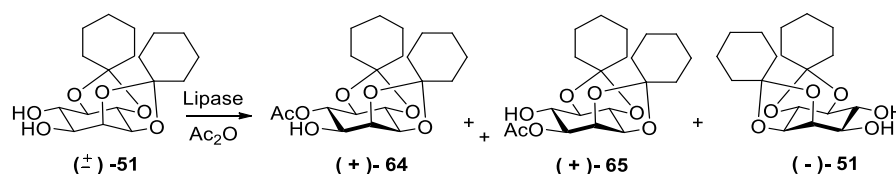
Scheme 34: Attempts to perform optical resolution of *myo*-inositol derivative in the presence of lipase according to Ling and co-workers (1993, 1994).

Based on the negative results described above, the preparation of the desired *myo*-inositol block was exploited by another synthetic approach, no longer employing the commercial *myo*-inositol as starting material. Thus, the conversion of a functionalized derivative of α-glucopyranoside in a cyclitol preserving the same stereochemistry of *myo*-inositol could be performed in 6 steps using *Ferrier* rearrangement (Scheme 35). Thus, the orthogonal protection and deprotection would be performed to obtain the functionalized *myo*-inositol **34**. The overall yield obtained in this rout was 9%.
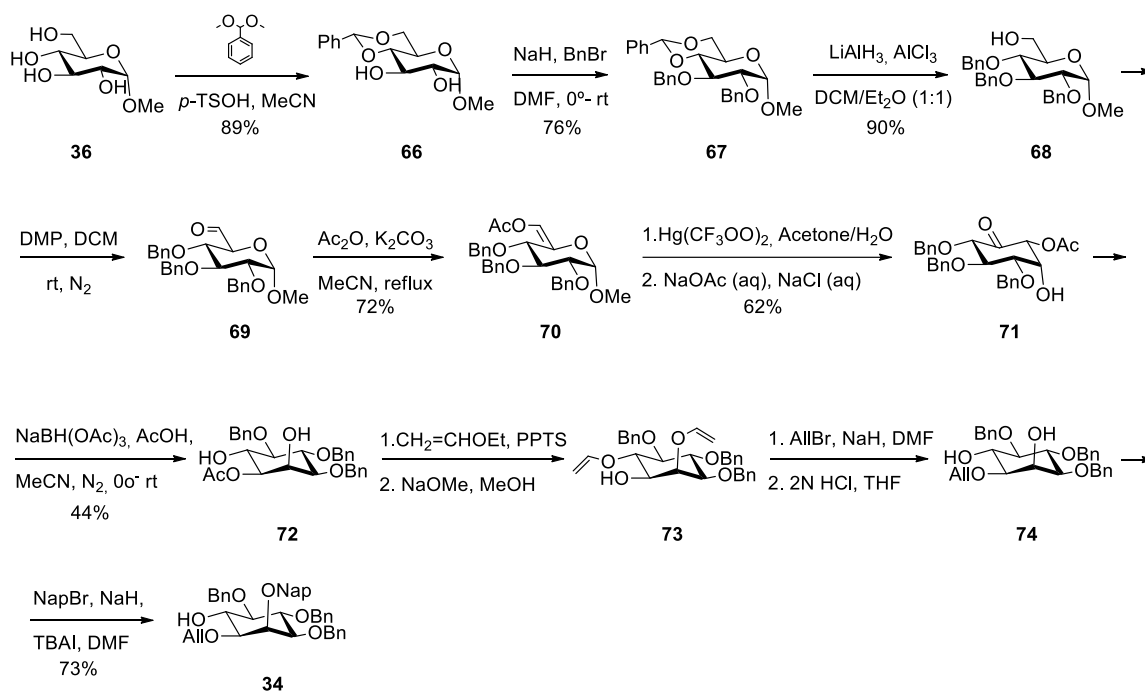
Scheme 35: New synthetic sequence proposed for the synthesis of acceptor 34.

Some advantages can be highlighted for this strategy: i) starting from a chiral precursor, α-glucopyranoside, can afford regio and stereoselective intermediates, such as cyclitol derivative **71** (Scheme 35), which carry already protective groups (three *O*-benzyl) that is not straightforwardly introduced into the *myo*-inositol scaffold (GUO; BISHOP, 2004); ii) acetyl and vinyl orthogonal protection allows the sequential removal of the former in basic conditions, for further introduction of a more stable allyl group (compounds **72-74**), whereas the vinyl groups (compound **73**) can be removed in acidic condition, consequently, no side products would be expected; iii) *O*-allyl groups are removed in very specific conditions, which would not interfere in any other protecting group; iv) given that the remaining unprotected hydroxyl groups at C-2 and C-6 would be displayed in a *trans* spatial orientation, their corresponding reactivity can be accessed. Therefore, *O*-naphthyl group was the group of choice at C-2 (compound **34**), that would allow derivatization of this position, such as addition of acyl chains, which frequently occurs on GPI anchor structures; v) initial reactions of this route have already been performed and standardized in our and other laboratories (CARVALHO; BORGES, 2012; BOONYARATTANAKALIN et al., 2008 MADSEN et al., 1995; XU, SCULIMBRENE, MILLER, 2006). The new strategy for the synthesis of the *myo*-inositol block is depicted on Scheme 35.

Initially, commercially available methyl α-D-glycopyranoside (**36**) was subjected to reaction with benzaldehyde dimethyl ketal and *p*-toluenesulfonic acid to form product **66** with 89% yield. The formation of benzylidene acetals was discussed with more details in Section 4.2.1.1 (Scheme 36).
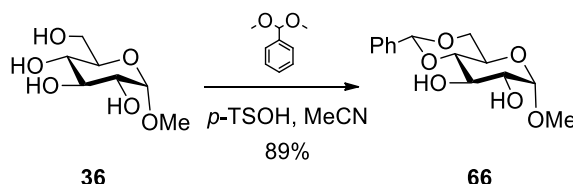
Scheme 36: Protocol for the synthesis of **66** from starting material **36**.

In the second step, the hydroxyl groups at C-2 and C-3 positions of glucopyranose **66** were protected with benzyl groups. The product **67** was generated in two different ways: by using benzyl chloride (BnCl) in excess, KOH and heating (50°C), or benzyl bromide (BnBr) with NaH as base at room temperature; both reactions gave the product with similar yields (around 70%) (Scheme 37). The mechanism of reaction is based on Williamson's ethers synthesis, previously described in Section *4.2.2.*
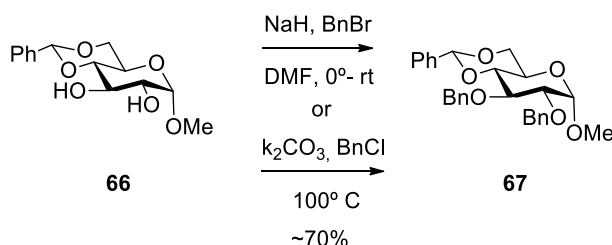
Scheme 37: *O*-benzylation of hydroxyl groups at C-2 and C-3 positions.

The ^{1}H NMR spectra presented multiplets in the region of 7.52-7.28 ppm, with relative integration for 15 aromatic hydrogens, and 4 doublets at 4.93-4.68 ppm with relative integral for 1 hydrogen each, related to the methylenic hydrogens of the benzyl groups (Appendix).

Next, Compound **67** was subjected to regioselective cleavage of the benzylidene ring by using LiAlH$_4$ and AlCl$_3$, under reflux and N$_2$, in a mixture of DCM and Et$_2$O (Scheme 38). Product **68** was obtained with 90% yield.
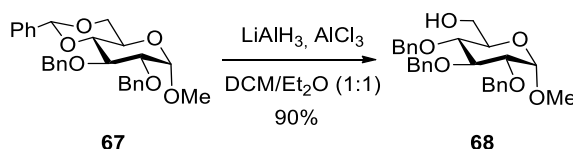
Scheme 38: Selective cleavage of the benzylidene acetal at C-6 promoted by LiAlH$_3$ and AlCl$_3$.

Selective dealkylation is possible due to the bulky benzyl group at position C-3 of the pyranose ring which redirects the cleavage complex to the C-6 position. Furthermore, LiAlH$_4$ reacts with AlCl$_3$ in Et$_2$O to form AlH$_3$ which acts as reductive agent (Scheme 39) (JOHNSSON; OLSSON; ELLERVIK, 2008).
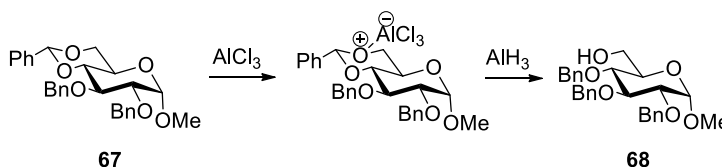
Scheme 39: Proposed mechanism of regioselective dealkylation of benzylidene ring proposed by Johnsson and co-workers.

The ^{1}H NMR spectra of compound **68** showed the absence of the singlet at 5.55 ppm related to the methinic hydrogen of the benzylidene group, when compared to starting material. The relative integration of the aromatic signals at 7.37 ppm to 7.25 ppm (15 hydrogens) as well as relative integral of methylene hydrogens at 5.0 ppm to 4.61 ppm (6 hydrogens) showed the presence of three aromatic rings (Appendix).

The oxidation of the primary alcohol at C-6 of the glucopyranoside **68** to aldehyde **69** was carried out with Dess-Martin periodinane (DMP) in dichloromethane, under inert atmosphere for two hours (Scheme 40).
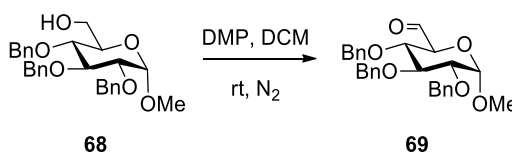
Scheme 40: Oxidation of the primary alcohol of **68** to afford the aldehyde **69**.

The mechanism of oxidation involves the displacement of an acetate from the Dess-Martin reagent by the alcohol, which becomes positively charged. The proton is then picked up by the acetate ion to stabilize it. Another acetate removes the proton

attached to the carbon atom leading to the formation of the carbon oxygen double bond of the aldehyde. The process leads to a release of another acetate molecule and a mono-acetoxy iodinane (Scheme 41). To neutralize the excess of acid formed, the reaction was worked up with a mixture of aqueous $NaHCO_3$ and $Na_2S_2O_3$.
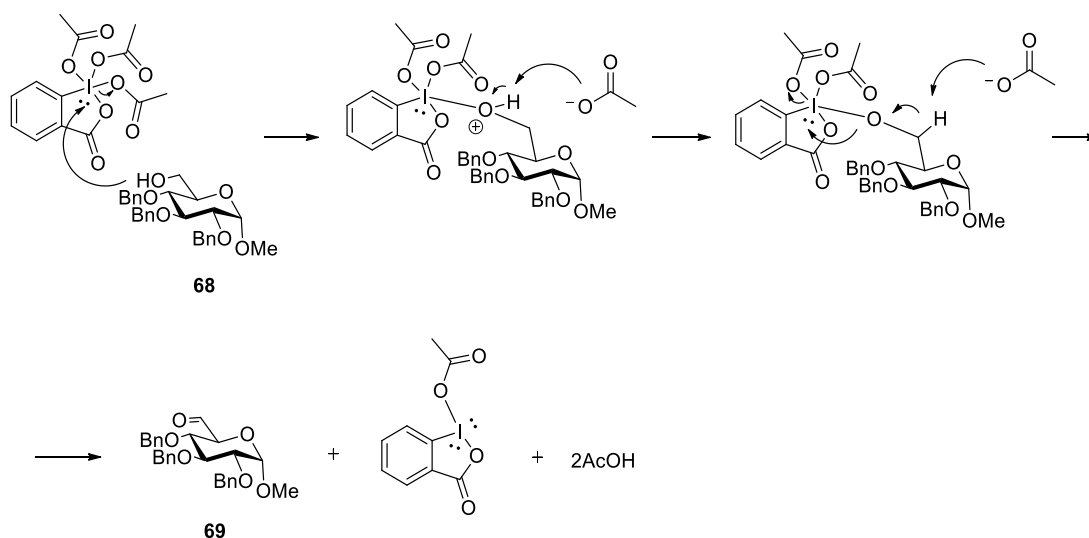
Scheme 41: Proposed mechanism of oxidation by DMP reagent.

Compound **69** followed to the next step, with no previous purification, which involves esterification and enolization of the aldehyde with acetic anhydride and potassium carbonate (K_2CO_3) (TAKAHASHI; KITTAKA; IKEGAMI, 2001; BENDER; BUDHU, 1991; HOUSE; KRAMAR, 1963). Product **70** was obtained after purification by silica flash chromatography in 70% yield (Scheme 42).

The ^{1}H NMR spectra revealed a singlet close to 7.0 ppm and relative integration for 1 hydrogen was observed related to the olefin proton at C-6. All signals were attributed according to literature (TAKAHASHI; KITTAKA; IKEGAMI, 2001).
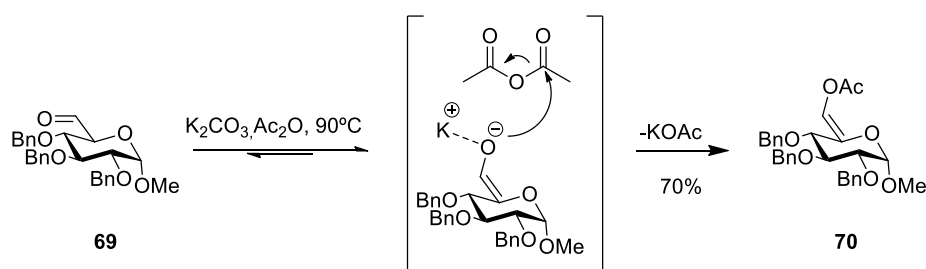
Scheme 42: Enolization followed by acetylation of compound **69** to afford **70**.

Next, the glucopyranoside ring **70** was converted into a carba-sugar derivative **71** under the treatment with mercury trifluoroacetate in a mixture of acetone and water (4:1). After stirring for 1-hour, aqueous solutions of NaOAc (3.0 M) and saturated solution of NaCl were added and reaction kept overnight (Scheme 43).
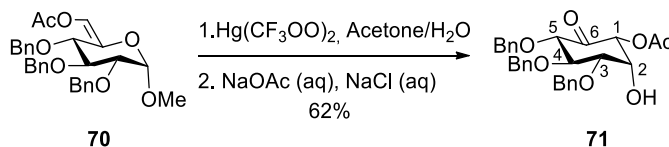
Scheme 43: *Ferrier* rearrangement to convert glucopyranoside **70** into *cyclitol* derivative **71**.

The products were purified by silica flash chromatography as a mixture of isomers in 82% yield. Two extra chromatography purifications were necessary for the isolation of the target α-isomer in 60% yield, as a clear oil (YU, GUO, 2009).
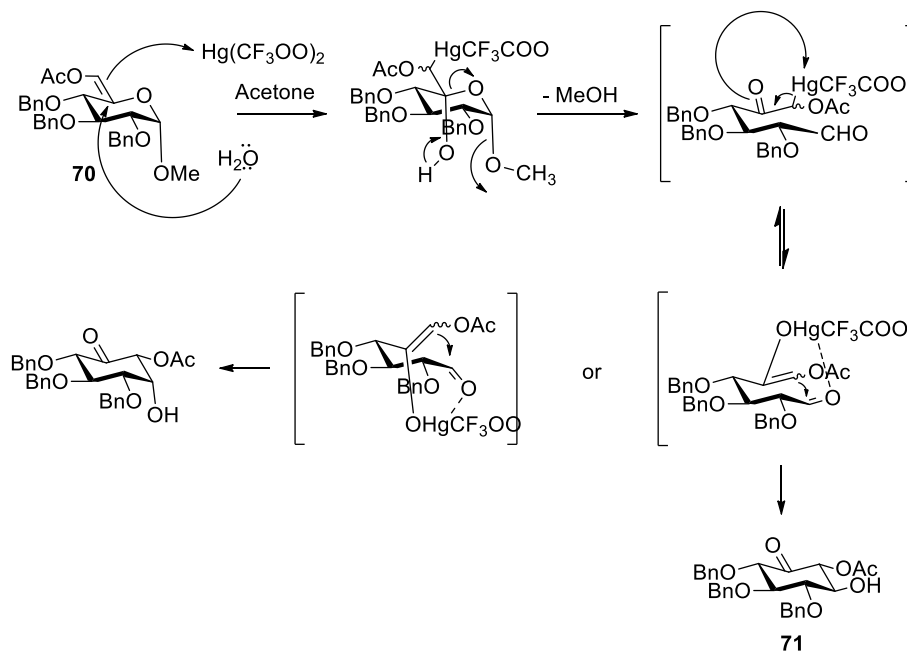
Scheme 44: Proposed mechanism of *Ferrier* rearrangement to afford compound **71**.

The ^{1}H NMR showed the absence of anomeric hydrogen. Relative integrals of the aromatic region (7.40-7.26 ppm) for 15 hydrogens were related to the *O*-benzyl groups, as well as the signals between 4.94 pppm and 4.52 ppm (methylenic hydrogens assigned to the *O*-benzyl groups). The triplet at 4.34 ppm with coupling constants (axial/equatorial) 2.5 Hz was related to the only axial substituent in the cyclitol ring at C-2 (Scheme 43). In addition, one singlet at 2.25 ppm with relative

integral to 3 hydrogens was associated to the methyl group of the *O*-acetyl. All the signals were attributed according to literature (Appendix) (TAKAHASHI; KITTAKA; IKEGAMI, 2001; BENDER; BUDHU, 1991).

The reaction mechanism involves the binding of mercury and a water molecule to the carbohydrate olefin. Then, the pyranose ring opens, and the mercury is released from the complex after addition of excess of Cl⁻ ions into the medium, leading to ring closure and consequent loss of the methoxy group (Scheme 44).

Subsequently, stereoselective reduction of inosose **71** was performed with sodium triacetoxyborohydride and acetic acid in order to obtain **72** (Scheme 45). The TLC analysis of the reaction showed several products, besides one major product, more polar than the starting material. After purification by silica flash chromatography using solvent gradient, **72** was isolated as colorless oil in 44% yield. NMR spectra and yields were in accordance with the literature (Appendix) (BENDER; BUDHU, 1991).
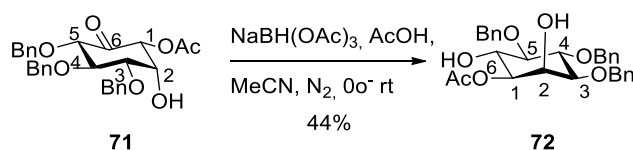
Scheme 45: Selective oxidation of the ketone of carba-sugar **71**.

A stereo-controlled reduction was achieved in the presence of sodium triacetoxy-borohydride with a complex formation between the triacetoxy-borohydride and the alcohol on the C-2 position of the ketone. The complex provides the intramolecular hydride attack on the same face as the axial alcohol, generating the desired equatorial alcohol **72** (Scheme 46).
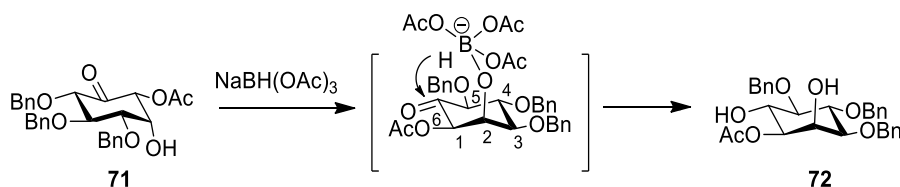
Scheme 46: Stereo-controlled oxidation of the equatorial ketone with assistance of the axial alcohol at C-2.

Both hydroxyl groups of inositol **72** were protected with vinyl groups by using ethyl vinyl ether and pyridinium *p*-toluenesulfonate (PPTS) through formation of acetals' methodology, which was previously described in Section 4.2.1.1. Further

deprotection of the acetyl group with NaOMe under heating (50ºC) was performed to give compound 73. (Scheme 47).
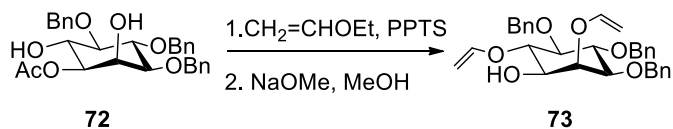
Scheme 47: Protection of remaining hydroxyl groups of **72** with vinyl ethers and removal of acetyl group.

The mechanism of deprotection of acetyl groups by using sodium methoxide in methanol, (Zemplén transesterification) is shown in Scheme 48. The methoxide ion attacks the carbonyl group of the acetate. Then, the carbonyl group reforms and expels the inositol leaving group. The reaction can either revert to the starting material or proceed to the transesterified product releasing methyl acetate (REN et al., 2015).

A different protecting group should be attached to the hydroxyl group at C-1 of the *myo*-inositol derivative **73** in order to allow orthogonal deprotection and further addition of a phosphodiester block at this position. The group of choice was allyl group, which could be easily prepared by Williamson reaction.
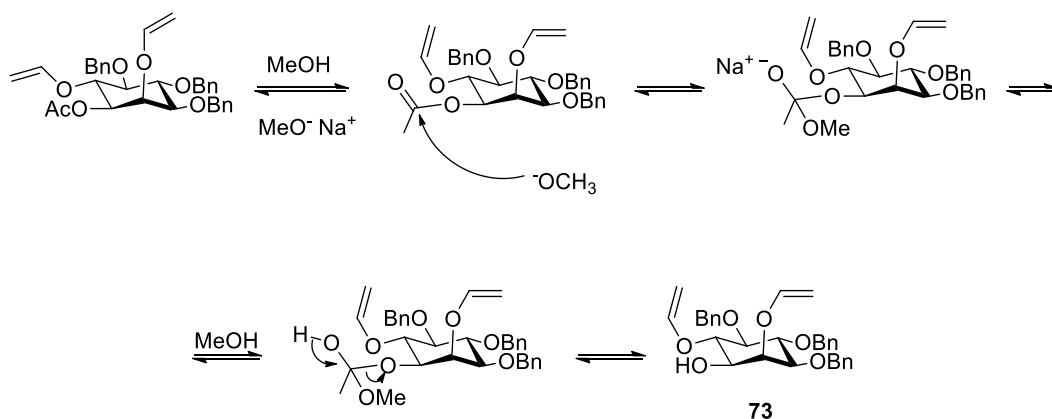
Scheme 48: Proposed mechanism for Zemplén trans-esterification for compound **73**.

The addition of the allyl group was achieved in DMF, using NaH as catalyst. Work up after conversion to the allyl intermediate was not necessary, since the sequential removal of the vinyl groups could be performed in "*one pot*" by adding THF and HCl 2N solution to the reaction mixture. Finally, compound **74** was obtained after purification by silica flash chromatography with 67% yield over the last 4 steps (Scheme 49).
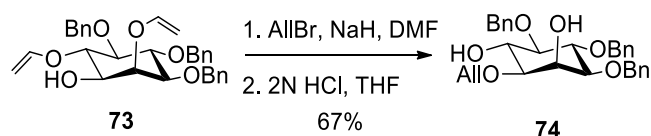
Scheme 49: Addition of *O*-ally at C-1, followed by deprotection of *O*-vinyl groups of **73** to afford **74**.

The final step of the route was the regioselective attachment of the methylnaphtyl group at position C-2 of compound **74** using 2-methylnaphtyl bromide in presence of tetrabutylammonium fluoride (TBAI) and NaH (Scheme 50). Lastly, the acceptor **34** was obtained after silica flash chromatography purification with 73% yield (SAYKAM et al, 2015).
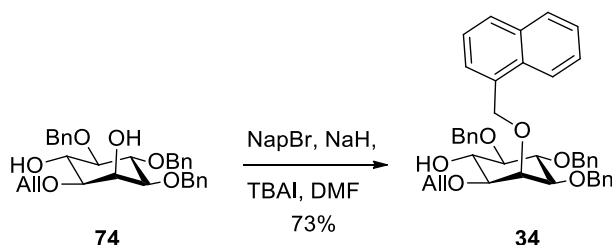
Scheme 50: Obtention of acceptor **34** from **74**.

The ^{1}H NMR of product **34** showed multiplets at 7.50-7.19 ppm with relative integration of 22 hydrogens which correspond to the three *O*-benzyl moieties and the *O*-naphtyl group. A multiplet at 5.82 ppm, two double-double doublets at 5.19 ppm and 5.10 ppm with relative integration for 1 hydrogen each are signals related to the *O*-allyl group (Appendix).

4.2.3. O-glycosylation reactions: Synthesis of pseudo-disaccharide 31.

4.2.3.1. *O*-glycosylation reactions using cyclohexanol as a model acceptor

O-glycosylation reactions were performed in Robert Field's laboratory, at John Innes Centre, Norwich/UK. The reaction conditions were investigated using donor **33a** and cyclohexanol **75** as model acceptor according to Scheme 51. The reaction was performed simultaneously in 3 different solvents (1,2-dichloroethane, toluene/Et$_2$O 1:1 and Et$_2$O), using trimethylsilyl trifluoromethanosulfonate (TMSOTf) as promoter. All reagents were added at -50⁰ C and then allowed to warm up

between -30⁰ C and -10⁰ C. The reactions were complete within 3 hours. They were monitored by TLC, being considered complete when observed the absence of donor **33a**. After neutralization with Et₃N and filtration over celite, the crude mixture was analysed by ^{1}H NMR.
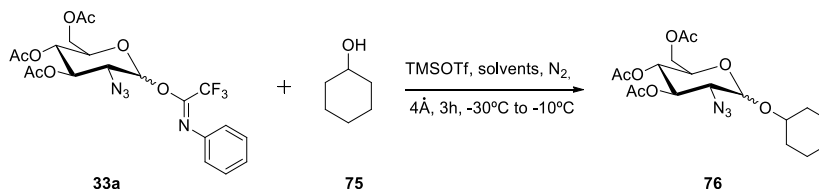
Scheme 51: Studies of *O*-glycosylation reaction using cyclohexanol **75** as model acceptor in the presence of different solvents.

The ^{1}H NMR spectra of crude compound **76** showed a doublet at 4.89 ppm with relative integration to 1 hydrogen related the α-glycosylated product (coupling constant $J_{1,2}$= 3.6 Hz). The hydrogen correspondent of the β anomer could be observed at 4.37 ppm with coupling constant $J_{1,2}$= 8.4 Hz. The α/β ratios were 1:1.5 for the reaction performed in 1,2-dichloroethane (DCE), 1:0.7 in the mixture toluene/Et₂O, and 1:0.4 in the Et₂O reaction. These results were already expected due to the solvent effect, which will be later discussed. Given the positive results, these conditions were applied to the next *O*-glycosylation reactions involving donors **33a-d** and acceptor **34**.

4.2.3.2. *O*-glycosylation between acceptor 34 and trifluoroacetimidate donors 33a-d

Parallel small-scale *O*-glycosylation reactions were performed with the *myo*-inositol block **34** as acceptor and the four different glycosyl donors **33a-d** in three different solvents (1,2-dichloroethane, Et₂O/toluene 1:1 and Et₂O), using molecular sieves (4 Å) and TMSOTf as activator (Scheme 52). These variations were pursued to establish the better glycosyl donor and solvent to afford the pseudo-disaccharide in higher yield and α-selectivity.

Reactions were prepared and carried out as previously reported. The average duration of reactions was 3 hours, although some of them were left overnight for completion. The glycosylations were considered complete when TLC plates showed

that donor **33a-d** was totally consumed (equivalent relationship between donor and acceptor was 1:1). Products were purified by semi-preparative TLC plates.

31a and 33a= R_1=R_2=R_3= OAc
31b and 33b= R_1=R_2= CHPh; R_3= OAc
31c and 33c= R_1=R_2=R_3= OBz
31d and 33d= R_1= OTBDPS; R_2=R_3= OBz
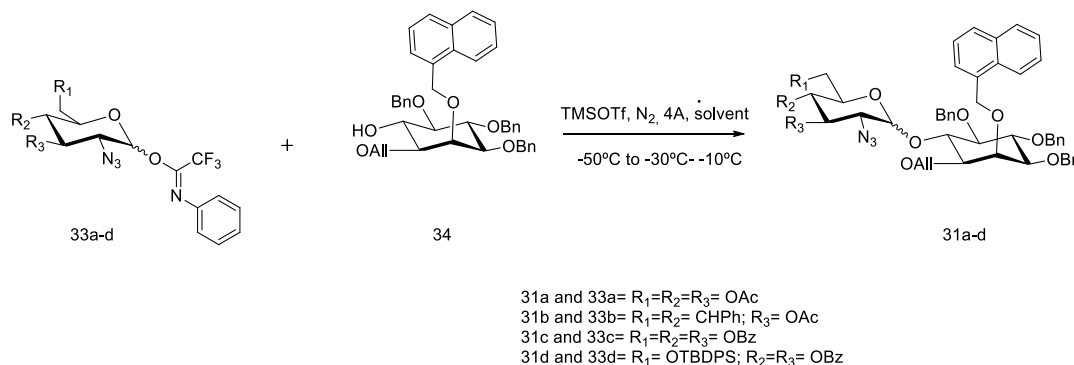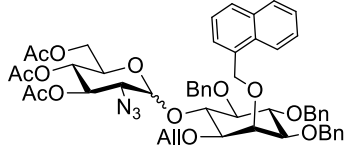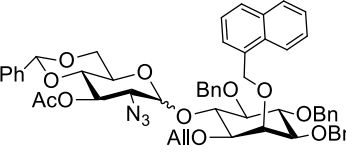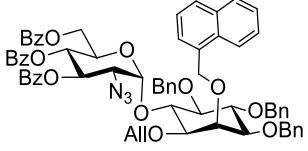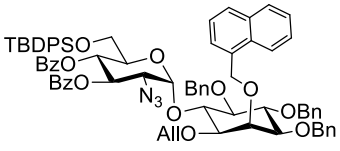
Scheme 52: *O*-glycosylation reactions in small scale performed between donors **33a-d** and acceptor **34**.

The separated α and β compounds were initially analysed by ^{1}H and HSQC NMR, which showed clear signals of glucose and *myo*-inositol moieties in same proportion, based on relative integrals. A doublet at the region around 5.75 ppm with coupling constant $J_{1,2}$= 3.7 Hz was referred to α-linked pseudo-disaccharides. For the β derivatives, the signal of the anomeric hydrogen appeared in more shielded region (around 4.98 ppm). These last referred hydrogen signals could only be checked by HSQC, since they are located in a region with many other signals in the spectra (Appendix). Thus, it was not possible to calculate the coupling constants for the β anomers. The α/β ratio was calculated by the weight[2] as well as the isolated yields of glycosides **31a-d** and results are presented on Table 2.

Based on the results of Table 2, it was evident that *O*-glycosylations performed with donors containing only benzoyl group (**33c**) and 6-OTBDPS group (**33d**) were more stereoselective, regarding formation of α-*O*-glycosides, with no detection of β anomers. Among the four donors, only the benzylidene **33b** gave more β glycosides rather than α. Acetyl donor presented products with α/β ratios close to 1:1, apart from the result of reaction performed in Et_2O, which seemed to be effective in favouring the product **31a** with α configuration.

---

[2] Reaction mixtures were purified by semi-preparative TLC and all isolated compounds were analysed by ^{1}H NMR. The α/β ratio was determined by comparing the weight of pure products, since it was not possible to integrate the signals of β-anomers by NMR.

Table 2: Yields and the α/β ratio of products from small-scale *O*-glycosylation reactions.

Compound	DCE		Toluene/Et2O		Et2O	
	Yield (%)	α/β ratio	Yield (%)	α/β ratio	Yield (%)	α/β ratio
31a	27	1.3:1	34	1.3:1	40	2:1
31b	82	1:1.25	74	1:1.5	68	1:1.5
31c	82	Only α	74	Only α	77	Only α
31d	63	Only α	68	Only α	68	Only α

Numerous factors are known to affect the stereoselectivity and yield of glycosylation reactions, which include temperature, solvent, type of donor/acceptor (and their reactivity), amount and type of promoter, protecting groups, etc. In addition to the complex glycosylation process, there are other competing processes that cannot be ignored. Side reactions, such as elimination, substitution (formation of unexpected substitution products or hydrolysis at the anomeric centre), cyclization (inter and intramolecular ortho-esterification), migration, etc. are some examples of phenomena that frequently complicate stereo-control and also impair the yield of glycosylation (NIGUDKAR; DEMCHENKO, 2015).

One of the main factors that favours the α or β glycosidic linkage is the influence of the neighbour group linked at C-2 of the pyranose ring, which was already discussed in Section *4.2.1*. In this context, preparation of donors with a non-participating group (azide) at C-2 would favour the better ration of α anomers as major products if the reaction would occur by S$_N$1 mechanism (ADERO et al, 2018). On the other hand, the non-participating group alone cannot ensure the stereoselectivity (NIGUDKAR; DEMCHENKO, 2015). Some of these factors can be correlacted to the results obtained from the *O*-glycosylation reactions performed in this work. In this context, they will be discussed with more detail hereafter.

The mechanism of reaction for *O*-glycosylations with imidates as leaving groups and promoted by TMSOTf may undergo S$_N$1 and S$_N$2 (Schemes 53 and 54). For the S$_N$1 mechanism, the electrophilic promoter TMSOTf activates the leaving group of the donor, giving the *oxocarbenium* ion in its flattened half-chair conformation. After this, nucleophilic attack by acceptor occurs, thereby leading to the required glycoside formation. However, the attack of the acceptor can occur via two pathways, owing to the structural property of the *oxocarbenium* intermediate. The attack of the glycosyl acceptor from the bottom of the sugar ring leads to the formation of α-glycoside, whereas attack of the glycosyl acceptor from the top of the sugar ring yields β glycoside (Scheme 53) (ADERO et al., 2018; KAFLE; LIU; CUI, 2016).
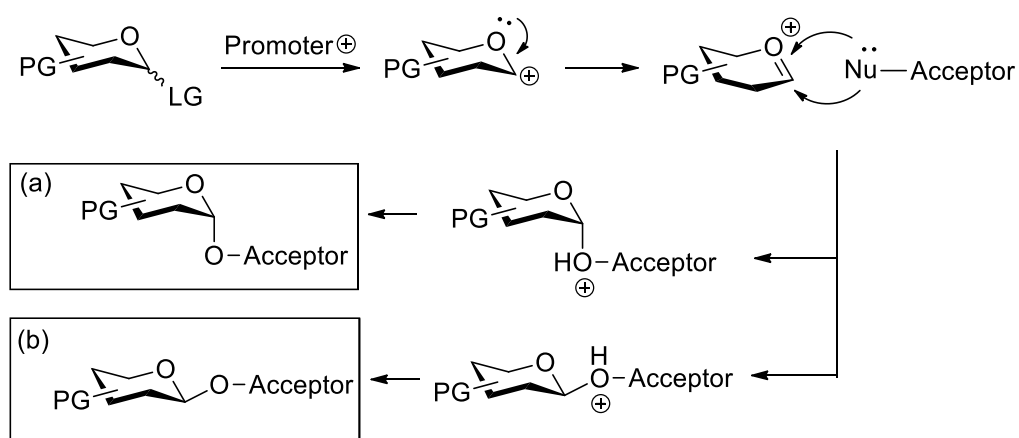
Scheme 53: Proposed mechanism of *O*-glycosylation by S$_N$1 mechanism.

The S$_N$2 mechanism of *O*-glycosylation, occurs with the function of the TMSOTf as Lewis acid, that promotes the exit of the leaving group in the anomeric position by removing a pair of electrons from the imidate group. The free position of

the acceptor performs the nucleophilic attack to the anomeric position, inverting the configuration of the glycosidic bond. Thus, the anomeric configuration is led accordingly to the previous configuration of the leaving group. The α-substituted leaving groups will favor formation of β glycosydic bond, and the contrary is also true (Scheme 54) (ADERO et al., 2018; KAFLE; LIU; CUI, 2016).
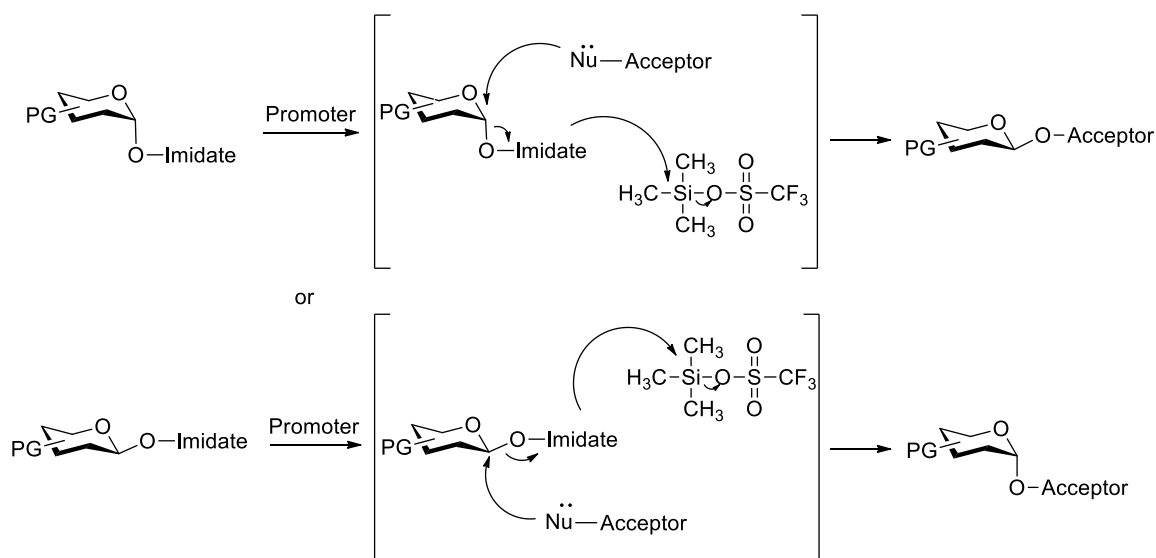
Scheme 54: Proposed mechanism of *O*-glycosylation by S$_N$2.

Regarding the influence of solvents in *O*-glycosilation reactions, several authors report the study of polar and non-polar solvents over the preference on the formation of α or β-glycosidic linkage. Ishiwata and Ito (2005) performed a series of reactions with different solvents at room temperature and at 50 $^{\circ}$C. Variable selectivity was observed among the halogenated hydrocarbon solvents, out of which, chloroform (CHCl$_3$) presented the best choice regarding its α-selectivity (α/β 10.9:1). Similarly, aromatic solvents were found to yield substantially higher α-selectivity (ISHIWATA; ITO, 2005).

In another study, anomeric α-selectivity of the products was enhanced when employing mixture of halogenated and ethereal solvents. The α/β ratios were significantly higher when compared to the use of individual solvents suggesting some forms of synergistic effect (ISHIWATA; MUNEMURA; ITO, 2008). The result also revealed that the α-selectivity of the reaction was found to decrease when the solvent (CHCl$_3$:Et$_2$O) ratio was diverged from 1:1. The authors proposed that the presence of ether in the mixture of solvents more possibly formed ether-coordinated intermediates E(α) and E(β), and more plausibly the reaction proceeded through the

more abundant E(β) resulting in α-anomer product (ISHIWATA; MUNEMURA; ITO, 2008) (Scheme 55). Similarly, Demchenko and co-workers (1997) observed higher rates of α-glycosylated products when reactions were performed in toluene/ Et$_2$O 1:1. The studies performed using only Et$_2$O did not deviate very much from the results found in the mixture of solvents toluene/Et$_2$O (DEMCHENKO; BOONS, 1997).

Wasonga and co-workers (2011) reported the use of Et$_2$O or DCM and evaluated their capacity to switch the stereochemical outcome of the reaction (WASONGA.; ZENG; HUANG, 2011). Et$_2$O favoured α-glycosides, whereas β-glycosides were the main products when solvent was changed to DCM. Supplementary, when the volume of the Et$_2$O was increased to 10-fold, the α-selectivity of the reaction increased, probably due to the higher accessibility of the solvent participation in the diluted condition. The authors proposed that in non-polar and non-nucleophilic solvent such as DCM, the reaction is favoured by an S_N2 type displacement to give β-selectivity (*O*-glycosylation via S_N2 mechanism is exemplified in Scheme 54).

The given studies encouraged this research regarding the solvents of choice to achieve the major α-glycosides (1,2-dichloroethane, toluene/Et$_2$O 1:1 and only Et$_2$O). The results encountered in this work corroborate with literature, being the diethyl ether the solvent of choice for further *O*-glycosylations in larger scale because it gave better yields and good α selectivity in most of the cases.
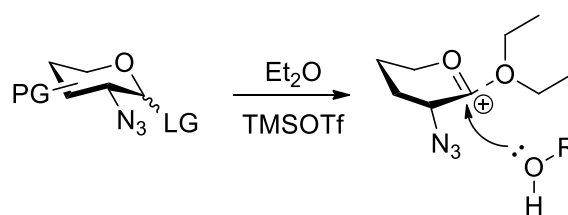
Scheme 55: Participation of Et$_2$O in *O*-glycosylation stereocontrol.

No variation of temperature was tested in this study although it may also influence in the α/β ratio over formation of the glycosidic bond. In theory, higher temperatures would lead to the thermodynamic product (α), whereas the lower one would favour kinetic products (β). On the other hand, it is also known that a fast *O*-glycosilation reaction renders very weak stereo-control (NIGUDKAR; DEMCHENKO, 2015). In this context, all the reagents were added to the reaction mixture at -50º C to avoid a fast conversion to any product for later warm up to a range of -30º to -10 ºC (NIGUDKAR; DEMCHENKO, 2015).

Protecting groups are key factors for the stereoselectivity of *O*-glycosylation reactions. Besides the anchimeric assistance from the 2-*O*-acyl groups, they also play important role in conformation-constraining factors. Furthermore, protecting groups help to increase or decrease the reactivity of a glycosyl donor, depending on their chemical characteristics (NIGUDKAR; DEMCHENKO, 2015; GUO; YE, 2010).

Acetyl donors are easier to prepare, in high yields and cheap reagents. This donor was proposed due to the straightforwardness regarding the study of *O*-glycosilation reactions. Furthermore, some authors have reported the effect of remote participation of acyl groups in positions C-3 and C-6 of carbohydrate moieties. They showed that acyl groups in positions C-3 and C-6 can lead to the stabilization of a *dioxocarbenium* intermediate between one of these positions and O-1, which enables the attack of the nucleophile by the α direction in the anomeric position (Scheme 56) (HAHM; HUREVICH; SEEBERGER, 2016; VIDAL; WERTZ, 2014; KOMAROVA et al., 2014; LI; ZHU; KALIKANDA, 2011).

On the other hand, the trufluoroacetimidate donor is a mixture of α and β anomers and, if the reaction underwent S*N*2 mechanism, the inversion of configuration will occur, rendering a mixture of anomers as product. This factor may have corroborated with the results regarding stereoselectivity presented in Table 2. Since *O*-acetyl donors lack reactivity, lower yields for donor **33a** when compared to donors **33b** and **33d**, may be explained by the longer time which led to degradation of the donor (GUO; YE, 2010; CRICH, 2010).

Remote participation by C-3   *Remote participation by C-6*
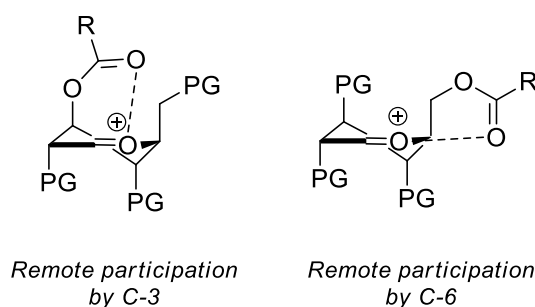
Scheme 56: Remote participation by acyl groups in C-4 and C-6 of glucose.

Regarding 4,6-*O*-benzylidene protecting groups, the function of the benzylidene acetal can favour both α and β anomers. Benzylidenes can act destabilising the glycosyl *oxocarbenium* by keeping the C-6/*O*-6 bond antiperiplanar to the C-5/*O*-5 bond. This would lead to formation of β glycosides instead of α and

can explain the rate of β anomers to be slightly higher, even in different solvents. On the other hand, the α-products can still be formed from a free *oxocarbenium* ion, according to the anomeric effect (CRICH, 2010).

The anomeric effect is based on molecular orbital interaction, using the hyperconjugation of the non-bonding electron pair of the oxygen atom on the ring with the vacant σ* orbital of the C-O bond, thereby stabilizing the axial configuration (Scheme 57) (LEMIEUX, 1971).
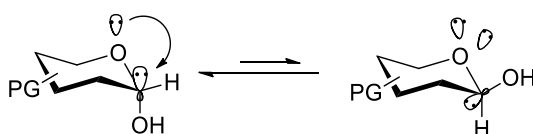
Scheme 57: Anomeric effect explained by molecular orbital interaction.

On the other hand, studies revealed that the energy due to hyperconjugation is not the bulk contributor in establishing the energy difference between the axial and equatorial configuration. Further, dipole moment theory aid that, in the equatorial isomer, the dipoles of the heteroatoms are partially aligned, thereby repelling each other. But, in the axial configuration, the opposite orientation of the dipoles stabilizes the system by implicating a lower energy barrier (ARDALAN; LUCKEN, 1973) (Scheme 58).
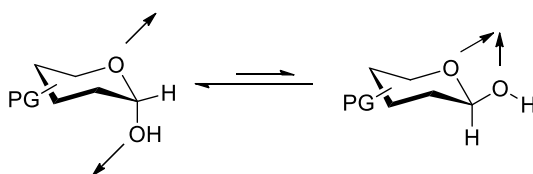
Scheme 58: Anomeric effect explained by dipole moment.

Benzoyl protecting groups, as well as acetyl groups, may promote remote participation with positions C-3 and C-6 in stabilization of a *dioxocarbenium* ion in the upper face of the carbohydrate. Moreover, the bulkiness of the benzoyl groups, when compared to acetyl groups, possibly prevents more effectively the attack of a nucleophile from the β face. In addition, these protecting groups are electron withdrawing groups (EWG), which reduce the reactivity of the glycosyl donors and decrease reaction velocity, possibly allowing a better stereo control on the product formation (BOLS & PEDERSEN, 2017; PARK et al., 2007; DOUGLAS et al., 1998).

Silyl protecting groups have frequently been used primarily as an orthogonal protective group together with more commonly used acyl and benzyl. The enhance reactivity of glycosyl donors bearing silyl groups has also been widely studied recently (HEUCKENDORFF; PEDERSEN; BOLS, 2010; JENSEN; PEDERSEN; BOLS, 2007). In this study, the aim of using bulky silyl group at C-6 position of the glucopyranose ring was to evaluate the hindrance of the equatorial face of anomeric position due to voluminous *O*-6 linked substituent. Thus, TBDPS proved to be effective for α-linked pseudo-disaccharide formation. However, the instability of the donor was a matter of concern and did not show much advantage by comparing to donor **33c**, which appeared to be more stable and easier to be synthesised.

Summing up all the results, the explanation for the high α anomer selectivity in most of the reactions may be due to the lack of neighbour participation azido group and the influence of the anomeric effect. The performance of *O*-glycosylation reaction using TMSOTf as promoter in relatively high temperatures have also been reported as favourable condition for development of α-glycosides (NIGUDKAR; DEMCHENKO, 2015; YANG; ZHANG, YU, 2012). Solvents of choice were in accordance to literature to render α anomers, since they are non-polar and etheric solvents. The best results could be observed with Et$_2$O, which was the solvent of choice to perform the large-scale *O*-glycosylations. The best results obtained for higher α– isomer formation was encountered with donors **33c** and **33d**, with possibly very low amounts of β anomer (non-detectable in this study). Given the low stability of donor **33d**, the *O*-benzoyl donor **33c** was selected for further large-scale *O*-glycosylations, which was conduced with 300 mg to 350 mg of donor (NIGUDKAR; DEMCHENKO, 2015; KIM; SUK, 2011).

4.2.3.3. *O*-glycosylation using tricholoroacetimidoyl donor 32

An attempt of *O*-glycosylation between donor **32** and acceptor **34** was performed to compare to *N*-phenyl trifluoroacetimidoyl donor containing the same protection groups **33b.** Conditions for the reaction were the same applied to previous *O*-glycosylations in this work, being Et2O the solvent of choice. Equivalent relationship between donor and acceptor was 1:1, accordingly to previous methodology. The reaction was left overnight for completion, which was determined by the complete consumption of the donor **32** (Scheme 59). The reaction was

monitored by TLC which showed one product with same R_f of the pseudo-disaccharide standard. After completion the reaction mixture was then neutralised with Et₃N, filtered over celite and concentrated. The product was isolated by semi-preparative TLC, in 35% yield.
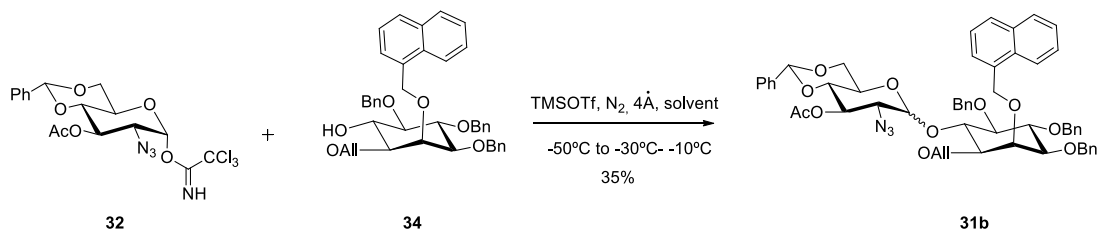
Scheme 59: *O*-glycosylation reaction with donor **32** containing trichloroacetimidate leaving group.

Despite the TLC showed only one product, the analysis of HSQC NMR showed a mixture of α/β anomers. In the ^{1}H NMR it was possible to observe one doublet at 5.87 ppm with relative integral of 1 hydrogen with coupling constants $J_{1,2}=$ 3.7 Hz, representing the hydrogen of the α-pseudo-disaccharide. It was not possible to calculate the coupling constants of the β anomer due to the overlapped region (Appendix).

The results showed that the trichloroacetimidate donor afforded the pseudo-disaccharide **31b** in lower yield (35%) when comparing to *N*-phenyl trifluoroacetimidate donor **33b** (68.6% in Et₂O). They also showed the presence of α/β anomers, which can be explained by the higher reactivity of trichloroacetimidoyl groups in comparison even to *N*-phenyl trifluoroacetimidoyl that leads to loss of stereoselectivity control (DEMCHENKO, 2008).

3.2.4. Synthesis of phospholipid and attachment to pseudo-disaccharide **30**.

After obtaining the pseudo-disaccharide block **31c** in good quantities, the next steps involved the attachment of the phospholipid core at C-1 of the *myo*-inositol unit. To accomplish this, the allyl group was selectively deprotected (compound **77**) for later introduction of the phosphodiester linkage (Scheme 60).
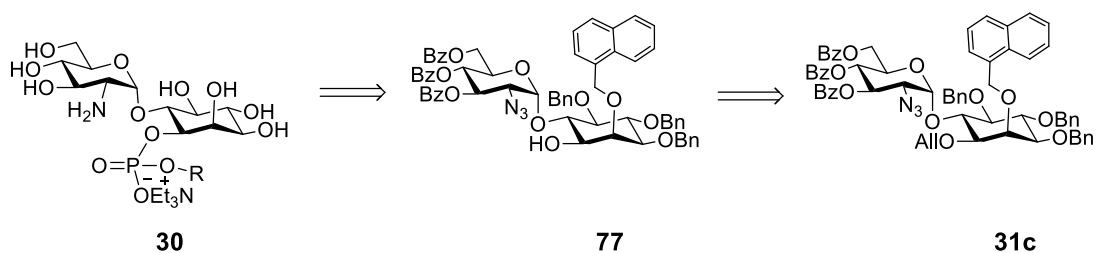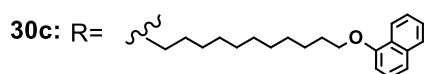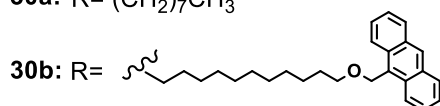
Scheme 60: Retrosynthesis of pseudo-disaccharide **30** containing phosphodiester linkage with lipid mimics.

4.2.4.1. Removal of Allyl group

To choose the right condition for the deallylation was essential to preserve the 2-azido group in the glucopyranoside moiety, since some conditions undergo reductive elimination, which could lead to reduction of the azido group to amine (VUTUKURI et al., 2003). Therefore, deallylation of **31c** was performed with palladium chloride (PdCl$_2$) in the presence of sodium acetate, acetic acid and water (Scheme 61). The deallylation did not reach completion, even after forcing conditions. Therefore, the product **77** was obtained in 83% yield after purification by flash column chromatography.
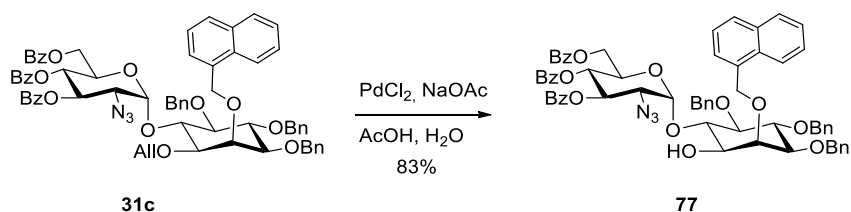
Scheme 61: Selective deallylation of **31** to give compound **77**.

Signals related to the allyl groups were absent at the ^{1}H NMR of the product (Appendix), when comparing to the starting material **31c** (Appendix).

The mechanism of deallylation by PdCl$_2$ is not totally elucidated. For instance, a proposed mechanism is presented on Scheme 62. The palladium complex A reacts

with the allyl group B to give a π-allyl-Pd(II) complex C. Next, the hydrogen ion is donated by equilibration of the acetate buffer D to this complex, affording the propene E and the deallylated product (CHANDRASEKHAR; REDDY; RAO, 2001).
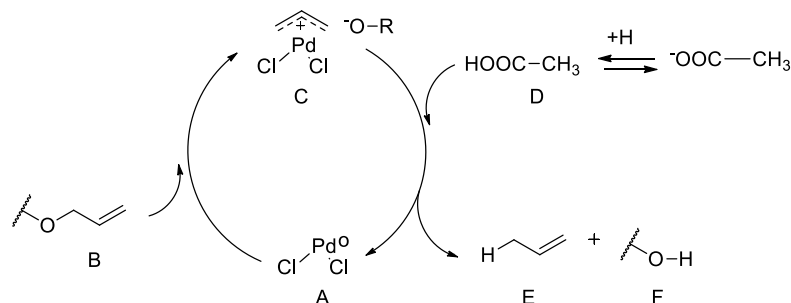
Scheme 62: Proposed Mechanism for deallylation with PdCl$_2$ in acetate buffer.

4.2.4.2. Preparation of the lipid chain analogues

In parallel, the synthesis of the lipid mimics containing naphthol and anthracenyl moieties was performed based on Brockhausen's works (RILEY; XU; BROCKHAUSEN, 20010; MONTOYA-PELEAZ et al., 2005). To achieve target compounds, commercial the terminal alcohol of 11-bromo-1-undecanol (**78**) was protected with tetrahydropyranyl (THP) group by reaction with 3,4-dihydro-2H-pyran and p-tuluenesulfonic acid, in DCM for 16 hours (Scheme 63). The acetal **79** was used in next steps without any purification.
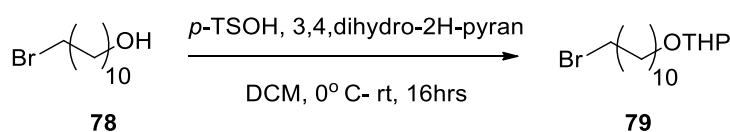
Scheme 63: Protection of alcohol of compound **78** with THP to afford protected intermediate **79**.

In sequence, Williamson reaction between compound **79** and 9-anthracenemethanol (**80**) or naphthalen-1-ol (**81**) afforded compounds **82** and **83**, respectively. Both reactions were worked up and crude products followed to the next step without previous purification (Scheme 64). The deprotection of THP was performed in methanol using excess of p-toluenesulfonic acid. Compounds **84** and **85** were obtained in 45% and 30% yields over three steps (Scheme 65).
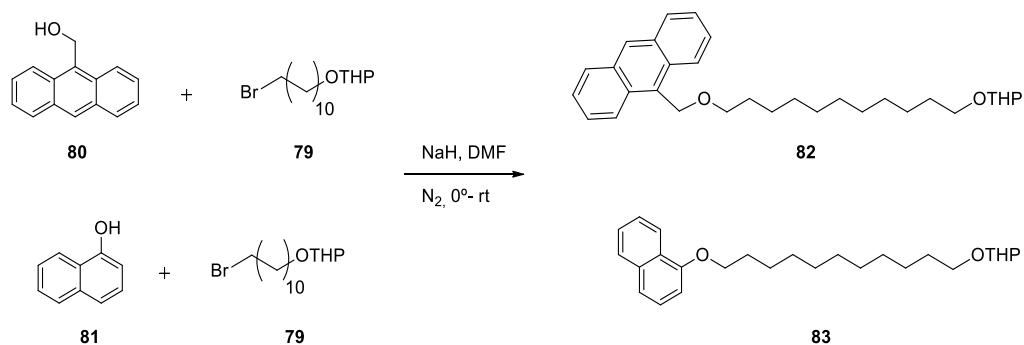
Scheme 64: Attachment of the aromatic moieties to chain **79**, affording products **82** and **83**.
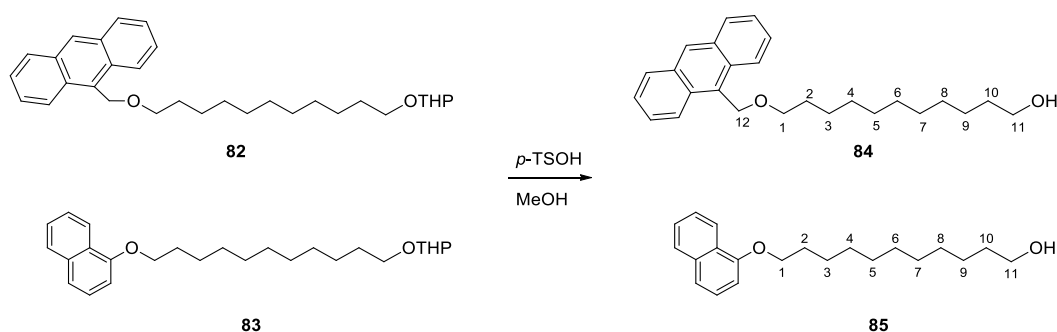
Scheme 65: Deprotection of group THP using p-toluenesulfonic acid to give products **84** and **85**.

The ^{1}H NMR spectra of compound **84** showed signals between 8.45 ppm and 7.44 ppm with relative integral to 9 aromatic hydrogens. One singlet at 5.45 ppm with relative integral to 2 hydrogens is related to the hydrogens of the methylene close to the anthracene group at C-12 (See Scheme 65 for atom numbers). A multiplet at 3.64 ppm with relative integral to 4 hydrogens indicates the 2 methylenes at C-1 and C-11, whereas other multiplets between 1.68 ppm to 1.15 ppm are related to the remaining hydrogens of the chain between C-2 and C-10.

In relation to ^{1}H NMR spectra of compound **85**, signals between 8.30 ppm and 6.76 ppm with relative integral adding up to 7 hydrogens are related to the naphthol moiety. Two triplets at 4.13 ppm and 3.62 ppm with relative integral to 2 hydrogens each are related to the methylene of C-1 and C-11, whereas multiplets between 1.96 ppm and 1.27 ppm are related to the remaining hydrogens of the chain between C-2 and C-10.

4.2.4.3. Synthesis of GPI derivative, compound 30a

A study performed by Brown and co-workers (2001) demonstrated that a series of synthetic mannosides containing a C-8 "lipid" chain were able to be recognized as substrates for mycobacterial mannosyltransferases (BROWN et al., 2001). Based on this, the first phospholipid proposed to be attached to the pseudo-disaccharide **77** comes from 1-octanol (compound **86,** Scheme 66). In this context, problems related to solubility of the final compound for assays would be avoided. Therefore, salicylchlorophosphite (SalCIP-**86**) was used as source of phosphorus during the work at John Innes Centre, generating the H-phosphonate derivative **87** to react with pseudo-disaccharide **77** in a convergent approach (CROSSMANN et al., 2002; MARUGG, et al., 1986). Thus, under inert atmosphere, 1-octanol together with pyridine was added dropwise over a solution of SalCIP in THF. The reaction was followed by TLC which showed a product with no mobility (mobile phase DMC/MeOH 9:1).
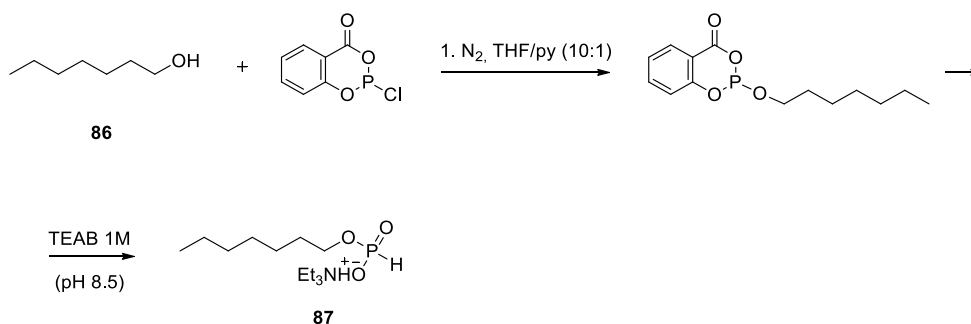
Scheme 66: Synthesis of the H-phosphonate **87** from reaction of **86** with SalCIP.

Next, the mixture was diluted with CHCl$_3$ and triethylammonium bicarbonate buffer (pH=~ 8.5) was added to the reaction mixture and stirred for more 1 hour. The mixture was then worked up and the product **87** followed to the next step without purification.
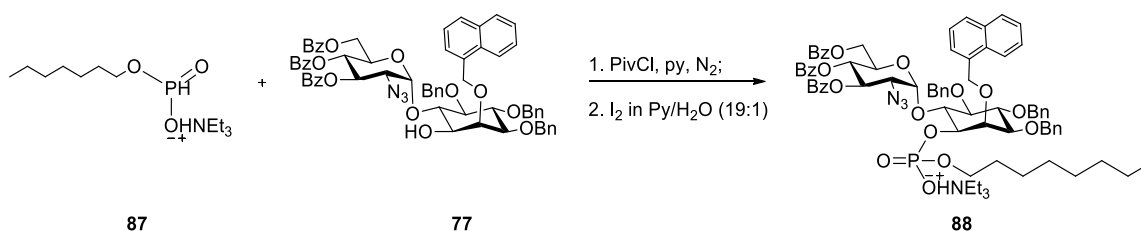
Scheme 67: Synthesis of phosphodiester product **88**.

Finally, compound **87** was attached to the pseudo-disaccharide **77** by using pivaloyl chloride (PivCl) in anhydrous pyridine (CROSSMANN, 2002). The later oxidation with molecular iodine in water gave the desired phosphodiester linkage in compound **88** (Scheme 67).

There are not many detailed mechanistic studies regarding the phosphodiester's formation from of H-phosphonates reacting with pivaloyl chloride and pyridine. A proposed mechanism involves the activation of the monophosphoester by pivaloyl chloride in the presence of pyridine, and the mixed anhydride formed is attacked by the nucleophile, in this case, the free position of the pseudo-disaccharide **77** (Scheme 68) (SOBKOWSKI; KRASZEWSKI; STAWINSKI, 2014; SIGURDSSON; STRÖMBERG, 2002; MARUGG et al, 1986).

R= Pseudo-disaccharide **77**
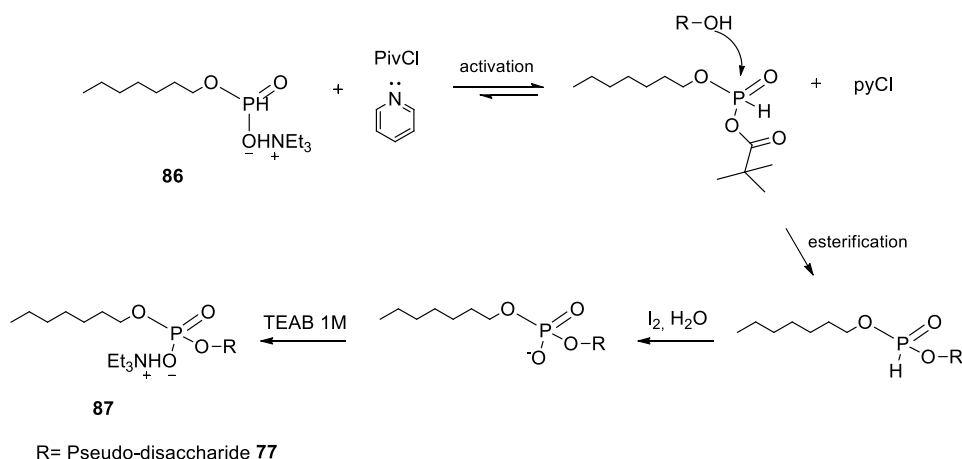
Scheme 68: Proposed mechanism for the formation of phosphodiester from H-phosphonates with PivCl and pyridine.

After the work up, the crude mixture underwent several attempts of separation by silica column chromatography with no success. The strategy of purification was then changed to reverse phase.
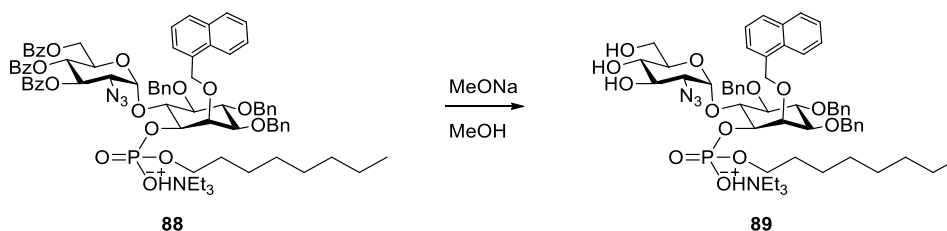
Scheme 69: Selective deprotection of O-benzoyl groups of intermediate 88 to afford product **89**.

To access this, the product **88** was then subjected to partial deprotection of the benzoyl groups with sodium methoxide in methanol giving compound **89**, for further purification by semi-preparative HPLC (Scheme 69).

Separation of **89** was performed in DIONEX Ultimate 3000 instrument equipped with UV/vis detector and using column Phenomenex Luna 5 C_{18} (10 x 250 mm). The sample in methanol was eluted with 50 mM Et_3NHOAc, pH 6.8 with 1.5% MeCN (Bottle A) and MeCN (Bottle B) at a flow rate of 5 mL/min and detection with on-line UV detector to monitor A_{274} (Figure 13). Product **89** had the retention time of 21 minutes and was obtained with 8% yield over 2 steps (Appendix).
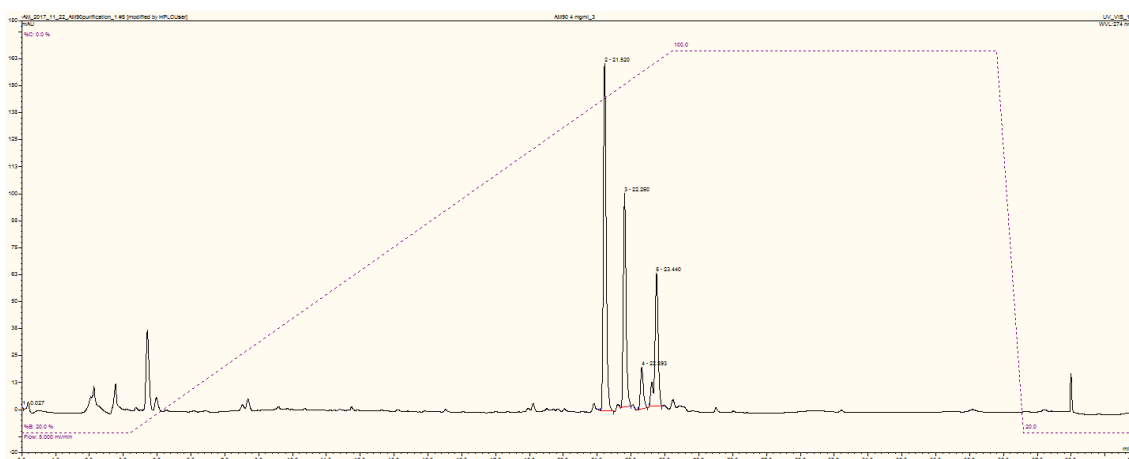
Figure 13: HPLC separation of compound **89**. The higher peak corresponds to the product (21 min).

The ^1H NMR of compound **89** showed multiplets at 1.52 ppm, 1.25 ppm and a triplet 0.83 ppm which are related to methylenes and the methyl group of the lipid chain. Signals between 7.88 ppm to 7.14 ppm with relative integral to 22 hydrogens are related to *O*-benzyl and *O*-naphtyl protecting groups of the inositol moiety. The ^{31}P NMR showed a signal at -0.55 ppm, which is typical of phosphate diester chemical shift. The high-resolution mass spectra in negative mode showed an ion with *m/z* 969.4152 $[M–Et_3N]^-$ calculated for $C_{52}H_{63}N_3O_{13}P^-$ (exact mass: 968.4182 g/mol) (Appendix).

Compound **89** underwent overall deprotection by hydrogenation with palladium in activated carbon in methanol and acetic acid under pressure (10.0 atm of H_2). The product **30a** was purified in C_{18} cartridge and obtained in 70% yield (Scheme 70).

The last steps in the synthesis of compound **30a** rendered the product in low yields (Scheme 70). Optimization of the final steps, such as attachment of the

phospholipid to the pseudo-disaccharide moiety and overall deprotection is still critical. Purification attempts of the phospholipid derivative **87** and variations of conditions of the phosphodiester formation between **77** and **87** are ongoing to circumvent problems regarding low yield.
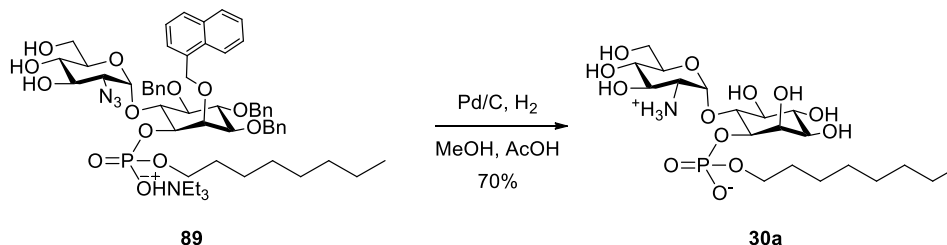
Scheme 70: Catalytic hydrogenation of 89 to afford final compound **30a**

4.2.4.4. Synthesis of GPI derivative, compound 30c

The attachment of the lipid mimic chain **85** to disaccharide derivative **77** was performed accordingly to methodology previously discussed for the synthesis of compound **30a** (CROSSMANN et al., 2002; MARUGG, et al., 1986). For instance, the steps depicted in Scheme 71 were performed, yielding the compound **91** in 20% yield.
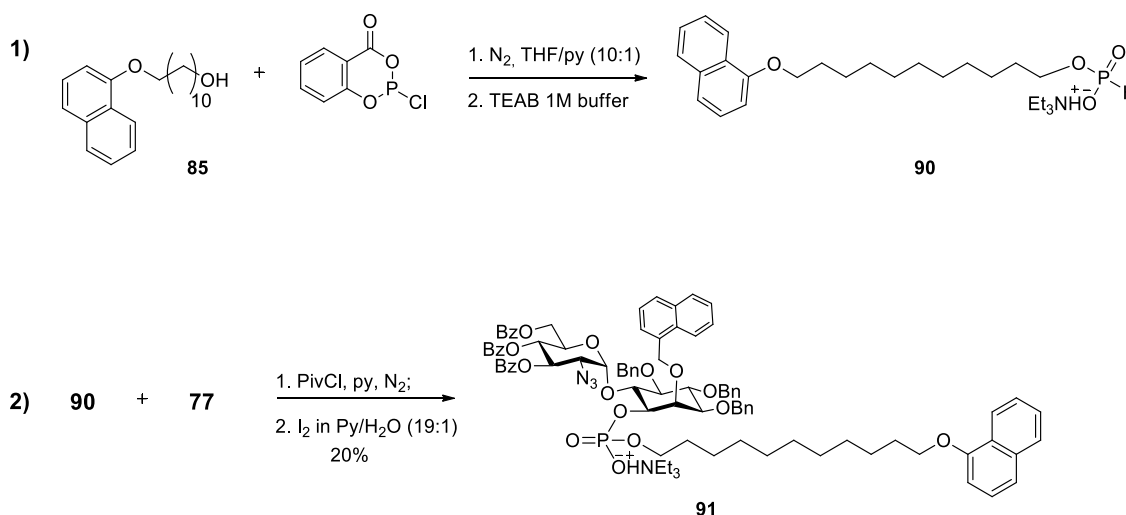
Scheme71: Synthesis of blocks **90** and **91** towards synthesis of compound **30c.**

The characterization of product **91** by ^{1}H NMR revealed the *O*-naphthyl at 6.80 ppm (other signals could not be observed due to very overlapped region between 8.30 ppm and 7.10 ppm). Signals at 1.96 ppm and 1.27 ppm related to the lipidic chain could also be observed. Moreover, high resolution mass spectra (negative

mode) showed an ion with *m/z* 1464.5713 [M–Et$_3$N]$^-$ calculated for C$_{86}$H$_{87}$N$_3$O$_{17}$P$^-$ (exact mass: 1464.5778 g/mol) (Appendix). Further reaction optimization and deprotection steps are being performed to achieve final compound **30c**. Regarding GPI derivative **30b**, the ongoing experiments will provide the better reaction conditions for its straightforward preparation.

4.2.4.5 Alternative synthesis of phosphodiesters

Based on the low yields of final product **30a** and intermediate **91**, beside the unvavailability of salicylchlorophosphite in Brazil, another attempt to attach the lipid chain was also studied, via Mitsunobu reaction in a linear synthesis (WANG, et al., 2008; KAYSER-BRICKER; JORDAN; MILLER, 2008; SCULIMBRENE; XU; MILLER, 2004). The proposed route would be an alternative to obtain the phosphodiester **30a** using the available diphenylchlorophosphate, even though in 7 steps (Scheme 72).
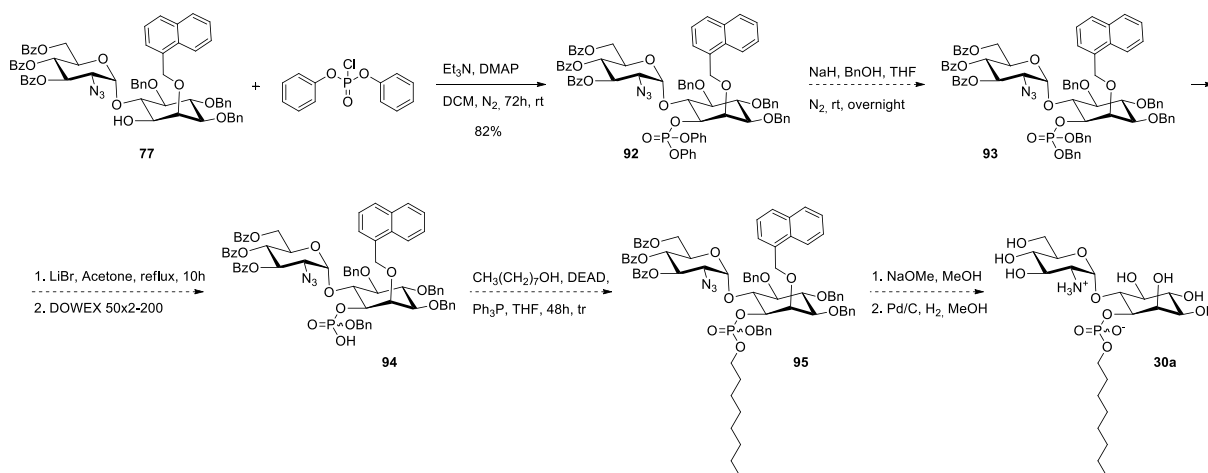
Scheme 72: Alternative synthesis to achieve phosphodiester **30a**.

Thus, pseud*o*-disaccharide **77** was treated with diphenyl-chlorophosphate in presence of Et$_3$N and dimethyl aminopyridine (DMAP) at room temperature. After 72 hours, a new product could be observed in Rf almost identical to starting material. Compound **92** was isolated by silica flash chromatography in 82% yield.

It was not possible to observe any changes in ^{1}H NMR spectra, since the only visible signals would be in the overlapped region of the aromatic hydrogens. On the other hand, high resolution mass spectra presented the ions related to the product in positive mode*: m/z* 1322.4409 [M+1]$^+$ calculated for C$_{77}$H$_{69}$N$_3$O$_{16}$P (Exact mass:

1321.4337 g/mol) (Appendix). Furhter attempts to replace the two phenyl by benzyl groups gave a product bearing both phenyl and benzyl groups even at forcing conditions. Due to the limited time, this route is still under investigation.

4.2.5. LC-MS/MS analysis of product **30a**
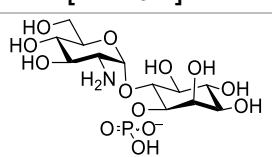
Injection of compound **30a** was performed on Zevo TQ-S Acquity UP-LC made by WATERS® for the stablishment of a chromatographyc method, required for comparison of extracts to be obtained after incubation *Euglena gracilis* microsomes with compound **30a**. For this reason, compound **30a** was sent to Dr. Irina Ivanova at John Innes Centre to carry out these assays that involve the incubation of microsomal membranes with product **30a** in presence of UDP-mannose. Thus, the possible new compounds in the extract will be analysed by the same LC-MS/MS method. In this context, the diluted compound **30a** was injected (2-7.5 µl, 10 µM in MeOH/water) in small column *Hypercarb* 1 x 100 mm, particle 5 µm, CV ~ 78.5 µL, and flow rate of 80 µl/min. Each injection lasted 50 minutes. Detection of the product was performed by ESI(-) and the results are shown on Table 3.

Table 3: Ion detected by LC-MS/MS peak at 22 minutes.

Compound	Formula/ Mass		Parent m/z	Cone Voltage	Daughters	Collision Energy	Ion Mode
30a	533.2237	1	532.26	94	78.92	44	ES-
		2	532.26	94	402.16	32	ES-

A peak identified at 22 minutes was related to the mass of compound **30a** (533.2237). The daughters of this parent ion were 78.92 and 402.16. (Table 3). The given daughter ions are related to fragments of compound **30a**, depicted on Table 4.

Table 4: Fragments related to the ions detected on LC-MS/MS in injection of **30a.**

Ion	Fragment
1- m/z 78.92	[Pi-H₃O]⁻
2- m/z 402.16	Chemical Formula: $C_{12}H_{23}NO_{13}P^-$ Exact Mass: 420,0912 **420-18=402**

The injections of compound **30a** on LC-MS showed that a chromatographic method was successfully stablished, that can be extended to compounds **30b-c**. Despite the microsomal membranes of *E. gracilis* were already obtained their incubation with GPI derivative **30a** are underway.

4.3. Phylogenetic trees

Phylogenetic trees were performed by the Ph.D. student Sakonwan Kuhaudomlarp by comparing known protein sequences related to the enzymes involved in GPI anchor biosynthesis of various organisms. Database BLAST (Basic Local Alignment Search Tool) was used to align and compare the sequences. Figure 14 shows a representative phylogenetic tree highlighting some important species involved in the preparation of the phylogenetic trees.
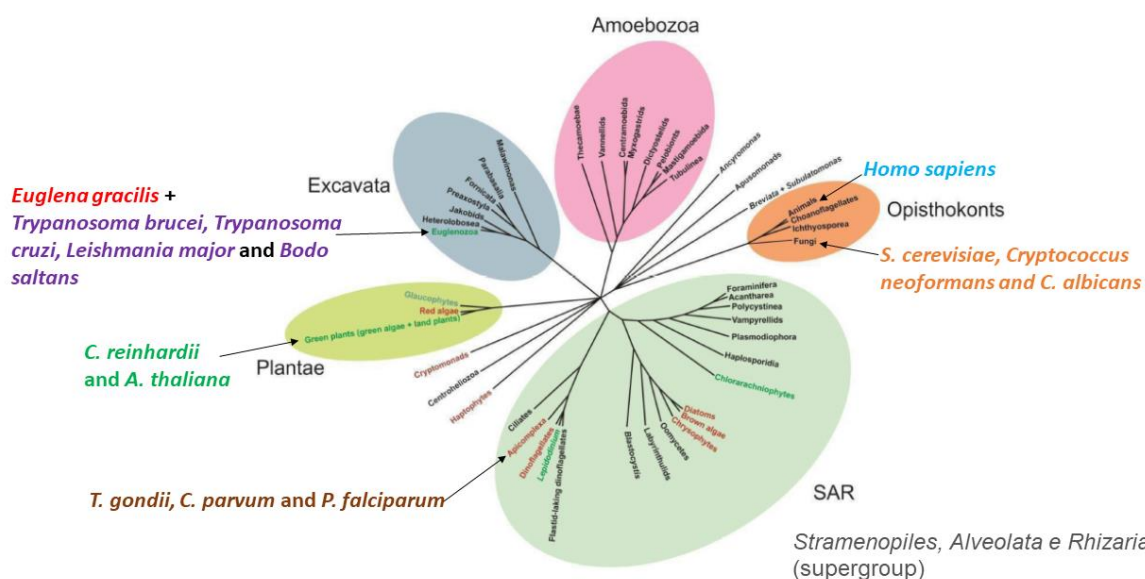
Figure 14: Tree of life for the species used in the protein sequence analyses. Colour code on the species names are used for the annotation of subsequent trees.

The main goal of the elaboration of these trees was to analyse the clustering of enzymes involved in GPI anchor biosynthesis between *E. gracilis* and protozoan, fungi, plants, mammalians and algae, giving clues of similarity among them. Thus, four phylogenetic trees were obtained to pursued enzymes, such as:

- PI deacylase

- α-1,2-mannosyltransferase
- Inositol acyltransferase
- α-1,4-mannosyltransferase

From all the enzymes mentioned above, α-1,4-mannosyltransferase showed common origin between *E. gracilis*, *Trypanosomatids* and *Bodo saltans*: a free-living protozoan which belongs to order *Kinetoplastidae*, closely related to protozoan parasites of the same order, such as *T. cruzi, T. brucei* and *Leishmania spp.* (JACKSON et al., 2016) (See Appendix for phylogenetic trees)*.*

No other enzymes showed such close relation between the organisms mentioned, apart from *E. gracilis*' inositol acyltransferase, which gives rise to acylated inositol, also presents common origin with *Bodo saltans*. Therefore, the lack of analogous sequence might suggest that inositol acyltransferase is not required for all GPI anchor biosynthesis because there is no evidence that all known GPI anchor pathways contain acylated inositol.

The enzyme 1,4-mannosyl transferase attaches the first residue of mannose to the block of glucosamine-PI during the biosynthesis of GPI anchors. Given the results from the phylogenetic trees, it is possible to affirm that the derivatives synthesised in this work are appropriate for the assays with mannosyltransferases in *E. gracilis* and extension of the tests in *T. cruzi.*

4.3.1. Microsomal membranes of Euglena gracilis

Based on the homology with known enzymes, O'Neill and co-workers (2015) resolved the transcriptome of *E. gracilis* and demonstrated that it contains sequences of all enzymes involved in the biosynthesis of *N*-linked glycoproteins and GPI anchors. Glycosyltransferases that participate in the biosynthesis of GPI anchors in ER and Golgi organelles (VARKI; ESKO; COLLEY, 2009), which are related to microsomal membranes (vesicle-like artefacts re-formed from pieces of ER). In this context, isolation of microsomes often leads to enzyme denaturation with subsequent loss of activity. Because of that, *E. gracilis* microsomal membranes were extracted following the literature procedure in order to preserve activities of membrane-bound glycosyltransferases (GILLOTT; TRIEMER; VASCONCELOS, 1980). In this study, microsomes were obtained from growing cultures in dark of *Euglena gracilis* var *saccharophila* Klebs (strain 1224/7a) in media supplemented with glucose for 13

days. After isolation, microsomal membranes, they were stored at -80 °C and can be used along one year without losing enzymatic activities.

4.4. Final considerations

Biologycal assays are being performed in *E. gracilis* microsomes with compound **30a** to test its ability of being either a GPI anchor biosynthesis precursor or inhibitor. The work is being carried out at John Innes Centre with the assistance of Dr. Irina Ivanova. It is important to deliberate that working with *E. gracilis* metabolism is very challenging, since there are not enough biochemical studies to point base on the lack of a known ligand in the assays. Thus, the synthesised compounds may help the validation of the assays, and if successful, the same procedure will be applied to *T. cruzi* microsomal membranes, which will be isolated by methodology already described in literature (PREVIATO et al., 1998).

Synthetic work is still ongoing to get the final product **30a** in good quantities for better standardization and relyability of biological assays. Compounds **30b** and **30c** could not be obtained in time until date, but their synthesis is still being performed for further completion of the proposed objectives. Some studies regarding optimization of reactions and alternative routes are being carried out in a search for more satisfactory yields and overall results.

5. CONCLUSIONS
_____

Glycosyl donors were prepared from α-D-Glucosamine hydrochloride (**35**) in good yields, being the donors **33c** and **33d** not previously described in the literature. Synthesis of *myo*-inositol acceptor unit was successful achieved using *Ferrier* rearrangement strategy, affording acceptor **34** in moderate yields. Donors and acceptor were all tested in small scale in *O*-glycosylation reactions to check conditions and select the best donor in terms of good α anomer ratio, yield and reproducibility. From these experiments, donor **33c** was selected for large scale *O*-glycosylations.

O-glycosylation α/β ratio proved to be more depend on donor chemical properties than on solvents. Despite most of reactions had a higher generation of α anomer, yields and effectiveness of reactions were different. For instance, 1,2-dichloroethane seemed to promote extended time for reaction completion, which led to decomposition of some donors to hemiacetals. Large scale of *O*-glycosylation of acceptor **34** with donor **33c** was accomplished in diethyl ether, using TMSOTf as promoter. A key step involving the deallylation of compound **31c** was successfully performed with $PdCl_2$ and NaOAc in acetic acid giving a novel pseudo-disaccharide **77** in good yields. All synthesised pseudo-disaccharides **31a-d** are unkown in the literature.

Phosphodiester linkage between octanoyl H-phosphonate **87** and **77** was conducted according to Crossman and co-workers (2002), giving compound **90** with low yield, after partial deprotection and successful purification by semi-preparative HPLC. Product **90** was then subjected to overall deprotection giving the target product **30a,** which was sent to John Innes Centre for further *E. gracilis* microsomes assays. Moreover, injections of compound **30a** on LC-MS allowed the establishment of appropriate conditions for further analysis of products to be obtained after incubation of **30a** with microsomal membranes. For this purpose, *E. gracilis* was grown in dark conditions for 13 days for later isolation of microsomal membranes,

Furthermore, synthesis of anthracenyl (**84**) and naphthyl (**85**) lipid chains were successfully synthesised according to Riley and co-workers (2010) in few steps and moderate yields. Compound **85** underwent H-phosphonate approach and further phosphodiester linkage to the deallylated pseudo-disaccharide **77**, giving compound **91** in low yield. Overall deprotection of **91** is ongoing and last steps of the synthetic route are being optimized to achieve better yields and purity. The anthracenyl

derivative **84** will be submitted to the same procedures of phosphorylation once the route is optimized.

As future perspectives, the synthesis of compounds **30b-c** will be performed and optimization of the synthetic route aiming to achieve the final products in better quantities will be performed. In addition, standardization and further validation of the assays *in E. gracilis* microsomes will be performed with the scope that it must be prepared to give information whether the synthesised compounds **30a-c** would be either an GPI pathway inhibitor or substrate. Once assays are set in *E. gracilis*, results will be analysed, and the same methods will be appliedto *T. cruzi* microsomal membranes.

6. REFERENCES

_____

ADERO, P. O.; AMARASEKARA, H.; WEN, P.; BOHÉ, L.; CRICH, D. The Experimental Evidence in Support of Glycosylation Mechanisms at the S_N1–S_N2 Interface. **Chemical Reviews, v.** *118*, n.17, p. 8242-8284, 2018.

AHMADINEJAD, N.; DAGAN, T.; MARTIN, W. Genome history in the symbiotic hybrid *Euglena gracilis*. **Gene**, v. *402*, p. 35-39, 2007.

AICH, U.; M. MELEDEO, A.; SAMPATHKUMA, S.-G.; F.; JONES, M. B.; WEIER, C. A.; CHUNG; S. Y.; TANG, B. C.; YANG, M.; HANES, J.; YAREMA K. Development of Delivery Methods for Carbohydrate-based Drugs: Controlled Release of Biologically-active Short Chain Fatty Acid-Hexosamine Analogs. **Glycoconjugate Journal**, v. 27, p. 445–459, 2010.

ANDRADE, L. O.; MACHADO, C. R.; CHIARI, E.; PENA, S. D.; MACEDO, A. M. Differential tissue distribution of diverse clones of *Trypanosoma cruzi* in infected mice. **Molecular and Biochemical Parasitology**, v.100, p. 163-172, 1999.

ANDRADE, P.; GALO, O. A.; CARVALHO, M. R. CARVALHO.; LOPES, C. D.; CARNEIRO, Z. A. SESTI-COSTA, R.; MELO, E. B.; SILVA, J. S.; CARVALHO, I. 1,2,3-Triazole-based analogue of benznidazole displays remarkable activity against Trypanosoma cruzi. **Bioorganic & Medicinal Chemistry**, v. 23, p. 6815-6826, 2015.

ANDRADE, P. **Síntese e atividade Biológica de Dissacarídeos acoplados a Aminoácios**, Dissertação de Mestrado, 2008.

ANSELME, J. P.; FISCHER, W. The reaction of anions of primary amines and hydrazones with *p*-toluenesulfonyl azide. **Tetrahedron**, v. 25, p. 855-859, 1969.

ARDALAN, E. A. C. LUCKEN, HELV. Nuclear Quadrupole Resonance and Stereochemistry I. α – Chloro ethers. **Chimica Acta**, v. 56, p.1715-1719, 1973.

BAEK, J.Y.; LEE, B.; JO, M.G.; KIM, K.S. β-Directing effect of electron withdrawing groups at O- 3, O-4, and O-6 positions and α-directing effect by remote participation of 3 *O*-acyl and 6-*O*acetyl groups of donors in Mannopyranosylations. **Journal of The American Chemical Society**, v. 131, p. 17705-17713, 2009.

BAESCHLIN, D. K.; CHAPERON, A. R.; CHARBONNEAU, V.; GREEN, L. G.; LEY, S. V.; LÜCKING; U.; WALTHER, E. Rapid Assembly of Oligosaccharides: Total Synthesis of a Glycosylphosphatidylinositol Anchor of *Trypanosoma brucei*. **Angewandte Chemie- International Edition**, v. 37, p.3423–3428, 1998.

BEDINI, E.; CIRILLO, L.; PARRILLO, M. Synthesis of the trisaccharide outercore fragment of *Burkholderiacepacia* pv. *vietnamiensis* lipooligosaccharide. **Carbohydrate Research**, v. 349, p. 24-32, 2012.

BENDER, S.; BUDHU, R. J. Biomimetic Synthesis of Enantiomerically Pure *myo*-Inositol derivatives. **Journal of The American Chemical Society**, v. 113, p. 9883-9885, 1991.

BOLS, M; PEDERSEN, C. M. Silyl-protective groups influencing the reactivity and selectivity in glycosylations. Hoffmann-Röder A. **Journal of Organic Chemistry**, v.13, p.93-105, 2017.

BOONYARATTANAKALIN, S.; LIU, X.; MICHIELETTI, M.; LEPENIES, B.; SEEBERGER, P. H. Chemical Synthesis of All Phosphatidylinositol Mannoside (PIM) Glycans from Mycobacterium tuberculosis. **Journal of The American Chemical Society**, v. 130, n. 49, p. 16791-16799, 2008.

BRASIL. Secretaria de Vigilância em Saúde. **Doenças infecciosas e parasitárias: guia de bolso**. 8. ed. rev. Brasília, D.F.: Ministério da Saúde, 2013.

BROWN, J. R.; GUTHER, M. L. S.; FIELD, R. A.; FERGUSON, M. A. J., Hydrophobic mannosides act as acceptors for trypanosome alpha-mannosyltransferases. **Glycobiology.** v.*7*, (4), 549-558, 1997.

BROWN, J. R.; FIELD, R. A.; BARKER, A.; GUY, M.; GREWAL, R.; KHOO, K-H.; BRENNAN, P. J.; BESRA, G. S.; CHATTERJEE, D. Synthetic mannosides act as acceptors for mycobacterial α1-6 mannosyltransferase. **Bioorganic & Medicinal Chemistry**, v.9, (4), p. 815–824, 2001.

BRUCKNER, R. **Organic Mechanisms-Reactions, Stereochemistry and Synthesis,** 1st Edition. Springer- Verlag Berlin Heidelberg, 2010.

BUETOW, D. E., *Euglena.* **Encyclopedia of Life Sciences,** 2011.

BUETOW, D. E., Differential effects of temperature on growth of *Euglena gracilis*. **Experimental Cell Research,** v. 27, p. 137-142, 1962.

CAMPBELL A. S., FRASER-REID B. Support studies for installing the phosphodiester residues of the Thy-1 glycoprotein membrane anchor. **Bioorganic and Medicinal Chemistry**, v. 2, p. 1209-1219, 1994.

CAMPBELL A. S., FRASER-REID B**.** First Synthesis of a Fully Phosphorylated GPI Membrane Anchor: Rat Brain Thy-1 **Journal of The American Chemical Society**, v.*117*, p. 10387-10388, 1995.

CAMPO, V. L.; IVANOVA, I. M.; CARVALHO, I.; LOPES, C. D.; CARNEIRO, Z. A.; SAALBACH, G.; SCHENKMAN, S.; SILVA, J. S.; NEPOGODIEV, S.A.; FIELD, R. A. Click chemistry oligomerisation of azido-alkyne-functionalised galactose accesses triazole-linked linear oligomers and macrocycles that inhibit *Trypanosoma cruzi* macrophage invasion. **Tetrahedron**, v. 71, p. 7344-7353, 2015.

CARDOSO, M. S.; JUNQUEIRA, C.; TRIGUEIRO, R. C.; SHAMS-ELDIN, H.; MACEDO, C. S.; ARAUJO, P. R.; GOMES, D. A.; MARTINELLI, P. M.; KIMMEL, J.; STAHL, P.; NIEHUS, S.; SCHWARZ, R. T.; PREVIATO, J. O.; MENDONCA-PREVIATO, L.; GAZZINELLI, R. T.; TEIXEIRA, S. M. R. Identification and Functional Analysis of *Trypanosoma cruzi* Genes That Encode Proteins of the Glycosylphosphatidylinositol Biosynthetic Pathway. **Plos Neglected Tropical Diseases***,* v.*7*, p.2369, 2013.

CARVALHO, I.; BORGES, E. B. Synthesis of (+)-(2R, 3S, 4R)-2, 3, 4-trihydroxycyclohexanone from d-glucose. **Carbohydrate Research**. v. 339, p. 361-365, 2012.

CHANDRASEKHAR, S.; REDDY, R.; R. RAO, J. Facile and selective cleavage of allyl ethers, amines and esters using polymethylhydrosiloxane– $ZnCl_2$/$Pd(PPh_3)_4$ **Tetrahedron**, v. *57*, p. 3435-3438, 2001.

CONZELMANN, A.; PUOTI, A.; LESTER, R.L.; DESPONDS, C., Two different types of lipid moieties are present in glycophosphoinositol-anchored membrane proteins of Saccharomyces cerevisae. **Embo Journal**, v.11, p. 457-466, 1992.

CRICH, D. Mechanism of a Chemical Glycosylation Reaction. **Accounts of Chemical Research**, v. *43*, p. 1144-1153, 2010.

CROSSMAN, A. T.; URBANIAK, M D, FERGUSON M. A.J. Synthesis of 1-d-6-O- [2-(N hydroxyaminocarbonyl) amino-2-deoxy-α-D-glucopyranosyl]-*myo*-inositol-1-(n-octadecylphosphate): a potential metalloenzyme inhibitor of glycosylphosphatidylinositol biosynthesis. **Carbohydrate Research**. v. 343, p. 1478-1481, 2008.

CROSSMAN, A.; PATERSON, M, J.; FERGUSON, M. A. J.; SMITH T. K., BRIMACOMBE J. S. Further probing of the substrate specificities and inhibition of enzymes involved at an early stage of glycosylphosphatidylinositol (GPI) biosynthesis. **Carbohydrate Research,** v. 337, p. 2049-2059, 2002.

DASGUPTA, S.; NITZ, M. Use of *N*, *O*-Dimethylhydroxylamine As an Anomeric Protecting Group in Carbohydrate Synthesis. **The Journal of Organic Chemistry***, v.* 76, p. 1918-1921, 2011.

DELACANAL, L.; PARODI, A. J. Glycosylation of proteins in the protozoan *Euglena gracilis.* **Comparative Biochemistry Physiology B***, v.* 81, p. 803-805, 1985.

DEMCHENKO*, A.* **Handbook of Chemical Glycosylation: Advances in Stereoselectivity and Therapeutic Relevance**. Wiley-VCH Verlag GmbH & Co. KGaA, 2008.

DEMCHENKO*, A;* BOONS, *G.* J. Solvent and other effects on selectivity of thioglycoside glycosidation. **Tetrahedron Letters**, v. 38, p. 1629-1632, *1997.*

DOERING, T.L.; RAPER, J.; BUXBAUM, L.U.; ADAMS, S.P.; GORDON, J.I.; HART, G.W.; ENGLUND, P.T., An analog of myristic acid with selective toxicity for African trypanosomes. **Science***, v. 252*, p. 1851-1854, 1991.

DOUGLAS, N. L.; LEY, S. V.; LUCKING, U.; WARRINER, S. L., Tuning glycoside reactivity: new tool for efficient oligosaccharide synthesis. **Journal of Chemical Society**, Perkin Trans, v.1, p. 51-66, 1998.

Drugs for Neglected Disease Initiative (DNDi)- Chagas Disease. Available at: https://www.dndi.org/?s=chagas, Accessed in September, 2018.

ECKERT, V.; GEROLD, P.; SCHWARZ, R.T. **Glycosciences: status and perspectives**. Gabius, H.-J.; Gabius, S., Eds.; Wiley-VCH Verlag GmbH & Co. KGaA: Weinheim, p. 223-243, 2002.

EDWARD J. T., Stability of glycosides to acid hydrolysis. **Chemistry & Industry**. p. 1102-1104, 1955.

FANKHAUSER, C.; HOMANS, S.W.; THOMASOATES, J.E.; MCCONVILLE, M.J.; DESPONDS, C.; CONZELMANN, A.; FERGUSON, M.A.J., Structures of glycosylphosphatidylinositol membrane anchors from *Saccharomyces cerevisae*. **Journal of Biological Chemistry***,* v. *268*, p. 26365-26374,1993.

FENG S.; BAGIA, C.; MPOURMPAKIS, G. Determination of Proton Affinities and Acidity Constants of Sugars. **Journal Physical Chemistry A**, v. 117, p. 5211–5219, 2013.

FERGUSON, M. A. J. The structure, biosynthesis and functions of glycosylphosphatidylinositol anchors, and the contributions of trypanosome research. **Journal of Cell Science***,* v. 112, p. 2799-2809, 1999.

FERGUSON, M.A.J., The surface glycoconjugates of trypanosomatid parasites. **Philosophical Transactions of the Royal Society of London Series B-Biological Sciences**, v. 352, p. 1295-1302, 1997.

FERGUSON, M. A. J.; HALDAR, K.; CROSS, G. A. *Trypanosoma brucei* variant surface glycoprotein has a sn-1,2-dimyristyl glycerol membrane anchor at its COOH terminus. **Journal of Biorganic Chemistry**, v. 260, n. 8, p. 4963-4968, 1985.

FERGUSON, M. A. J.; HART, GERALD, W.; KINOSHITA, T. **Essentials of Glycobiology,** 3rd edition. Cold Spring Harbor (NY):Cold Spring Harbor Laboratory Press, 2017.

FIANDOR, J.; GARCÍA-LÓPEZ,M. T.; DE LAS HERAS,F. G.; MÉNDEZ-CASTRILLÓN,P. P. A Facile Regioselective 1-*O*-Deacylation of Peracylated Glycopyranoses. **Synthesis,** v. 12, p.1121-1123,1985.

FONTAINE, T.; MAGNIN, T.; MELHERT, A.; LAMONT, D.; LATGÉ, J. P.; FERGUSON, M. A. J. Structures of the glycosylphosphatidylinositol membrane anchors from *Aspergillus fumigatus* membrane proteins, ***Glycobiology***, v. 13, p. 169–177, 2003.

FRASER-REID, U. E. UDODONG, Z. F. WU, Z. H. OTTOSSON, J. R. MERRITT, C. S. RAO, C. ROBERTS, R. MADSEN. *n*-Pentenyl Glycosides in Organic Chemistry: A Contemporary Example of Serendipity **Synlett**, p. 927 –942, 1992.

GAO, J.; ZHOU, Z.; GUOA, J.; GUO Z. Synthesis of biotin-labelled core glycans of GPI anchors and their application to the study of GPI interaction with pore-forming bacterial toxin. **Chemical Communications**. v. 53, p. 6227–6230. 2017.

GAREGG, P. J.; IVERSEN, T.; JOHANSSON, R.; LINDBERG, B. Synthesis of some mono-*O*-benzyl- and penta-*O*-methyl-*myo*-inositols. **Carbohydrate Research**, v. 130, p.322-326, 1984.

GILLOTT, M. A.; TRIEMER, R. E.; VASCONCELOS, A. C., Isolation of dictyosomes from *Euglena gracilis*. **Protoplasma**, v.105, p. 45-51, 1980.

GREENE, T. W.; WUTS, P. G. M. **Protective Groups in Organic Synthesis**, Wiley-Interscience, New York, 1999.

GREENE, T. W.; WUTS, P. G. M. **Protective Groups in Organic Synthesis**, 3rd ed. John Wiley & Sons: New York, 2007.

GUO, J.; YE, X.-S. Protecting Groups in Carbohydrate Chemistry: Influence on Stereoselectivity of Glycosylations. *Molecules, v.15, p.7235-7265, 2010.*

GUO, Z.; BISHOP, L. Chemical Synthesis of GPIs and GPI-Anchored Glycopeptides. **European Journal Organic Chemistry**, *p.* 3585-3596, 2004.

HAHM, H. S.; HUREVICH, M.; SEEBERGER, P. H. Automated assembly of oligosaccharides containing multiple *cis*-glycosidic linkages. **Nature Communications**, v. 7, article number: 12482, 2016.

HATAKEYAMAA, S.; SUGIHARAB, K.; SHIBATA, T., K.; NAKAYAMAC, J.; AKAMA, T., O.; TAMURA, N.; WONGA, S.; BOBKOVA, A., A.; TAKANOA, Y.; OHYAMAD, C.; FUKUDA, M.; FUKUDA, M., N. Targeted drug delivery to tumor vasculature by a carbohydrate mimetic peptide. **PNAS**, v. 108, p. 19587–19592, 2011.

HEDEROS M.; KONRADSSON P. Synthesis of the Core Tetrasaccharide of *Trypanosoma cruzi*Glycoinositolphospholipids: Man*p* (α1→6)-Man*p* (α1→4)-6-(2-aminoethylphosphonic acid)-GlcN*p* (α1→6)-*myo*-Ins-1-PO$_4$. **The Journal of Organic Chemistry**, v. 70, p. 7196–7207, 2005.

HEUCKENDORFF, M.; PEDERSEN, C. M.; BOLS, M. Quantifying Electronic Effects of Common Carbohydrate Protecting Groups in a Piperidine Model System Chem. – Eur. J., v.16, p.13982–13994, 2010.

HOUSE; H; KRAMAR, V. The Chemistry of Carbanions. V. The Enolates Derived from Unsymmetrical Ketones. **The Journal of Organic Chemistry**, v. 28, i.12, p. 3362-3379, 1963.

IMHOF I.; FLURY, I., VIONNET, C.; ROUBATY, C.; EGGER, D.; CONZELMANN, A. Glycosylphosphatidylinositol (GPI) Proteins of Saccharomyces cerevisiae Contain Ethanolamine Phosphate Groups on the 1,4-linked Mannose of the GPI Anchor. **The Journal of Biological Chemistry**, v. 279, No. 19, Issue of May 7, pp. 19614–19627, 2004.

ISHIWATA, A.; ITO, Y. High throughput screening of *O*-glycosylation conditions. **Tetrahedron Letters**, v. 46, p. 3521- 3524, 2005.

ISHIWATA, A.; MUNEMURA, Y.; ITO, Y. Synergistic solvent effect in 1,2-*cis*-glycoside formation. **Tetrahedron**, v. 64, p. 92-102, 2008.

IVANOVA I. M., NEPOGODIEV, S. A., SAALBACH, G., O'NEILL, E. C., URBANIAK, M. D., FERGUSON, M A. J., GURCHA, S. S, BESRA G. S., FIELD, R. A. Fluorescent mannosides serve as acceptor substrates for glycosyltransferase and sugar-1-phosphate transferase activities in *Euglena gracilis* membranes. **Carbohydrate research***, v.438, p.26-38, 2017.

JACKSON, A. P.; OTTO T. D.; ASLETT, M.; ARMSTRONG, S. D.; BRINGAUD, F.; SCHLACHT, A.; HARTLEY, C.; SANDERS, M.; WASTLING, J. M.; DACKS, J. B.; ACOSTA-SERRANO, A.; FIELD, M. C.; GINGER, M. L., BERRIMAN, M. Kinetoplastid Phylogenomics Reveals the Evolutionary Innovations Associated with the Origins of Parasitism. **Current Biology,** v. 26, p. 161–172, 2016.

JENSEN, H. H.; PEDERSEN, C. M.; BOLS, M. Going to Extremes: "Super" Armed Glycosyl Donors in Glycosylation **Chemistry – A European Journal**, v.13, p. 7576–7582, 2007.

JOHNSSON, R.; OLSSON, D.; ELLERVIK U. Reductive openings of acetals: explanation of regioselectivity in borane reductions by mechanistic studies**. Journal of Organic Chemistry**, v. 73, p. 5226-5232, 2008.

KAFLE, A.; LIU, J.; CUI, L. Controlling the stereoselectivity of glycosylation via solvent effects. **Canadian Journal of Chemistry**, v. 94, n.11, p. 894-901, 2016.

KAYSER-BRICKER, K.; JORDAN, P. A.; MILLER, S. J. Catalyst-Dependent Syntheses of Phosphatidylinositol-5 Phosphate-DiC8 and its Enantiomer. **Tetrahedron**, v. 64, p. 7015-7020, 2008.

KIM, J.-H.; YANG, H.; BOONS, G.-J., Stereoselective glycosylation reactions with chiral auxiliaries. **Angewandte Chemmie., Int. Ed**., v. 44, p.947-949, **2005**.

KOMAROVA, B. S.; OREKHOVA M. V.; TSVETKOV, Y. E.; NIFANTIEV, N. E. Is an acyl group at O-3 in glucosyl donors able to control a-stereoselectivity of glycosylation? The role of conformational mobility and the protecting group at O-6. **Carbohydrate Research**, v. 384, p. 70–86, 2014.

KRNACOVA, K.; VESTEG, M.; HAMPL, V.; VLCEK, C.; HORVATH, A., *Euglena gracilis* and *Trypanosomatids* possess common patterns in predicted mitochondrial targeting pre-sequences. **Journal of Molecular Evolution***, v. 75, p. 119-129, 2012.

KWON, Y-U.; SOUCY, R. L.; SNYDER, D. A.; SEEBERGER, P. H. Assembly of a Series of Malarial Glycosylphosphatidylinositol Anchor Oligosaccharides. Chemistry-A European Journal, v.11, p. 2493–2504, 2005.

LEMIEUX, R. U. Effects of unshared pairs of electrons and their solvation on conformational equilibria. **Pure Applied Chemistry.** v. 25, p. 527– 548, 1975.

LI, Z.; ZHU, L.; KALIKANDA, J. Development of a highly a-selective galactopyranosyl donor based on a rational design. **Tetrahedron Letters**, v. 52, p. 5629–5632, 2011.
LI, J. AND YU, B., A Modular Approach to the Total Synthesis of Tunicamycins. **Angewandte Chemie. Int. Ed.**, v. 54, p. 6618–6621, 2015.

LINDBERG, J.; ÖHBERG, L.; GAREGG, P. J.; KONRADSSON, P. Efficient routes to glucosamine-myo-inositol derivatives, key building blocks in the synthesis of glycosylphosphatidylinositol anchor substances. **Tetrahedron**, v. 58, p. 1387-1398, 2002.

LING, L.; LI, X; WATANABE, Y.; AKIYAMA, T.; OZAKI, S. Enzymatic resolution of racemic 1,2:5,6-di-O-cyclohexylidene and 1,2:3,4-di-O-cyclohexylidene-myo-inositol. **Bioorganic & Medicinal Chemistry**, v, 1, i. 2, p. 155-159, 1993.

LING, L.; OZAKI, S. A chemoenzymatic synthesis of D-*myo*-inositol 1,4,5-trisphosphate. **Carbohydrate Research**, v. 256, p. 49-58, 1994.

LIU, X.; STOCKER, B. L.; SEEBERGER, P. H. Total Synthesis of Phosphatidylinositol Mannosides of Mycobacterium tuberculosis. **Jornal of The American Chemical Society,** 128, 3638-3648, 2006.

LU, L.; GAO, J.; GUO, Z. Labeling cell surface GPIs and GPI-anchored proteins through cell metabolic engineering with artificial inositol derivatives. **Angewandte Chemie- *International Edition***, v. 54, p. 9679–9682, 2015.

MACEDO, C. S.; SHAMS-ELDIN, H.; SMITH, T. K.; SCHWARZ, R. T.; AZZOUZ, N. Inhibitors of glycosyl-phosphatidylinositol anchor biosynthesis. **Biochimie**, *v. 85*, p. 465-472, 2003.

MADSEN, R.; UDODONG, U. E.; ROBERTS, C.; MOOTOO, D. R.; KONRADSSON, P.; FRASER-REID, B. Studies Related to Synthesis of Glycophosphatidylinositol Membrane-Bound Protein Anchors. 6. Convergent Assembly of Subunits. **Journal of The American Chemical Society**, *v.* 117, p. 1554–1565, 1995.

MARCHIORI, M. F.; RIUL, T. B.; BORTOT, L., O.; ANDRADE, P.; JUNQUEIRA, G. G.; FOCA, G.; DOTI, N.; RUVO, M.; DIAS- BARUFFI, M.; CARVALHO I.; CAMPO, V., L. Binding of triazole-linked galactosyl arylsulfonamides to galectin-3 affects *Trypanosoma cruzi* cell invasion. **Bioorganic & Medicinal Chemistry**, v. 25, p. 6049–6059, 2017.

MARTINS- TEIXEIRA, M., B.; CAMPO, V., L.; BIONDO M.; SESTI-COSTA, R.; CARNEIRO, Z., A.; SILVA, J., S.; CARVALHO, I. Selective glycosylation affords mucin-related GalNAc amino acids and diketopiperazines active on *Trypanosoma cruzi*. **Bioorganic & Medicinal Chemistry**, v. 21, p.1978–1987, 2013.

MARUGG, J. E.; BURIK, A.; TROMP, M.; VAN DER MAREL, G. A.; VAN BOOM J. H. A convenient and general approach to the synthesis of properly protected d-nucleoside- 3′- hydrogenphosphonates *via* phosphite intermediates. **Tetrahedron Letters**, v.27, p. 2271, 1986.

MAYER, T.G.; SCHMIDT, R. R. Glycosyl Phosphatidylinositol (GPI) Anchor Synthesis Based on Versatile Building Blocks – Total Synthesis of a GPI Anchor of Yeast. **European Journal of Organic Chemistry**, p. 1153–1165, 1999.

McCONVILLE, M. J.; FERGUSON, M. A. J., The structure, biosynthesis and function of glycosylated phosphatidylinositols in the parasitic protozoa and higher eukaryotes. **Biochemical Journal**, v. *294*, p. 305-324, 1993.

MENDONCA-PREVIATO, L.; TODESCHINI, A.R.; HEISE, N.; AGRELLOS, O.A.; DIAS, W.B.; PREVIATO, J.O. Chemical structure of major glycoconjugates from parasites. **Current Organic Chemistry**, v. *12*, p. 926-939, 2008.

MILJKOVIC, M. **Carbohydrates- Synthesis, Mechanisms, and Stereoelectronic Effects.** Springer-Verlag New York, 2009.

MITRAGOTRI, S., BURKE, P. A.; LANGER, R. Overcoming the challenges in administering biopharmaceuticals: formulation and delivery strategies. **Nature Reviews Drug Discovery**. v.13, p. 655–672, 2014.

MONTOYA- PELEAZ, J. G.; RILEY, W. A.; SZAREK, M. A.; VALVANO, J. S.; SCHUTZBACH, I.; BROCKHAUSEN. Identification of a UDP-Gal: GlcNAc-R galactosyltransferase activity in *Escherichia coli* VW187. **Bioorganic & Medicinal Chemistry Letters**. v. 15, p. 1205-1211, 2005.

MOROTTI, A. L. M.; MARTINS-TEIXEIRA, M. B.; CARVALHO, I. Protozoan parasites glycosylphosphatidylinositol anchors: Structures, functions and trends for drug discovery. **Current Medicinal Chemistry**, in press.

MOROTTI, A. L. M.; LANG, K. L.; CARVALHO, I.; SCHENKEL, E. P.; BERNARDES, L. S. C. Semi-Synthesis of new glycosidic triazole derivatives of dihydrocucurbitacin B. **Thetrahedron Letters**. v. 56, p. 303-307, 2015.

MURAKATA, C.; OGAWA, T. Synthetic studies on cell- surface glycans. 78. A total synthesis of GPI anchor of Trypanosoma brucei. **Tetrahedron Letters**, v. 32, n. 5, p. 671-674, 1991.

MURAKATA, C.; OGAWA, T. Stereoselective synthesis of glycobiosyl phosphatidylinositol, a part structure of the glycosyl-phosphatidylinositol (GPI) anchor of Trypanosoma brucei. **Carbohydrate Research**, v. 9 n. 234, p. 75-91, 1992.

NAIK, R. S.; KRISHNEGOWDA, G.; GOWDA, D. C. Glucosamine inhibits inositol acylation of the glycosylphosphatidylinositol anchors in intraerythrocytic *Plasmodium falciparum*. **Journal of Biological Chemistry**. v. *278*, p. 2036-2042, 2003.

NAIK, R. S.; DAVIDSON, E. A.; GOWDA, D. C., Developmental stage-specific biosynthesis of glycosylphosphatidylinositol anchors in intraerythrocytic *Plasmodium falciparum* and its inhibition in a novel manner by mannosamine. **Journal of Biological Chemistry**. v**.** *275*, p. 24506-24511, 2000.

NAKANO, Y.; URADE, Y.; URADE, R.; KITAOKA, S., Isolation, purification, and characterization of the pellicle of *Euglena gracilis*. **Journal of Biochemistry**. v. 102, p.1053-1063, 1987.

NEVES, D. P. **Parasitologia Humana**. São Paulo: Atheneu, 2000.

NIEHUS, S.; SMITH, T.K.; AZZOUZ, N.; CAMPOS, M.A.; DUBREMETZ, J.F.; GAZZINELLI, R.T.; SCHWARZ, R.T.; DEBIERRE-GROCKIEGO, F., Virulent and avirulent strains of *Toxoplasma gondii* which differ in their glycosylphosphatidylinositol content induce similar biological functions in macrophages. **Plos One**. v. 9, 2014

NIGUDKAR; S. S.; DEMCHENKO, a. V. Stereocontrolled 1,2-cis glycosylation as the driving force of progress in synthetic carbohydrate chemistry. **Chemical Science**, v. 6, v. 2687-2704, 2015.

NIKOLAEV, A. V.; AL-MAHARIK, N. Synthetic glycosylphosphatidylinositol (GPI) anchors: how these complex molecules have been made. **Natural Product Reports,** v. 28, n. 5, p. 970-1020, 2011.

NOIREAU F.; DIOSQUE P.; JANSEN A. M. *Trypanosoma cruzi*: adaptation to its vectors and its hosts. **Veterinary Research**, v. 40, p. 26, 2009.

NYFFELER, P. T.; LIANG, C. H.; KOELLER, K. M.; WONG, C. H. The chemistry of amine-azide interconversion: catalytic diazotransfer and regioselective azide reduction. **Journal of the American Chemical Society**, v. 124, p. 10773-10778, 2002.

O'NEILL, E. C.; TRICK, M.; HILL, L.; REJZEK, M.; DUSI, R. G.; HAMILTON, C. J; ZIMBA, P. V.; HENRISSAT, B.; FIELD, R. A. The transcriptome of Euglena gracilis reveals unexpected metabolic capabilities for carbohydrate and natural product biochemistry. **Molecular BioSystems.** v. 11, p. 2808-2820, 2015.

PARK, J.; KAWATKAR, S.; KIM, J.- H.; BOONS, G.-J., Stereoselective glycosylations of 2-azido-2-deoxy-glucosides using intermediate sulfonium Ions. Organic Letters. v. 9, p. 1959-1962, 2007.

PEKARI, K.; TAILLER, D.; WEINGART, R.; SCHMIDT, R., R. Synthesis of the fully phosphorylated GPI anchor pseudohexasaccharide of *Toxoplasma gondii*. **Journal of Organic Chemistry**. *v. 66*, p. 7432-7442, 2001.

PÉTURSSON, S. Protecting Groups in Carbohydrate Chemistry. **Journal of Chemical Education**, v. 74 n. 11, 1997.

PREVIATO, J. O.; SOLA- PENNA, M.; AGRELLOS, O. A.; JONES, C.; OELTMANNI, T.; TRAVASSOS, L. R.; MENDONÇA-PREVIATO, L. Biosynthesis of O-N-Acetylglucosamine-linked Glycans in *Trypanosoma cruzi*. **The Journal of Biological Chemistry.** v. 273, p. 14982- 14988, 1998.

RAJAO, M. A; FURTADO, C.; ALVES, C. L.; PASSOS- SILVA, D. G.; MOURA, M. B.; SCHAMBER- REIS, B. L.; Unveiling Benznidazole's mechanism of action through overexpression of DNA repair proteins in *Trypanosoma cruzi.* **Environmental Molecular Mutagenesis,** 2014.

RALTON, J. E.; MCCONVILLE, M. J. Delineation of three pathways of glycosylphosphatidylinositol biosynthesis in *Leishmania mexicana* - Precursors from different pathways are assembled on distinct pools of phosphatidylinositol and undergo fatty acid remodeling. **Journal of Biological Chemistry**. v. *273*, p. 4245-4257, 1998.

REN, B.; WANG M.; LIU; J.; GE, J.; ZHANG, X.; DONGA, H. Zemplén Transesterification: A Name Reaction Having Been Misleading Us for 90 Years, **Green Chemistry**, v. **17,** p. 1390-1394, 2015.

RILEY, J. G.; XU, C.; BROCKHAUSEN, I. Synthesis of acceptor substrate analogues for the study of glycosyltransferases involved in the second step of the biosynthesis of *O*-antigen repeating units, **Carbohydrate Research,** v.345, p. 586-597, 2010.

SALES-JUNIOR, P. A., MOLINA, I., FONSECA MURTA, S. M., SÁNCHEZ-MONTALVÁ, A., SALVADOR, F., CORRÊA-OLIVEIRA, R., & CARNEIRO, C. M. Experimental and Clinical Treatment of Chagas Disease: A Review. *The* **American Journal of Tropical Medicine and Hygiene**. v. 97, p. 1289–1303, 2017.

SATO, E.; SATO, M.; TANABE, Y.; NAKAJIMA, N.; OHKUBO, A.; SUENAGA, K. Total Synthesis of Biselyngbyaside. **Journal of The American Chemical Society.** v. 82, p. 6770-6777, 2017.

SAYKAM, V.; DARA, S.; YADAV, S.; PAL SINGH, R.; VISHWARKARMA, R. A. Dimethyltin Dichloride Catalyzed Regioselective Alkylation of cis-1,2- Diols at Room Temperature. **The Journal of Organic Chemistry**. v. 80, p. 11916-11925, 2015.

SCHMIDT, R. R.; MICHEL, J. Facile Synthesis of α- and β-*O*-Glycosyl Imidates; Preparation of Glycosides and Disaccharides. **Angewandte Chemie Int. Ed**. v. *19*, p. 731 – 732, 1980.

SCHMIDT, R. R.; KINZY, W. Anomeric-oxygen activation for glycoside synthesis: The trichloroacetimidate method. **Advances in Carbohydrate Chemistry and Biochemistry**. v. 50, p. 21-123, 1992.

SCULIMBRENE, B.; R.; XU, Y.; MILLER, S. J. Asymmetric Syntheses of Phosphatidylinositol-3-Phosphates with Saturated and Unsaturated Side Chains through Catalytic Asymmetric Phosphorylation. **Journal of The American Chemical Society**, p. 126, v. 13182-13183, 2004.

SERRANO, A. A.; SCHENKMAN, S.; YOSHIDA, N.; MEHLERT, A.; RICHARDSON, J. M.; FERGUSON, M. A. J., The lipid structure of the glycosylphosphatidylinositol-anchored mucin-like sialic acid acceptors of *Trypanosoma cruzi* changes during parasite differentiation from epimastigotes to infective metacyclic trypomastigote forms. **Journal of Biological Chemistry. 1995**, v. 270, p. 27244-27253, 1995.

SIGURDSSON S.; STRÖMBERG, R. The H-phosphonate approach to oligonucleotidesynthesis. An investigation on the mechanism of the coupling step. **Journal of the Chemical Society- Perkin Transactions 2**, Issue 12, p. 1961-,2164, 2002.

SHARMA, D. K.;. SMITH, T. K.; WELLER C.; CROSSMAN, T. A.; BRIMACOMBE, J. S.; FERGUSON M. A. Differences between the trypanosomal and human GlcNAc-PI de-N-acetylases of glycosylphosphatidylinositol membrane anchor biosynthesis. **Glycobiology**, v. 9, p. 415-422, 1999.

SMITH, M. B.; MARCH, J. **March's Advanced Organic Chemistry: Reactions, Mechanisms, and Structure**, 7th Edition, John Wiley & Sons, Inc., 2013.

SMITH, T. K.; GEROLD, P.; CROSSMAN, A.; PATERSON, M.J.; BORISSOW, C.N.; BRIMACOMBE, J. S.; FERGUSON, M. A. J.; SCHWARZ, R. T. Substrate specificity of the *Plasmodium falciparum* glycosylphosphatidylinositol biosynthetic pathway and inhibition by species-specific suicide substrates. *Biochemistry*, v.*41*, p.12395-12406, 2002.

SMITH, T. K.; CROSSMAN, A.; BORISSOW, C. N.; PATERSON, M. J.; DIX, A.; BRIMACOMBE, J. S.; FERGUSON, M. A. J. Specificity of GlcNAc-PI de-N-acetylase of GPI biosynthesis and synthesis of parasite-specific suicide substrate inhibitors. **Embo Journal**. v. *20*, p. 3322-3332, 2001.

SMITH, T. K.; CROSSMAN, A.; BRIMACOMBE, J. S.; FERGUSON, M. A. J. Chemical validation of GPI biosynthesis as a drug target against African sleeping sickness. **The EMBO Journal**, v. 23, p. 4701-4708, 2004.

SMITH, T. K.; CROSSMAN, A.; BRIMACOMBE, J. S.; FERGUSON, M. A. J. Chemical validation of GPI biosynthesis as a drug target against African sleeping sickness. **EMBO Journal**. v. 23, p.4701–4708, 2014.

SMITH, T. K.; KIMMEL, J.; AZZOUZ, N.; SHAMS-ELDIN, H.; SCHWARZ, R. T., The role of inositol acylation and inositol deacylation in the *Toxoplasma gondii* glycosylphosphatidylinositol biosynthetic pathway. **Journal of Biological Chemistry**. v.*282*, p. 32032-32042*,* **2007**.

SOBKOWSKI, M.; KRASZEWSKI, A.; STAWINSKI, J. Recent Advances in H-Phosphonate Chemistry. Part 1. H-Phosphonate Esters: Synthesis and Basic Reactions. **Top Current Chemistry**, v. 361, p. 137-177, 2015.

SOMMER, J. R., The ultrastructure of the pellicle complex of *Euglena gracilis. J.* **Cell Biology**. *v. 24*, p. 253-257, 1965.

SUETH-SANTIAGO, V.; DECOTE-RICARDO, D.; MORROT, A.; FREIRE-LIMA, C. G.; FREIRE-LIMA, M. E. **World Journal of Biological Chemistry**. v. 8, p. 57-80, 2017.

SUKHAREVA-BUELL, N., N. **Biologically Active Substances of Protozoa**. Springer Science+Business Media, Netherlands, p. 46-54, 2003.

SURESHAN, K. M.; SHASHIDHAR, M. S.; PRAVEEN T.; DAS T. Regioselective Protection and Deprotection of Inositol Hydroxyl Group. **Chemical Reviews***, p. 4477-4503, 2003**.

SWARTS B. M.; GUO, Z. **Synthesis of glycosylphosphatidylinositol anchors bearing unsaturated lipid chains**. *Journal of The American Chemical Society*. v. *132*, p. 6648–6650**, 2010**.

TAKAHASHI, H; KITTAKA, H; IKEGAMI, S. Novel Synthesis of Enantiomerically Pure Natural Inositols and Their Diastereoisomers. **Journal of Organic Chemistry**, v. 66, p. 2705-2716, 2001.

TANAKA, S.I.; TAKASHINA, M.; TOKIMOTO, H.; FUJIMOTO, Y.; TANAKE, K.; FUKASE, K. Highly β-Selective Mannosylation towards Manβ1-4GlcNAc Synthesis: TMSB(C_6F_5)$_4$ as a Lewis Acid/Cation Trap Catalyst. **Synlett,** p. 2325- 2328, 2005.

TSAI, Y. H.; LIU, X. Y.; SEEBERGER, P. H., Chemical Biology of Glycosylphosphatidylinositol Anchors. **Angewandte Chemie- International Edition**. v. *51*, p. 11438-11456, 2012.

URBANIAK, M. D.; YASHUNSKY, D. V.; CROSSMAN, A.; NIKOLAEV, A. V.; FERGUSON, M. A. J. Probing Enzymes Late in the Trypanosomal Glycosylphosphatidylinositol Biosynthetic Pathway with Synthetic Glycosylphosphatidylinositol Analogues. **ACS Chemical Biology**. v. 3, p. 625-634, 2008.

VARKI, A.; ESKO, J. D.; COLLEY, K. J., **Cellular Organization of Glycosylation. Essentials of Glycobiology**, 2nd ed. Cold Spring Harbor (NY), 2009.

VARMA, Y.; HENDRICKSON, T. Methods to Study GPI Anchoring of Proteins. **ChemBioChem,** v. 11, p. 623 – 636, 2010.

VIDAL, S. & WERTZ, D. (eds). Modern Synthetic Methods in Carbohydrate Chemistry- From Monosaccharides to Complex Glycoconjugates. Wiley, 2014.

VUTUKURI, D. R.; BHARATHI, P.; YU, Z.; RAJASEKARAN, K.; TRAN, M-H.; THAYUMANAVAN, S. A Mild Deprotection Strategy for Allyl-Protecting Groups and Its Implications in Sequence Specific Dendrimer Synthesis. **The Journal of Organic Chemistry**. v. *68,* p. 1146–1149, 2003.

WALVOORT M. T. C.; MOGGRÉ, G.-J.; LODDER, G.; OVERKLEEFT, H. S.; CODÉE, J. D. C.; VAN DER MAREL., G. A. Stereoselective Synthesis of 2,3-Diamino-2,3-dideoxy-β-d-mannopyranosyl Uronates. **The Journal of Organic Chemistry**, v. *7,* p. 7301-7315**, 2011.**

WANG, Y. K.; CHEN, W.; BLAIR, D.; PU, M.; XU, Y.; MILLER, S.; REDFIELD, A. G.; CHILES, T. C.; ROBERTS, M. G. Insights into the Structural Specificity of the Cytotoxicity of 3-Deoxyphosphatidylinositols**. Journal of The American Chemical Society**, v. 130, p. 7746-7755, 2008.

WASONGA, G.; ZENG, Y.; HUANG, X. Pre-activation based stereoselective glycosylations: Stereochemical control by additives and solvent. **Science China Chemistry**, v.*54*, p.66-73, 2011.

WHO, **Chagas Disease Fact Sheet.** March, 2017. Available on: http://www.who.int/mediacentre/factsheets/fs340/en/. Accessed in September, 2018.

WHO, **Bulletin of the World Health Organization Past issues**. v, 87, n. 7, July 2009. Available in http://www.who.int/bulletin/volumes/87/7/09-030709/en. Accessed in September, 2018.

WICHROSKI, M. J.; WARD, G. E. Biosynthesis of glycosylphosphatidylinositol is essential to the survival of the protozoan parasite *Toxoplasma gondii*. **Eukaryotic Cell**. v. 2, p. 1132-1136, 2003.

WINSTEIN, S.; BUCKLER, R. E. *J. Am. Chem. Soc.*, **1942**, *64* (12), pp 2780–2786.

XU, Y.; SCULIMBRENE, B. R.; MILLER, S. J. Synthesis of Phosphatidylinositol (PI), PI3P, PI3,5P2, and Deoxygenated Analogues as Potential Biological Probes. **The Journal of Organic Chemistry**, v. *71*, p. 4919–4928, 2006.

XUE, J.; SHAO, N.; GUO, Z. First Total Synthesis of a GPI-Anchored Peptide. **Journal of Organic Chemistry**, v. 68, p.4020-4029, 2003.

YAN, L.; KAHNE, D. Generalizing Glycosylation: Synthesis of the Blood Group Antigens Le[a], Le[b·], and Le[x] Using a Standard Set of Reaction Conditions. **Journal American Chemical Society.** v.*118, p.* 9239–9248, 1996.

YANG, W.; SUN, J.; YANG, Z.; HAN, W.; ZHANG, W.- D.; YU, B. Efficient synthesis of kaempferol 3,7-*O*-bisglycosides via successive glycosylation with glycosyl ortho-alkynylbenzoates and trifluoroacetimidates. **Tetrahedron Letters**, v. 53, p. 2773-2776, 2012.

YANG, Y.; ZHANG, X.; YU, B. *O*-Glycosylation Methods in the Total Synthesis of Complex Natural Glycosides. **Natural Product Reports.** *v. 32, p. 1332, 1355, 2015.*

YU, B; TAO H., Glycosyl trifluoroacetimidates. Part I. Preparation and application as new glycosyl donors. **Tetrahedron Letters**, v.42, p. 2405-2407, 2001.

YU, B.; SUN, J. Glycosylation with glycosyl *N*-phenyltrifluoroacetimidates (PTFAI) and a perspective of the future development of new glycosylation methods. **Chemical Communications.** v. 46, p. 4668, 2010.

7.APPENDIX

Phylogenetic tree of 94033 α-1,4- mannosyltransferase (common origin is highlighted)

Phylogenetic tree 93529 inositol acyltransferase (common origin is highlighted)

Phylogenetic tree 93529 inositol deacylase (common origin is highlighted)

Phylogenetic tree 85690 α- 1,2-mannosyltransferase

Infra-red of compound **37**

¹H NHR of compound **37** (MeOD; 300 MHz)

^{1}H NHR of compound **41** (CDCl$_3$; 400 MHz)

^{1}H NHR of compound **42** (CDCl$_3$; 400 MHz)

¹H NHR of compound **33a** (CDCl₃; 400 MHz)

HSQC of compound **33a** (CDCl₃; 400 MHz)

¹H NMR of compound **38** (CDCl₃; 300 MHz)
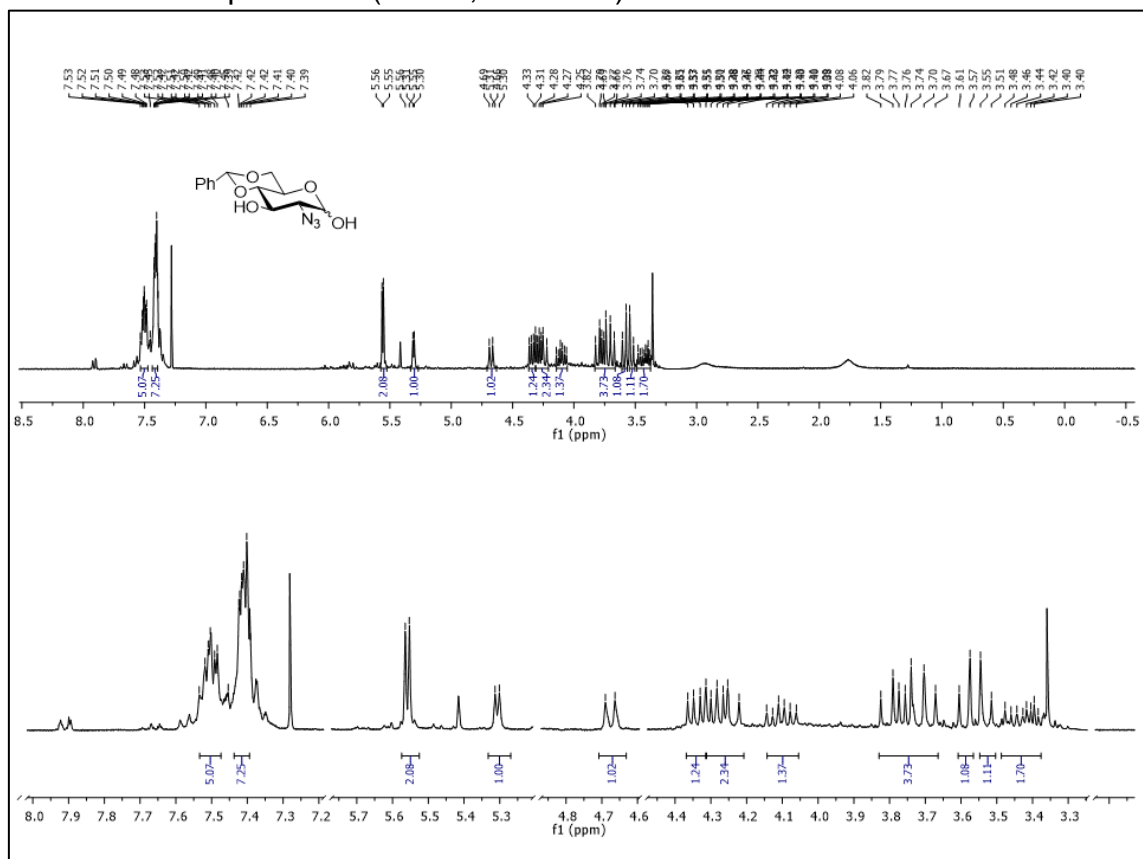
¹H NMR of compound **39** (CDCl₃; 300 MHz)
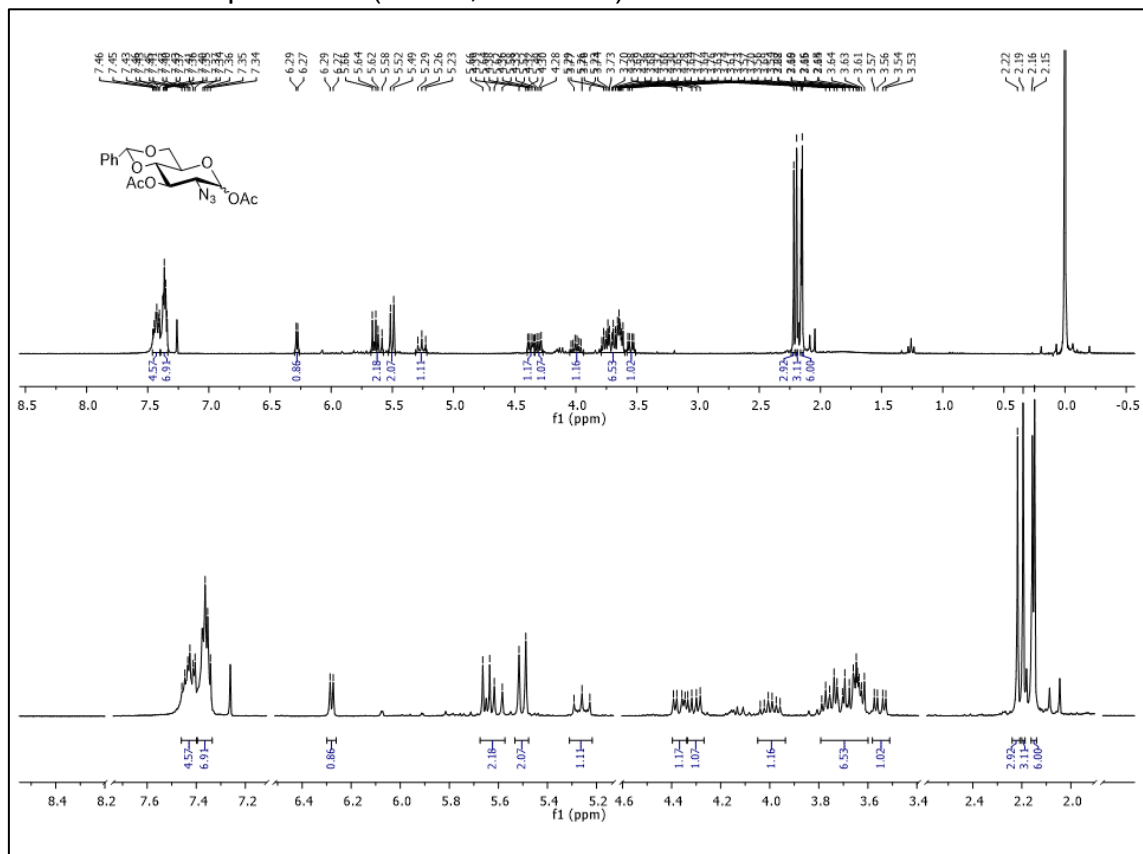
¹H NMR of compound **40** (CDCl₃; 300 MHz)

¹H NMR of compound **32** (CDCl₃; 400 MHz)

^{1}H NMR of compound **33b** (CDCl$_3$; 400 MHz)

HSQC of compound **33b** (CDCl$_3$; 400 MHz)
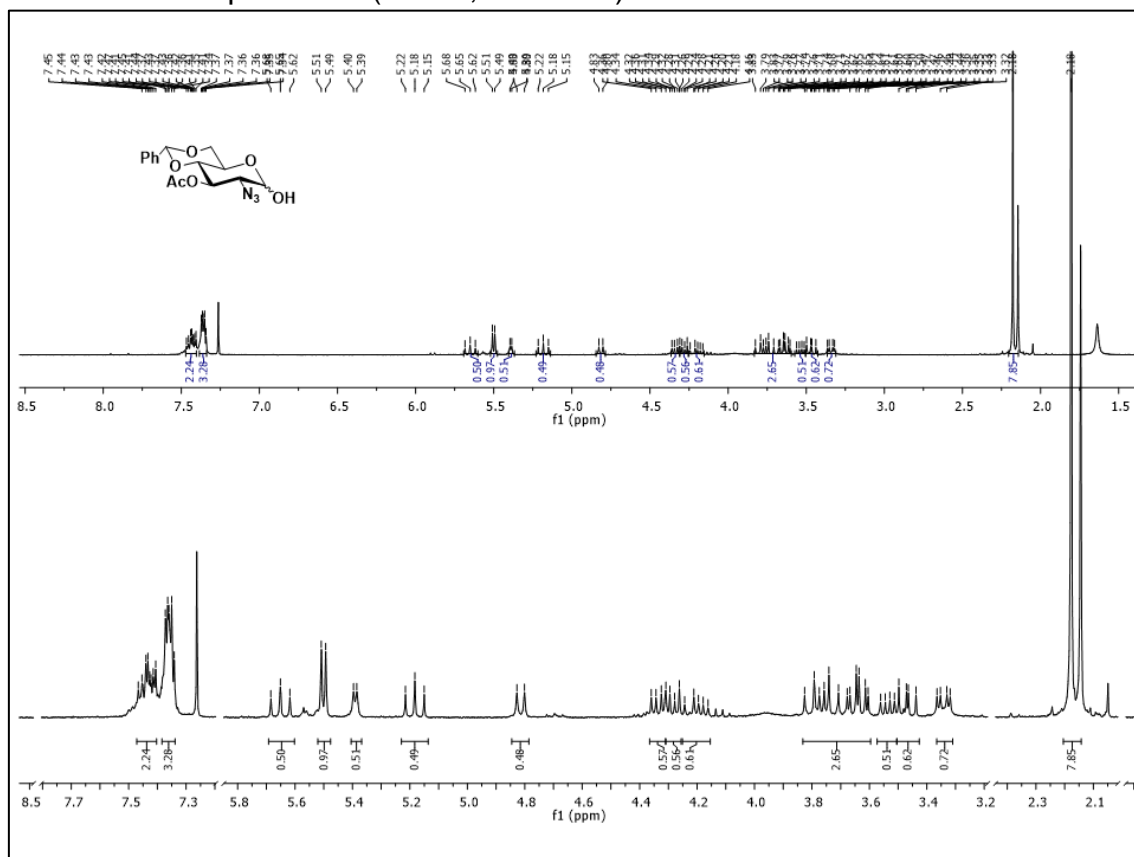
¹H NMR of compound **43** (CDCl₃; 400 MHz)
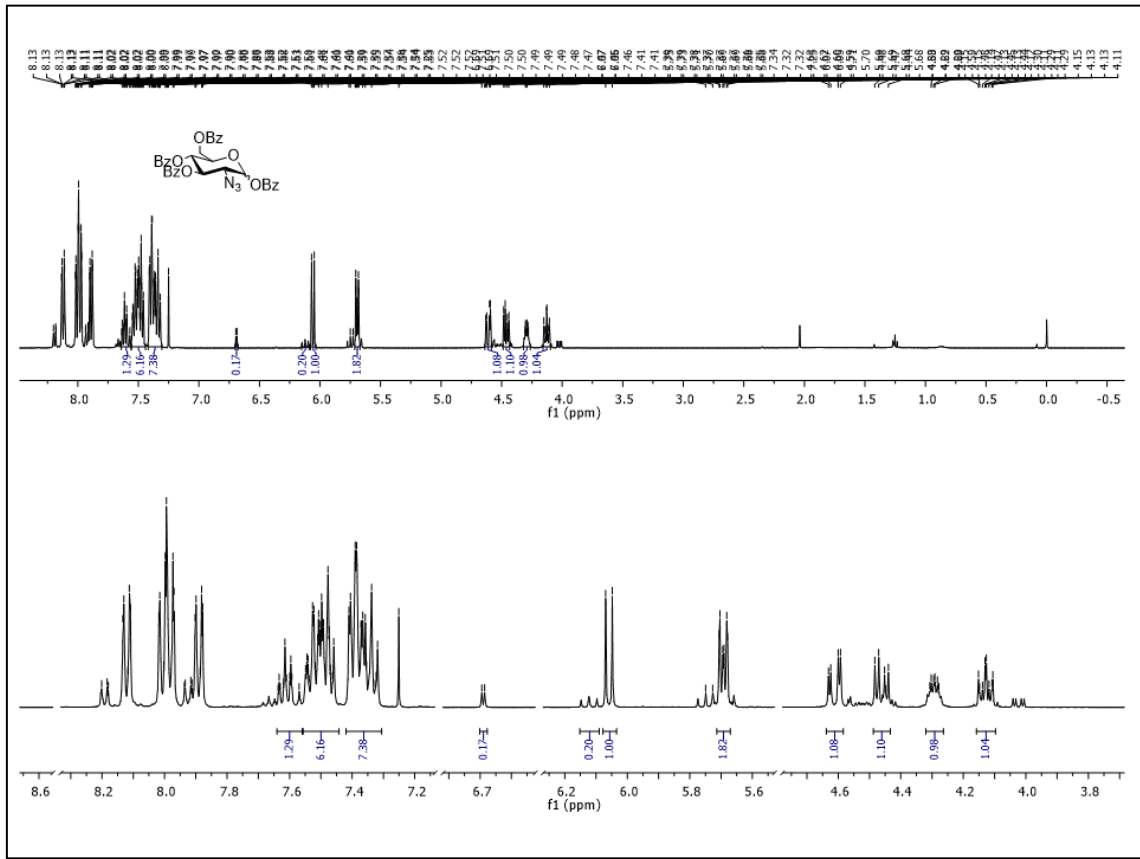
¹H NMR of compound **44** (CDCl₃; 400 MHz)
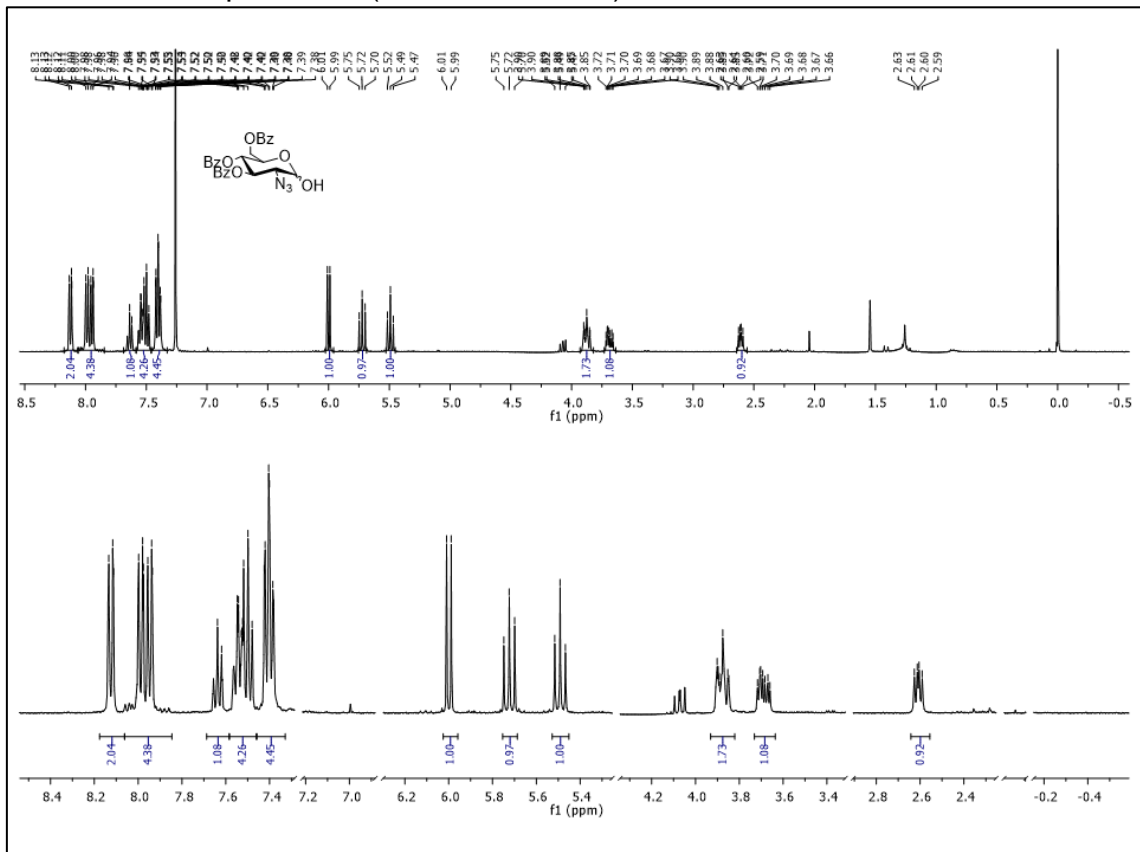
¹H NMR of compound **33c** (CDCl₃; 400 MHz)
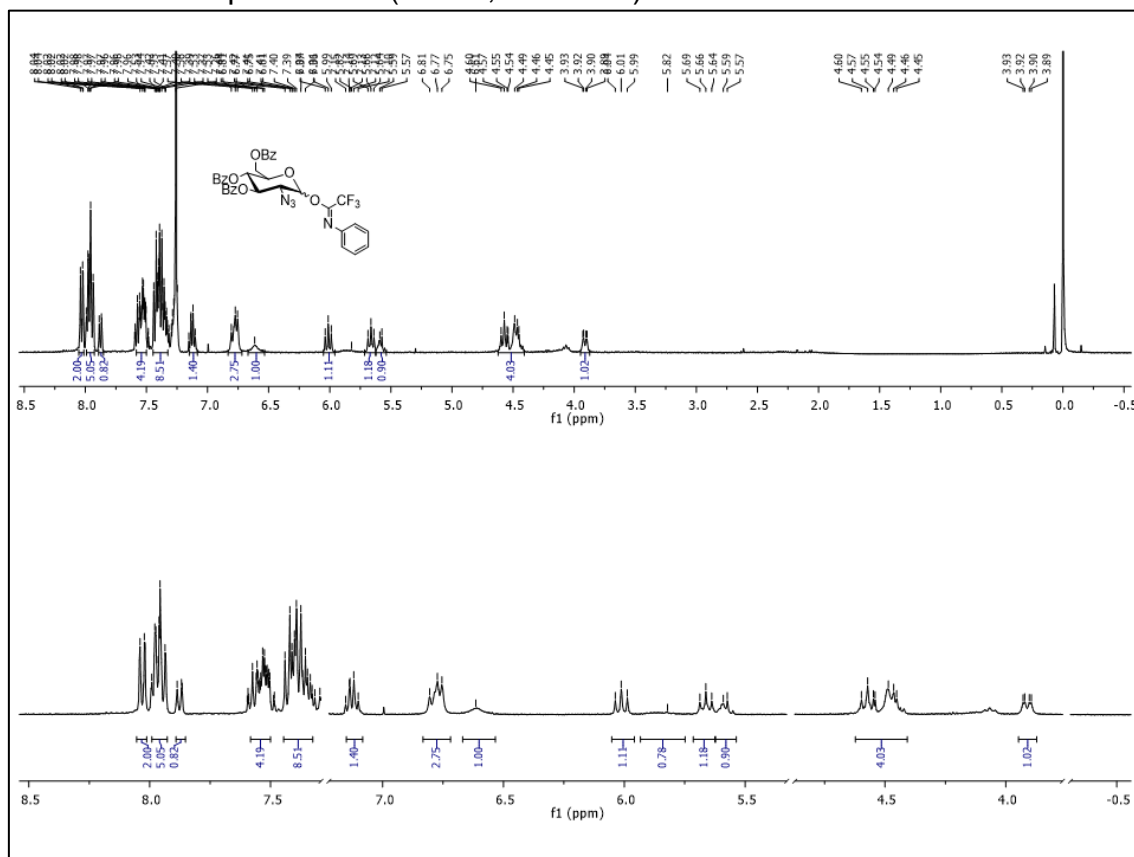
COSY NMR of compound **33c** (CDCl₃; 500 MHz)
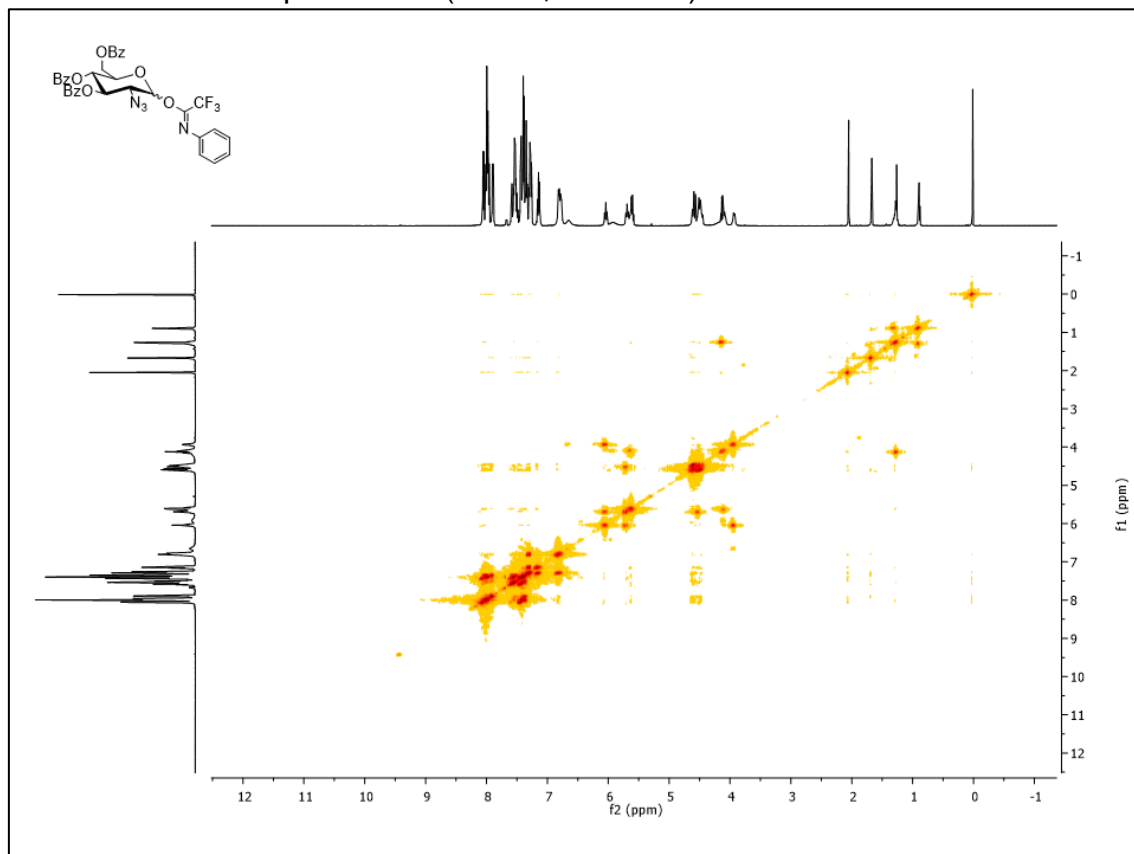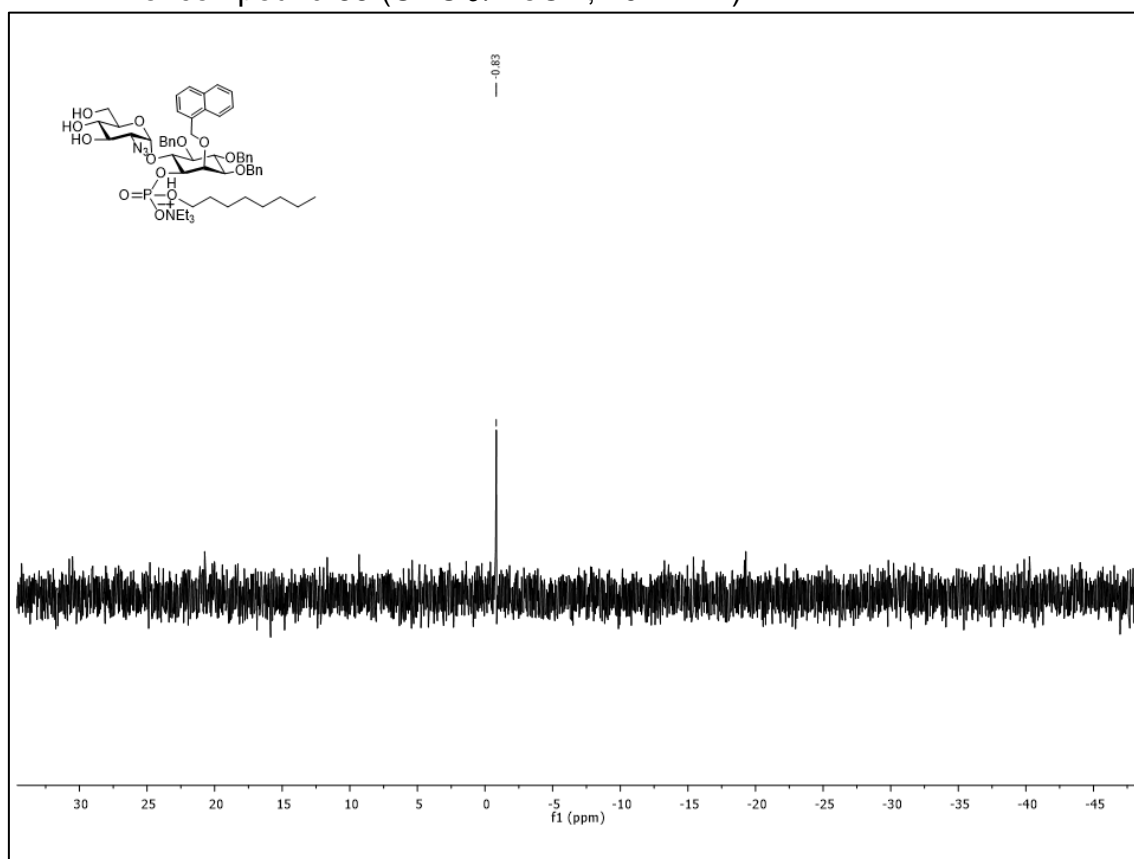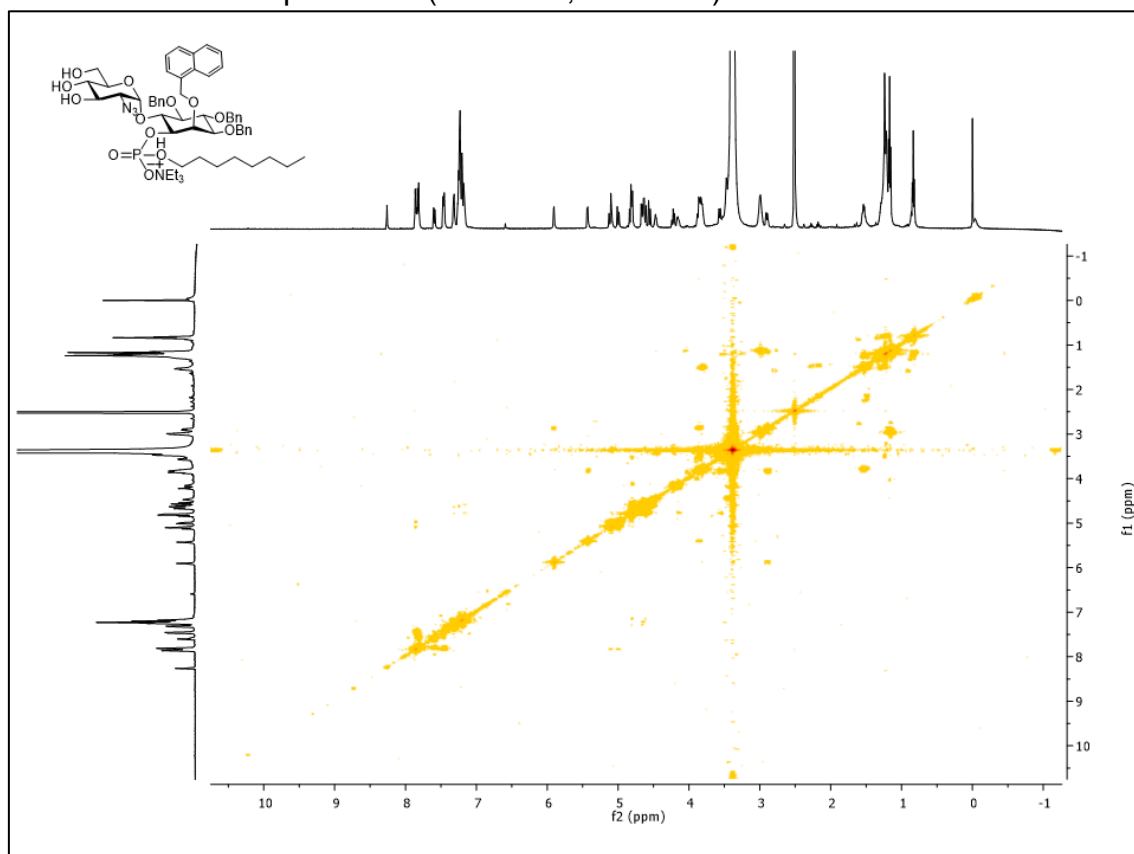
HSQC NMR of compound **33c** (CDCl₃; 500 MHz)

HMBC NMR of compound **33c** (CDCl₃; 500 MHz)

^{1}H NMR of compound **45** (CDCl$_3$; 400 MHz)
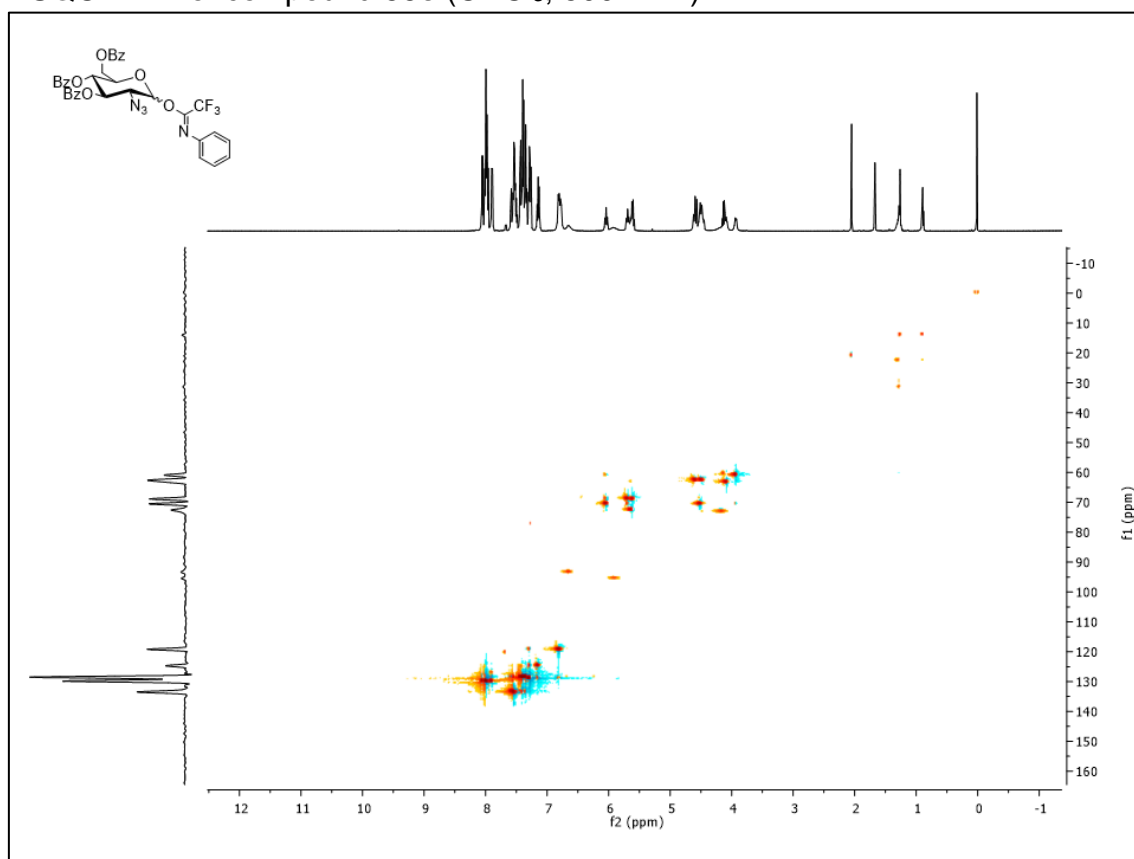
^{1}H NMR of compound **46** (MeOD; 400 MHz)
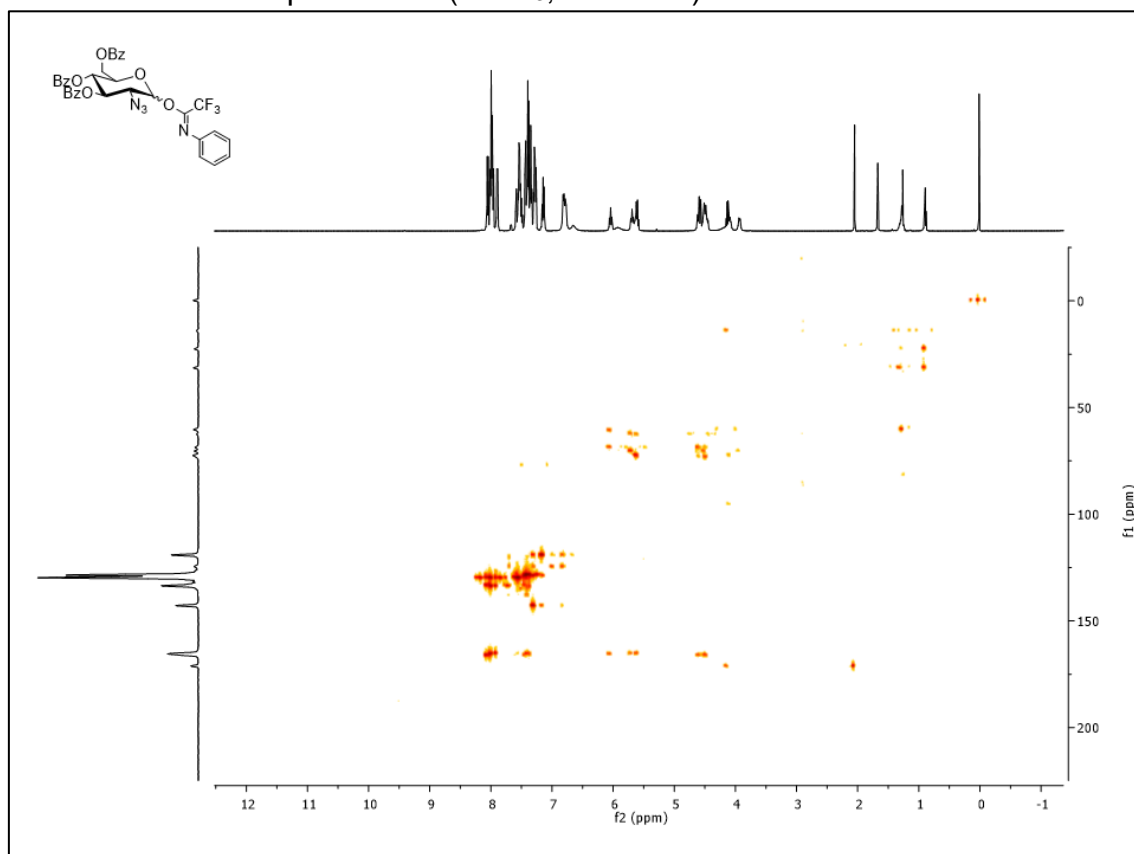
^{1}H NMR of compound **49** (CDCl$_3$; 400 MHz)
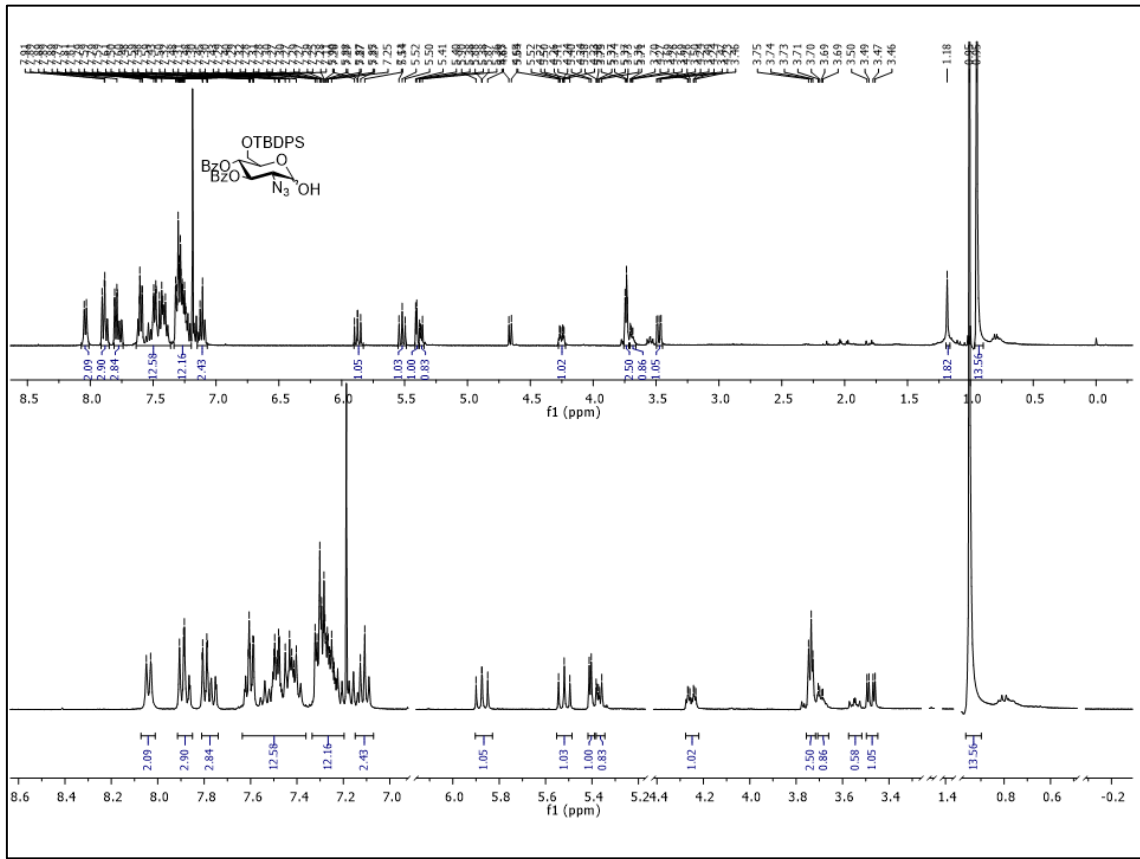
^{1}H NMR of compound **51** (CDCl$_3$; 400 MHz)

¹H NMR of compound **52** (CDCl₃; 300 MHz)

¹H NMR of compound **66** (CDCl₃; 300 MHz)
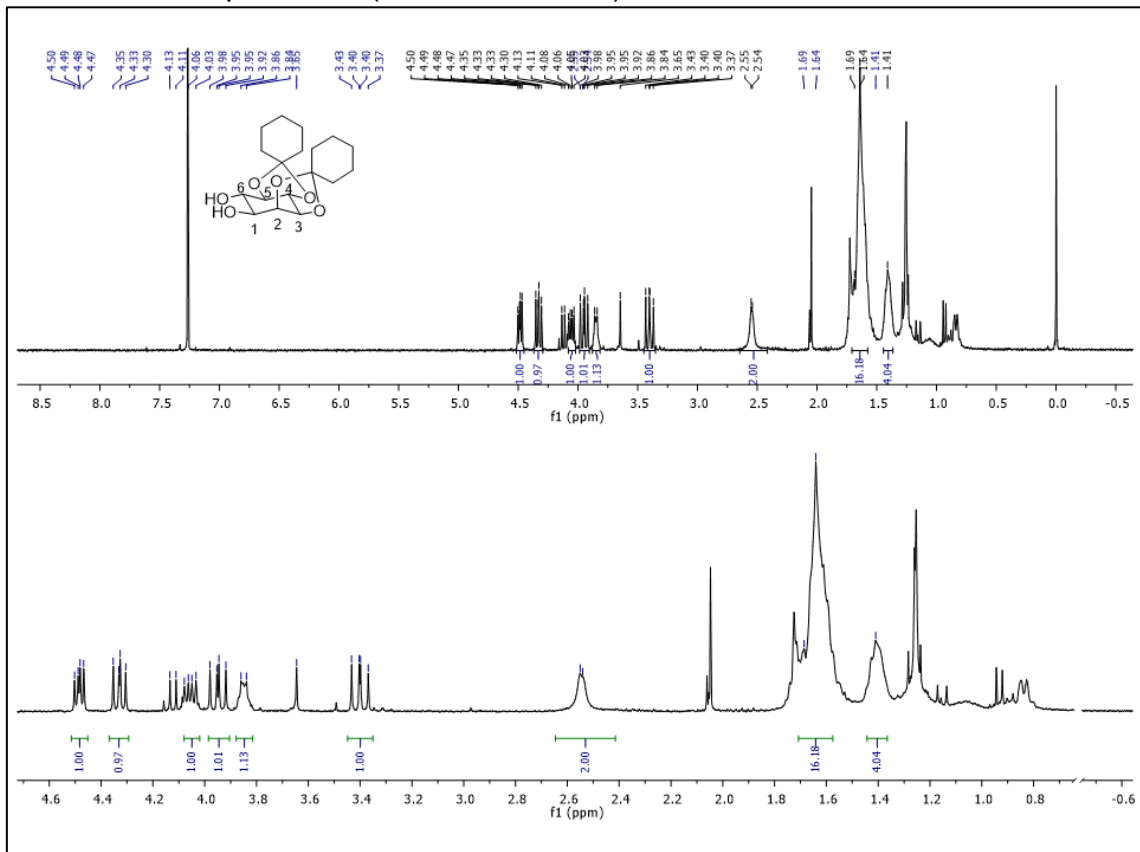
¹H NMR of compound **67** (CDCl₃; 300 MHz)
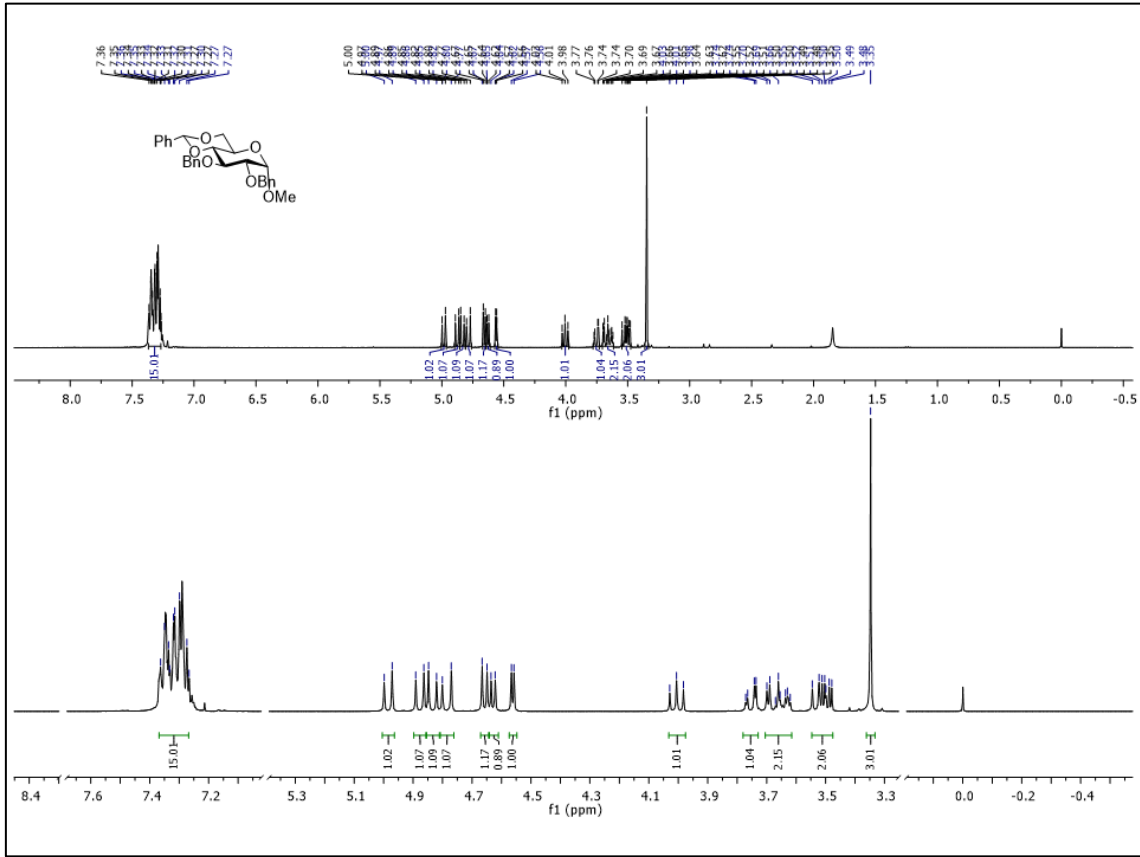
¹H NMR of compound **68** (CDCl₃; 300 MHz)

^{1}H NMR of compound **70** (CDCl$_3$; 300 MHz)

^{1}H NMR of compound **71** (CDCl$_3$; 500 MHz)
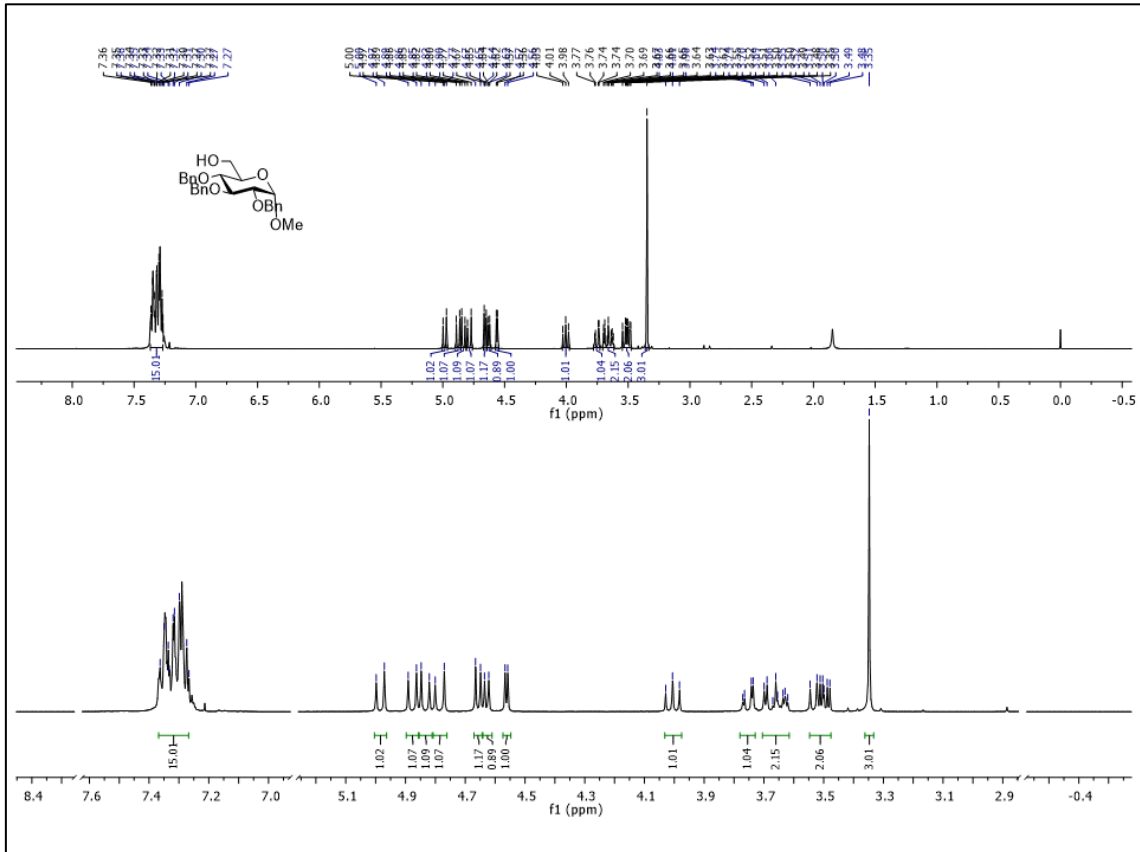
^{1}H NMR of compound **72** (CDCl$_3$; 400 MHz)
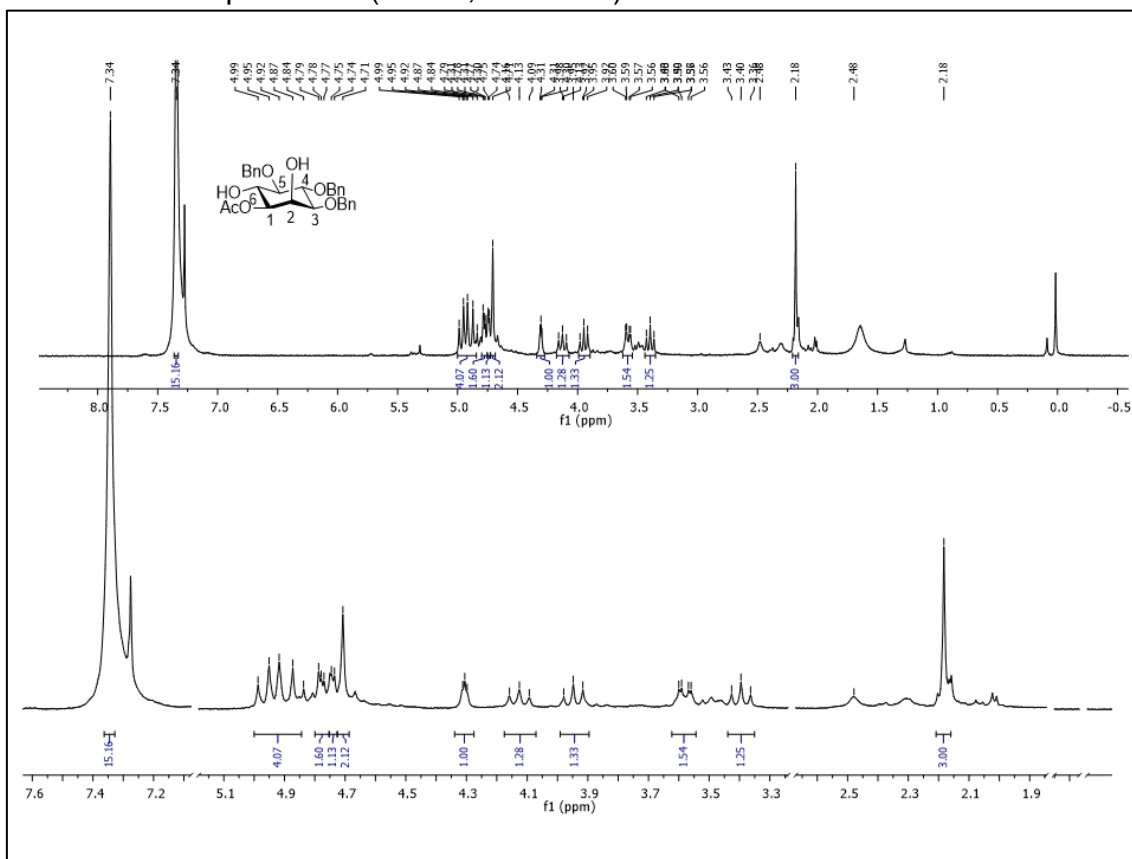
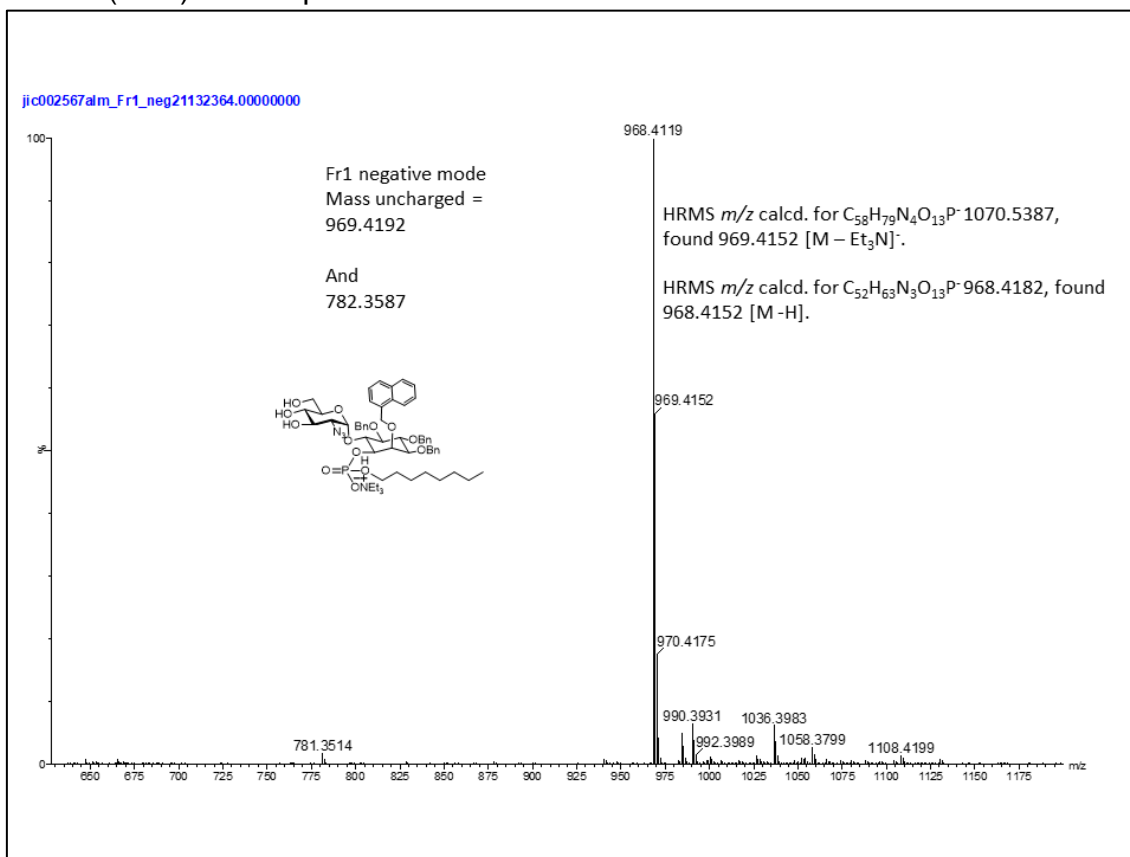# ^{1}H NMR of compound **74** (CDCl$_3$; 400 MHz)
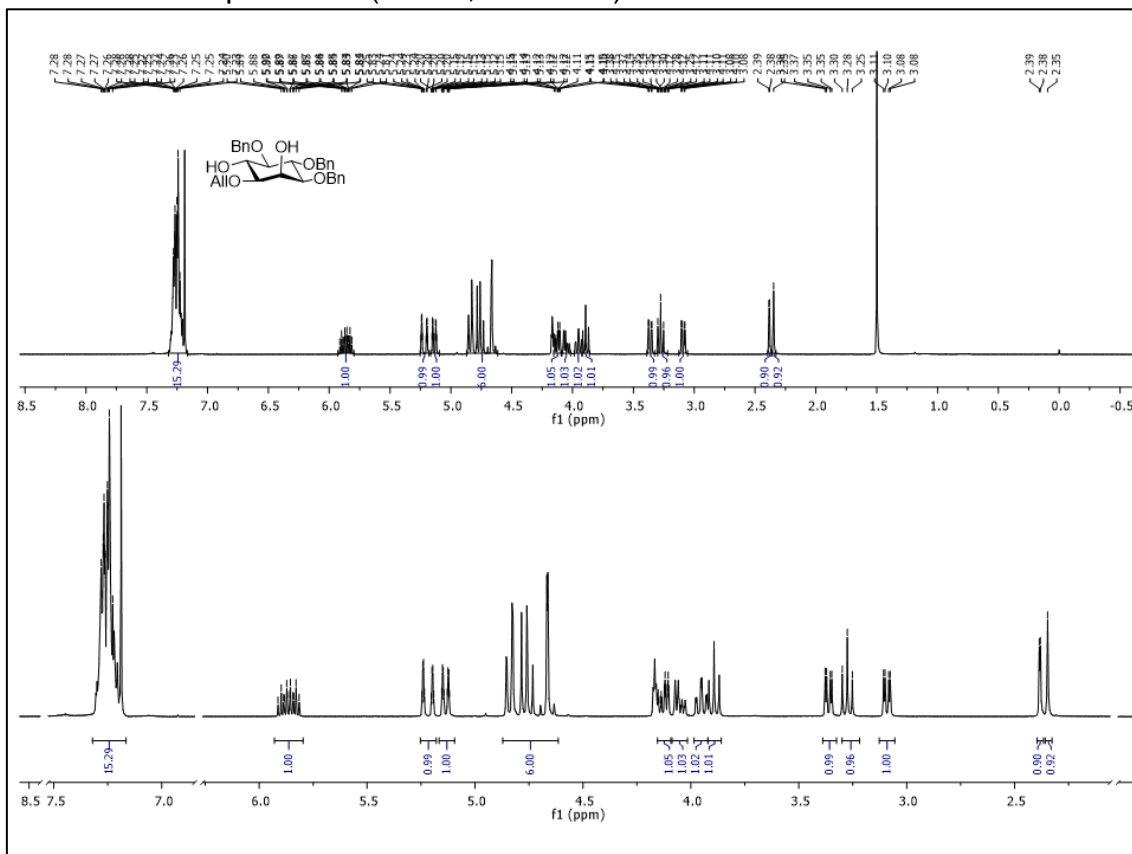
COSY of compound **74** (CDCl₃; 400 MHz)
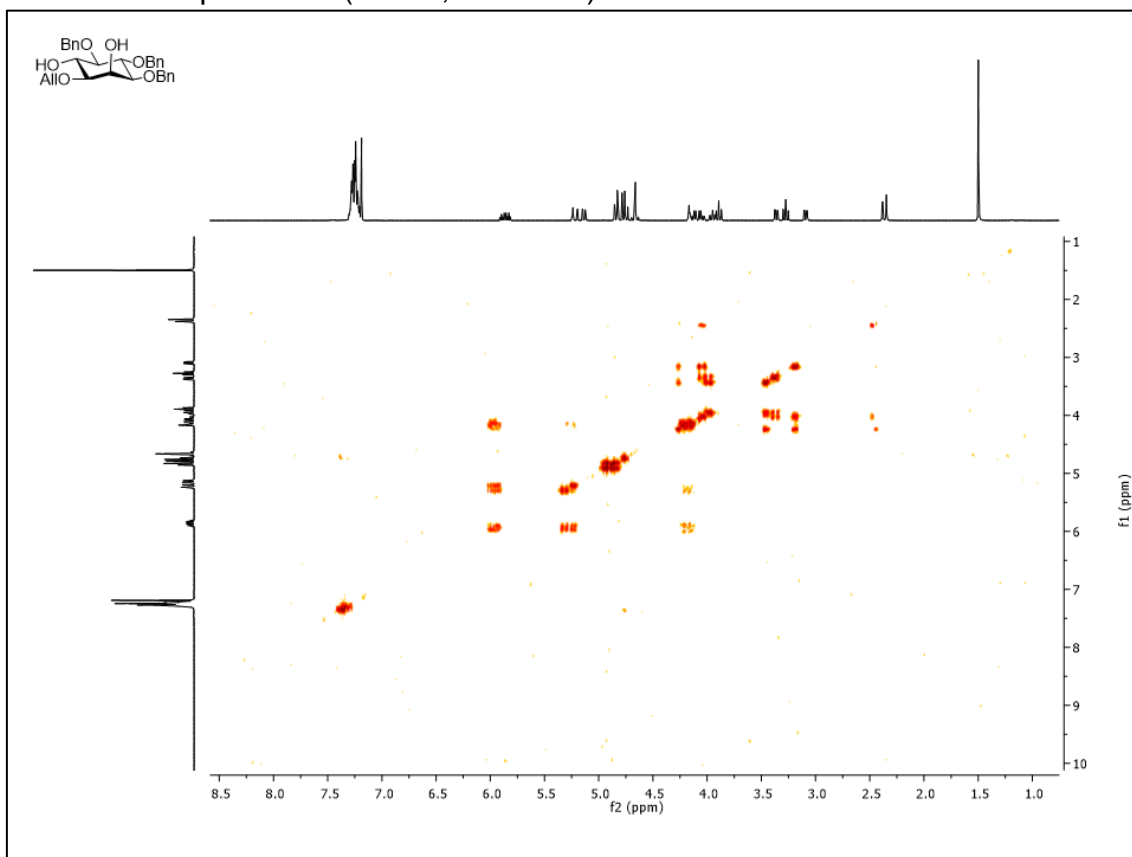
¹H NMR of compound **34** (CDCl₃; 400 MHz)
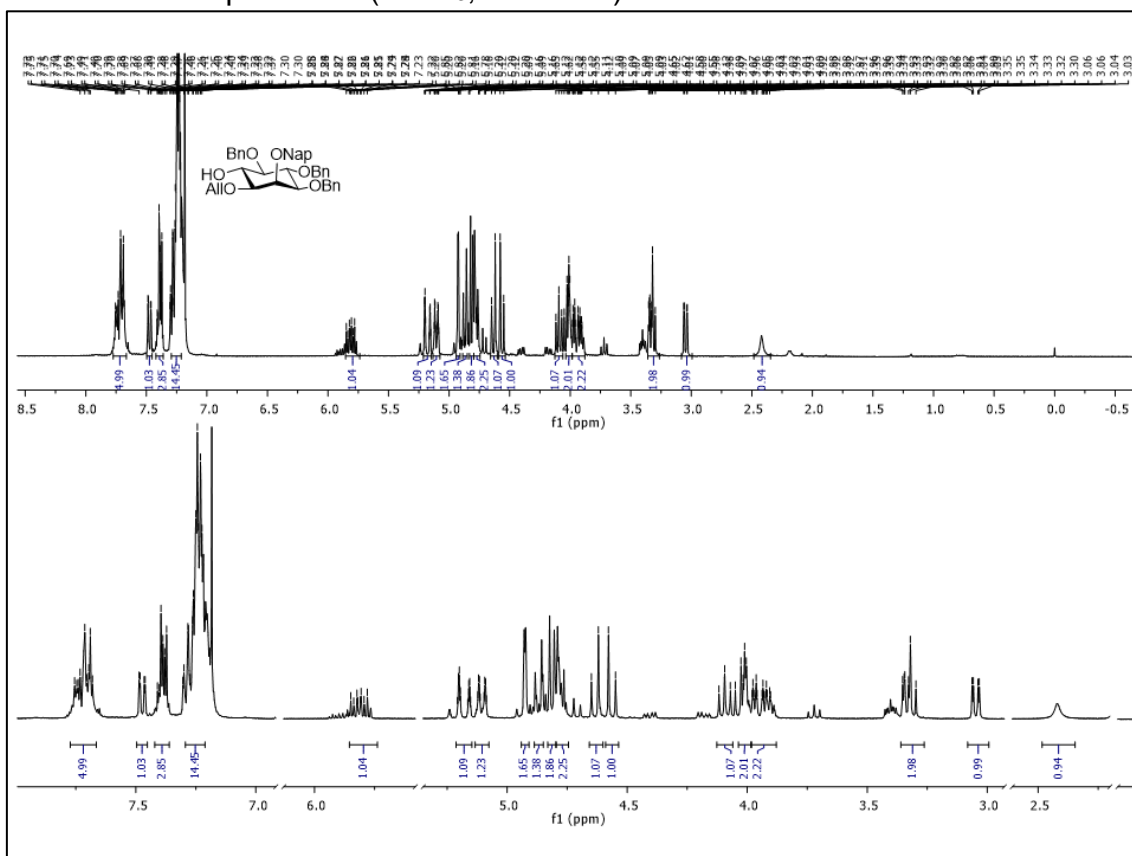
^{1}H NMR of compound **31aα** (CDCl$_3$; 400 MHz)

COSY NMR of compound **31aα** (CDCl$_3$; 400 MHz)

HSQC NMR of compound **31aα** (CDCl₃; 400 MHz)
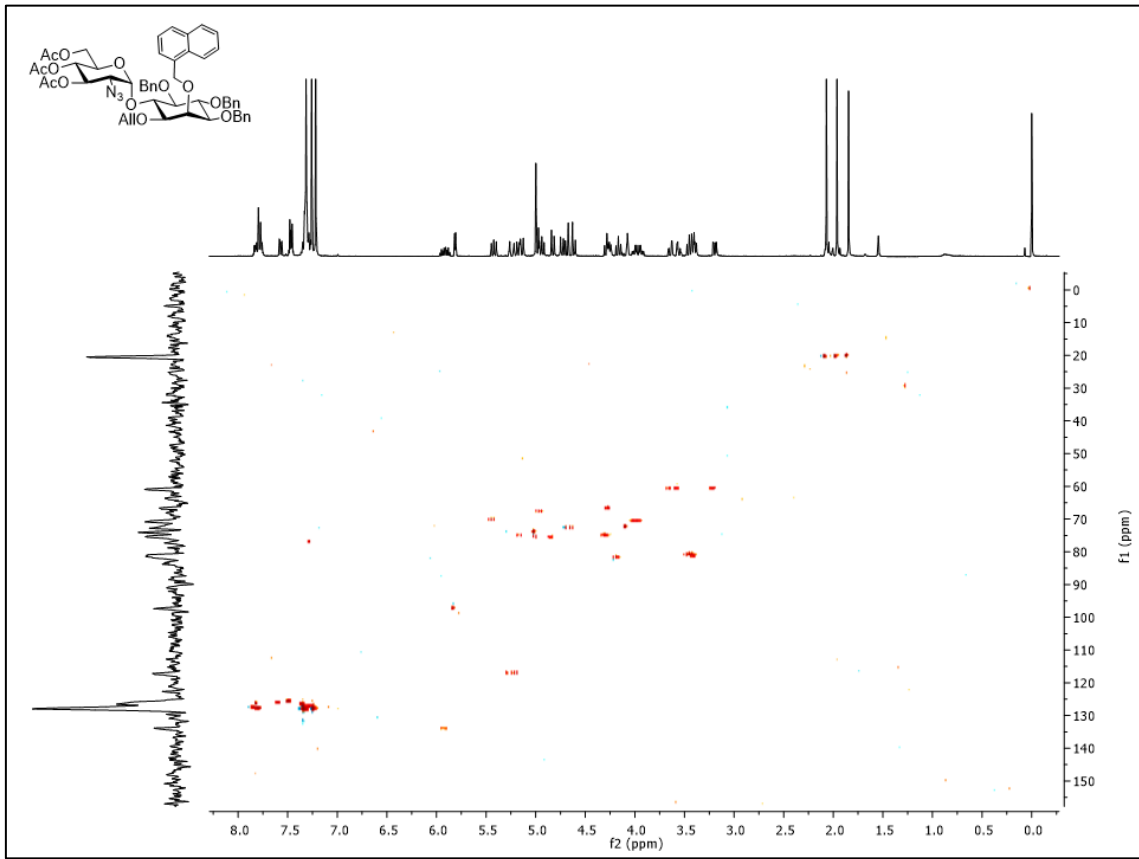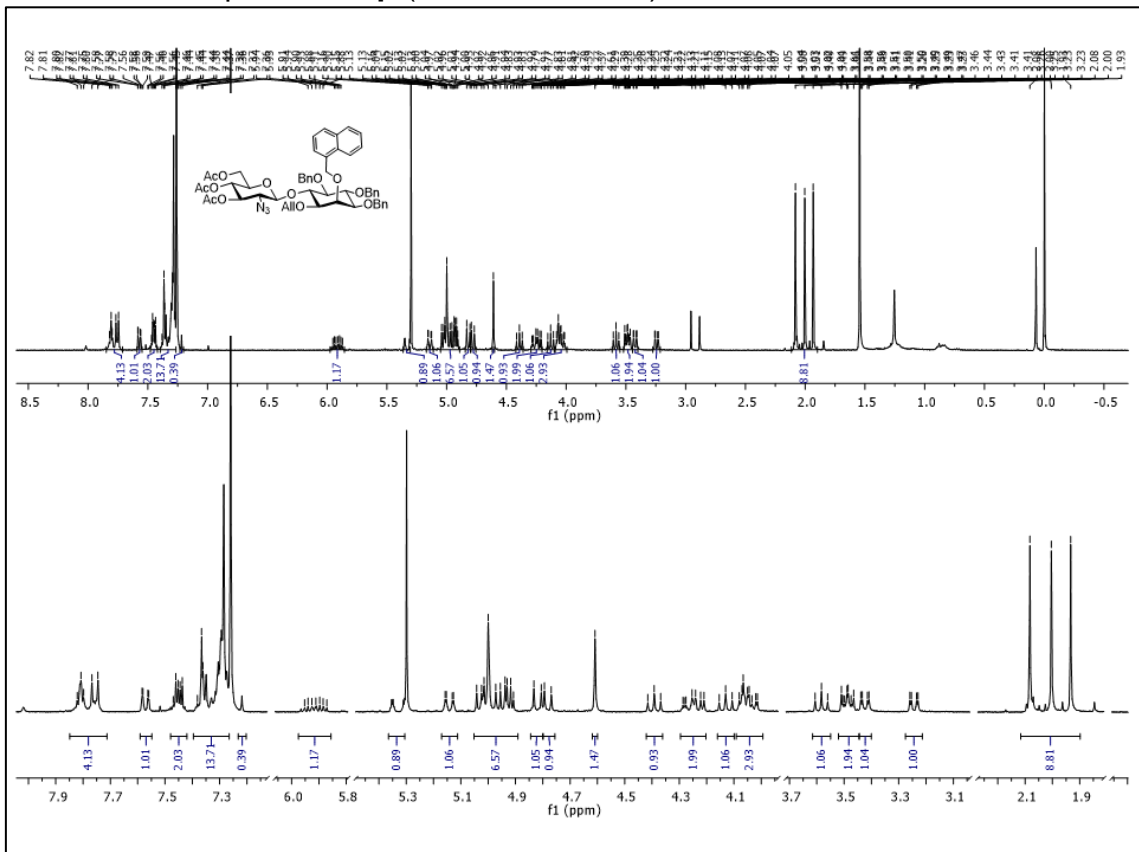
¹H NMR of compound **31aβ** (CDCl₃; 400 MHz)

COSY NMR of compound **31aβ** (CDCl$_3$; 400 MHz)

HSQC NMR of compound **31aβ** (CDCl$_3$; 400 MHz)

HRMS (ESI +) of compound **31a**
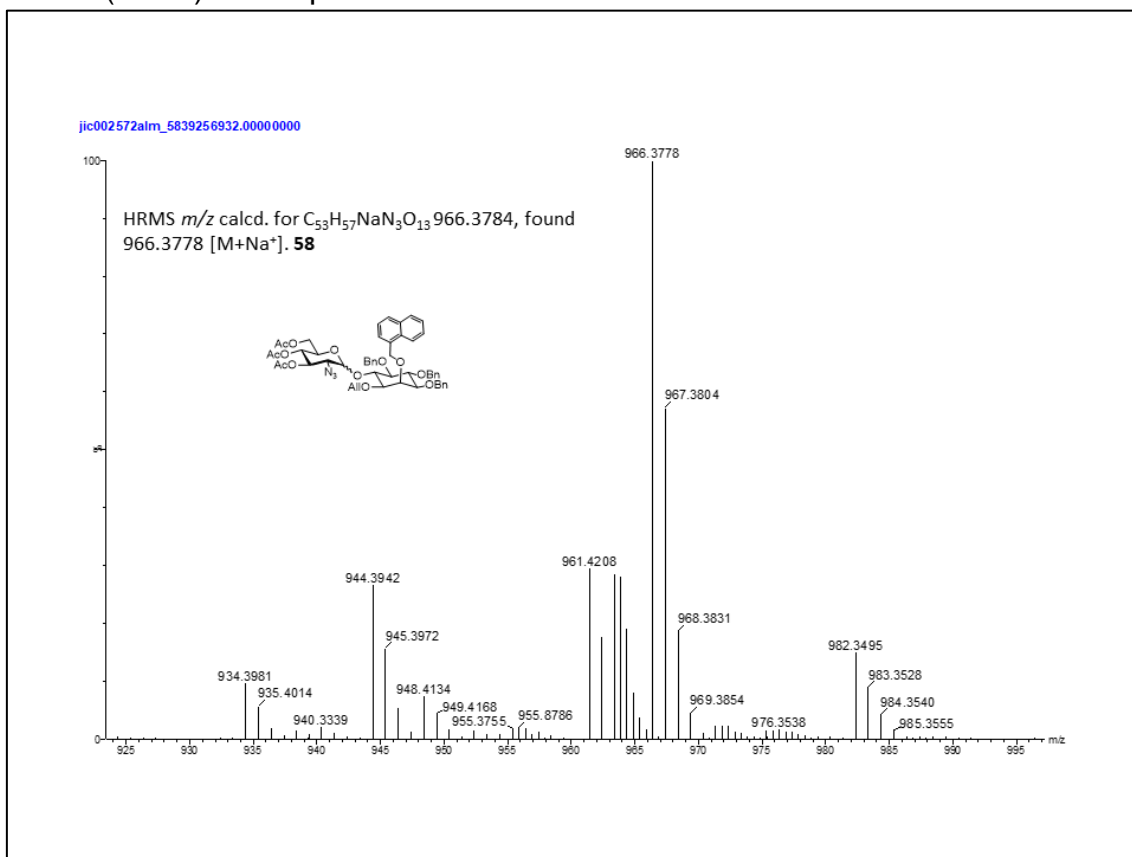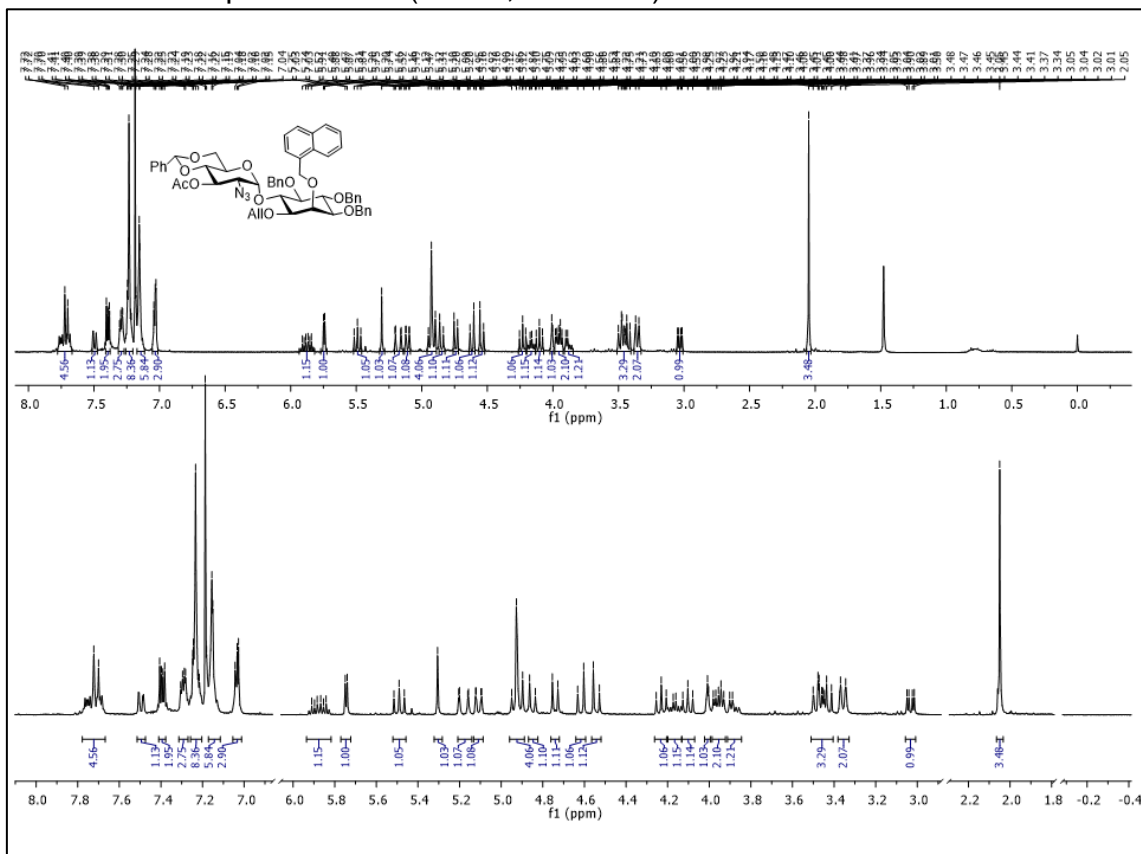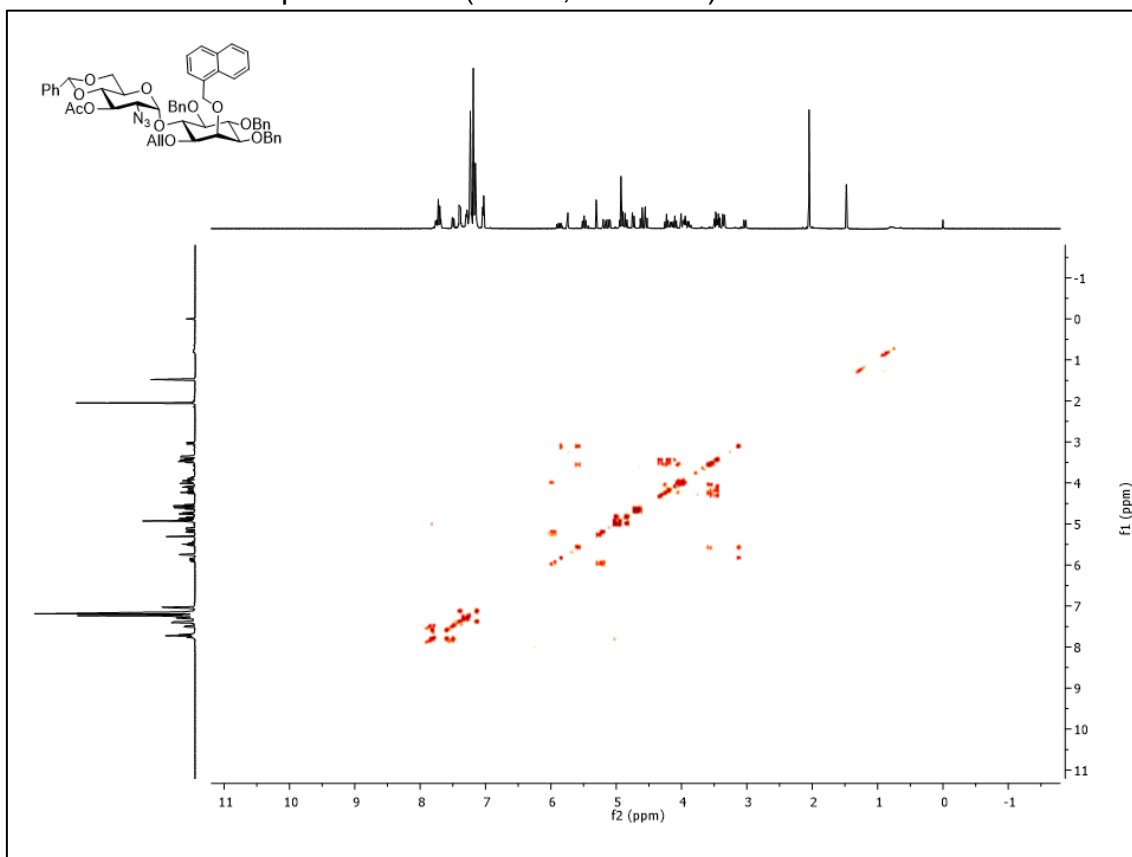
jic002572alm_5839256932.00000000

HRMS m/z calcd. for $C_{53}H_{57}NaN_3O_{13}$ 966.3784, found 966.3778 [M+Na$^+$]. **58**

^{1}H NMR of compound **31bα** (CDCl$_3$; 400 MHz)

COSY NMR of compound **31bα** (CDCl₃; 400 MHz)

¹H NMR of compound **31bβ** (CDCl₃; 400 MHz)

COSY NMR of compound **31bβ** (CDCl₃; 400 MHz)

HRMS (ESI +) of compound **31b**

jic002572alm_6212036670.00000000

HRMS *m/z* calcd. for $C_{56}H_{57}N_3NaO_{11}$ 970.3885, found 970.3870 [M+Na⁺]. **62**
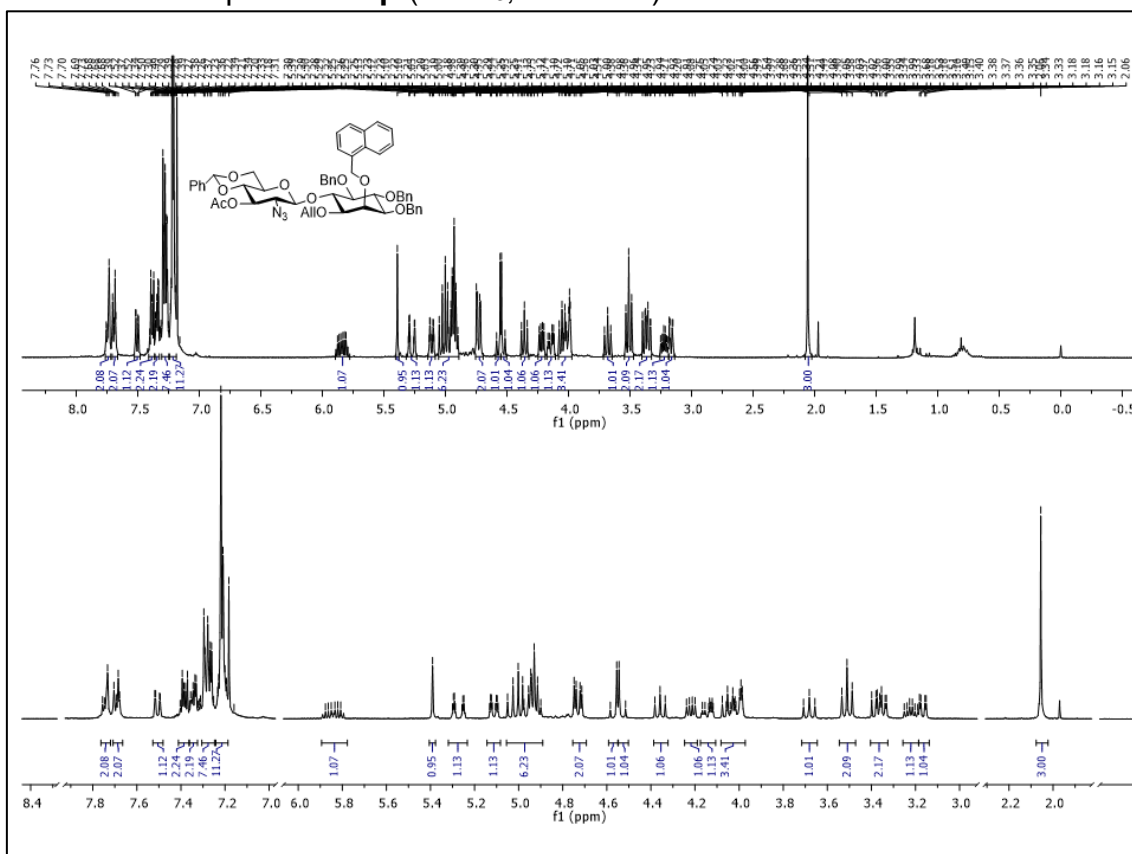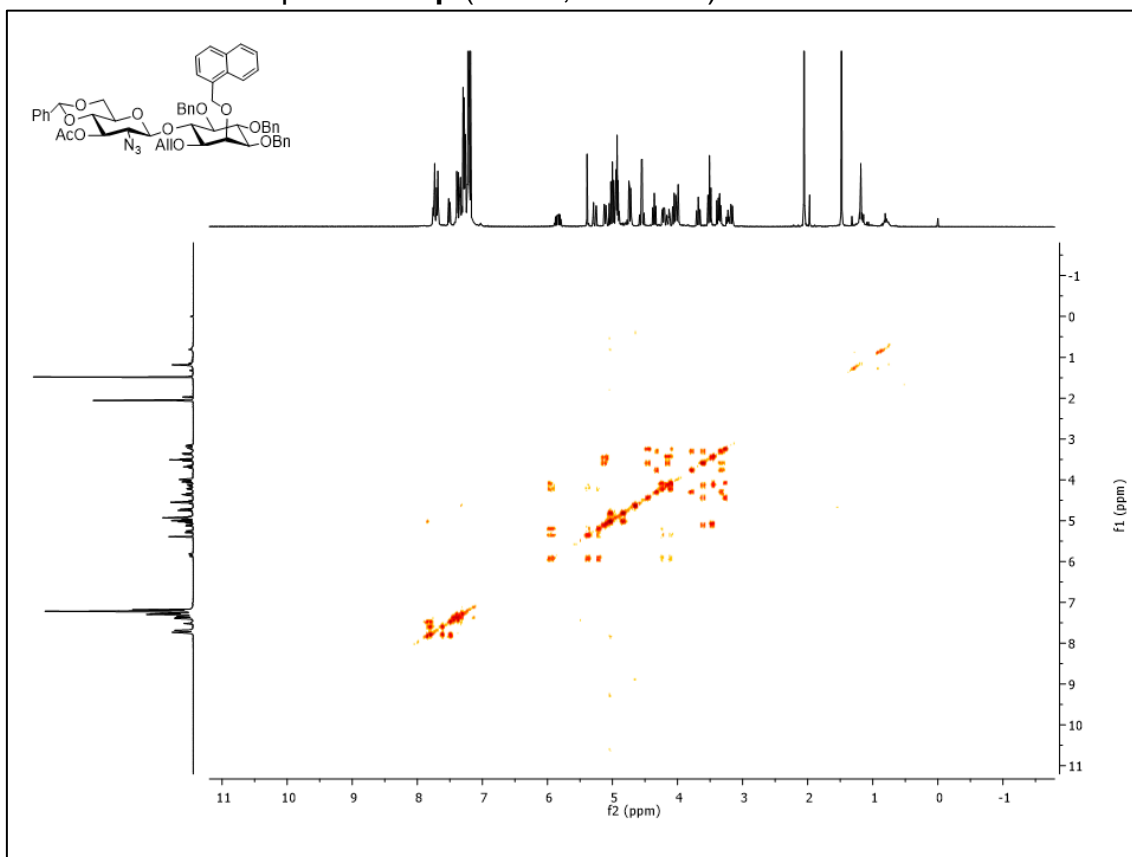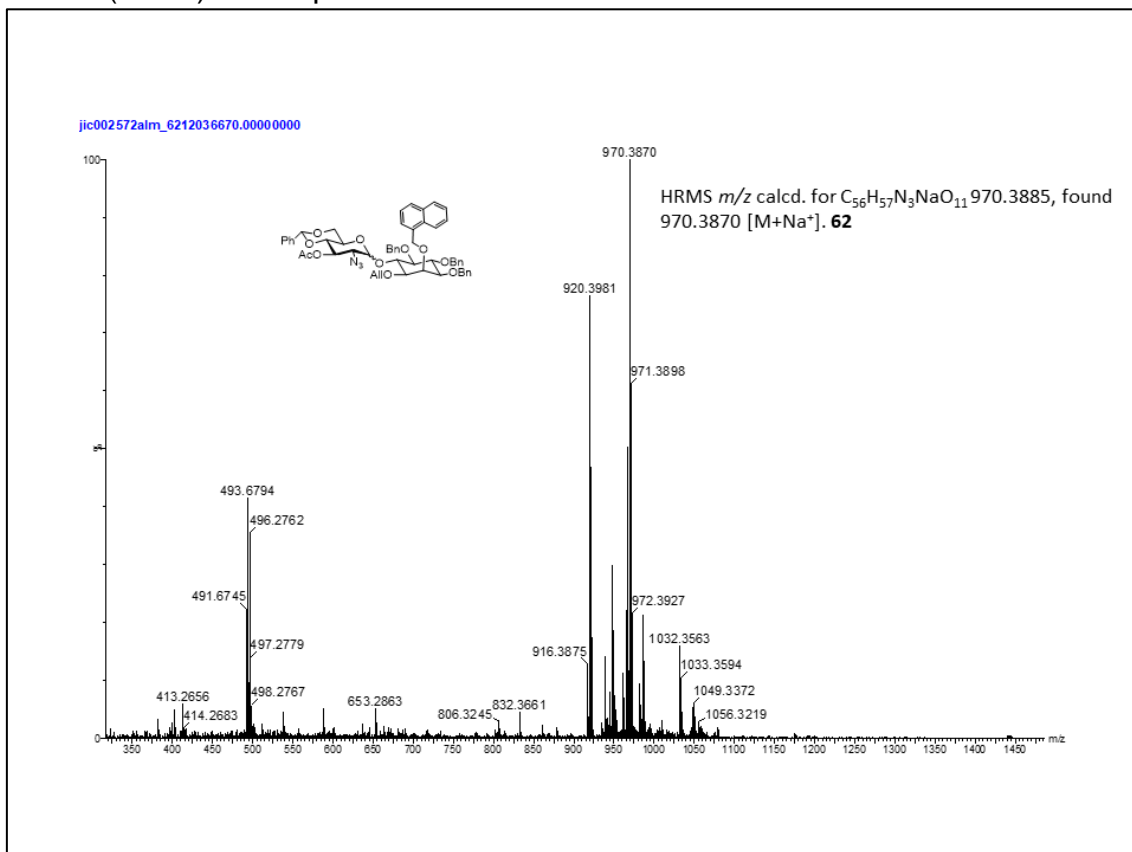
¹H NMR of compound **31c** (CDCl₃; 400 MHz)

¹³C NMR of compound **31c** (CDCl₃; 100 MHz)
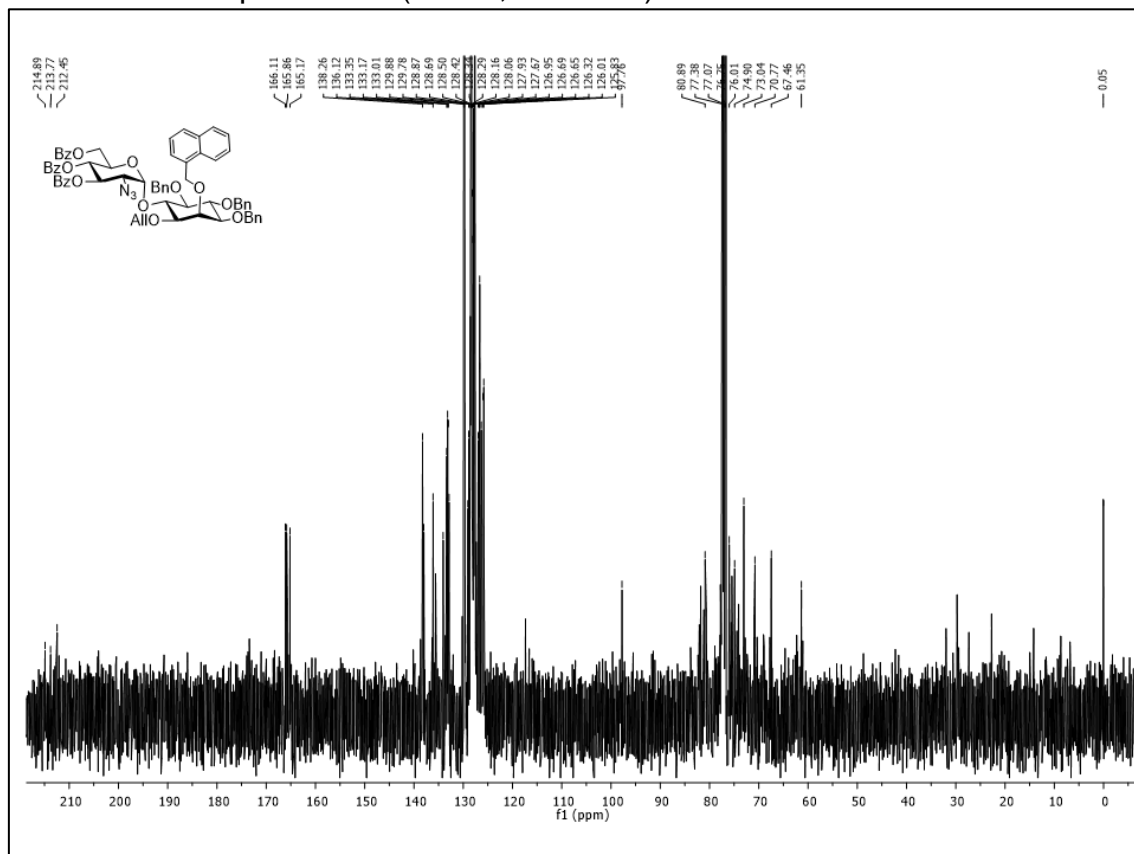
COSY NMR of compound**31c** (CDCl₃; 400 MHz)
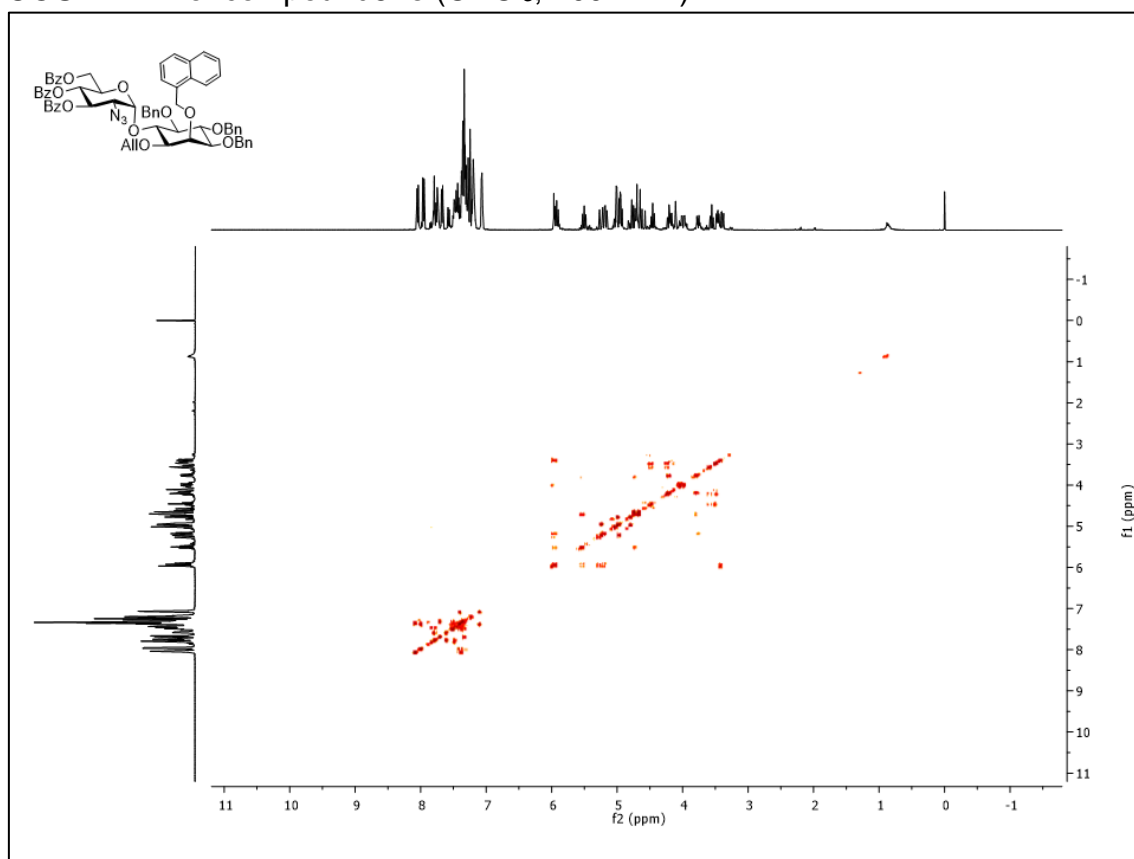
HSQC NMR of compound **31c** (CDCl₃; 400 MHz)

HRMS (ESI+) of compound **31c**

jic002572alm_63144046912.00000000

HRMS *m/z* calcd. for $C_{68}H_{63}NaN_3O_{13}$ 1152.4253, found 1152.4415 [M+Na⁺].
63
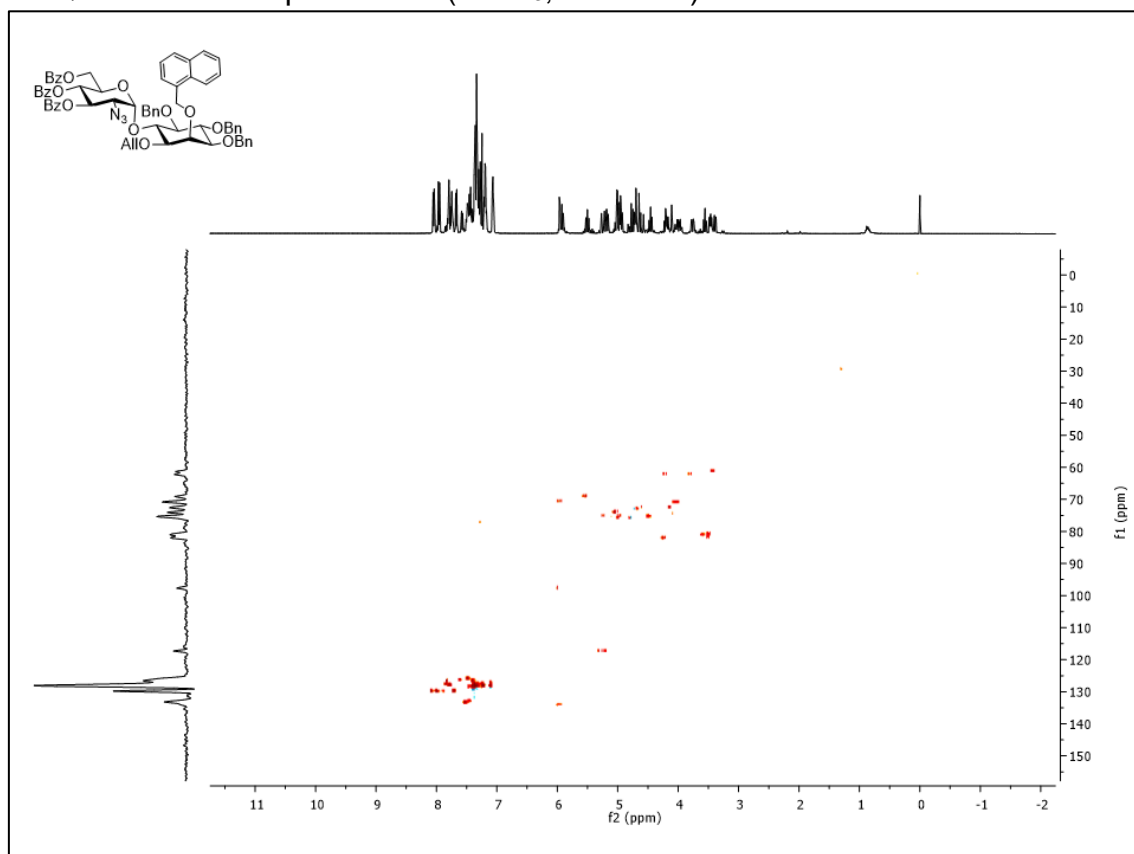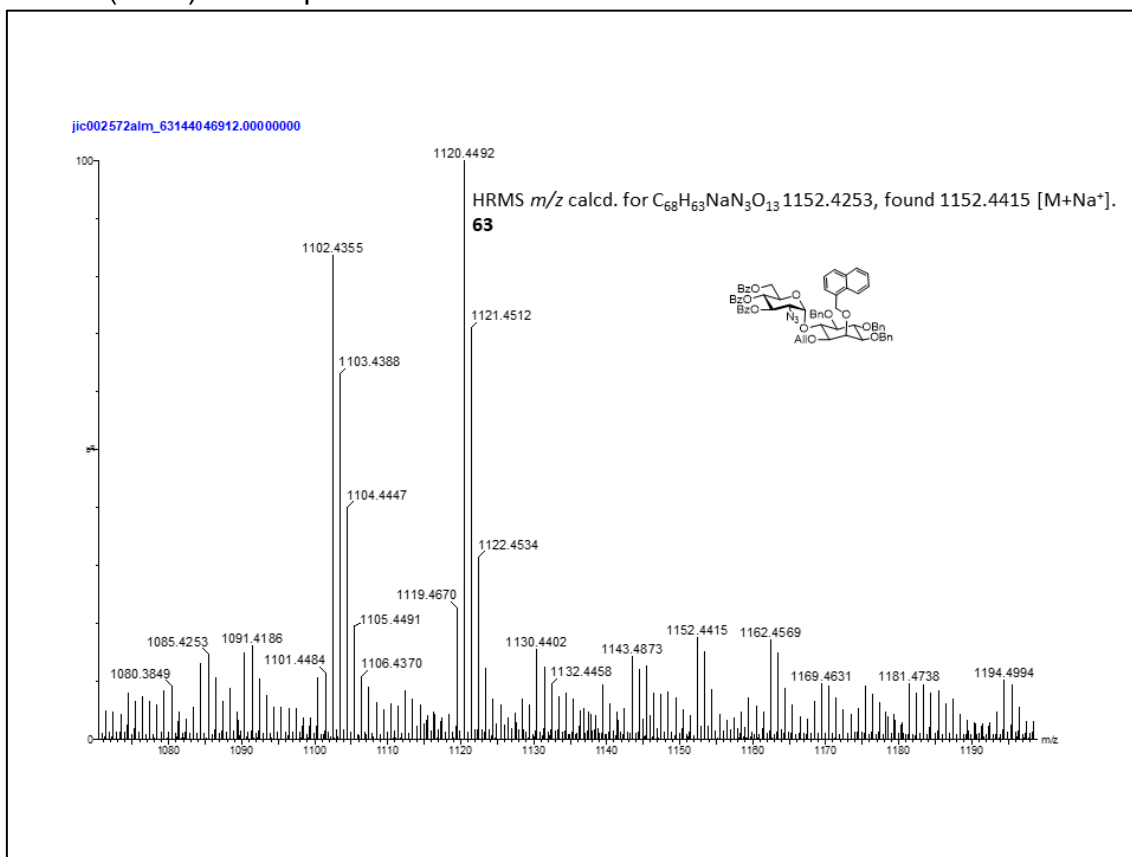
¹H NMR of compound **31d** (CDCl₃; 400 MHz)
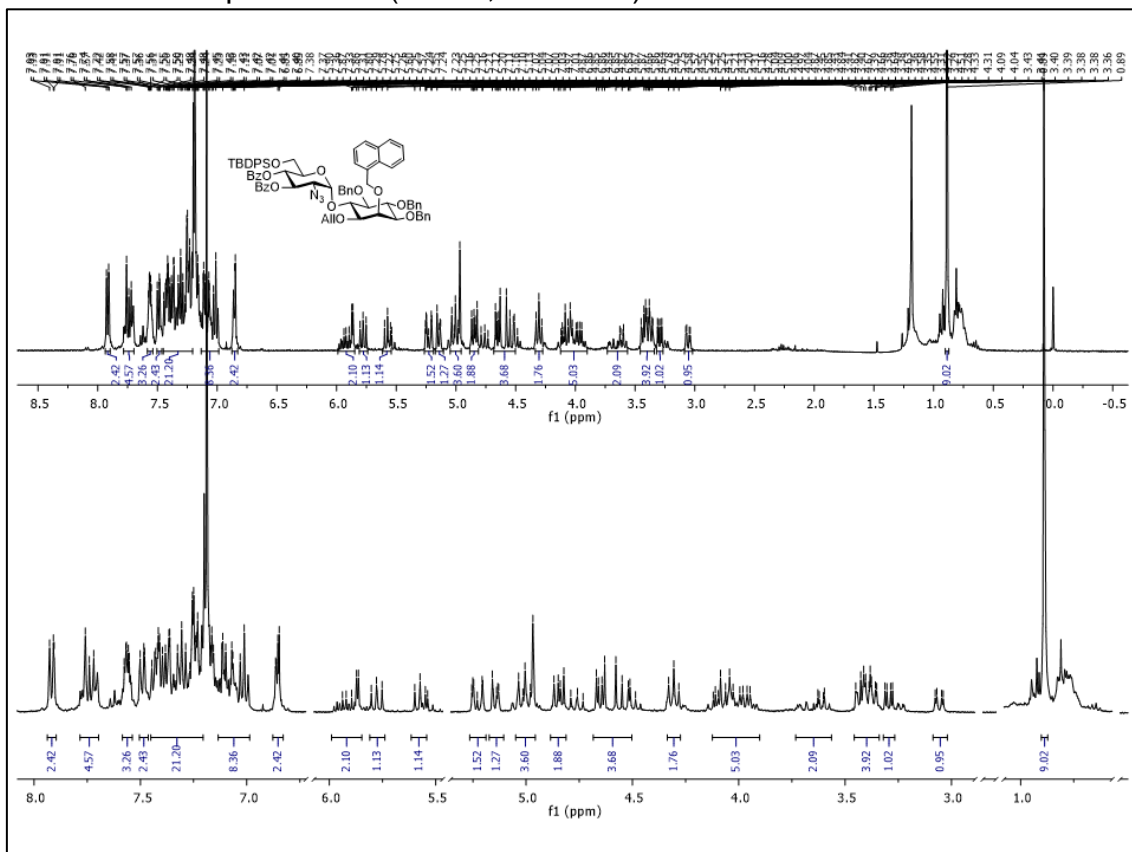
COSY NMR of compound **31d** (CDCl₃; 400 MHz)

HRSM (ESI+) of compound **31d**

HRMS *m/z* calcd. for $C_{77}H_{77}NaN_3O_{12}Si$ 1286.5169, found 1286.5621 [M+Na⁺].
65
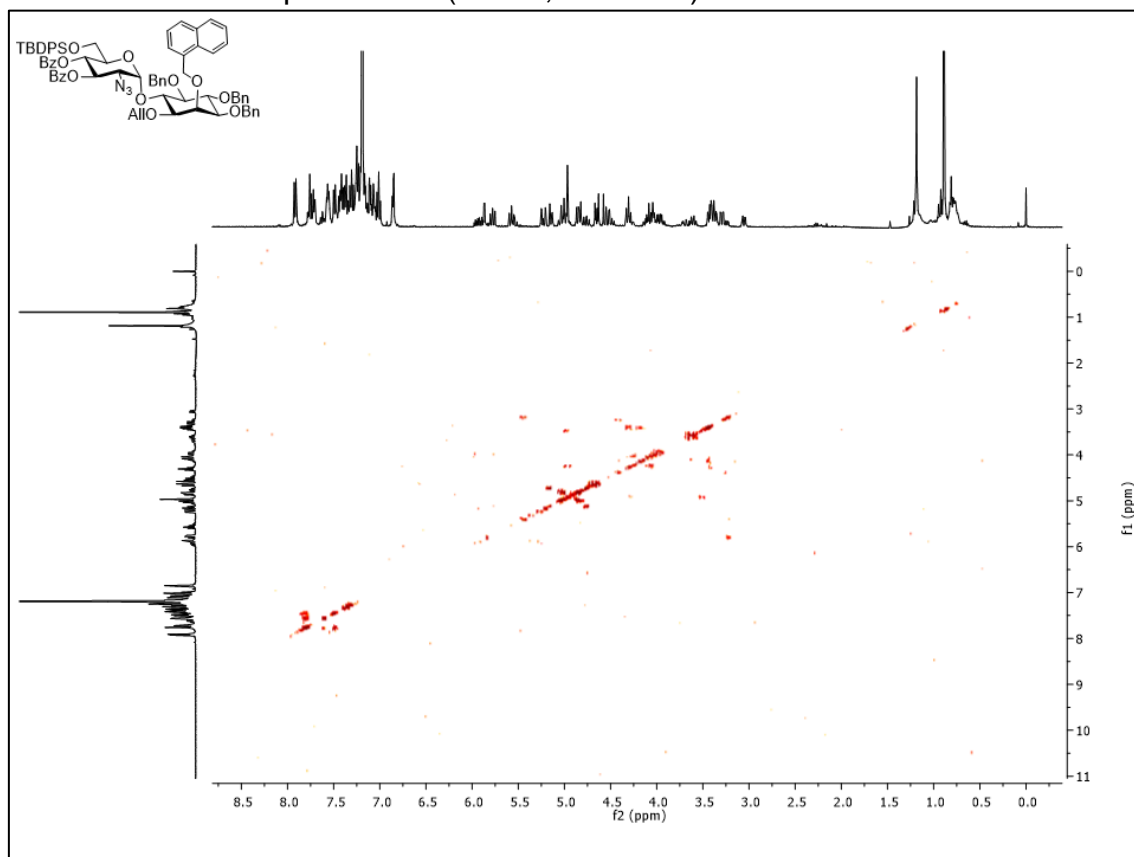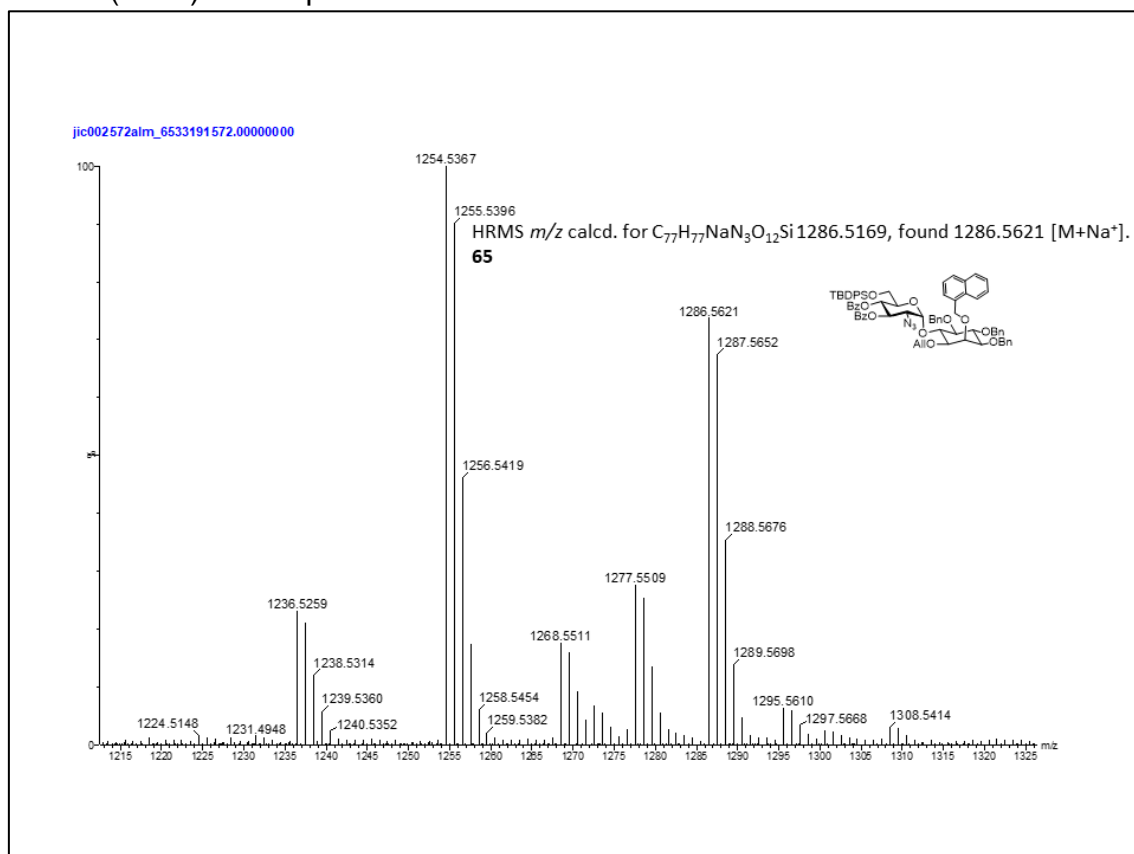
^{1}H NMR of compound **77** (CDCl$_3$; 400 MHz)
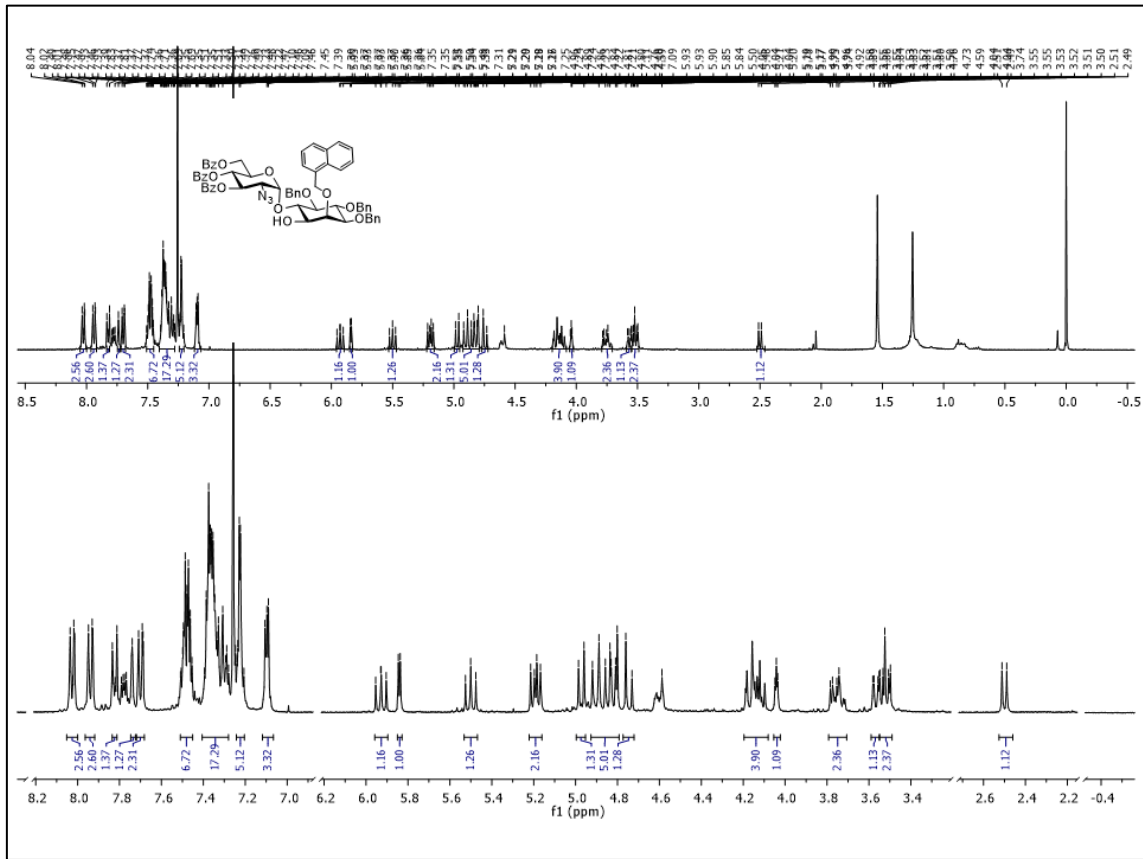
^{13}C NMR of compound **77** (CDCl$_3$; 100 MHz)
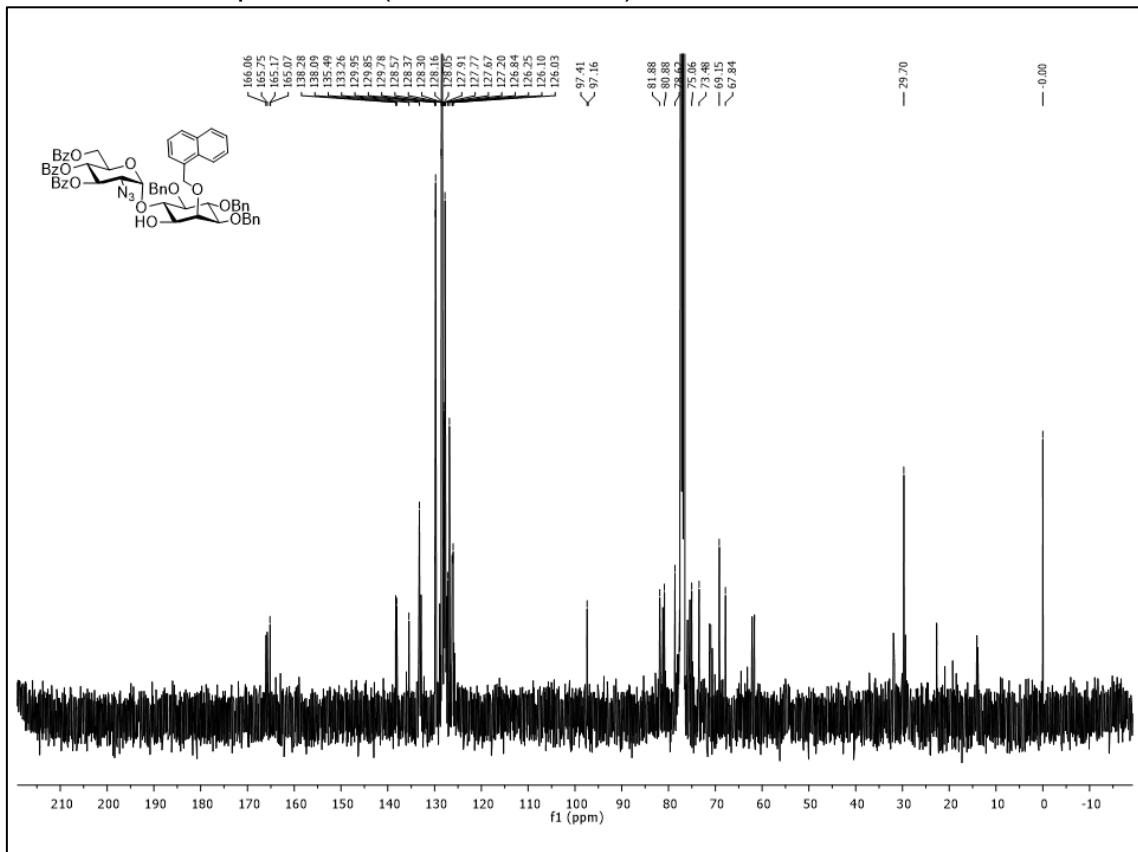
HSQC NMR of compound **77** (CDCl₃; 400 MHz)
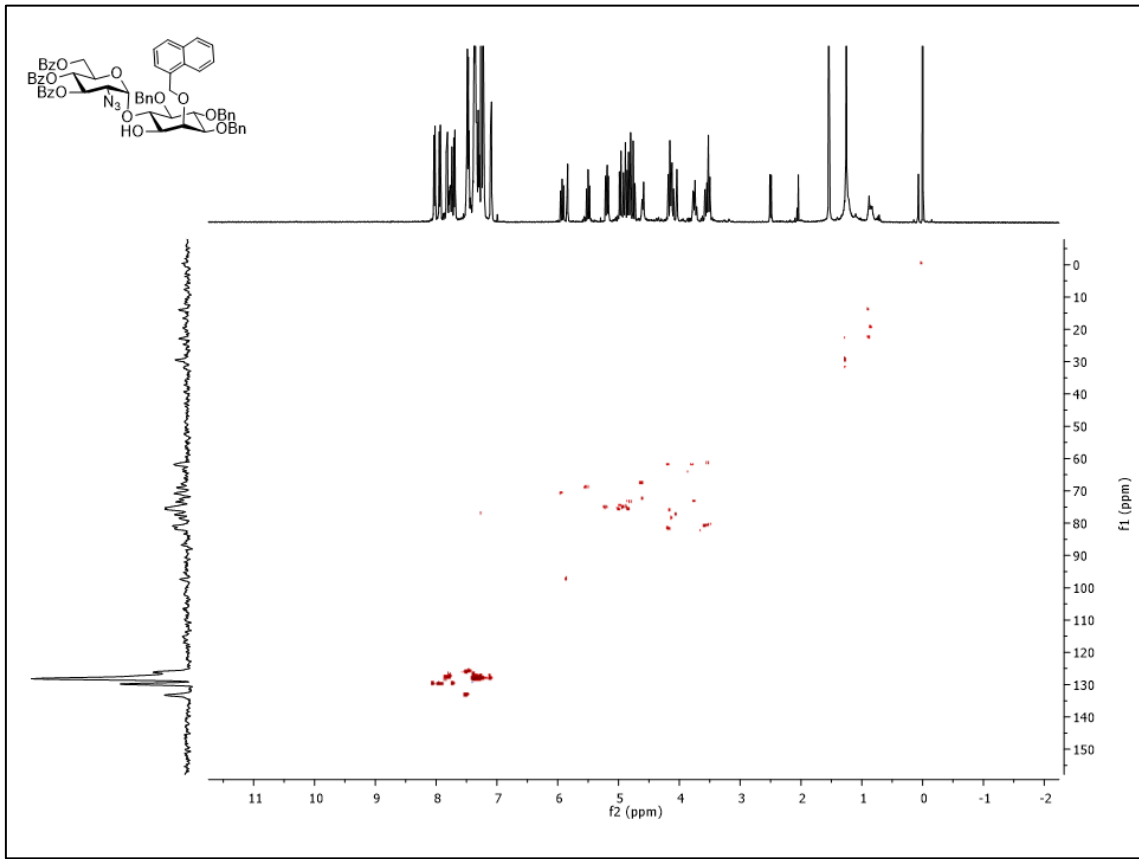
¹H NMR of compound **89** (DMSO-D; 500 MHz)
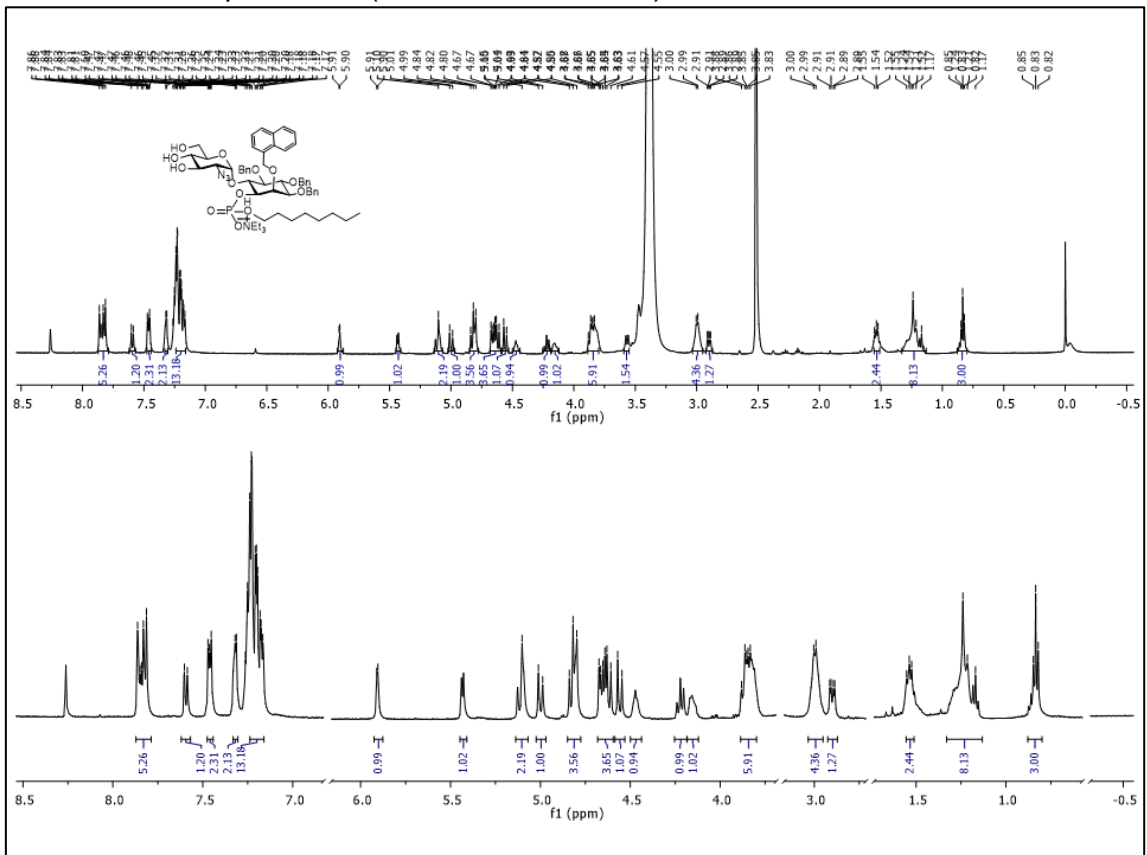
^{31}P NMR of compound **89** (CDCl$_3$ /MeOD; 202 MHz)

COSY NMR of compound **89** (DMSO-D; 500 MHz)

HSQC NMR of compound **89** (DMSO-D ₃; 500 MHz)
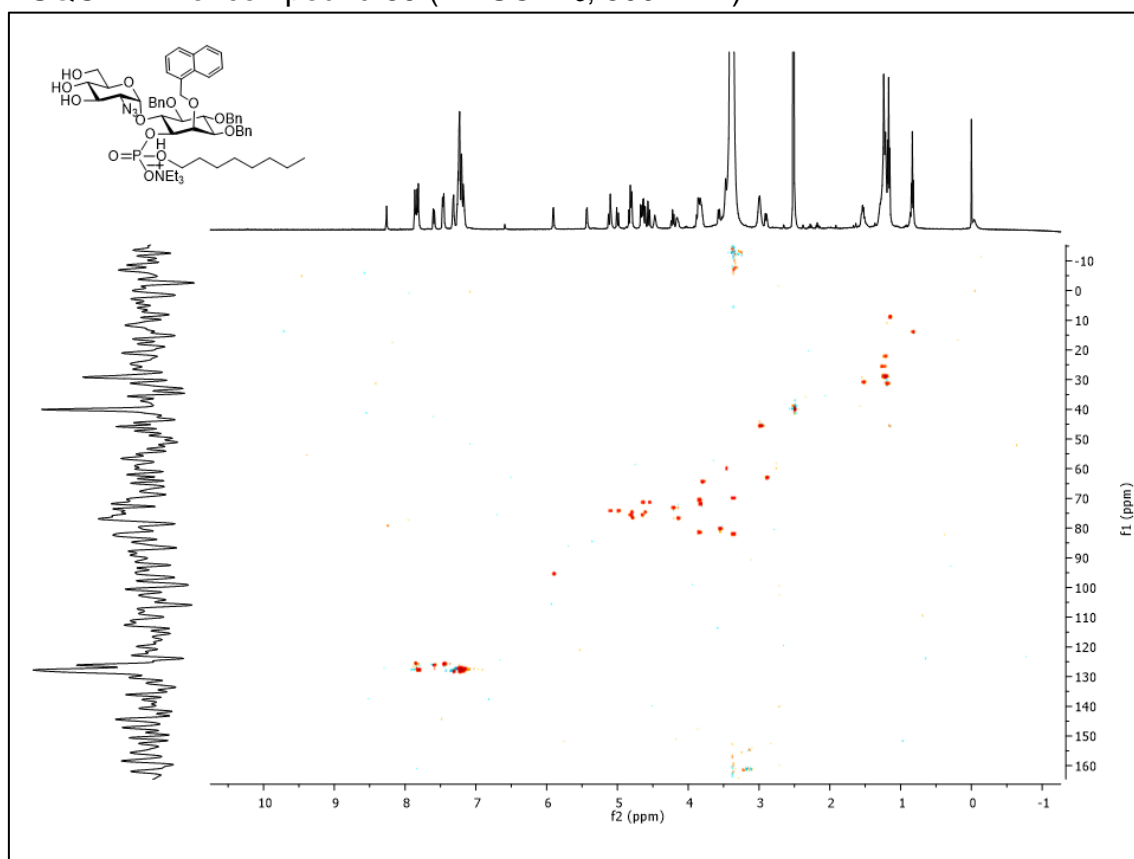
HMBC NMR of compound **89** (DMSO-D; 500 MHz)
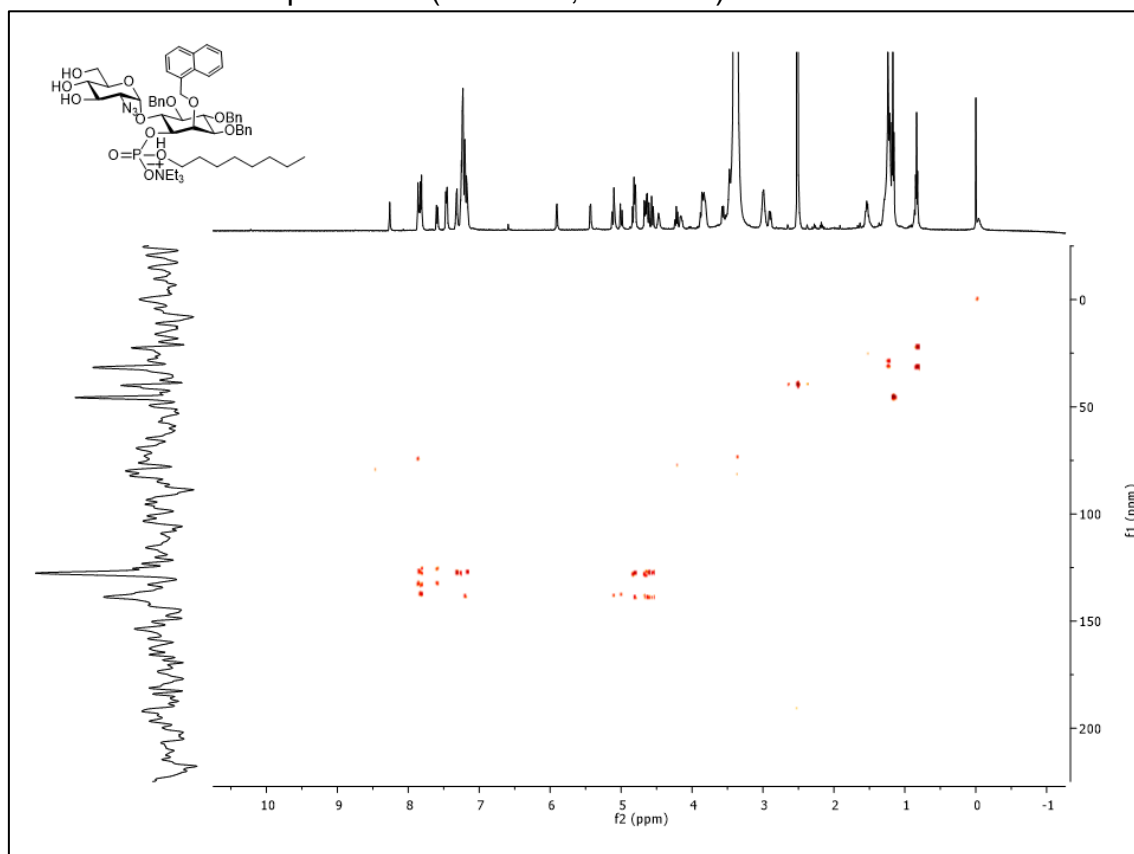
HRMS (ESI-) oc compound **89**

HRMS (ESI-) of compound **30a** *m/z* calcd. For $C_{20}H_{40}NO_{13}P^-$ 533.2237, found 532.2170 [M – H]$^-$ and 533.2195.
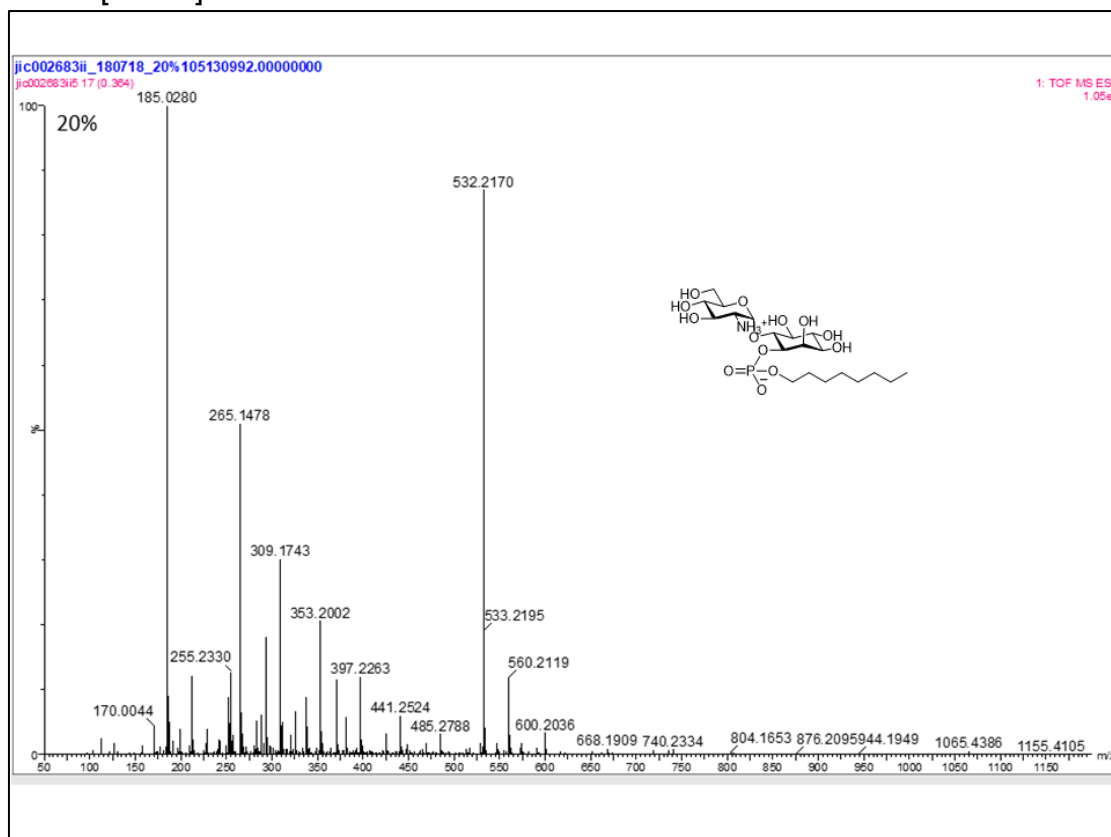
^{1}H NMR of compound **91** (CDCl$_3$; 500 MHz)
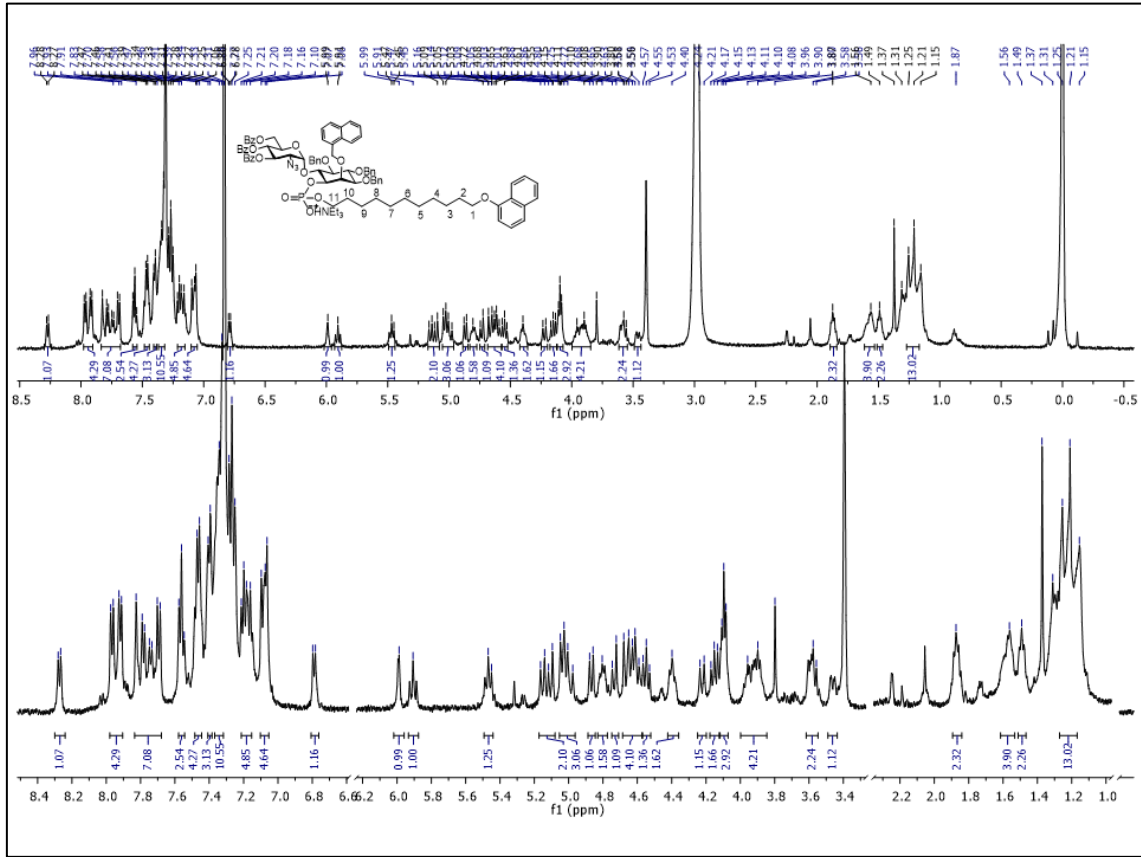
COSY NMR of compound **91** (CDCl$_3$; 500 MHz)
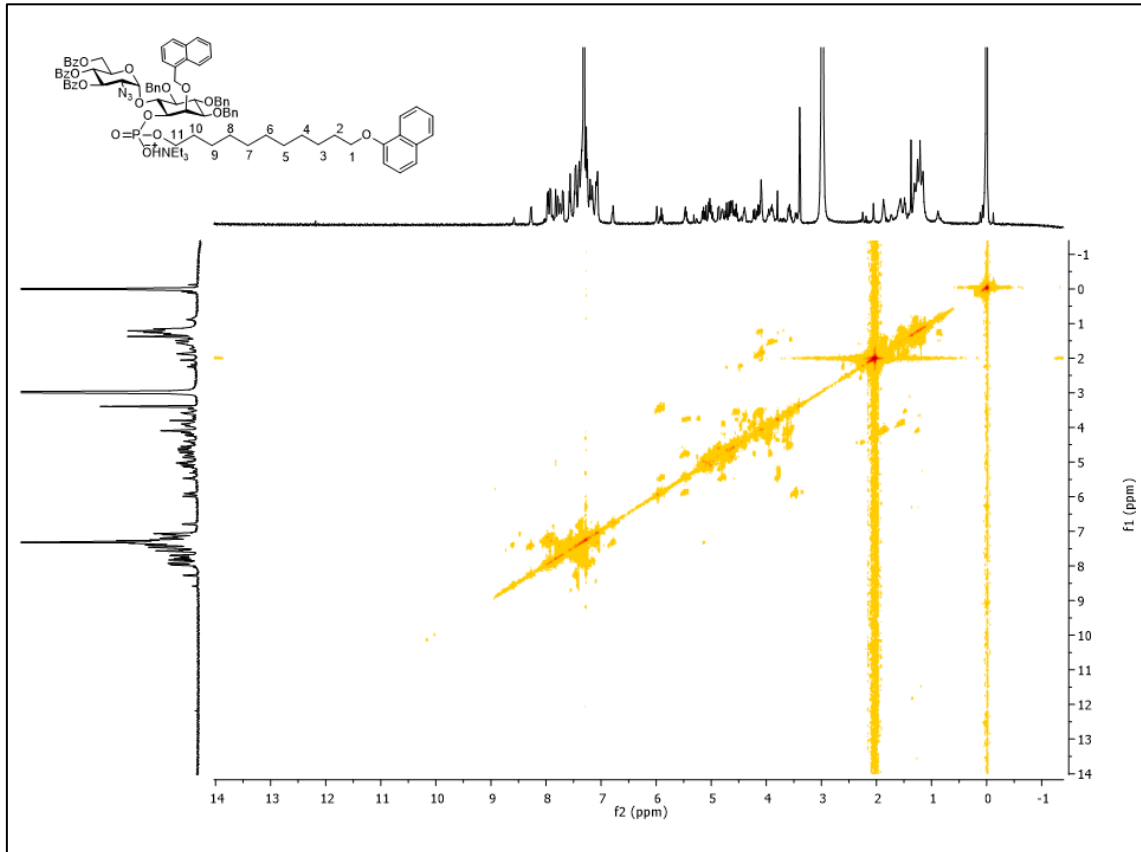
HSQC NMR of compound **91** (CDCl₃; 500 MHz)
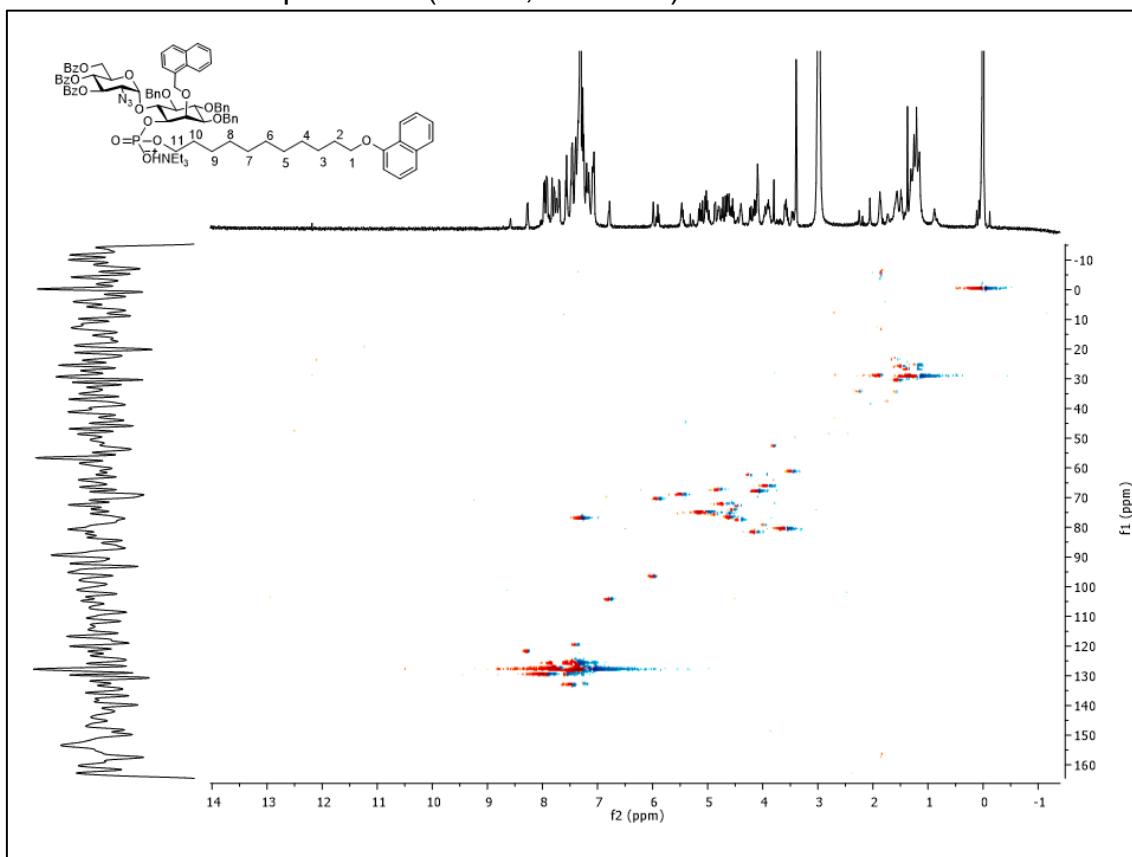
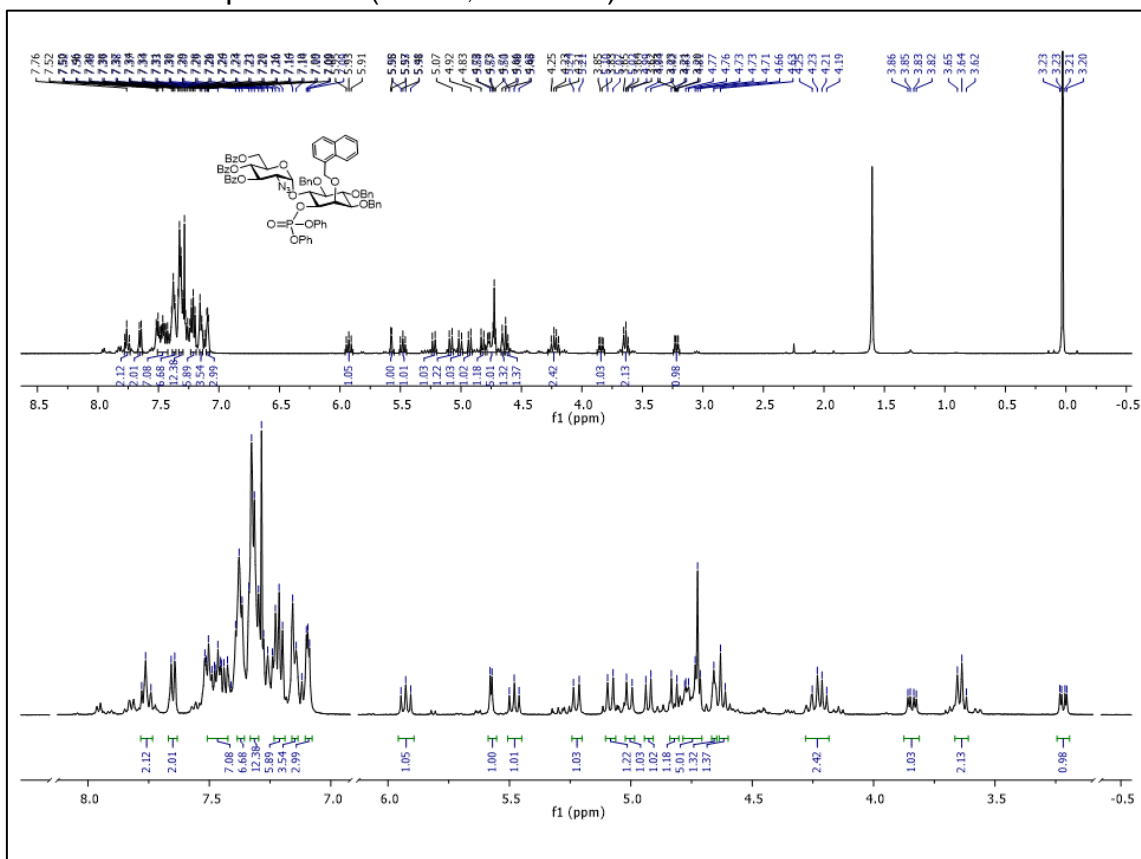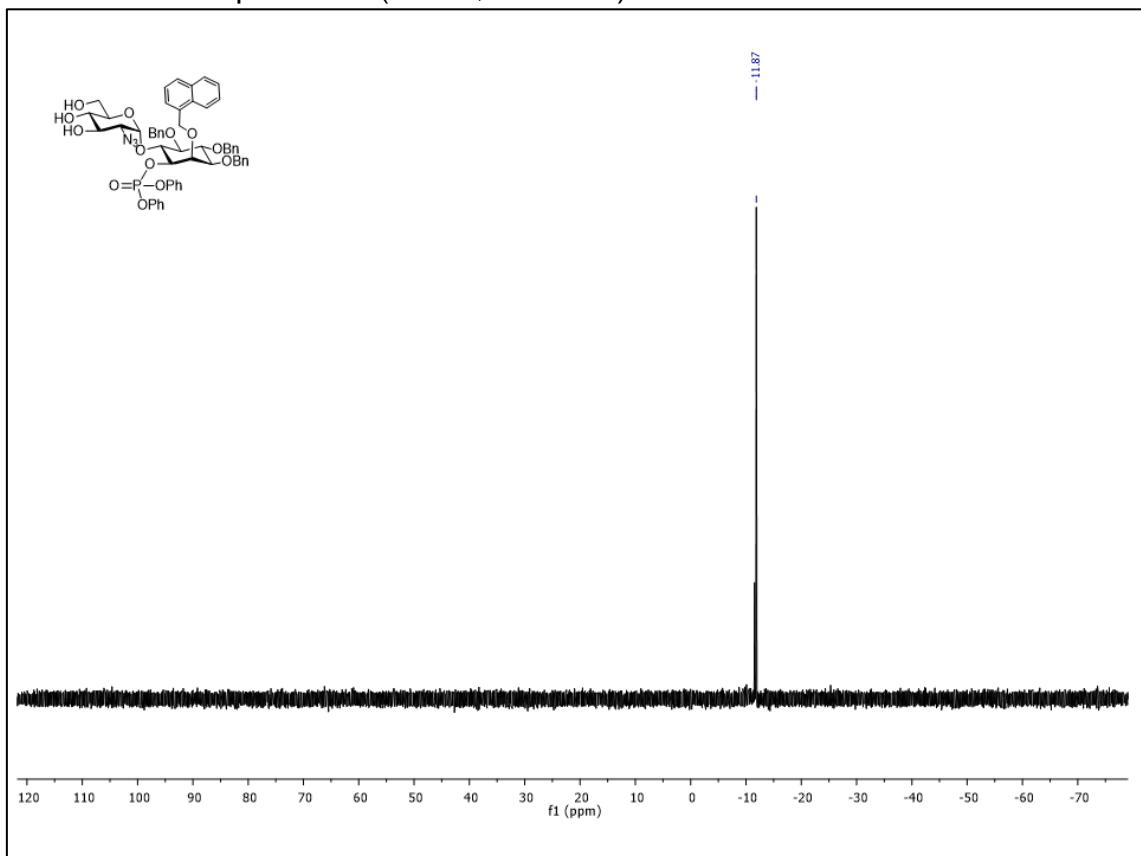HMBC NMR of compound **91** (CDCl₃; 500 MHz)
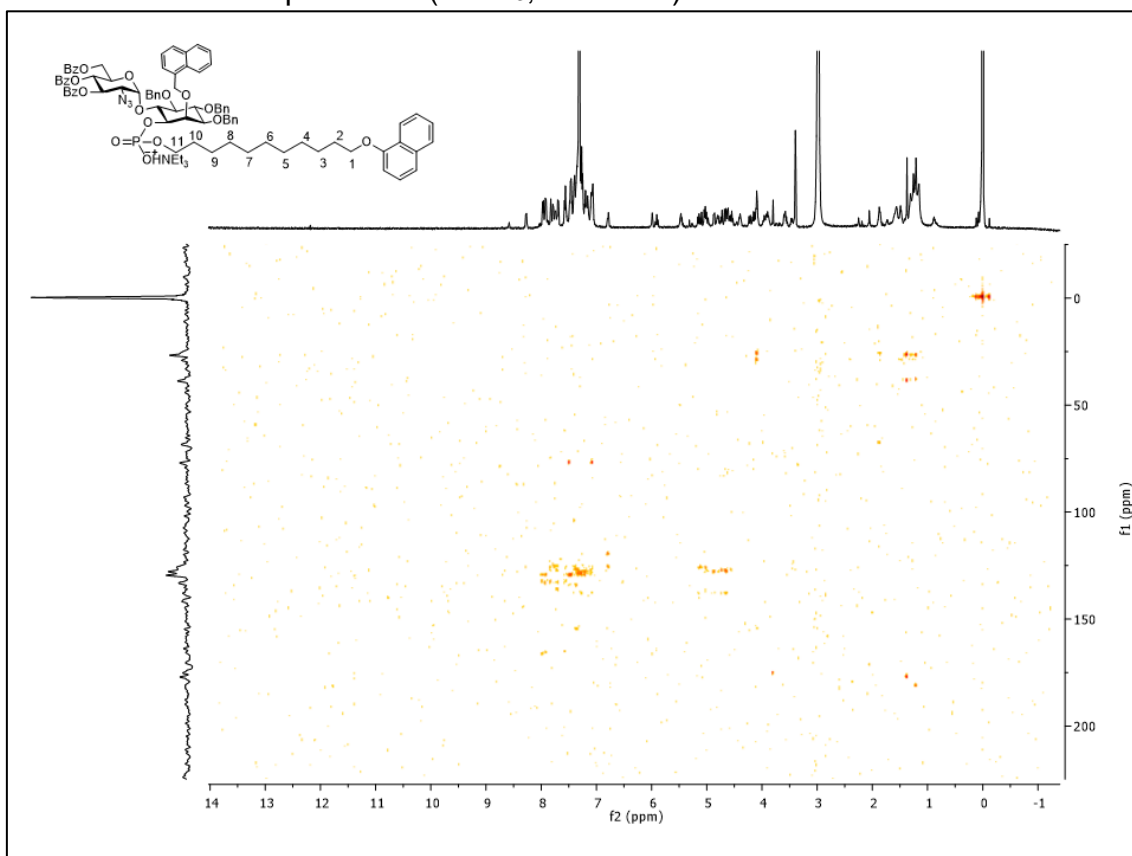
³¹P NMR of compound **91** (CDCl₃; 202 MHz)
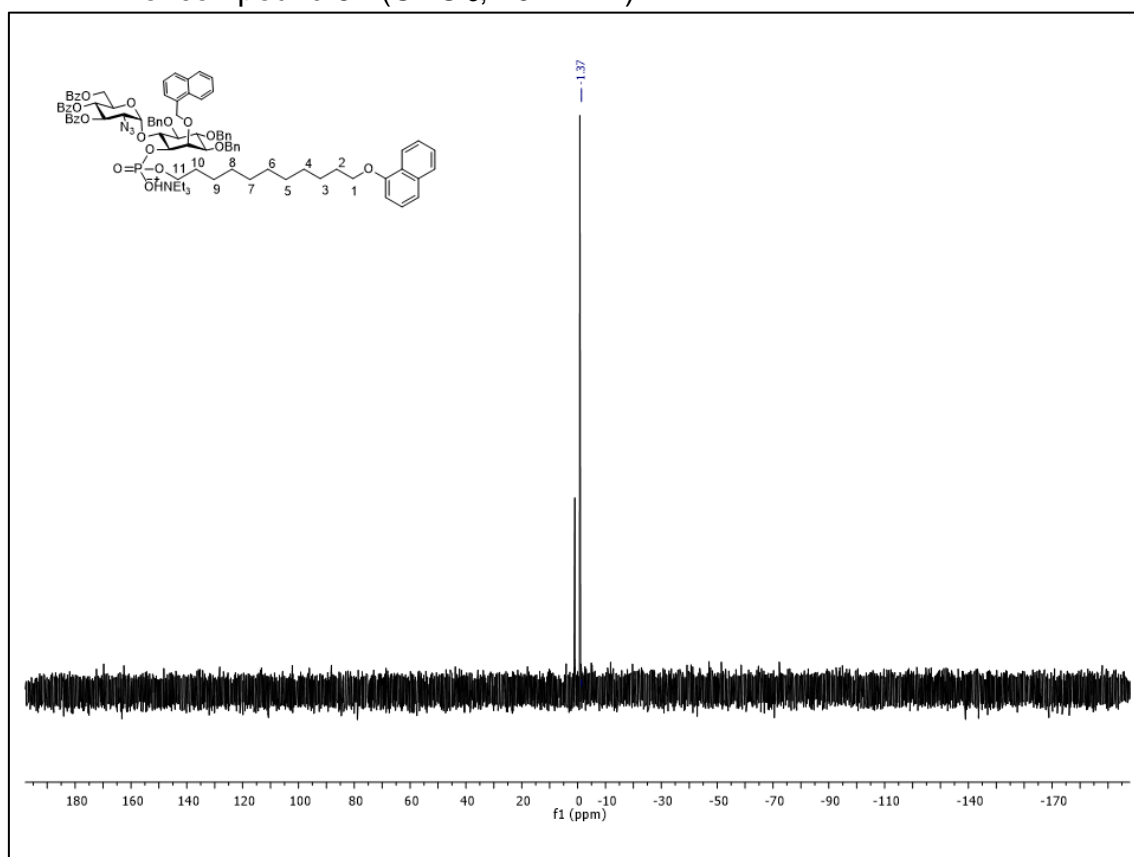
HRMS (ESI-) of compound **91** *m/z* calcd. For $C_{86}H_{87}N_3O_{17}P^-$ 1464.5778, found 1464.5713 [M – Et_3N]$^-$.
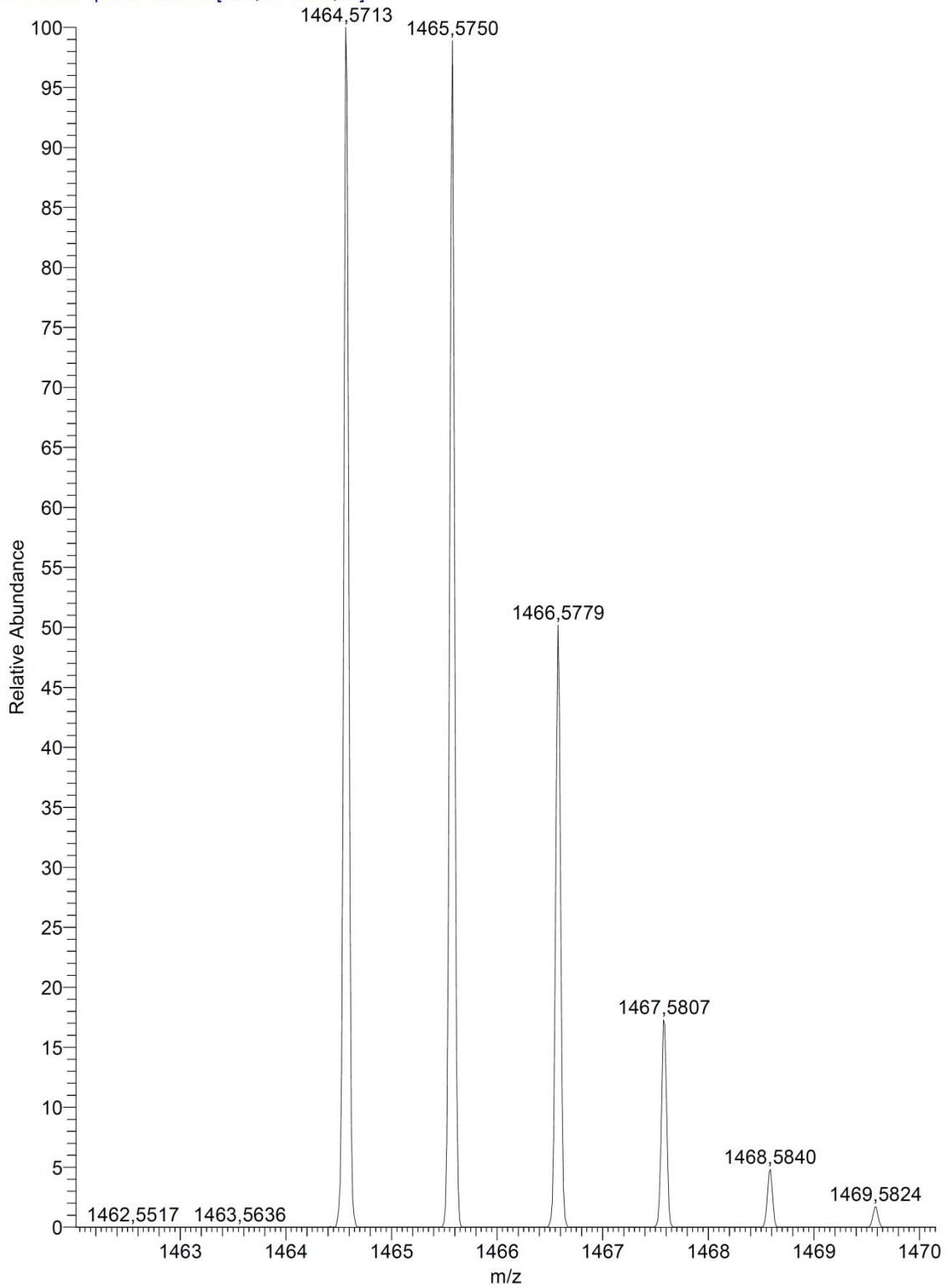
^{1}H NMR of compound **92** (CDCl$_3$, 500 MHz)

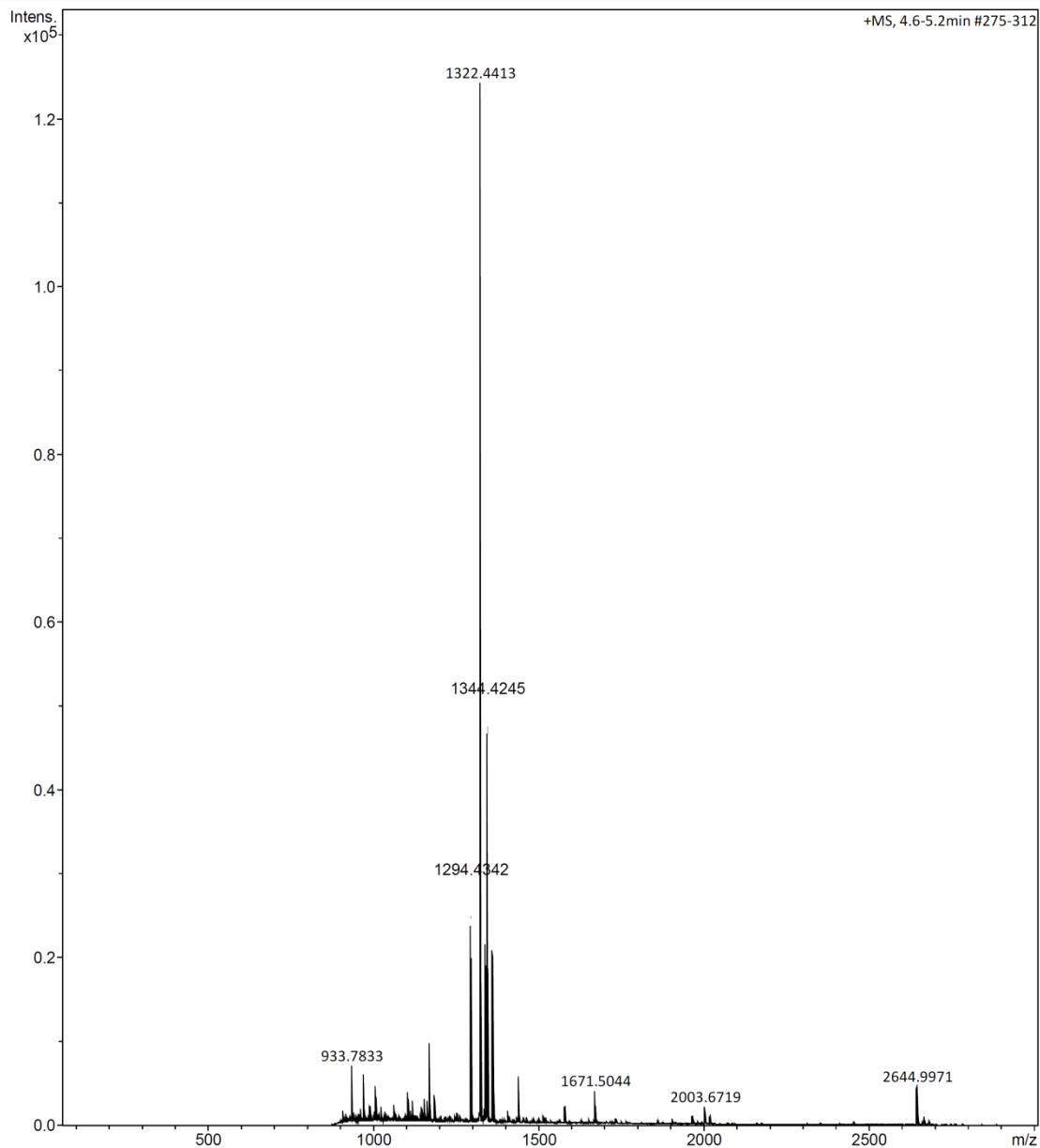# ^{31}P NMR of compound **92** (CDCl$_3$, 500 MHz)

HRMS (ESI +) of compound **92** *m/z* calcd. for $C_{77}H_{69}N_3O_{16}P$ 1321.4337, found 1322.4409 [M+1]$^+$ and *m/z* calcd. for $C_{77}H_{69}N_3O_{16}$ 1321.4337, found 1344.4245 [M+Na]$^+$.
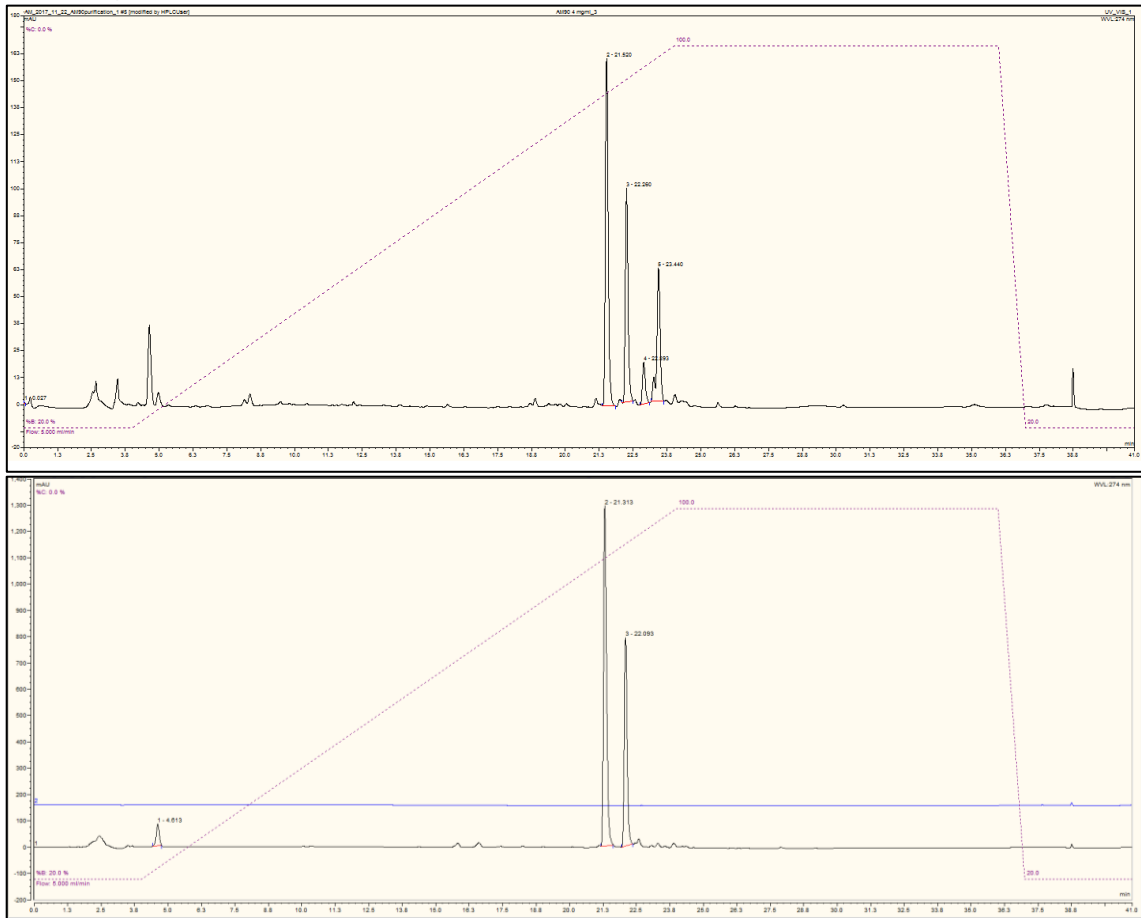
Analysis Info

Analysis Name	D:\Data\PROF. IVONE\ALM 63 B_Fr 1_POS.d	
Method	tune_high_pos.m	
Sample Name	ALM 63 B_Fr 1_POS	
Comment		

Acquisition Date   7/2/2018 2:18:25 PM

Operator   TOMAZ
Instrument   micrOTOF-Q

Chromatograms of compound **89** purified in DIONEX Ultimate 3000, C$_{18}$ column.

Chromatogram of compound **30a** in Zevo TQ-S Acquity UP-LC.